DESIGN OF CONTROLLER FOR STABLE MICROGRID OPERATION

A Thesis

submitted in fulfillment of the requirements for the award of the degree of

Doctor of Philosophy

in

Engineering

Submitted by

Sahil Mehta
(Registration no.: 951804002)

Under the guidance of

Dr. Prasenjit Basak
Associate Professor, DEIE

Department of Electrical and Instrumentation Engineering
Thapar Institute of Engineering & Technology, Patiala
(Declared as Deemed-to-be-University u/s 3 of the UGC Act., 1956)
Post Bag No. 32, Patiala – 147004
Punjab (India)

October 2024

Dedicated

To

My Parents

Mr. Deepak Mehta & Mrs. Nimmy Mehta

CERTIFICATE

This is to certify that the thesis entitled "**DESIGN OF CONTROLLER FOR STABLE MICROGRID OPERATION**" being submitted by Mr. Sahil Mehta to the Department of Electrical & Instrumentation Engineering, Thapar Institute of Engineering & Technology (Deemed to be University), Patiala, Punjab, India for the award of the degree of **Doctor of Philosophy**, is a record of bonafide research work carried out by him under my guidance and supervision and has fulfilled the requirements for the submission of this thesis, which to my knowledge has reached the requisite standard.

The results embodied in the thesis have not been submitted in part or full to any other Institute or University for the award of any diploma or degree.

22/10/2024

Dr. Prasenjit Basak
Associate Professor
Department of Electrical & Instrumentation Engineering,
Thapar Institute of Engineering & Technology (Deemed to be University),
Patiala, Punjab, India

ACKNOWLEDGMENT

I would like to extend my thanks and gratitude to the many people who generously contributed to the work presented in this thesis. I honestly find myself short of words to acknowledge all those who helped me directly and indirectly during this research work.

With due regards and great delight, I convey my heartfelt gratitude and indebtedness to my supervisor, **Dr. Prasenjit Basak**, Associate Professor in the Department of Electrical & Instrumentation Engineering at Thapar Institute of Engineering & Technology (Deemed to be University), Patiala. I appreciate his skillful guidance, persistent encouragement, proficient evaluation, and conscientious supervision throughout this academic endeavor. Dr. Basak was always available to assist me with utmost care, kind attention, and prudent suggestions during odd hours of the job. His hardworking nature and methodical suggestions were a constant source of encouragement to me. I find my vision even more broadened owing to his guidance, expertise, inquisitive attitude, and tireless efforts, apart from his working hours. I earnestly thank him from the core of my heart for being a consistent source of inspiration from the beginning to the end.

I am very thankful to **Dr. Mukesh Singh**, Associate Professor in the Department of Electrical & Instrumentation Engineering, **Dr. Nitin Narang**, Associate Professor in the Department of Electrical & Instrumentation Engineering, and **Dr. Neeraj Kumar**, Professor in the Department of Computer Science Engineering, for being members of the Doctoral Committee and spending their valuable time reviewing and critically examining the work.

I am also thankful to the present Chairman of the Doctoral Committee, **Dr. Sunil Singla**, Professor & Head of the Department of Electrical & Instrumentation Engineering, for the much-needed support throughout the work.

My heartfelt gratitude is due to Honorable Director **Dr. Padmakumar Nair** and **Dr. N. Tejo Prakash**, Professor & Dean of Research and Sponsored Projects, for their support, encouragement, and providing the necessary facilities to carry out and complete this work on a steady course.

I also wish to express my deep sense of gratitude to all the faculty and staff members of the Department of Electrical & Instrumentation Engineering. Their encouraging and caring words, constructive criticism, and suggestions have contributed directly or indirectly in a significant way towards the completion of this research work. My deepest appreciation is due to all the research scholars, especially **Dr. Jitender Kaushal, Dr. Amit Kumar Roy**, **Dr. Manjeet Singh**, **Dr. Arshdeep Singh**, and **Dr. Zaid B. Siddique** under the supervision of Dr. Prasenjit Basak. They have always stood by me in all difficult times and reinforced my confidence. Their

never-ending support was a constant source of motivation and always kept me going. Besides, I would like to express my gratitude to all those laboratory technicians with whom I have worked and interacted and whose thoughts have helped me further my grasp and understanding of the work.

I bow with gratitude to my parents, **Mr. Deepak Mehta** and **Mrs. Nimmy Mehta**, who are the most precious people in my life. Without their efforts, I would not have achieved this milestone. I also feel highly honored to recognize my sister, **Dr. Jimmy Mehta**, and my brother-in-law, **Mr. Karan Saneja**, for their constant support, that has motivated me throughout this journey. I am also profoundly grateful to my fiancée, **Dr. Aastha**, for her unwavering support and encouragement, which have strengthened me during this endeavor.

I would also like to express my gratitude to the Copperpod family, especially **Mr. Rahul Vijh and Mrs. Purva Sharma,** for their support, which significantly contributed to the successful completion of my Ph.D.

Last but not least, I bow in reverence to **Almighty God**, who has always showered blessings on me at each and every step in completing this thesis.

ABSTRACT

Microgrids are integral to sustainable energy infrastructure, offering localized control over power generation, distribution, and consumption. Despite their multiple advantages in resilience and renewable integration, various challenges persist, particularly in maintaining stability amidst the dynamic and uncertain nature of renewable inputs like solar and wind. Thus, to address such issues, robust controllers are essential for managing uncertain renewable energy sources (RES) and ensuring stable microgrid operation. An inclusive literature survey reveals that the current literature lacks a robust controller that maintains stable microgrid operation while considering multiple system parameters such as voltage and frequency. Besides, in line with this, the literature also lacks an approach to performing strategic load shedding given load priority in the presence of uncertain RES. In addition, the literature also lacks a comprehensive approach to microgrid assessment, especially focusing on all the performance aspects, i.e., technical, economics, and implementation. Lastly, given the microgrid assessment, an ideology of a comprehensive stability assessment index is unavailable in the existing literature.

Thus, focusing on such issues, this work presents a stage-wise control strategy that utilizes a fuzzy logic controller to regulate frequency and voltage in islanded microgrids. Divided into three stages, the approach manages minor perturbations with battery support and strategically sheds non-critical loads during significant perturbations to enhance stability. Additionally, a robust energy management system employing a cascaded dual-fuzzy logic-based control approach to effectively manage battery operation, microgrid mode of operation, and load distribution has also been presented. In addition, this work also presents the use of HOMER Pro software for the economic assessment of developed microgrids, considering Kibber Village, India, as an exemplary system. In addition to the economic and technical assessment, this work proposes a hardware test bench for real-time validation using a programmable logic-based controller (PLC). Lastly, considering the factor for stability assessment, this research presents a novel methodology for determining the Microgrid Stability Index (MGSI), employing a fuzzy inference system. Validation via MATLAB simulations, multiple case studies, and comparison with existing topologies demonstrate the effectiveness of the proposed approaches in ensuring stable microgrid operation.

Keywords: Microgrid Stability, Fuzzy Logic Control, Renewable Energy Integration, Energy Management System, PLC, HOMER Pro, Microgrid Stability Index (MGSI)

TABLE OF CONTENTS

LIST OF FIGURES

LIST OF TABLES

LIST OF ACRONYMS

AC	Alternating Current
AHP	Analytic Hierarchy Process
AI	Artificial Intelligence
ANFIS	Adaptive Neuro-Fuzzy Inference System
APE	Active Power Estimation
AREP	Accelerated Rural Electrification Program
BESS	Battery Energy Storage System
CCW	Connected Components Workbench
CI	Clearness Index
CL	Critical Load
COE	Cost of Energy
CPL	Constant Power Loads
DC	Direct Current
DER	Distributed Energy Resources
DFTC	Distributed Finite-Time Control
DG	Distributed Generation
DSM	Demand Side Management
EMS	Energy Management System
EPS	External Power System
ESS	Energy Storage Systems
EV	Electric Vehicle
F	Frequency
FC	Fuel Cell
FIE	Fuzzy Inference Engine
FIS	Fuzzy Inference System
FLC	Fuzzy Logic Control
GHI	Global Horizontal Irradiance
H∞	H-Infinity
HESS	Hybrid Energy Storage Systems
HIL	Hardware In Loop
HOMER	Hybrid Optimization of Multiple Energy Resources
ICT	Information And Communication Technology
IEA	International Energy Agency

IEGC	Indian Electricity Grid Code
INR	Indian Rupee
KJP	Kutir Jyoti Program
LC	Local Controllers
LFC	Load Frequency Control
LV	Low-Voltage
MCB	Miniature Circuit Breaker
MF	Membership Functions
MG	Microgrid
MGCC	Microgrid Central Controller
MGS	Microgrid Stabilizer
MGSI	Microgrid Stability Index
MNP	Minimum Needs Program
MNRE	Ministry Of New and Renewable Energy
MPC	Model Predictive Control
MPPT	Maximum Power Point Tracking
NCL	Non-Critical Load
NPC	Net Present Cost
NREL	National Renewable Energy Laboratory
O&M	Operation And Maintenance
P	Proportional
P&O	Perturb and Observe
PCC	Point of Common Coupling
PDC	Power Droop Controller
PI	Proportional-Integral
PID	Proportional-Integral-Derivative
PLC	Programmable Logic-Based Controllers
PLECS	Piecewise Linear Electrical Circuit Simulation
PLL	Phased Locked Loop
PMGY	Pradhan Mantri Gramodaya Yojna
PMSG	Permanent Magnet Synchronous Generator
PR	Proportional-Resonant
PV	Photovoltaic
RES	Renewable Energy Sources
REST	Rural Electricity Supply Technology Mission

RNCES	Renewable And Non-Conventional Energy Sources
RSCAD	Real-Time Structured Computer-Aided Design
RV	Relative Variation
SC	Secondary Control
SI	Solar Irradiance
SMPS	Switch Mode Power Supply
SOC	State of Charge
THD	Total Harmonic Distortion
UG	Utility Grid
VD	Voltage Deviation
WES	Wind Energy Source
WS	Wind Speed

CHAPTER 1
INTRODUCTION

This research addresses various aspects of stable microgrid operation, including multiple control approaches and assessment methodologies. Focusing on microgrid control, firstly, the research work presents a brief introduction and review of microgrid stability aspects and causes related to small-signal, transient, and voltage stability, comparing existing controllers, such as conventional controllers, intelligent controllers, and hybrid controllers, various control schemes, and exploring the scope of stability improvement. Secondly, the research presents different control approaches for stable microgrid control, including a novel stage-wise approach that employs a fuzzy logic controller to regulate frequency and voltage parameters under various perturbations. In addition, the work also presents a cascaded dual-fuzzy logic-based control approach for energy management, ensuring stable microgrid operation under variable renewable sources and load fluctuations. Thirdly, the work presents a comprehensive performance assessment of a residential microgrid planned for Kibber village, Himachal Pradesh (India). The comprehensive assessment includes technical assessment using MATLAB Simulink, economic assessment using HOMER Pro, and implementation assessment using a PLC-based hardware test bench prototype. Lastly, the work presents a decision-making methodology for the Microgrid Stability Index (MGSI), considering fundamental electrical parameters, such as microgrid voltage and frequency, while considering various case studies for validation.

Conclusively, this work presents state-of-the-art research on stable microgrid operation, providing valuable insights related to the fuzzy-based control approach, details related to comprehensive assessment, including design and development of a PLC-based hardware test bench, and lastly, an in-depth understanding of microgrid stability index [1-5].

1.1.Motivation of research

The motivation of this research work is to understand the complex issues involved in establishing and maintaining a stable microgrid operation, especially in view of various uncertainties. One of the key reasons for such issues is because of distributed energy resources (DERs) that present significant challenges for microgrid systems, where the DERs are low-voltage (LV) networks of interconnected energy sources, especially renewable energy sources scattered geographically in the microgrid boundary. The dynamic and unpredictable nature of these resources, especially wind and photovoltaic (PV), complicates this integration even further, i.e., the power output of these resources is majorly affected by climate conditions, such

that with a slight change in the climatic conditions, the severe effect is observed in the renewable energy sources power output. Besides, the variable nature of the load causes additional complexity in handling and maintaining stable microgrid operation. Thus, this leads to the need for robust and adaptive microgrid control that includes efficient power management and productive use of other resources, such as power storage units. One of the most renowned and effective power storage units is batteries, which are an ancillary support that plays a pivotal role in maintaining stable microgrid operation and a resilient power supply.

Besides this, the other challenges include smooth integration of DERs, the bi-directional flow of power (sources, including battery storage unit to load and sources to the battery (acting as a load)), effective battery control, unbalanced and variable conditions, and efficient load management. The inherent challenges associated with these factors affect the overall performance assessment and, thus, the reliability and efficiency of microgrid systems. Therefore, considering such factors and recognizing the importance of stable microgrid operation, this research is focused on comprehensively understanding and addressing the issues that arise by proposing and developing an adaptive control approach for wind, solar, and battery-based microgrid systems. An adaptive controller or adaptive control approach is an approach that reacts quickly to changes in load fluctuations, renewable energy output variations, and other dynamic elements that impact microgrid stability. The development and application of an adaptive control approach successfully navigates the uncertainties associated with many parameters, which is one of the focuses of this research, while aiming for stable microgrid operation.

In addition to the significance of an adaptive control approach in view of microgrid control and stable operation, the benefits of stable microgrid operation exceed mere reliability and extend to the seamless integration of renewable energy sources. Stable operation empowers the microgrid to harness renewable energy more effectively, support sustainable practices, and mitigate environmental impact. Thus, this research also emphasizes to provide insights and practical methodology for quantifying and measuring microgrid stability by delving into the microgrid stability index (MGSI). This comprehensive approach is geared towards assessing, monitoring, and enhancing stability in the face of dynamic and uncertain conditions, thereby fortifying the resilience of microgrid systems in an ever-evolving energy landscape. Besides being motivated to understand the challenges and issues related to microgrid planning and implementation, another branch of this work is oriented towards the comprehensive microgrid assessment in view of technical, economic, and implementation aspects. Notably, the work focuses on assessing the designed microgrid's technical performance via MATLAB Simulink,

economic planning and assessment via HOMER Pro software and implementation possibility, and evaluation and control via PLC hardware test bench controller.

Thus, in conclusion, this Ph.D. research work is propelled by the overarching goal of advancing stable operation within microgrids, precisely considering the uncertain nature of renewable energy sources, uncertain and fluctuating electrical load, and the vitalness of the adaptive controller. The study aspires to contribute thoughtful insights and practical solutions to address the multifaceted challenges associated with microgrid stability, ultimately enhancing the reliability and resilience of microgrid systems in the dynamic and rapidly evolving energy scenario.

The introduction to microgrids, including microgrid components and types of microgrids, is discussed in sub-section 1.2. Further, the microgrid control and stability, including various factors influencing stable microgrid operation, control schemes, etc., are elaborated in sub-section 1.3, followed by the organization of the thesis.

1.2.Introduction to Microgrids

This sub-section aims to provide a comprehensive understanding of microgrids, contributing to their role in shaping the future of sustainable and resilient energy infrastructures. Particularly, microgrids represent a paradigm shift in modern energy systems, embodying a sophisticated and distributed approach to electricity generation, storage, and consumption [6-8]. These systems are localized, autonomous energy networks integrating diverse distributed energy resources (DERs), including renewable energy sources like solar and wind, along with conventional sources like diesel generators and storage units like batteries [9]. These modern-day energy systems (referring to microgrids) operate in multiple modes, such as grid-connected and islanded modes. Significantly, the ability of the microgrid to operate in an islanded mode of operation (referred to as operating independently with respect to the utility grid) is vital and allows the microgrid to operate during grid disturbances and emergencies [10-11].

At the heart of microgrid functionality lies the nuanced operation of advanced control systems that dynamically optimize electricity generation, storage, and distribution [12]. Employing such smart algorithms ensures a highly efficient and adaptive energy ecosystem, reducing losses associated with transmission and distribution [1, 3, 5, 11, 13]. Further, the ability of microgrids to seamlessly transition into the islanded mode of operation during grid failures, faults, etc., enhances their resilience, thus making them a reliable source of continuous power supply to critical loads, especially in the presence of the battery storage system [14-15].

Besides, the benefits of microgrid systems, especially working in an islanded mode of operation and in the presence of only renewable energy sources, go beyond technical

considerations, such as economic, environmental, and social [1, 5, 16]. Their integration of renewable energy sources aligns with global sustainability goals, contributing to reducing carbon emissions, fostering a cleaner energy landscape, rural electrification, and many more [1, 5, 17-18].

1.2.1. Microgrid components

The operational architecture of the microgrid is developed by integrating multiple components, affecting the system's capacity for efficient and independent operation. Distributed Energy Resources (DERs) are crucial and vital system components; these include wind turbines, solar arrays, and traditional generators such as diesel generators [19]. While wind turbines capture wind energy, photovoltaic arrays use sun energy to generate electricity, offering a diverse and sustainable energy generation solution that differs from the traditional fossil fuel-centric approaches.

Complementing DERs, energy storage systems (ESS) are vital in energy generation. ESS effectively retains excess energy produced during peak hours through the use of cutting-edge battery technologies. In times of increased demand or intermittent or uncertain renewable energy output, this stored energy acts as a reservoir to maintain system stability [20–22]. The adaptive control system of the microgrid, a multifaceted entity with sophisticated algorithms and real-time monitoring capabilities, is in charge of setting up the DERs and ESS [1, 12, 16]. The control system serves as the brains of the microgrid, regulating energy flow dynamically, adapting to changes in demand, and maximizing overall system performance.

The controller is a key component in the microgrid architecture as it manages the communication between DERs, energy storage, and other grid accessories, such as different types of loads. In addition to energy management, the controller ensures smooth transitions by assisting with islanding and reconnecting procedures during grid disruptions [1]. The operational integrity of the microgrid is strengthened by its connection with communication networks. Thus, to conclude, this subsection provides brief insights into the design of microgrids by introducing PV systems, wind turbines, energy storage, and adaptive controllers as vital microgrid components [1]. Supporting the above description, Figure 1.1 presents a typical microgrid framework including significant DERs, such as solar photovoltaic, wind, battery storage, conventional diesel generators, utility grid, and different loads integrated with a central controller. Besides, local controllers (LC) are also shown in the figure, individually representing decentralized control and combined with the central controller representing distributed control.

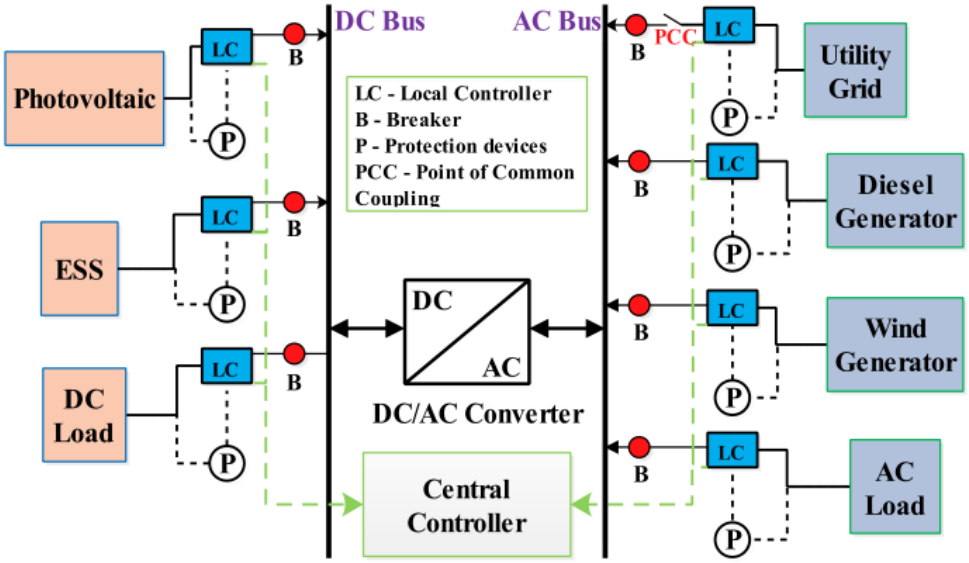

Figure 1.1. Typical Microgrid framework [1]

1.2.2. Type of Microgrids

Microgrids are dynamic, ever-evolving energy networks that take on a variety of topologies according to their electrical properties. The main differentiation is based on whether the microgrid runs on a direct current (DC) or alternating current (AC) source or on the combination of the two in an AC-DC hybrid microgrid configuration [7, 11, 17, 19]. Because the microgrids are based on the utilization of alternating current, AC microgrids are quite similar to the conventional electrical infrastructure seen in centralized power grids. This type of microgrid arrangement works well in industrial and urban settings where interoperability with various appliances and gadgets is crucial. In order to increase resilience and efficiency, AC microgrids frequently incorporate storage, adaptive control systems, and renewable energy sources. AC microgrids are a traditional yet flexible option in various situations due to their adaptability to varied electrical needs. On the other hand, DC microgrids benefit from employing direct current as their main power source. This setup is becoming increasingly popular. Various benefits of DC microgrids include lower conversion losses and better integration with equipment that runs on direct current by nature, easy battery integration, modularity, and better scalability. These microgrids are typified by their simplicity and appropriateness for specific applications [11, 13, 16, 22].

However, the most reliable and advantageous type of microgrid is AC-DC hybrid microgrids, which are cutting-edge microgrid inventions that integrate the advantages of both AC and DC systems into a single network. This hybridization is especially useful when AC and DC loads or various power sources with different power generation capability (AC or DC) are present. With AC-DC hybrid microgrids, energy management is maximized, total system

performance is improved, and adaptability to the changing needs of contemporary energy consumption patterns is raised [11, 16].

1.3.Microgrid control and stability

Considering the problems and challenges associated with microgrid (MG) stability or stable microgrid operation, the primary classification includes voltage stability, transient stability, and small-signal stability. Unexpected and uncertain fluctuations in load, under-voltage load shedding, loss of distributed energy resources (DER), MG failures and faults, and uncontrolled islanding are some of the elements that cause these problems. In particular, small-signal stability describes the power system's capacity to sustain synchronism in the face of frequent, minute, and transient disruptions brought on by supply and load generation uncertainties. Small-signal stability problems are caused by DER power limit restrictions, slow feedback controllers, and erratic changes in noncritical loads. Further, on the other hand, transient stability refers to the power system's capacity to sustain synchronism in the face of significant transient disturbances. MG islanding, power generator (DER) failure resulting in unbalanced power, different electrical problems, and adding or removing heavy loads in the MG are common sources of transient instability. Lastly, voltage stability refers to the MG's capacity to sustain steady-state voltage levels under a controller's supervision in typical and uncertain operation scenarios. Voltage stability conditions include unbalanced real/reactive power, various load types (particularly inductive loads), and substantial load shedding during under-voltage conditions [1, 23–24]. Regarding the above description, Figure 1.2 illustrates a comprehensive layout of various MG stability issues and common reasons for their occurrence within the system.

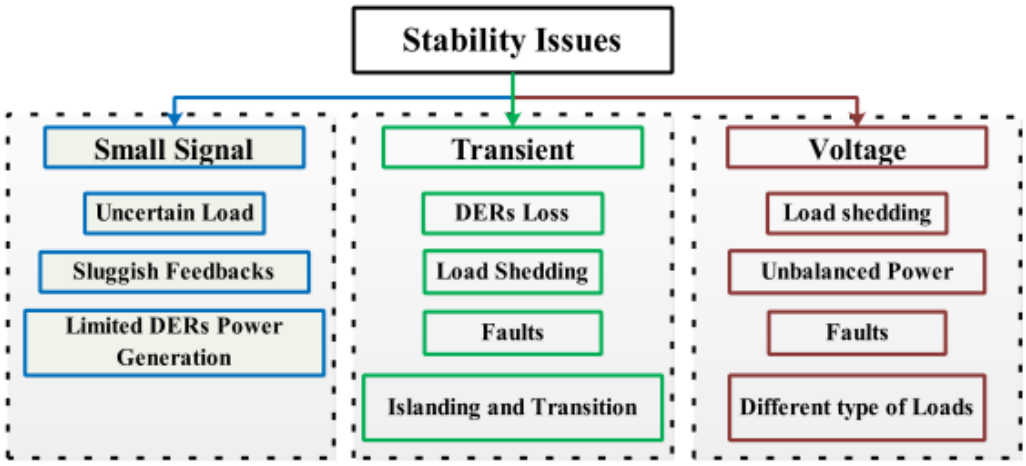

Figure 1.2. Microgrid Stability Issues [1]

Emphasizing these problems, the uncertain and unpredictable nature of all DERs, especially renewable energy sources, is an important issue, making microgrid control

necessary. For such purpose, i.e., stable microgrid operation in the presence of an effective and adaptive controller, the stability and dependability are maintained by the microgrid's ability to adjust to variations in generation, demand, and system circumstances. An essential component of microgrid control is energy management, which is well defined as the optimization of energy supplies (generation) to fulfill the electrical load demand. Diverse control strategies are utilized to tackle the complicated dynamics present in microgrids. Specifically, these include centralized, decentralized, and distributed control strategies, where decentralized control allows individual components to make decisions based on local data, making the microgrid operations more flexible and scalable. On the other hand, the centralized control strategy entails coordinating many components' actions by a single controller, mostly an intelligent and adaptive controller, to accomplish system-wide goals. Combining centralized and decentralized control components, hybrid control techniques provide a well-rounded solution that takes the benefit of both centralized and decentralized control strategies [25–30].

Conclusively, microgrid technology is essential to the advancement of renewable energy sources in power systems. They exhibit versatility in a variety of contexts, spanning from islanded to grid-connected models. A thorough grasp of the relationships between distributed energy resources, energy storage systems, AC/DC electrical loads, and different stability concerns is necessary for successfully modeling these systems. Further, controlling such systems becomes critical to maintaining stability, particularly as renewable energy sources are increasingly integrated. Sophisticated control strategies, such as a centralized approach, are necessary to function and integrate various energy resources in microgrids smoothly. The constant improvement of these methods is a reflection of the ongoing endeavor to improve microgrid operations' resilience, efficiency, and dependability.

Therefore, this study investigates the stable microgrid operation, considering various challenges and concerns. Particularly, to ensure stability during disturbances, this work presents a stage-wise and cascaded control mechanism based on fuzzy logic-based adaptive control. Additionally, this work thoroughly evaluates the future planning and deployment of microgrids to electrify rural areas. Lastly, a decision-making process for the Microgrid Stability Index (MGSI) is also demonstrated in order to assess a developed microgrid's stability level under various circumstances.

1.4.Organization of thesis

To describe the entire research work for achieving the objectives as mentioned in Sub-section 2.3, the thesis has been organized into seven chapters, and a brief outline is appended below.

CHAPTER 1: This chapter introduces the motivation of research, microgrid components and types, and stable microgrid operation.

CHAPTER 2: This chapter presents a comprehensive literature survey in the area of microgrid operation and control. The operation and control of microgrid systems, especially the stable operation, have been analyzed as a major issue considering microgrid design and role of the controller in the presence of variable renewable energy resources and other uncertainties. Further, the prominent research gaps and outcomes have been identified, followed by the objectives of research work for optimum microgrid performance.

CHAPTER 3: The design and modeling of microgrid systems comprising solar PV, wind energy systems, and battery storage have been comprehensively presented in this chapter in the perspective of their stable operation. Additionally, the design and development of a fuzzy logic-based controller have been presented in this chapter, including the selection of fuzzy membership functions and the design of the rule base.

CHAPTER 4: In this chapter, the proposed centralized stage-wise and cascaded dual fuzzy logic methodology for stable microgrid operation has been applied under the influence of small and large perturbations. These novel methodologies have been compared with significant state-of-the-art literature for their validation and feasibility in the area of microgrid topologies.

CHAPTER 5: This chapter presents the research methods for implementation assessment of a control approach aiming at stable microgrid operation using a PLC-based hardware test-bench prototype. The chapter presents the performance of the developed hardware test bench under multiple real-time scenarios.

CHAPTER 6: This chapter presents the research methods for comprehensive assessment and validation of developed microgrid systems. Particularly, it includes the details related to technical validation using MATLAB Simulink software and economic feasibility using HOMER Pro software.

CHAPTER 7: This chapter presents the proposed research method for determining microgrid stability index (MGSI) using the developed fuzzy inference system (FIS). The chapter highlights the conceptualization and significance of MGSI and the role of MGSI in stable microgrid operation.

CHAPTER 8: This chapter presents a brief summary, contribution, and conclusions of the thesis and the strategic initiatives for future propositions of the current research.

CHAPTER 2
LITERATURE SURVEY

With recent advancements at the worldwide level in various fields, the world's electrical system has started to face the trend of 3d's. These 3d factors (decarbonization, decentralization, and democratization) driven by various factors like reduction in CO_2 emissions, replacement of conventional power systems, cost of energy, rural electrification, environmental concerns, reliable and uninterrupted supply of electricity, etc., have given rise to the concept of microgrid technology [31]. These power system structures can balance the present issues in the electricity market while employing the various DERs, energy storage systems (ESS), and types of loads like electric vehicles. However, with all the benefits, MG also possess various technical and operational challenges with its integration with the existing system. Some are geographical location, voltage and frequency mismatch, depreciated voltage and power profiles, power generation and consumption uncertainty, and weak ESS. Integrating low voltage MGs consisting of uncertain load, ESS, and various RESs to resolve the multiple issues that existed a dozen years ago [1, 32]. With various RESs like photovoltaic, wind turbine, biomass, microturbines using CHP systems, fuel cells, and batteries for storage facilities, the least complex and approachable MG was the combination of PV and battery storage units.

Furthermore, as per the recent studies, the MG can be classified as AC and DC as well as AC/DC MG based on the type of voltage available at the point of common coupling (PCC) while operating in the grid-connected mode, whereas based on the type of source/load in case of the islanded mode of operation. With such developments, the droop control method initially dealt with various performance-related issues. In the presence of power converters and other electronic devices, the droop control method could regulate the bus voltage while maintaining the cooperative operation of paralleled converters. The droop control method was implemented based on adding virtual resistance related to the current loop with the voltage regulator of the power converters, allowing current sharing, plug, and play capability along with active damping. Despite the above advantages, the droop control method has various drawbacks, such as its incapability to follow the load-dependent voltage deviations affecting MG control and the deterioration of the current sharing in the system due to several issues. In addition, this method is non-consistent in maintaining the coordinated control between the various MG components, thus failing in quick and controlled actions. Thus, overcoming the above issues and in addition to the number of benefits, the centralized, decentralized, or distributed control scheme can play a crucial role. With such control schemes, the decision to maintain MG's stable and healthy condition concerning the available power generation via various RESs becomes simplified. Thus, considering the MG with various elements, it becomes essential to maintain the

coordination between the components, leading to a stable MG operation [1-2, 4-5, 7, 13]. Intending to develop a stable MG, this section presents various control techniques/strategies for MG, considering the trending issues affecting its stability.

2.1. Review of the operation and control of Microgrid

2.1.1. Review of various control schemes employed in MG

With the integration of the various RESs and other energy sources like ESS, ensuring MG's stable and efficient operation is challenging. Thus, while performing such integration, direct control of DGs plays a vital role [33]. Considering the flexibility provided by such RESs in utilizing the benefits of an MG is a boon for the energy sector. Still, the unpredictable nature of these RESs makes it complex to stabilize the performance of the MG [34]. In the earlier research phase, emphasis was placed on centralized control to provide stable operation for MG [35]. In general, the central controller or the centralized approach for controlling the MG operation worked on balancing the MG load while focusing on voltage and frequency regulation and other significant factors like real/reactive power demand, etc. Besides, research on microgrid central controller (MGCC) discussed its various applications, including load shedding, smooth transition, RESs assessment, communication and sharing signals with the entire MG, etc. [36]. The other benefits offered by MGCC include cost benefits [37-40] and efficient and optimized energy balance between the load demand and the energy generated in the MG while maintaining its stability [41-43]. But, with an increase in the complexity of MG, the centralized controller fails to cope with the system. Considering the number of RESs in MG, the amount of data to be collected and analyzed tends to increase at a gradual rate, making it multifaceted for MGCC [44]. Thus, in the case of MG with an increased number of components, the MGCC is incapable of data collection, feasibility, economics, complex decision-making, etc.

Hence, to overcome such challenges, the other control scheme includes a decentralized and distributed control scheme. As per the literature, these control schemes for low-level MG have been employed and tested under various conditions while coping with the issues related to the stable operation of MG [45-47]. Also, these control schemes offer several other advantages like reduced power losses, flexibility in a future system extension, cost benefits, etc., and thus are highly recommended for such complex systems [48].

A. Centralized control scheme

It can be defined as the central processing element that can handle the system alone. The scheme allows the use of various communication links and control distribution systems while connecting all the other elements of the system. Such a connection includes the various sensors, control devices, and a central brain like the controller for decision-making purposes. In the bi-

directional flow of information, the sensors process the information of the data gathered to the central controller, which is further responsible for the data handling, analysis, calculations, etc. For decision-making aimed at the stable MG operation, the central controller communicates with the various sensors available in the system for the necessary actions [49-50]. As per the literature, the significance of centralized control for the stable MG operation under various contingencies, constraints, and conditions has been discussed in [51-56]. Moreover, the drawbacks of centralized control include reduced flexibility and expandability, limitation of data collection, low communication networks, and other issues related to the control of various parameters for stable operation in the island mode of operation [51-53].

B. Decentralized control scheme

This scheme can be explained as the system equipped with several local controllers responsible for the data collection, its analysis, and stable MG operation. Compared to the central controller, this scheme is employed in complex and high-order MGs where the centralized scheme would be unable to perform appropriately, resulting in the decaying performance of MG [48].

C. Distributed control scheme

The distributed control scheme for the smooth and stable operation of the MG can be explained as an approach where the local controllers communicate with each other and a central controller via communication and networking channels. The central controller is responsible for the system monitoring and control, whereas the local controllers are linked with the various individual MG components [46-47].

2.1.2. Review of various control techniques (controllers) employed in MG

A. Conventional techniques

This subsection discusses MG's various conventional control techniques while aiming at its stability. These include Proportional (P), Proportional-Integral (PI), Proportional-Integral-Derivative (PID), and Proportional-Resonant (PR) controllers. Table 2.1 presents the brief features along with their other related parameters. As per the table, the various aspects for assessing these controllers include peak overshoot, settling time, rise time, steady-state error, etc.

B. Intelligent techniques

- Deadbeat Controller: An effective and dynamic controller working for the current inverter control. The controller facilitates the system with high bandwidth with instantaneous current tracking at the required points. Being an intelligent controller, the derivatives of control parameters depict the system's future state and, hence, the control action. For

research purposes, a deadbeat controller benefits the system with error compensation in the inverter current but is also sensitive to the network parameters [57-59]. In Figure 2.1, the schematic layout of the deadbeat controller with reference signal r(z) processed through the controller to the designed system with y(z) as the primary output where e represents an error signal to the controller unit, Q and P represents the polynomials of the transfer function, u represents the manipulated signal. P represents the actual system/model.

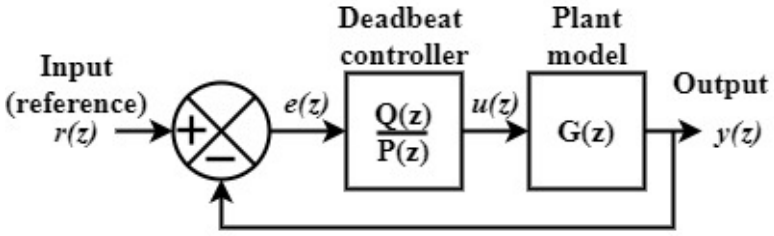

Figure 2.1. Deadbeat controller

- Model Predictive Control (MPC): It minimizes forecast errors while aiming to track the current parameter accurately. The advantages of MPC include its ability to maintain all the general and non-linear constraints of the network in the presence of multiple inputs/outputs. Based on the present values of various parameters, the model predicts the future values for the network, aiming at its stable operation. Also, the method is sensitive, especially concerning the existence of mathematical equations [60-62]. Figure 2.2 presents the block layout of MPC with various constraints and objectives as the critical input to the controller, based on which the control signal is processed to the actual system.

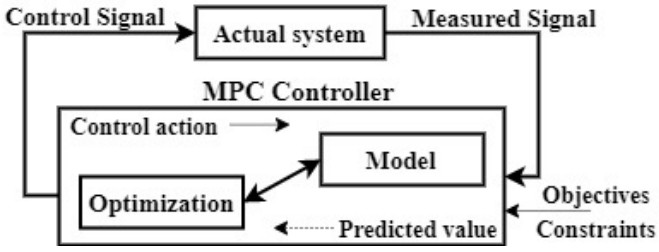

Figure 2.2. Model Predictive Controller

- Hysteresis Controller: A less complex technique for controlling the current error signal while comparing it with the reference signal. The advantages of a hysteresis controller include its fast and adaptive response to the inverter, easy implementation, etc. Also, the controller provides an inherent current protection scheme and reduces the system's THD [63-64]. Figure 2.3 presents the hysteresis controller where, based on the relay operation, the signal is processed to the designed system for its smooth operation.

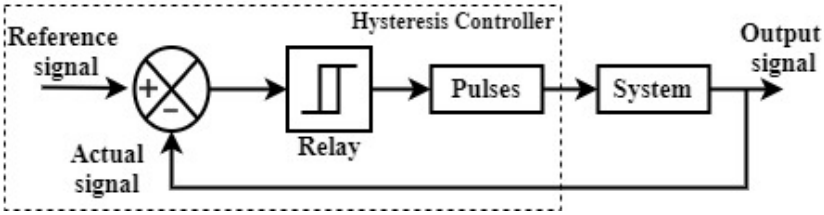

Figure 2.3. Hysteresis controller

- Repetitive Controller: An error minimization and elimination tool based on the internal model principle. This principle represents the error terms as pole pairs at multiple selected frequencies. The complete combination of an integral, proportional, and resonant controller, while connected in parallel, has been considered a repetitive controller in literature. The significant advantage of the repetitive controller in the stability of MG includes the low harmonic distortion in different parameters like voltage, current, etc., while in the presence of non-linear inductive loads [65-67]. Figure 2.4 shows the block structure of the controller with r as raw input, e as error, CR and u as processed inputs, and y as the main output of system G.

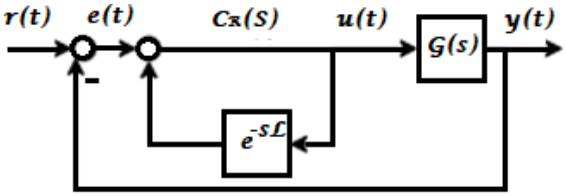

Figure 2.4. Repetitive Controller

- H-infinity (H∞) Controller: A robust controller able to alter the value of any parameter causing a disturbance in the system and stabilizing the system with quick responsive action. The objective of the controller is to eliminate the parameter causing disturbance in the system. Initially, the problem formulation in terms of optimization is defined followed by the controller action, where, the system specification(s) are formulated as constraints on the singular values of different loop transfer functions. The advantages of the controller include its robust nature in the presence of uncertain parameters, reduced error, and less complex implementation. Although, there are several advantages, the design, development, and understanding of the complex mathematical expressions with slow dynamics are the negatives of the controller [68].

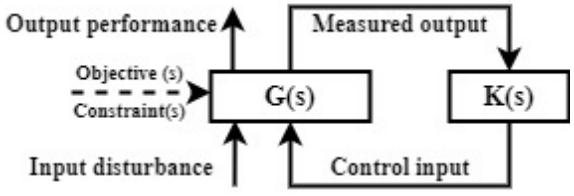

Figure 2.5. H∞ Controller

Figure 2.5 presents the basic structure of the H∞ Controller with G(s) as the plant or system and k(s) as the system compensator. The controller aims to determine k(s) to stabilize the designed system.

- Neural Network: The neural network-based controller passes the desired data to the central processor, working like the human psyche with some given time delay. Its basic architecture includes an input/output layer, activation function, and weights, and it is hidden later in a closed-loop manner for transmitting the information to one another while minimizing the error or desired function. Being an adaptive, intelligent, and self-learning controller, the neural network allows more flexibility and less complex design and implementation for different operating conditions. The other advantages of neural networks include their robust behavior and quick decision-making while working for the stability of MG [69-70]. Figure 2.6 presents the brief schematic layout of the neural network-based controller. The smooth operation is based on the system's reference signal, input/hidden/output layer, and regulator.

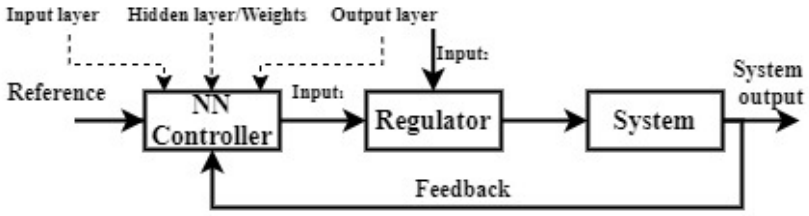

Figure 2.6. Neural Network Controller

- Fuzzy Controller: This logical controller relates and deals with various linguistic values while eliminating the logic of the crisp value in decision-making, as shown in Figure 2.7. The range of fuzzy varies from 0 to 1. In terms of MG stability, being a highly robust and user-friendly controller, fuzzy logic has been widely used in the control of MG. In addition to decision-making and robust performance, the fuzzy logic controller has been used to minimize overshoots and improve tracking performance [71-73].

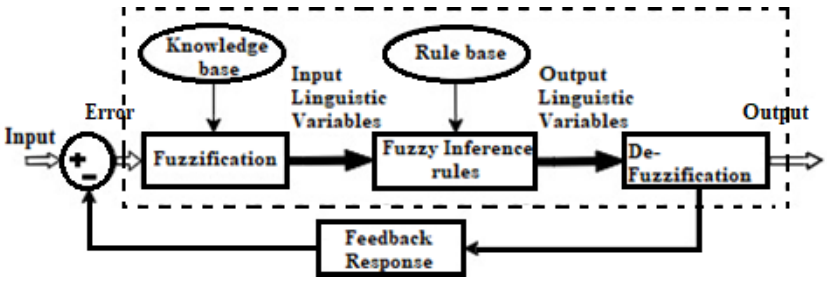

Figure 2.7. Fuzzy Logic Control

- Sliding Mode Control: It can be defined as the robust and adaptive controller working for the variation in the system parameters based on its operating conditions. The range of such

a variation varies widely to provide stability to the system in a short period. The main objective of the controller is to maintain the system's steady state, whereas, in case of uncertain change, the controller must respond with a quick control action. The controller cannot adapt to uncertain changes and the non-linear system's dynamic behavior; therefore, to avoid such an issue, the controller optimizes the parameters based on the output ripple waves. The primary advantages of the sliding mode controller include its straightforward implementation in the MG and the low-level sensitivity against the change in parameter values [74-75].

- Linear Quadratic Regulator: This method for MG stability can be defined as an effective and robust controller for stabilizing a system even under uncertain and transient conditions. The significant advantages of employing this method include inherent stable characteristics and independence of system order. The disadvantages include - delay in decision-making and lag in tracking accuracy during change in load type [76-77].
- Linear Quadratic Integrator: This method can be employed for a fast and dynamic response while minimizing the steady-state error of different parameters, especially voltage. Considering minimization, the actual values for error measured between the grid voltage and the reference voltage during the uncertain load change are fed to the controller, as shown in Figure 2.8. Further, the controller is responsible for minimizing the error produced in the system. Considering the advantages, the control approach is less complex as it is easy to calculate the optimal gain that provides acceptable tracking with minimized steady-state error [78-79].

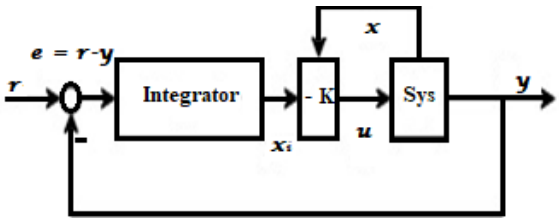

Figure 2.8. Linear Quadratic Integrator

Where x_i is the integrator output, x is the input fed to the gain block, r is the reference signal, e represents error, sys is the state-space model, and y is the output with k as gain.

C. *Hybrid Techniques*

- Fuzzy – PI/PID controller: With significant advantages of PI/PID controller in stability enhancement of an inverter-based MG, the vague, uncertain, and sudden system disturbances affecting their performance is a significant challenge. Thus, the fuzzy inference system can handle conditions that can be utilized for tuning PID while adapting the disturbances in the system. The significant advantage of such integration is the robust

and quick decision-making by fuzzy logic and enhanced PID controller tuning. The input to the system usually includes various components of system error [80-81]. Figure 2.9 presents the Fuzzy/PID-based hybrid controller employed for smooth operation. In Figure, x and E represent the input in primary and derivative form processed to the fuzzy controller, which further transports the crisp value to the PID controller. Based on the values of gains, the control signal/output (u) is forwarded to the system.

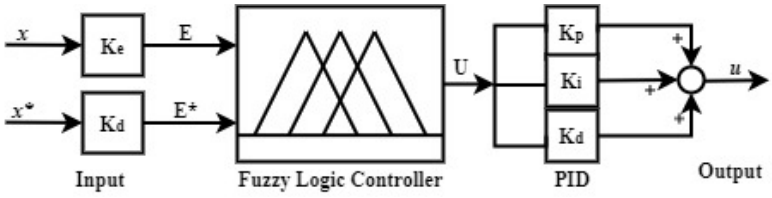

Figure 2.9. Fuzzy/PID controller

- Adaptive Neuro-Fuzzy Inference System (ANFIS) controller: The combination of neural networks and fuzzy techniques that utilize their benefits is called the ANFIS-based control technique. The technique is based on neural networks' learning and feedback capability and an adaptive, robust fuzzy inference system for better representation of the system information/knowledge. Working for error minimization in the system for stability enhancement, the gradient descent method is used to update the weights based on the feedback from the output layer to the input layer. This way of weight tuning is generally termed backpropagation, while the stages included in the process are precondition tuning (first layer) and consequent tuning (fourth layer). Figure 2.10 illustrates the corresponding layer architecture of the ANFIS controller [82-83].

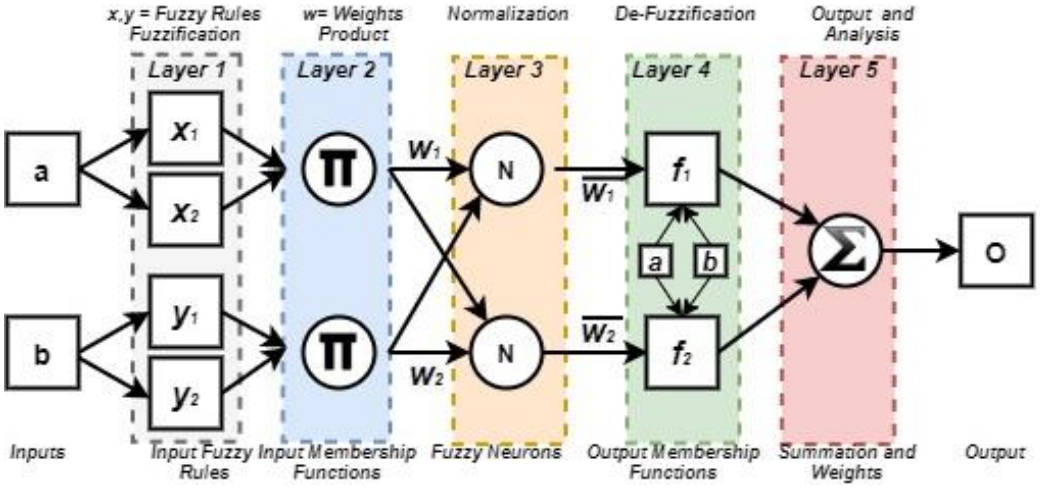

Figure 2.10. Architecture of Adaptive Neuro-Fuzzy Inference System (ANFIS)

The advantages and disadvantages of all the controllers aiming for MG stability have been summarized in Table 2.2.

Table 2.1 Various features of conventional control techniques

Controller	Equation	Remarks/Features
P [84]	$\frac{U(s)}{E(s)} = K_p$ Where, K_p= Proportional gain	• Reduces rise time and steady-state error • Increase in overshoot • Slight effect on settling time
PI [84-85]	$\frac{U(s)}{E(s)} = K_p + \frac{K_i}{s}$ Where, K_p= Proportional gain K_i = Integral gain	• Reduced rise time and significant decrease in steady-state error • Slight increase in overshoot and decrease in settling time • Improved performance with feed-forward voltage along with the cross-coupling term. • Effective for dq reference frame with current as the reference, considering high-level power flow control in the system.
PID [86]	$\frac{U(s)}{E(s)} = K_p + \frac{K_i}{s} + K_d s$ Where, K_p = Proportional gain K_i = Integral gain K_d = Derivative gain	• Combination of all gain values (Kp, Ki, and Kd). • Low-level decrease in settling time, overshoot, and rise time. • Significant effect on steady-state error. • Improved response to uncertain and sudden changes. • Enhanced performance with low value of kd
PR [65, 87-89]	$\frac{U(s)}{E(s)} = K_p + K_i \frac{s}{s^2 + \omega^2}$ Where, ω = Resonant frequency K_p = Proportionality gain K_i = Integral gain	• Effective in both abc and αβ reference frames. • With high gain value - closer to the value of ω, the steady-state error is decreased significantly. • ω regulates the controller performance in various conditions. • Lag in time delay, accurate tuning, and high sensitivity against frequency variations are its demerits.

Table 2.2 Summary of various controllers

Controller	Advantages	Disadvantages
P [84]	• Easy implementation • Low rise time	• High overshoots during the transient stage • Low stability
PI [84-85]	• Low rise time • Minimized steady-state error in *dq* reference frame	• Unfitting steady-state response during transients • High steady-state error for uncertain system
PID [86]	• Low overshoot • Minimized steady-state error	• Inappropriate for transient and time-delayed system with low flexibility
PR [65, 87-89]	• Minimized rise time • Low steady-state error	• Time delay lag • Inaccurate gain tuning • Sensitive to uncertain conditions
Deadbeat [57-59]	• Appropriate for harmonics control • Fast and dynamic transient response with low harmonic distortion	• Require accurate filter and inverter model • Complex network parameters
Model Predictive [60-62]	• Appropriate for non-linear system • Require less switching frequency • Precise current control with minimized THD level	• Accurate filter and inverter model • Complex calculations • Sensitive to change in parameter values
Hysteresis [63-64]	• Easy implementation • Fast and dynamic transient response • Inherent current protection	• Resonance related issues • Imprecise current tracking and harmonic issues
H-infinity [68]	• Minimized THD. • Robust performance for linear, non-linear and unbalanced loads • Reduced tracking error	• Require complex mathematical equations and understanding • Slow response and dynamics

Repetitive [65-67]	• Robust performance during uncertain and transient condition • Reduced steady-state error at a various range of harmonic frequencies	• Issue related to system stabilization • Slow response during load fluctuations
ANN [69-70]	• Impactful performance in current control • Self-learning controller	• Slow and complex response • Require huge data
Fuzzy logic [71-73]	• No effect via parameter variations • Suitable for a small as well as a large-scale non-linear system	• Slow control method • Complex rule development
SMC [74-75]	• Consistent performance during fluctuations and transients • THD minimization	• Chattering Phenomenon in discrete implementation • Complex design procedure
LQR [76-77]	• Inherent stable characteristics • Effective and robust	• Delay in decision • Lag in tracking accuracy
LQI [78-79]	• Fast and dynamic response • Simple structure and design steps • Accurate tracking performance	• Phase shift issue in voltage tracking • Complexity in extracting model properties and characteristics
Fuzzy – PI/PID [80-81]	• Improved performance in vague and non-linear systems • Self-tuning gain capability	• Complex structure and implementation
ANFIS [82-83]	• Adaptive and robust • Ability to work with linear/non-linear systems • Learning ability	• Complex data collection and analysis

2.1.3. Review of various control parameters affecting stability

A. Voltage control

- Based on centralized control

The impact of preplanned MG islanding on the system performance can be balanced using the central MG controller [84]. The controller deals with the power electronic interfaced DERs to minimize the system transients while maintaining the voltage and angle stability of the DERs. Considering the issue of high load penetration, voltage fluctuations, and load sharing, a centralized droop-based compensator for maintaining the MG stability has been used [85]. The controller manages the system voltage while maintaining stability via load shedding/sharing between various DGs. Focusing on power sharing and voltage transients causing MG instability, a centralized controller with DC-link voltage control proves advantageous as it adjusts the input reference voltage of the inverter as a function of DC-link voltage. It minimizes the system transients and enhances the overall stability. Aiming to compensate for the unbalanced/fluctuating frequency in MG due to uncertain load and power generation mismatch, the controller for MG stability enhancement shows its significant importance [86]. Investigating the aspects of MG stability, [88] discusses various MG stability issues and improvement techniques for remote, facility, and grid-connected MG. Considering the issue of smooth transitioning and MG stability in islanded mode, the data analytics-based ANFIS controller is critical [89]. The ANN is trained with PMPP-Temp, against VMPP characteristics based on the P&O approach, where the work presents the significance of data analytics in the MG system for maintaining stability. Targeting the instability due to unbalanced voltage, uncertain load, and generation in MG, supercapacitors, and BESS are used for stabilizing the DC bus voltages. Fuzzy logic with frequency, DC voltage, and battery charge state as its input is presented as the central controller [90]. For the issue of controlling the DC link voltage level for stable MG occurring due to unstable load and other conditions, an interleaved converter operating as a power interface for regulating the power flow is discussed [91]. The work employs the control strategy to provide high-quality voltage to the MG via the proposed controller. The damping controller that can adapt and perform during sudden disturbances has been used for the developed microgrid MG [92]. The controller mitigates the voltage fluctuations due to uncertainty, balancing the other MG parameters to maintain system stability. A centralized DC-link voltage controller is investigated to address the issue of voltage variation due to uncertain conditions in supercapacitor-based DC-MG [93]. The controller calculates and provides the operating voltage and gain/phase margin to maintain stable operation. A centralized Fuzzy-PI controller is investigated to address the issue of voltage instability due to variable load conditions in DC-MG [94]. The work focuses on calculating the controller parameters, such as

maintaining the DC-link voltage constant under uncertain load conditions. Influenced by the issue of impedance mismatch in MG and, therefore, power-sharing, voltage fluctuations, etc., a phase supplementary loop in comparison to the frequency loop for stabilizing DC link voltage has been investigated [95]. Based on the assessment, calculating droop gain values via the participation factor method under such instability-causing conditions is considered crucial as it affects the system's performance. Resolving the issues related to voltage fluctuations and harmonics present due to variable load and generation in hybrid MG, intelligent centralized controllers like enhanced ANFIS-PID, SVPWM, and fuzzy logic are discussed [96]. The role of ESS in stabilizing the system performance is highlighted in the work while focusing on the design perspective of the controllers. Considering the issue of voltage imbalance present due to various conditions, a centralized controller is investigated based on analyzing and balancing the terminal voltage level [97]. Considering the islanded operation, the importance of eliminating the current sensors from the system to diminish the cost and complexity of the system is also discussed.

- Based on decentralized control

The decentralized control approach proves advantageous for the problem of voltage imbalance, deviation from the setpoint, and its compensation in autonomous MG [98]. The local droop controllers connected to the controller at PCC via a communication link are responsible for maintaining the voltage imbalance and its compensation. The scheme provides ease of expanding the network, such as incorporating more resources and load. Similarly, a novel decentralized control system is employed for managing energy in islanded DC microgrids, enhancing load-sharing accuracy and voltage regulation. With the BESS unit SoC level and superimposed AC voltage as defining parameters, the system achieves improved performance, which is validated through piecewise linear electrical circuit simulation (PLECS) simulation and experimental studies [99]. The controller gains are automatically adjusted based on the reference and actual terminal voltage. The scheme provides better control for complex structures compared to a centralized manner. Committed to the issue of load sharing and voltage regulation in complex MG, multiple local controllers based on a decentralized scheme are investigated in [100]. Based on the operation and processing of terminal voltage as feedback to the controllers for every component, precise load sharing can be achieved along with voltage balance, affecting the stability. With a change in load demand/generation, the controller gains value changes correspondingly, thus improving performance.

- Based on distributed and hierarchical control

The hierarchical scheme's primary and secondary level control features for minimizing voltage deviations and fluctuations caused in MG due to uncertain conditions and faults, local

PR, and PI controllers have been employed [101]. The various case studies are investigated based on uncertain load, etc., such that the MG stability is not compromised under the impact of uncertainty. The primary level controller balances the voltage to a nominal level, whereas the secondary controller eliminates the voltage deviations. For the issue of a smooth power-sharing mechanism and balanced system voltage, [102] deals with AC/DC dynamic voltage control via a cascaded control scheme. The work discusses an adaptive power-sharing mechanism and implementation of an AC dynamic voltage compensator based on distributed BESS. The distributed secondary control algorithm without droop control for voltage stability and load sharing facility for the problem of communication delays leading towards system instability is investigated in [103]. For the selection of control parameters, delay-dependent stability criteria under constant delay and time-varying delay-dependent criteria using linear matrix inequality have been used. The work shows the distributed control technique's significance in communication and networking issues. Based on the distributed control scheme, the problem related to voltage fluctuations and deviations in convoluted MG architecture in the application of sliding mode controller is discussed in [104]. The work highlights eliminating communication delays in the system and focuses on the robustness of the controller. Similarly, [105] proposed a hierarchical control algorithm for managing an islanded DC microgrid comprising batteries, supercapacitors, and PV arrays. It features a supervisory layer utilizing fuzzy logic control to oversee device states and a local control layer for each device using PI control. The algorithm aims to stabilize the DC-bus voltage amidst load and PV variability while optimizing power flow to prevent the battery from over-discharging, leveraging the rapid response of supercapacitors.

B. Frequency control

- Based on Centralized control

For stability enhancement of islanded MG, the energy management system with frequency droop control characteristics in the presence of a central controller can be employed [106]. The proposed approach can balance the output power of the generators and load changes to maintain MG stability. Virtual resistance and capacitance-based droop controllers have been employed in work, while system validation has been performed via detailed frequency domain analysis and Middlebrook stability criterion. Considering different RESs, modes of MG operation, transients, and types of loads, the controller resolves the issue of frequency regulation in the system [107]. A centralized load frequency controller for the problem related to the frequency balance/regulation of an islanded MG has been investigated [108]. The proposed model predictive controller (MPC) has been compared with the conventional PI controller and validated via steady-state power balance equations. The work shows significant advantages of

using the feedback and learning-based controller in maintaining the system frequency and, thus, the MG stability. Working on minimizing frequency fluctuations and stabilizing the EV/ESS integrated MG, the centralized MPC has been investigated and proposed [109]. The study shows the significance of ESS while working in centralized control for stabilizing the MG in various fluctuating conditions. The controller's performance shows its ability to balance the system under load and generation variation.

- Based on decentralized control

Specifying the benefits of decentralized control, [110] discusses the challenges of applying centralized, hierarchical control strategies to islanded microgrids and, thus, the benefits of decentralized and distributed control approaches in enhancing performance, ensuring stability during faults and facilitating deeper DER penetration. Common decentralized and distributed control approaches are reviewed, and current design trends and technical challenges are discussed to comprehensively understand controlled microgrids. Similarly, [111] discusses a decentralized secondary control (SC) for AC MGs, emphasizing frequency as a critical parameter. Active power estimation (APE) based on frequency regulates the MGs frequency, ensuring accurate power sharing. Besides, [112] discusses a decentralized consensus-based secondary control strategy for multiple DC microgrid clusters with hybrid energy storage systems (HESS), aiming for proportionate current sharing, voltage synchrony, and frequency-based power sharing.

- Based on distributed and hierarchical control

Highlighting the significance of hierarchical control in maintaining the system stability, [113] investigated the power flow modeling of droop-controlled DERs with secondary frequency and voltage restoration control for an islanded MG. The authors incorporated the Newton-Raphson method and validated its performance via various software tools. Thus, primary droop control and secondary control to minimize voltage and frequency deviation are highly important for smooth MG operation and control. Resolving the issues of frequency restoration present in the complex autonomous MGs, [114] investigated the distributed control scheme for such a system. The work discussed the significance of the communication network and its application in MG control. The system's stability has been maintained based on the frequency and voltage controllers employed in a distributed manner. Thus, with a minimized communication network, the central unit communicates with the various local controllers to maintain and restore the system frequency under different circumstances. Utilizing the advantages of distributed control for a complex MG structure, [115] proposed a hierarchical control scheme to enhance microgrid performance, focusing on the stability of voltage/frequency and active/reactive power parameters. It utilizes a multi-layered approach,

including a power droop controller (PDC) and secondary distributed V/F control strategies like distributed finite-time control (DFTC), ensuring efficient system modification and restoration.

C. Active/reactive power control

- Based on Centralized control

Highlighting the significance of maintaining system voltage and issues related to its regulation, the application of a central controller has been investigated in [116]. Specifically, it presents an Energy Management System (EMS) for an AC/DC microgrid with renewable energy sources (RES) and a battery, ensuring energy stability. Operating modes selected by users and RES power generation status dictate microgrid regulation, prioritizing continuous energy supply to critical loads and optimizing RES efficiency. The EMS maintains a generation-consumption balance, utilizing the battery when necessary. Likewise, [117] proposed an advanced energy management strategy for hybrid AC/DC microgrids to improve fuel efficiency and mitigate renewable intermittency challenges. Combining conventional gas turbine generators with solar photovoltaic (PV) systems ensures high fuel efficiency, virtual inertia provision, fast DC-link voltage regulation, and seamless transition between grid-forming and grid-following modes. In coordination with the P-F droop, the fuzzy droop control can achieve optimized power sharing and prevent the system from overloading conditions [118]. The control approach varies the droop coefficients based on the scheduling demands of MG, whereas it serves various advantages like enhanced stability and improved economic operation. Considering the mismatch issue of constant power loads (CPLs) and uncertain power generation in DC-MG, the high-capacity ESS can be employed under the supervision of a robust fuzzy-based central controller or with the load-side compensation technique [119]. Thus, as evident from experimental results, the ESS balances the load and generation uncertainty, whereas the closed-loop approach for MG control is healthier than others. The dynamic phasor concept can be used to understand the impact of unbalanced conditions on the inverter output and system stability [120]. In work, under various conditions like faults, uncertain load, etc., the different parameters like DC link voltage, inverter output, controller parameters, etc., get affected. Thus, the complete system analysis has been investigated. Considering efficient MG operation, [121] proposed an energy management strategy for grid-connected microgrids with a hybrid energy storage system (HESS), emphasizing power and energy control. It addressed challenges in managing distributed renewable energy resources, particularly in AC-coupled microgrids, by facilitating efficient energy usage under different operational modes. The strategy ensures quick voltage build-up at the DC bus, optimal energy and power sharing between the battery and supercapacitor, and enhanced compatibility with the grid, leading to improved battery life, enhanced power quality, and seamless transition between operational

modes. The phased locked loop (PLL) can be used when dealing with the MG with ESS under contingency conditions [122]. The technique, along with the adaptive power management algorithm, can be employed for voltage and frequency regulation and, therefore, the better power balance such that MG stability under different operating modes can be enhanced. [123] discusses efficient energy and power control mechanisms for stand-alone microgrids, featuring a photovoltaic system, wind turbine, and battery energy storage device. The developed controller ensures power stability, mainly regulating the bidirectional DC/DC converter linking the Li-ion battery to the DC bus. The study emphasizes the development of a wind/photovoltaic power generation system and employs Maximum Power Point Tracking (MPPT) techniques like perturb and observe (P&O). Simulation results demonstrate the effectiveness of the proposed method, utilizing only power and voltage system data for bidirectional control. [124-125] presented energy management methods for standalone DC microgrids, emphasizing power control and stability of the DC bus voltage. It employs a centralized energy management strategy (EMS) utilizing fuzzy logic and sliding mode control for maximum power extraction from renewable sources and effective control of storage converters. The strategy ensures production/consumption balance, limits battery stress, and enhances longevity while reducing hydrogen intake. The results validate the effectiveness of the proposed approach in ensuring reliability, improving BESS longevity, and minimizing battery deep discharge under various operating conditions, both in simulation and hardware prototype environments. The reactive power balance plays a significant role in dealing with the voltage stability issue present in MG. This issue can be resolved using the centralized controller to balance the power injection/consumption under various circumstances [126].

- Based on decentralized control

To balance the reactive power demand of complex MG, the modified droop controller can be employed in a decentralized manner [127]. The decentralized manner of controlling such a system is advantageous as it improves performance, reduces response time, and enhances stability. The system validation for steady-state and transient response has been done using a digital time-domain simulation study using PSCAD/EMTDC software. The wireless communication-based decentralized control scheme is highly significant for optimal power sharing/injection aiming at stable MG operation. The conventional droop or advanced sliding mode controller combined with this scheme has been validated for uncertain load and variable power generation conditions [128]. Also, the proposed scheme can be well utilized to minimize the reactive power-sharing error present in the system. This leads to accurate power sharing and improved voltage control of the MG system [129].

- Based on distributed and hierarchical control

The hierarchal control, as per ISA-95 and electrical dispatching standards, discusses the role of the power flow balance in maintaining flexibility and system stability [130]. Considering an MG with an issue related to frequency deviation and power exchange, the scheme can be well employed. Also, to minimize power-sharing errors in parallel operating DGs in complex MG architecture, the scheme provides various benefits compared to centralized or decentralized schemes. The system validation for such an MG structure can be done using a small-signal state-space model, stability assessment techniques, and experimental setups [131]. A distributed networked-based power-sharing scheme can be well utilized to improve the MG dynamic performance, minimize power-sharing errors, and ensure system stability [132]. The scheme ensures the stable operation of MG under various unnecessary conditions like load and generation mismatch, etc. Considering the problem related to smooth power sharing and power management for MGs, applying a distributed scheme in supervisory control can be employed. The various controllers that can be used for such purposes include fuzzy logic, state machine approach, conventional local controllers, etc. [133]. Similarly, intelligent MPC can also be deployed for optimal power sharing and maintaining the system scheduling [134]. The local controllers maintain the converter output in such systems, whereas the secondary controller deals with the energy management system. Working on the MG stability enhancement, a flexible distributed control strategy can be used using a non-linear microgrid stabilizer (MGS) for different operation modes [135]. The technique can be utilized to balance the system fluctuations while improving the power exchange between various DGs connected through different converters. The distributed technique also proves advantageous in balancing the uncertain load, leading to complex resonance phenomena and, therefore, MG instability [136]. The control scheme is highly robust and responds better to such uncertainties. Hence, the distributed control scheme significantly demonstrates its effectiveness for enhanced power sharing, voltage and frequency regulation, power management, etc.

Comprehensively considering the present state of research and uncertain conditions, intelligent and adaptive control techniques, especially fuzzy logic-based algorithms, need much attention due to their nature of solving complex, vague, and uncertain data-related problems. This user-friendly approach can provide a crisp and quick decision based on comprehensive data analysis of renewable sources, system parameters, etc., leading to an accurate solution to the present power system-related problem. Besides, it can be applied to any system configuration by changing the type and range of input parameters and a slight change in its rule base if required. Thus, focusing on the same, this section has reported some literature on fuzzy logic control (FLC) for MG's stable operation and EMS. From the analysis, the implementation

of fuzzy logic controllers (FLCs) is effective for energy management systems (EMS) in microgrids (MGs). These controllers aim to ensure stable and smooth transitions between different MG operation modes based on power, voltage, and battery state of charge. Robust FLCs have been developed and validated for improved EMS performance, considering factors like variable Photovoltaic (PV) output and battery storage. Various input parameters, including the rate of energy change, battery SOC, net power, and total system power, have enhanced controller robustness and stability.

Additionally, studies have explored the application of adaptive FLCs considering DC link voltage, system frequency, and other critical inputs. Despite advancements, there is a need to consider system uncertainties further to optimize MG performance. Other control methods, such as fuzzy-based consensus control and adaptive neuro-fuzzy, have also been proposed to ensure stable MG operation. The integration of cascaded controllers and fuzzy-PID, PD-PI, and optimized fuzzy controllers has been highlighted for smooth operation and inverter control in MGs. Comparative analyses of different input parameters employed in EMS decision-making further contribute to understanding stable MG operation.

Further, the analysis extensively explores the application of fuzzy logic-based controllers (FLC) for voltage and frequency regulation in islanded MG systems. Various studies demonstrate the effectiveness of FLC in managing voltage and frequency deviations caused by load disturbances, fluctuating power generation, and other factors. Compared to conventional controllers like PI, FLC offers faster response times and adaptive control, making it preferable for MG stability. Additionally, centralized control schemes and the integration of storage devices are proposed to enhance voltage and frequency regulation in MGs. Moreover, the literature highlights the significance of FLC's adaptability and robustness in ensuring efficient voltage and frequency regulation. Alongside fuzzy-based control, other techniques such as multiagent-based control, model-predictive control, and optimization-based strategies are also explored, each serving different purposes in microgrid management, including power extraction, size optimization, and active/reactive power management.

The other aspects of MG assessment while aiming for a stable operation include control algorithm validation for a planned MG model using various laboratory hardware setups. Specifically, real-time implementation of microgrids involves implementing and validating control schemes in hardware test benches using robust controllers that integrate critical parameters and facilitate rapid decision-making. Existing literature offers hardware setups, platforms, and toolboxes for validating simulated MG systems under uncertain conditions, including PSCAD/EMTDC, TRNSYS, HOGA, RSCAD, and Hardware in Loop simulations.

However, these tools are mainly confined to laboratory setups and simulations, lacking feasibility for real-world application due to environmental constraints.

In addition, rural electrification in remote areas is crucial for poverty alleviation and socioeconomic development in India, providing continuous electricity for residential and commercial needs. Microgrids offer a promising solution by integrating renewable energy sources, but their optimal design and planning must consider local resources and demand. Thus, techno-economic feasibility analysis plays a pivotal role in evaluating factors like system cost, resource availability, load demand, storage types, and microgrid operation modes. The previous studies have employed various approaches, such as single RES with energy storage systems (ESS), PV-wind-fuel cell hybrids analyzed via HOMER Pro, and PV-diesel-flywheel systems. These analyses assess economic viability, environmental impact, and operational efficiency under different scenarios.

In addition, a comprehensive microgrid stability index is the need of the hour concerning the stable microgrid operation. However, the literature discloses multiple such indexes, but in view of the individual parameters such as voltage and frequency. These indexes majorly focus on the individual parameters, while the level of the microgrid's stable operation is still unknown. Thus, a detailed literature survey concerning the PLC-based control algorithm validation and its significance, as discussed in the previous state-of-the-art work, has been presented in respective Chapters.

2.2. Outcomes of the literature survey

The stability of Microgrids (MGs) faces various challenges, including small-signal, transient, and voltage stability issues exacerbated by uncertain conditions, different loads, and variable Renewable Energy Sources (RESs). These conditions can lead to partial or complete system shutdowns, underscoring the need for special attention during MG design and validation. Dynamic loads like induction motors significantly impact stability, especially with system uncertainties. Resolving MG issues often involves three control strategies: centralized, decentralized, and distributed. Distributed control is particularly effective in complex MG structures, offering accessible data collection, analysis, and decision-making. However, ensuring the healthy operation of all local controllers remains crucial. Hybrid control techniques, incorporating conventional, intelligent, and hybrid approaches, hold promise for enhancing MG stability. Robust and adaptive controllers are favored due to hybrid microgrid components' uncertain and non-linear nature. Integrating RESs requires careful voltage and frequency regulation to prevent system instability, with power balance between generation, load demand, and losses playing a vital role. Unbalanced power distribution is a significant research

focus, especially in islanded mode. Parameters like Total Harmonic Distortion (THD), power quality, and power factor must also be managed to maintain stability. Backup devices like battery storage and electric vehicles respond rapidly to fluctuations, crucial for balancing system transients. Supercapacitors and fuel cells are also valuable for enhancing system stability.

In particular, the controllers mentioned above consider only the selective input parameters. However, while aiming for microgrid stability, it is essential to consider the combined influence of parameters like net power shared, DC-Link voltage, grid parameters, uncertain renewable sources, battery SOC, etc. Besides, it has also been observed that the simultaneous decision-making for load management, battery operation, and mode of MG operation have yet to be much explored. Therefore, it is necessary to highlight that the work done in previous literature does not incorporate a few of the critical points that are significant in power system research. Thus, from the analysis, the identified gaps in research include the deficiency in the research on adaptive and robust EMS for the MG model using the fuzzy-based cascaded controller, especially under the effective influence of real-time experimental conditions. Also, the literature lacks an intelligent control approach for multiple decision-making while combining all the controllable/non-controllable parameters for stable MG operations.

Further, the analysis also highlights significant drawbacks associated with previously proposed controllers in microgrid management, hindering adaptation to changing configurations and intelligent decision-making processes. While FLC shows promise, its design exploration remains limited, particularly considering multiple parameters. Existing literature overlooks the impact of environmental conditions and load fluctuations on microgrid performance under FLC control. Addressing these gaps necessitates the development of a robust, centralized control approach adaptable to evolving scenarios. Additionally, exploring microgrid configurations reveals the superiority of the DC-link configuration due to its reduced complexity and ease of resource coordination, offering a promising path for simplifying microgrid architecture.

Following the research gap in control algorithm validation in a hardware setup, industrial programmable controllers (PLC) are crucial for real-time implementation. PLCs are renowned for their robustness, reliability, flexibility, and quick decision-making capabilities, making them ideal for automatic operations in diverse engineering fields. Previous literature highlights numerous applications of PLCs across various domains, further endorsing their suitability for stable MG operation. These aspects are essential from the validation point of view.

The feasibility analysis of solar, wind, and battery-based MGs remains unexplored mainly despite the high renewable potential in these areas, necessitating focused attention.

Additionally, economic analyses based on various parameters like Cost of Energy (COE), Net Present Cost (NPC), emissions, and component sizing are lacking for islanded MGs in rural India, where the renewable potential is high, but the proper analysis is scarce. Technical assessments through simulations are also insufficient, particularly in evaluating the reliability and security of planned MGs under specific geographical and weather conditions. Furthermore, while robust controllers for stable MG operation are crucial, the implementation assessment for real-time rural and remote locations is not adequately addressed in the existing literature.

Besides, the literature also highlights a significant gap in comprehensively addressing the stability assessment of MG systems, particularly in considering key parameters, uncertain conditions, and diverse electric loads. While exploring conventional power system stability and multi-area control criteria, existing methodologies often fail to evaluate overall system stability comprehensively. This gap underscores the need for specialized methods tailored to MGs' unique characteristics to establish a more accurate stability index, enhancing control and management.

2.3. Objectives of research work

1. To study different types of microgrid considering various energy resources.
2. To develop a simulation model for microgrid.
3. To design a control scheme(s) for frequency and voltage regulation of microgrid.
4. Performance evaluation of proposed microgrid for stable operation.

Moving from the stability challenges and control strategies discussed in Chapter 2, the next chapter presents the practical aspects of microgrid design and modeling, setting the stage for implementing the control approaches. The chapter thoroughly conceptualizes microgrid design and modeling, emphasizing the integration of renewable energy sources such as solar PV, wind, and battery-based energy storage. It details the development of a comprehensive microgrid model using MATLAB Simulink, covering procedures for modeling solar, wind, battery, and power converters. Economic assessment using HOMER Pro software is also introduced, highlighting critical factors such as net present cost and renewable fraction. Lastly, the chapter also explores the implementation of control algorithms through a PLC-based hardware test bench, providing insights into the block diagram and wiring architecture. This chapter thus allows for an understanding of practical design and modeling and facilitates a deeper understanding of how robust and adaptive control strategies can be effectively applied. The modeling concepts and tools introduced in the next chapter are essential for the subsequent

chapters, which focus on validating the proposed control approaches through simulation and hardware implementation, ensuring stable and efficient microgrid operation.

Chapter Summary

This chapter presented a comprehensive overview of the stability challenges faced by Microgrids (MGs), including small-signal, transient, and voltage stability issues exacerbated by uncertain conditions, diverse loads, and variable energy sources. Particularly, the work presented three control strategies: centralized, decentralized, and distributed. Additionally, considering the uncertain and non-linear nature of microgrid components, the preferred robust and adaptive controllers, including fuzzy logic controller and other, such as neural network, and hybrid, have also been well presented. Further, the chapter presented a comprehensive review of the state-of-the-art literature on energy management and stable microgrid operation while considering the three major microgrid parameters: voltage, frequency, and power. Lastly, the chapter presented the outcomes of the literature survey based on the major objectives. Thus, focusing on the major work objectives, the next chapters present microgrid modeling, followed by the discussion related to the proposed controller and results.

CHAPTER 3
DESIGN AND MODELING OF MICROGRID SYSTEM

This chapter discusses modeling a microgrid model from the perspective of simulation, hardware, and economic assessment. Specifically, the microgrid design employed in this work incorporates solar photovoltaic, wind turbine, lithium-ion-based battery storage units, and various converters.

3.1.Basics of Microgrid Design

Microgrid design is a diverse process that creates localized energy systems capable of operating independently or communicating with the main power grid. The design process typically includes planning that involves a detailed analysis of energy demand, available resources, and grid connectivity options. Besides this, load forecasting is crucial in determining the optimal sizing and configuration of generation and storage assets to meet expected demand patterns effectively. In addition, source management entails integrating various energy sources, such as solar, wind, and conventional generators, to ensure a reliable power supply. Further, the controllers are essential components that manage the operation of different elements within the microgrid, optimizing energy production, storage, and distribution in real-time. Converters facilitate the seamless energy conversion between AC and DC forms, ensuring compatibility with the grid and enhancing system efficiency. Lastly, energy storage devices like batteries provide crucial backup power during peak demand periods or when renewable sources are unavailable. Grid connectivity enables microgrids to interact with the main utility grid, allowing for bi-directional energy flow and providing additional resilience and flexibility to the system. Overall, a well-designed microgrid offers increased energy resilience, sustainability, and reliability in diverse applications, ranging from remote communities to urban environments. This section briefs about the various aspects of microgrid design, including microgrid planning, monitoring, control, management, and design process [137].

3.1.1. Microgrid planning

Microgrid planning ensures reliable power supply while optimizing economic efficiency and minimizing environmental impact. The key aspects and considerations involved in microgrid planning are as follows:

- Load and Resource Analysis: Understanding the demand profile and available energy resources is fundamental to microgrid planning. This analysis involves assessing both

current & future and minimum & maximum energy consumption patterns and identifying potential renewable energy sources like solar, wind, or biomass.

- DER and Energy Storage Configuration: Determining the optimal mix of distributed energy resources (DERs) such as solar panels, wind turbines, and energy storage systems (ESS) is critical. This includes selecting appropriate sizes and locations for DER installations and deciding on the types of energy storage technologies to integrate.
- System Operation Strategy: Developing an effective operation strategy involves defining how the microgrid will respond to different operating conditions and grid disturbances. This includes a strategy for islanded operation, grid-connected operation, and seamlessly transitioning between the two modes.
- Alternative Energy Forms: Beyond traditional electrical energy storage, exploring alternative forms of energy storage such as phase-change heat, compressed air, or hydrogen storage can provide additional flexibility and resilience to the microgrid.
- Planning Objectives: Microgrid planning objectives typically include economic efficiency, system reliability, and environmental sustainability. These objectives are tailored to specific application scenarios and customer requirements, ensuring that the microgrid design aligns with stakeholders' priorities.
- Multi-Objective Optimization: In many cases, microgrid planning involves balancing multiple objectives simultaneously. This requires trade-offs between economic benefits, reliability, and environmental considerations to achieve the most optimal design outcome.
- Application-specific Considerations: Microgrid construction must address the requirements of various application scenarios, such as in remote areas without access to grid infrastructure; minimizing costs and maximizing self-sufficiency are primary goals, whereas grid-connected microgrids prioritize reliability and economic viability [9, 49, 138].

3.1.2. Load Planning

A. Load forecasting is a pivotal pillar in microgrid planning, directing decisions regarding deploying distributed generation (DG), configuring energy storage, and selecting appropriate power supply solutions. The process entails:

- Present Load Analysis: A statistical examination of existing load conditions within the microgrid's planning domain, including identifying primary power load types and peak load demands. It also involves studying typical daily load curves for each month.
- Forecasting: Predicting load demand for the planning period by leveraging historical load data and anticipated development requirements. This involves forecasting growth trends in

peak load, introducing additional load types and levels, overall annual load demand, typical daily load demand, and dynamic load characteristics.

- Factors Influencing Forecasting: The various factors that affect the accuracy of load forecasting, including economic conditions, temporal considerations (e.g., weekdays vs. weekends, seasonal fluctuations), meteorological aspects (e.g., temperature, humidity), and other variables such as shifts in consumer behavior and fluctuations in electricity prices.

B. Load classification serves to ensure efficient power distribution during periods of scarcity and in outage scenarios:

- Critical Load: Categories of load with a high risk of personal injury, potential economic losses, or disruption to essential operations of consumers during power interruptions fall under this classification.
- Non-Critical Load: Load that can be temporarily interrupted or reduced during peak periods or emergencies, with the following contractual obligations, is classified as intermittent load [139-140].

3.1.3. Power Generation Forecasting

Before power generation forecasting, a comprehensive resource analysis is imperative. This includes assessing available resources such as solar, wind, biomass, and natural gas. Additionally, the geographic environment in the planning region is evaluated to devise a viable distributed generation (DG) configuration plan, considering the type and location of resources. Power output forecasting forms the cornerstone for determining electric power and energy balance. For accurate forecasting:

- Solar and Wind Power Forecasting: Monitoring data on solar radiation and wind speed within the microgrid area is collected and analyzed over a minimum of one year. This data aids in analyzing annual energy generation, generation curves, and typical daily generation patterns. Collected data includes representative monthly irradiance and wind speed values, hourly radiation and wind speed data for at least a year, monthly average temperatures, maximum wind speeds, and extreme weather occurrences.
- Biomass, Natural Gas, and Diesel Power Generation: In addition to generator unit characteristics, fuel conditions significantly impact power output forecasting. Factors such as fuel quality, supply, and price are investigated and collected from historical and current periods to evaluate and forecast generating output within the planning horizon [141-142].

3.1.4. System Configuration

The objective of system configuration within a microgrid is to establish a construction plan, including the type and capacity of distributed generators (DGs) and energy storage devices, to meet the power demand effectively. Load classifications, load forecasting, and power output predictions guide this process.

Specifically, factors such as economy, reliability, and environmental impact are thoroughly assessed when configuring DGs. Electric power and energy balance calculation is integral to this planning phase. Analysis of power source status, load demand, and generation resources guides the adaptive configuration of power sources. It's crucial to establish a ratio of DG installed capacity to load to ensure continuous power supply in standalone mode, with a recommendation for a proportion of renewable energy sources. Technical characteristics of generating equipment, operation strategy, and microgrid operation mode are considered, and various combinations are compared to determine the most suitable configuration.

When configuring energy storage, its function in the microgrid, such as smoothing power fluctuations and supporting voltage and frequency in standalone mode, is paramount. Energy storage type and capacity are selected accordingly, and a replacement program should be devised for the planning period. The capacity configuration of DGs and energy storage must meet the maximum electrical load demand.

3.1.5. Microgrid Primary System Design

Determining the voltage levels within the microgrid and its connection to the External Power System (EPS) is critical for efficient operation. The voltage levels within the microgrid are chosen based on factors such as internal energy resources, load size, planned area, and cost considerations. Generally, voltage levels do not exceed 35 kV and include options like 23 kV, 13.8 kV, 0.48 kV, 480 V, and so on to 230 V. The selection process aims to minimize the voltage levels while ensuring compatibility with the installed series of renewable energy resources. Similarly, the voltage level of the EPS that the microgrid accesses should be determined based on the maximum exchange power between the two systems, with recommendations below 35 kV.

Further, the point of common coupling (PCC) is the connection point between the microgrid and the power system. Typically, each microgrid has a single PCC, i.e., a node on the high-voltage side for those with a step-up substation or the input/output convergence point for those without.

3.1.6. Power Flow Calculation

Power flow calculations for the microgrid must account for various operating conditions throughout the planning/design period. This includes scenarios such as peak and off-peak loads, maintenance or fault conditions, and maximum and minimum generation periods from Distributed Generators (DGs).

- Boundary Definition: Establishing boundaries for power flow calculations involves combining different generation and loading conditions. This includes scenarios like maximum generation with minimum loading and vice versa. Extreme conditions, such as when all renewable generation resources are offline and energy storage is fully discharged, must also be considered. For grid-connected microgrids, calculations should extend to abnormal conditions when the microgrid is disconnected from the main grid. At the 400 V level, power flow calculations may be simplified, but precautions should be taken to avoid exceeding branch power flow or nodal voltage limits.
- Grid Integration Verification: In grid-connected microgrids, power flow calculations verify the integration scheme with the main grid, the selection of conductor cross-sections, and the configuration of electrical apparatus parameters. This validation ensures seamless integration and optimal performance under normal and abnormal operating conditions [143-144].

3.1.7. Monitoring, Control, and Energy Management

The primary objective of microgrid monitoring, control, and energy management is to oversee, regulate, and optimize the operation of the microgrid, ensuring efficient energy flow in real-time. Specifically, the monitoring and control system is designed to uphold the microgrid stability by gathering data related to distributed generators, storage units, and the grid. This system presents the collected information through graphical interfaces, facilitating intuitive monitoring and control. Additionally, it ensures the timely storage and updating of relevant data, which is crucial for informed decision-making and system optimization. In addition, the energy management system focuses on fostering the economical operation of power generation, distribution, and consumer equipment within the microgrid. This system strives to optimize overall performance while minimizing operational costs by efficiently allocating and utilizing energy resources [145-147].

3.1.8. Control Architectures

As discussed in Chapter 2, microgrid energy management systems typically employ two technical approaches: centralized mode and distributed mode. In the centralized mode, the

system configuration comprises three logical layers: device, management, and optimization. Conversely, in the distributed mode, the local monitoring and control layer (a) and coordinated control layer (b) are often combined. The details related to the layers are as follows –

- The local monitoring and control layer is primarily responsible for local data acquisition, information upload, and command execution within the microgrid. Essential functions include real-time data collection, information transmission, and command execution.
- The coordinated control layer focuses on coordinating the control of distributed energy resources and controllable loads within the microgrid. Its objectives include achieving internal stability and facilitating access to distributed energy resources.
- The energy management layer is dedicated to real-time information monitoring, historical data storage, system operation control, advanced energy management, and report generation. Its functions encompass real-time monitoring, historical data storage, system operation control, advanced energy management, and statistical reporting.

3.1.9. Energy Management

A microgrid's energy management system (EMS) is a crucial computer-aided tool for operators to monitor, control, and optimize the microgrid's performance. The primary functions of EMS in a microgrid encompass:

A. Power Generation Forecasting:

- The EMS uses historical and measurement data to forecast power generation and integrates prediction data from power generators.
- Special considerations are made for microgrids with intermittent power sources like wind and solar, with the EMS equipped with resource monitoring functions.
- The EMS is configured with appropriate capabilities for estimating and further considering power generation levels from renewable sources for stable microgrid operation.

B. Distributed Energy Resources Management:

- Manages power generation, maintenance, and fuel for distributed energy resources and energy storage systems within the microgrid.
- Implements fuel management for various power generation devices, including fuel consumption tracking, residual fuel calculation, and early fuel inventory warnings.
- Manages maintenance schedules for power generation equipment and monitors the state of charge for energy storage systems, issuing alerts for abnormal charge levels.
- Sets the primary power supply among multiple sources and establishes standby sequences for other sources.

C. Load Management:

- Classifies and manages loads based on power supply reliability requirements and safety considerations.
- Predefines load-switching strategies for different operating conditions based on load classifications.
- Implements load forecasting based on real-time monitoring data and load consumption plans.
- Under standalone mode, power reduction strategies are implemented for each load terminal.

D. Electricity Generation Plan:

- Based on optimization calculations, power generation plans and storage charge/discharge plans for distributed energy resources are arranged.
- Includes day-to-day power generation and intra-day electricity consumption plans with specific time resolutions.
- Allows for manual input and automatic generation of power generation plans.

E. Voltage and Power Management:

- Optimizes the setting of reactive voltage operation modes, providing parameter settings for selected control modes.
- Sets the input order of reactive power compensation equipment.

Thus, considering the points mentioned above, the following sections present the modeling approach for a microgrid system from the perspective of simulation, economic assessment, and implementation [146-147].

3.2.Microgrid modeling and simulation

In detail, Figure 3.1 depicts various Distributed Energy Resources (DERs), such as solar, wind, and battery storage-based microgrid systems interconnected with the main utility grid via the Point of Common Coupling (PCC). The centralized control unit (MGCC) is responsible for managing all components within the system, including load management, grid management, DER management, etc., ensuring system stability. However, this centralized approach can limit system flexibility. In such scenarios, either operating the microgrid less flexibly, rendering it unsuitable for all modes of operation, or modifying the control scheme to maintain system health becomes necessary. Consequently, combining the advantages of centralized and decentralized control schemes within a hierarchical structure, the distributed mode of operation becomes crucial.

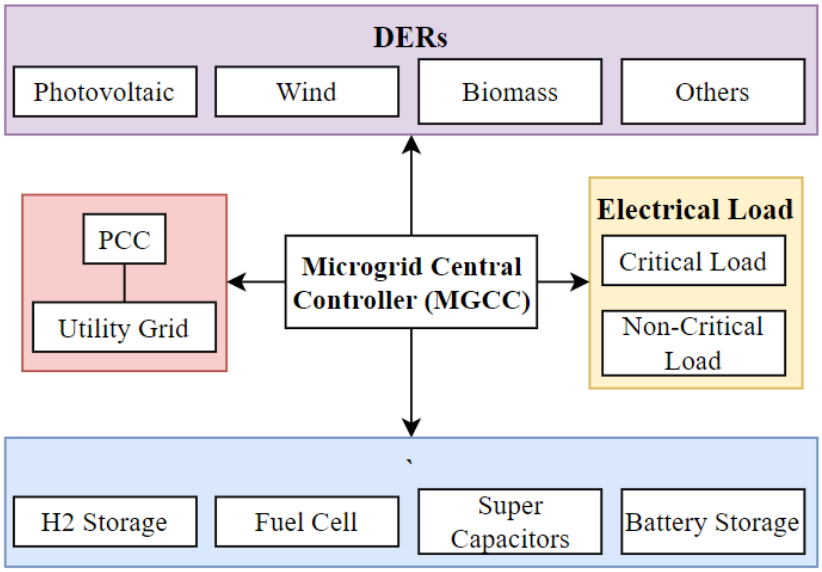

Figure 3.1. Schematic diagram of a microgrid system

According to the figure, all components of the microgrid system—utility grid, load, storage system, and various DERs—are equipped with local controllers. These local controllers are tasked with managing individual components of the entire system. For instance, a dedicated controller is assigned to the photovoltaic system, ensuring its monitoring and control for seamless system operation. This controller takes necessary actions concerning photovoltaics to ensure system smoothness, with relevant information communicated to the central controller for further monitoring and data handling. Similarly, other local controllers oversee individual system components, communicating with the central controller for higher-level energy and load management decisions.

Hence, following the power system approach, the related equations are given by Equations 3.1 to 3.3.

$$P_{gen.} = P_{PV} + P_{WT} \quad (3.1)$$

$$P_{net} = P_{PV} + P_{WT} - P_{L} \pm P_{B} \quad (3.2)$$

$$SOC_{(min)} < SOC_{(battery)} < SOC_{(max.)} \quad (3.3)$$

$P_{gen.}$ represents the overall power generation within the RNCES, comprising P_{PV} (power from PV) and P_{WT} (power from the wind turbine). Pnet denotes the total power distributed among the sources and the total load (P_L), which includes the power provided or consumed by the battery storage (P_B). As defined in Equation 3.3, SOC signifies the state of charge for the battery integrated into the system, and it must remain within the specified minimum and maximum limits.

Following the sample microgrid system, the below part of this section discusses the modeling approach of the various power components employed in the developed MG model [148]. Notably, equations 3.4 – 3.13 have been used to develop a complete microgrid system

where the sources are integrated via different power electronics components so that the proposed control algorithm can be validated.

3.2.1. PV Modeling

In the context of microgrid modeling, solar photovoltaic (PV) systems play a crucial role in advancing sustainable energy generation practices. By integrating solar PV models within microgrids, the efficient utilization of solar energy resources becomes possible, effectively addressing local electricity demands while reducing reliance on conventional power sources. Solar PV modeling entails a comprehensive characterization of various components and parameters to accurately capture the behavior and performance of PV systems within microgrid environments. This modeling process encompasses intricate photovoltaic modules, inverters, tracking systems, and control algorithms, all interacting dynamically with environmental factors such as solar irradiance, temperature variations, and shading effects. The complexity of solar PV modeling lies in its ability to simulate these interactions accurately, ensuring that the model reflects real-world conditions and provides valuable insights into system performance and energy yield within microgrid contexts. Given this, the modeling of a PV array consists of module strings connected in series/parallel combinations. The mathematical model of the PV system is given by the equation 3.4 – 3.6 [148-150].

$$I_p = GI_{phg} - i_0 exp\left(\frac{q}{nTK_b}\left(V_p + I_p R_{sg}\right) - 1\right) - \left(\frac{V_p + I_p R_{sg}}{R_{shg}}\right) \tag{3.4}$$

$$i_{ph} = \left(i_{sc} + k_i(T - T_r)\right)s \tag{3.5}$$

$$i_0 \exp\left[\frac{qE_g}{Ak_b}\left(\frac{1}{T_r + 273} - \frac{1}{T + 273}\right)\right]\left(\frac{T + 273}{T_r + 273}\right)^3 i_r \tag{3.6}$$

Where n is the total number of PV cells, G is the solar irradiance (W/m^2), k_b represents the Boltzmann constant in j/K, R_{sh}, and R represents the circuit resistances in Ω. Besides, T represents the PV panel temperature, T_r represents the reference temperature for the PV panel in ºC, A represents the diode ideality constant for the PV panel. E_g represents the bandgap energy for the PV panel. In addition, the PV panel's current parameters include q representing the electron charge, i_r representing the saturation current, and i_{ph} representing the photogenerated current. In addition, the MPPT controller based on panel voltage and current has been used to boost the power output in case of varying solar radiation. The controller works in combination with the boost controller. In the case of low solar radiation, the Maximum Power Point Tracking (MPPT) controller, based on voltage and current, follows the P&O algorithm to achieve maximum power for enhanced system operation. Specifically, MPPT is vital for solar energy systems, optimizing output by adjusting photovoltaic parameters. Besides, the Perturb

and Observe (P&O) is a widely used MPPT algorithm that continuously perturbs the operating point and observes power changes to converge toward the maximum power point. It's simple and efficient, enhancing solar panel efficiency and overall energy yield [151].

3.2.2. Wind Turbine Modeling

In the context of microgrid modeling, wind turbines play a pivotal role in harnessing renewable energy to ensure sustainable power generation. Integrating wind turbine models within microgrid systems enables the efficient utilization of wind energy resources to meet local energy demands. Specifically, wind turbine modeling involves the characterization of various parameters and components to accurately simulate the behavior and performance of wind turbines within the microgrid. Further, these models encompass intricate mechanical and electrical components, including rotor blades, drivetrains, generators, and control systems, all interacting dynamically with environmental factors such as wind speed, direction, and turbulence. Considering the same, this subsection provides the key mathematical equations related to modeling a wind turbine model, where the mechanical power is given by equations 3.7 and 3.8 [148-150].

$$P_m = \frac{1}{2} C_p(\lambda, \beta) \rho A v^3 \tag{3.7}$$

$$\lambda = \frac{\omega R}{v} \tag{3.8}$$

In equations 3.7 and 3.8, P_m represents the mechanical power of the wind turbine, ρ represents the air density in kg/m^3, and A represents the total area swept by the blades in m^2. Further, A is calculated as $A = \pi R^2$, v represents the wind speed in m/s, C_p represents the power coefficient, β represents the pitch angle, and λ represents the tip speed ratio for the wind turbine. Further, for calculating λ, the parameters include ω representing the blade angular velocity in rad/sec and R representing the rotor radius in meters. For the present case, a salient pole permanent magnet synchronous generator (PMSG) has been considered. The stator voltage equations as per the Parks transformation are given by equations 3.9 – 3.10.

$$\frac{di_{sd}}{dt} = -\frac{R_{sa} i_{sd}}{L_{sd}} + \frac{\omega_s L_{sq} i_{sq}}{L_{sd}} + \frac{v_{sd}}{L_{sd}} \tag{3.9}$$

$$\frac{di_{sq}}{dt} = -\frac{R_{sa} i_{sq}}{L_{sq}} - \omega_s \left(\frac{L_{sd} i_{sd}}{L_{sq}} + \frac{\psi_p}{L_{sq}} \right) + \frac{v_{sq}}{L_{sq}} \tag{3.10}$$

Where v_{sd} represents the voltage of stator resistance in the d-axis, i_{sd} represents the current of stator resistance in the d-axis, v_{sq} represents the voltage of stator resistance in the q-axis, i_{sq} represents the current of stator resistance in the q-axis. Further, R_{sa} represents the stator

resistance, ω_s represents the angular velocity of the generator, L_{sd} represents the inductance of the generator in the d-axis, L_{sq} represents the inductance of the generator in the q-axis, and ψ_p represents the permanent flux. Besides, the MPPT has been employed for extracting the maximum power from the developed wind turbine, for which parameters such as v representing wind speed and β representing pitch angle have been considered. Notably, the controller varies the turbine pitch angle to attain the maximum power under varying conditions [96].

3.2.3. Battery Modeling

Similar to solar PV and wind turbine modeling for a microgrid system, battery storage systems are a vital component contributing to the sustainability and resilience of energy generation. Integrating battery storage models within microgrids facilitates the effective management and optimization of energy resources, enabling reliable power supply and grid stability. Battery storage modeling involves a comprehensive characterization of various components and parameters to accurately simulate the behavior and performance of storage systems within microgrid contexts. These models encompass intricate battery chemistries, charging and discharging control mechanisms, energy management algorithms, and thermal management systems, all interacting dynamically with factors such as load demand, renewable energy generation, and grid conditions. The complexity of battery storage modeling lies in its ability to capture the dynamic interactions between these components and external factors. This ensures that the model provides insights into energy storage capacity, efficiency, and overall system performance within microgrid environments. In the context of mathematical modeling of the battery, the significant parameters are terminal Voltage (V_t) and the battery's percentage state of charge (SOC). Thus, equations 3.11 and 3.12 can be referred to in the following manner [150].

$$v_t = v_{oc} + i_b R_b - v_p \frac{Ah}{Ah + \int i_b dt} + v_a e^{B \int i_b dt} \tag{3.11}$$

$$SOC = \left(1 + \frac{\int i_b dt}{Ah}\right) \times 100 \tag{3.12}$$

In the equations, v_t represents the voltage across the battery terminals, v_{oc} represents the open-circuit battery voltage, i_b represents the battery current, r_b represents the battery resistance, v_p represents the polarization voltage of the battery, v_a represents the exponential voltage and B represents the exponential capacity of the battery. The battery sizing can be decided based on equation 3.13 as given below.

$$Battery\ rating = \frac{Load\ Demand * backup\ time}{Battery\ Terminal\ Voltage * Depth\ of\ Discharge} \tag{3.13}$$

It is important to note that, from reproducibility aspects, the battery's given capacity has to be modified for a system with high load capacity. In such a case, these modifications will lead to a stable operation with the controller working similarly. However, the system's stability will be hindered if such changes are not made.

3.2.4. Power Converter Modeling

Further, in microgrid modeling, power converter systems are pivotal in facilitating the seamless integration and management of diverse energy sources. Including power converter models within microgrids enables the efficient conversion of electrical energy between different forms, ensuring compatibility and stability within the grid. Power converter modeling entails a comprehensive characterization of various components and parameters to accurately simulate the behavior and performance of converter systems within microgrid contexts.

As depicted in Figure 3.2, the DC-AC converter module is a critical component in the microgrid infrastructure and is responsible for converting DC voltage into a consistent AC supply with a constant frequency. The control strategy implemented in this module involves the regulation of current (voltage) in continuous coordinates (dq0) using closed control loops. This strategic choice is made for its capability to deliver rapid transient responses and maintain stable performance under varying operating conditions.

These converter models encompass intricate control algorithms, modulation techniques, and switching mechanisms, all interacting dynamically with the input voltage, load demand, and grid conditions. The complexity of power converter modeling lies in its ability to accurately capture the dynamic interactions between these components and external factors, ensuring reliable energy conversion and grid synchronization within microgrid environments. By accurately simulating the behavior of power converters, microgrid operators optimize system efficiency, mitigate grid instability, and enhance overall energy management. Additionally, these models provide valuable insights into converter performance, efficiency, and reliability, facilitating informed decision-making and system optimization in microgrid applications.

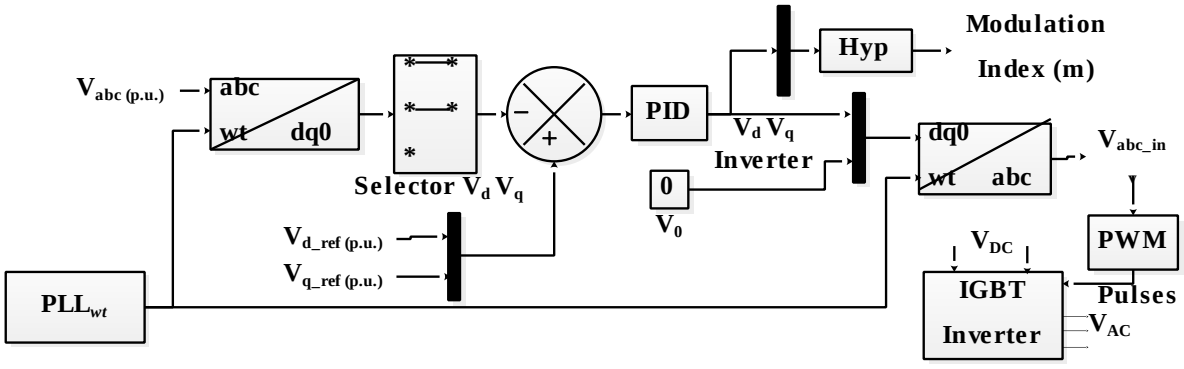

Figure 3.2. DC-AC converter modeling

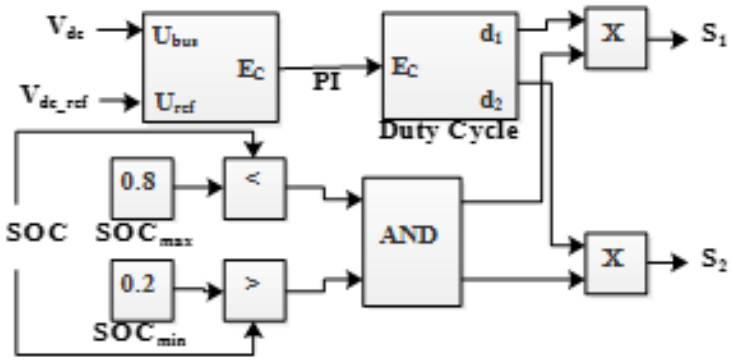

Figure 3.3. DC-DC bidirectional converter for a battery device

In Figure 3.2, the control strategy transforms $V_{abc(p.u.)}$ into the dq0 frame of the voltage source inverter, guiding V_{abc_inv} via PWM modulation to produce V_{AC} in the IGBT-based inverter module. A PID controller ensures controlled voltage supply and load current regulation. Meanwhile, Figure 3.3 displays battery connectivity through a bidirectional DC-DC converter on the DC bus. This converter maintains V_{dc} at a constant reference value, allowing adjustments for fluctuations. Vdc is compared to V_{*dc}, and the error signal enters a regulator. Its output (duty cycle D1 and D2) controls switches Q1 or Q2 in the converter module, staying within the SOC range (0.2 – 0.8) to safeguard the battery and prolong its life.

3.3.Microgrid modeling in perspective of Economic Assessment

The key components for economic assessment have been presented in this section. The components shown in Figure 3.4 include various power sources like generators, grids, and REs, different types of loads, converter and controller modules, various storage units, etc. [5, 152]. Subdividing the components, the different types of loads available include residential, industrial, and commercial loads. Different renewable and non-renewable sources are available for power sources, including solar PV, wind, biogas, utility grids, diesel generators, etc. Also, considering the specific location, the input data for resources like GHI, windspeed, etc., can be accessed from various online/offline sources. Considering the reliability of microgrid systems in islanded mode, storage units are of great importance. Thus, various types of storage units, like batteries, fuel cells, etc., are available in the software. The converter modules are accessible in the system to develop the AC/DC microgrid model while focusing on microgrid compatibility.

Figure 3.5 shows the basic steps in the form of a flowchart for developing the microgrid model using the HOMER Pro software. As per the flowchart, the different components involved in modeling and their subcomponents have been discussed stepwise. The solid lines in the flowchart represent the major steps for the design and development of the microgrid model. In

contrast, the dotted lines represent the various available options for the given parameter. It must be noted that for designing the microgrid model under a constrained and specific condition, the flowchart can be modified as per the requirement, whereas the basic steps remain the same [1].

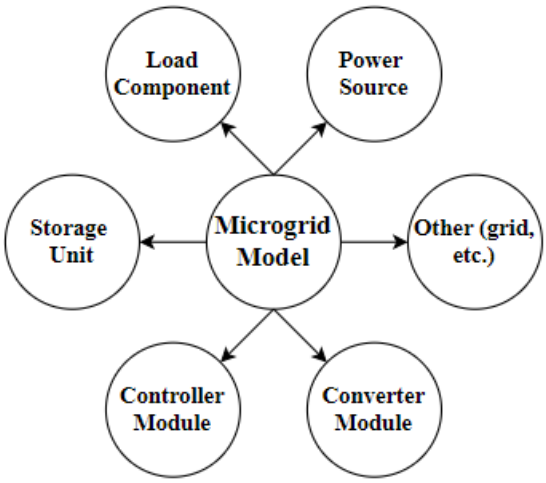

Figure 3.4. Components of HOMER Pro for a microgrid model

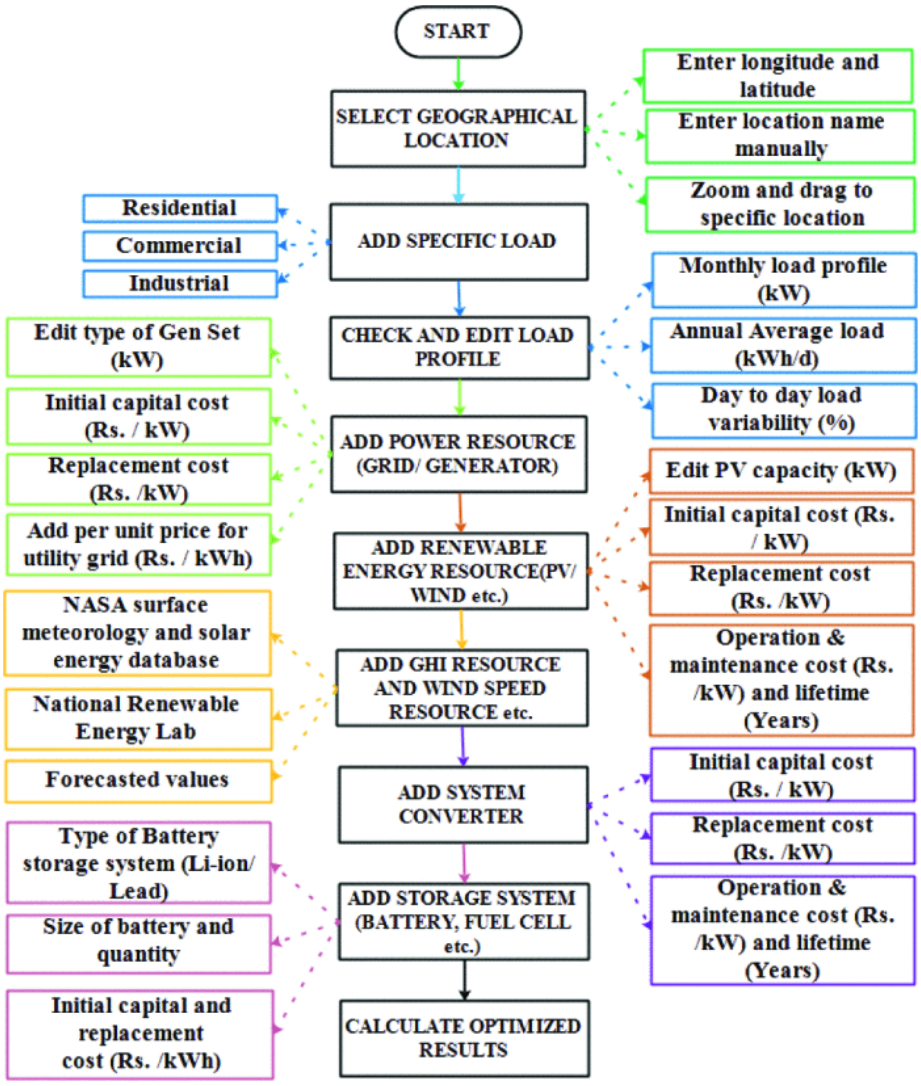

Figure 3.5. Working and operating flowchart of HOMER Pro software

Referring to the Figure 3.5, the first step is to select a specific geographical location for setting up the microgrid. Step two is to specify the type of load and set the respected load profile. Step three is to add the utility grid or the conventional generator in the model while specifying different parameters. Step four is adding different renewable energy resources like PV, wind, etc., followed by resource data. In the case of a hybrid microgrid model with both AC/DC sources, the converter module can be added to create the AC/DC bus in step five. In step six, the storage module available in the HOMER Pro library can be added to develop a stable microgrid model for specific geographical locations. This leads to improving the stability and feasibility of the system, although it slightly increases the per-unit energy cost. In the final step, calculated results can be analyzed using the controller and software optimization tool. In addition, the other output parameters for all number of possible combinations, like a renewable fraction, percentage of unmet load, amount of gases released in kg/year, etc., can also be investigated.

The various parameters associated with the economic assessment are as follows [153] -

- Cost of Energy (COE): The per-unit COE consumed at the consumer end is the total energy cost. The mathematical expression is mentioned in equation 3.14 below.

$$COE = \frac{C_{ann,tot} - C_{boiler} H_{served}}{E_{served}} \tag{3.14}$$

where, $C_{ann,tot}$ represents total annualized cost of the system (Rs./year), H_{served} represents the total thermal load served (kWh/yr), C_{boiler} represents the boiler marginal cost (Rs./kWh) and E_{served} represents the total electric load served (kWh/yr).

- Net Present Cost (NPC): The total cost analysis of system components, operations, and the revenue collected gives the NPC of the designed MG. It includes the cost of operations, initial cost, and revenue collection for a given period. The mathematical expression is mentioned in equation 3.15 below.

$$C_{NPC} = \sum_{n=i}^{n} \frac{CF_n}{(1+i)^n} \tag{3.15}$$

where, C_F represents the cash flow, i represents the discount rate, and n represents the time period.

- Renewable Fraction (f_{ren}): The quantity of power delivered to the load at the consumer end via different RESs (in percentage) is a renewable fraction. In the system assessment process regarding renewable extraction and usage, f_{ren} is the critical parameter. The increase in f_{ren} leads to reduced emission and COE. Below, the mathematical expression has been mentioned in equation 3.16.

$$f_{ren} = 1 - \frac{E_{nonren} + H_{nonren}}{E_{served} + H_{served}} \quad (3.16)$$

where E_{nonren} represents non-renewable electrical energy production(kWh/yr), H_{nonren} represents non-renewable thermal energy production, H_{served} represents total thermal load served (kWh/yr), $E_{grid,sales}$ represents total energy sold to the main grid(kWh/yr), and E_{served} represents total electrical load served in the grid(kWh/yr).

- Operating Cost ($C_{operating}$): The cost analysis focuses on the component's analytical value, excluding its initial and installation cost. Below, the mathematical expression of operating cost has been mentioned in equation 3.17.

$$C_{operating} = C_{ann,tot} - C_{ann,cap} \quad (3.17)$$

where, $C_{ann,tot}$ represents the total annualized cost (Rs./yr) and $C_{ann,cap}$ represents the total annualized capital cost (Rs./yr).

- Operation and Maintenance costs (O&M): It is the total sum of the cost involved in the operation and maintenance of the system components. The other charges related to O&M include costs related to the penalties, etc. Below, equation 3.18 presents the mathematical equation for operation, maintenance and other costs.

$$C_{om,other} = C_{om,fixed} + C_{cs} + C_{emission} \quad (3.18)$$

where $C_{om,fixed}$ represents fixed operation and maintenance cost of the system, C_{cs} represents the penalty for penalty for capacity shortage and $C_{emissions}$ represents the penalty for emissions, all in (Rs./yr).

3.4.Microgrid modeling in perspective of Hardware Validation

The planning and construction of a PLC test bench for stable microgrid operation, especially effective energy management systems (EMS), are thoroughly examined in this part. The section mainly covers the test bench prototype's electrical design, component overview, and block diagram. Figure 3.6 depicts the essential building components of the evolved system.

The primary subjects of the first block are the power switch and the 230 V AC power supply. The second block contains the SMPS module, which converts the 230 V AC into the 24 V DC required for subsequent modules. The SMPS module is a crucial part of the test bench since it may be configured in various ways based on the power requirements of all other system components. The third block includes an integrated Allen-Bradley - Micro820 PLC module (catalog ID - 2080-LC20-20QBB) with 4 analog inputs, 8 digital inputs, 1 analog output, and 7 digital outputs. As a result of its adaptability, affordability, and ease of expansion, if necessary, this particular PLC module was chosen. The fourth block, which has 4 analog inputs and 8 digital inputs, is the integral and only part of the test bench's input section. The analog inputs

imitate how different resources in the MG system change over time. The MG design can be reconfigured using digital inputs, enabling system disturbances and MG configurations, such as wind, wind-battery, PV-battery, etc. Additional input/output modules for the PLC can improve its capacity to adapt to different configurations. Furthermore, an 8-channel 24 V DC relay card, which is normally open, is connected to the system to facilitate improved and secure load-switching. Each channel of the relay card corresponds to a potential output connection that the PLC's output signal can activate. The different sets of LEDs are incorporated to provide visual indicators of each channel's status during the real-time operation. Lastly, it includes the output section, which features eight LEDs mounted on the prototype. These LEDs, labeled D0 to D7, serve distinct purposes. D0, the initial LED, is the dump LED representing the analog output. LEDs D1 to D3, identified as S1 to S3, indicate the status of the power sources, specifically whether they are turned on or off. The four LEDs that serve as indicators for the electrical load are also included on the test bench.

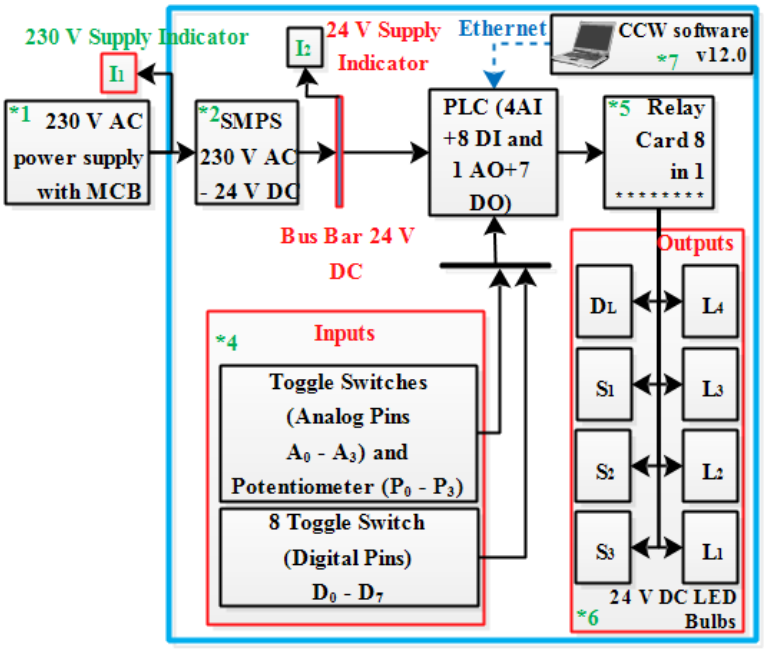

Figure 3.6. Block diagram of PLC test bench

As the last element of the test bench, the computer system is crucial since it houses the crucial software for creating the control logic. The CCW Standard Edition v12.0 software associated with the reconfigurable PLC module has been used in this research work. The software has been employed to design the logic aiming a stable and reliable microgrid (MG) operation, where, the logic is uploaded in the PLC for validation. In present research, authors laptop with Intel Core i5-5200 CPU operating at 2.20 GHz, 16 GB RAM, and a 64-bit operating system is used. Further, Table 3.1 provides the key features and details related to the developed system, such as power supply ratings, PLC configuration, inputs/outputs, etc.

Table 3.1. Details of the hardware test bench

Sr. No.	Feature	Details and Configuration
1.	Power Supply from Utility Grid	230 – 240 V AC
2.	Switch Mode Power Supply Unit (SMPS)	230 – 240 V AC to 24 V DC
3.	Programmable Logic Controller Module (PLC)	Reconfigurable 12 Inputs, 8+1 outputs and 24 V DC supply voltage (via SMPS)
3(A)	PLC with Catalog ID	Micro820 (Catalog ID - 2080-LC20-20QBB)
3(B)	Associated Software for PLC programming	CCW Standard Edition v12.0
3(C)	Reconfigurable	Yes
3(D)	Dimensions	90mm*100mm*80mm
3(E)	User/operator Defined Function Blocks	Yes
3(F)	Available Programming Languages	Ladder Logic, Structured Text, and Function Blocks
3(G)	Maximum Program Steps	10,000
3(H)	MicroSD Card Slot	32 GB
3(I)	Serial Port	RS232/485 non-isolated, CIP Serial, Modbus RTU, ASCII
3(J)	Programming Port	Embedded Ethernet Port
3(K)	Relay card	24 V DC 8 channel card
4.	Relay card indicators	Yes, LED indicators (Red) with 22.5mm diameter
5.	Other LEDs (Input and Output Indicators)	Pilot LEDs
6.	Potentiometer	5 kΩ with knob 0-180̊
7.	Input Toggle switches	6 A (Metallic)

Hence, the following section delves into the electrical design of the PLC test bench, expanding upon the provided block diagram and associated details. It is noteworthy that there is a limited amount of literature that extensively explores the design and diverse features of hardware test benches.

3.4.1. Electrical design of test bench

This section focuses on the electrical layout of a PLC-based hardware test bench that represents a model of a microgrid system with battery, wind, and solar photovoltaic (PV) technologies (presented in Figure 3.7).

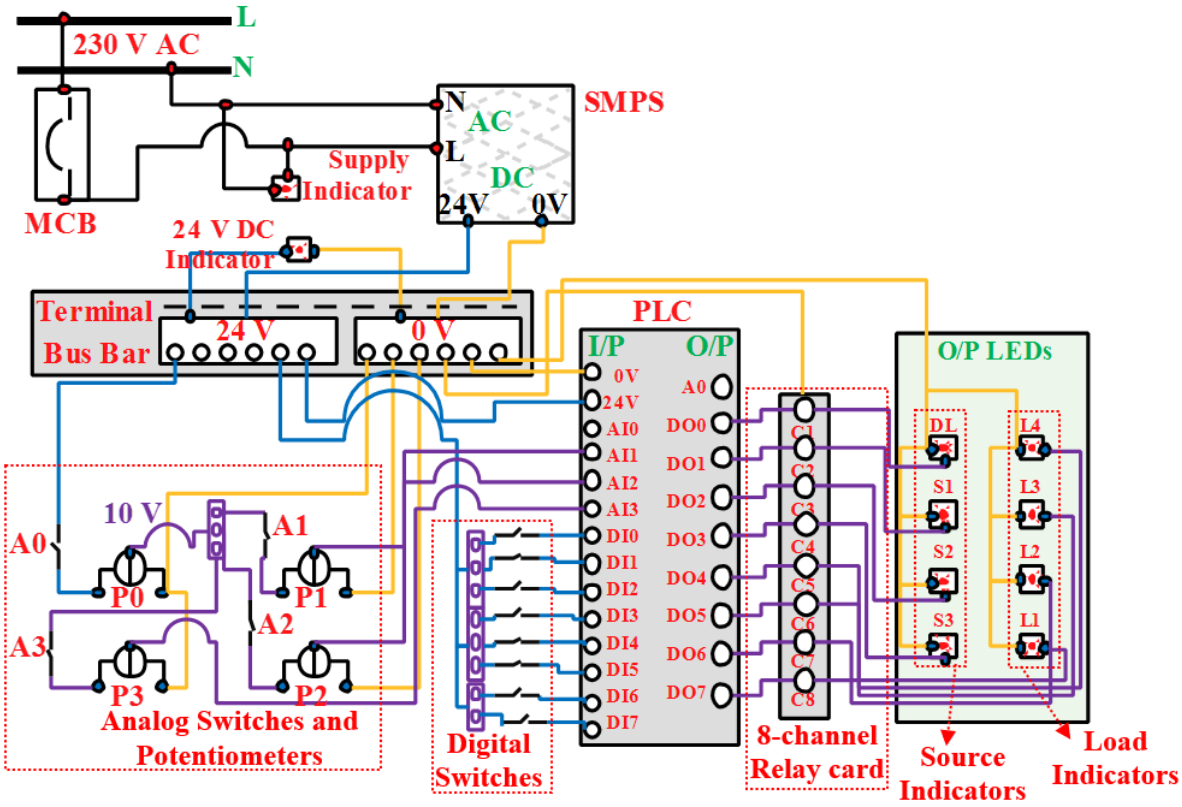

Figure 3.7. Internal Electrical connections of PLC-based test bench prototype

Figure 3.7's complete wiring diagram divides the system into three pieces: connections for 230 V AC to 24 V DC, wiring for potentiometers, and connections for analog and digital pins with the relay card and LEDs. Firstly, a switch-mode power supply (SMPS) is initially connected to the input ports of the 230 V AC main power supply through a miniature circuit breaker (MCB). The SMPS effectively transforms the input into a consistent 24 V DC output using a transformer, a rectifier, and filters. The existence of power is indicated via an LED indicator. The diagram shows a 24 V terminal DC busbar powered by the SMPS, which is the focal point for all electrical connections on the test bench. Secondly, the potentiometer (P0-P3) and analog switches (A0-A3) connections are carried out. These components' 0 to 10 V operational range makes ladder logic design in the Connected Components Workbench (CCW) software more straightforward and easier to understand. To ensure seamless operation, toggle switches are placed to turn the analog inputs on or off. The PLC's analog input command reads the output signals from the potentiometers and converts them into a format that may be used. A scaling process is also used to translate/convert/scale actual values into a percentage range

of 0 % to 100 %. The digital input port of the PLC (DI0 - DI7) is controlled by digital toggle switches that are directly linked to the busbar. These switches give users control over the test bench's digital features by activating or deactivating digital inputs.

Overall, supported by the thorough wiring diagram shown in Figure 3.7, the electrical design of the PLC-based hardware test bench for PV, wind, and battery-based microgrid configurations is an innovative and critical contribution to microgrid control algorithm testing and validation. The importance of the DI0 - DI3 digital switches in modeling disruptions brought on by turbulence, an abrupt shade over PV panels, and communication noise cannot be overstated. As previously mentioned, combining numerous analog and digital switches enables the replication of various setups and states. These conditions and scaled values are the foundation for the PLC logic, producing 75 combinations. Furthermore, the 8-channel relay card, which runs on a typical 0 V and 24 V DC supply, is connected to the output signals (DO0 - DO7). As a result, the PLC provides an output signal based on the designed logic that activates the relevant load lamp through the relay card. As annotated in the figure, S1-S3 indicates the source indicators, i.e., whether the source has been turned on or is presently in the off state. Further, L1-L4 represents the load indicators, i.e., based on the developed logic, whether the connected load is powered on or is presently in the off state. Notably, the output LEDs (L1-L4) indicate that the load is powered on or in the off state.

3.4.2. PLC test bench – Programming Overview

The process of creating code for the automated PLC involves two stages. The input and output parameters, addresses, and memory bits are assigned in the first stage. The memory bits, such as M0, M1, M3,.., and Mx, handle the combinations and logic within the main PLC program. Additionally, the comparators and scaling blocks are employed in this stage to process the input parameters and ensure that the parameters are formatted correctly for further operations. This initial stage of code creation establishes the foundation for the effective functioning of the automated PLC system.

The sample program in Figure 3.8(a) demonstrates the initial input step of system operation, which involves reading and scaling the analog data. The output logic is developed in the second code generation phase to establish correlations between the input parameters and various combinations. Figure 3.8(b) illustrates the usage of additional memory bits in the output logic. According to the logic, all the output LEDs should be activated when the input status is high. Conversely, when there is a drop in input status, the LEDs must be automatically turned off based on the priority list chart. The crucial requirement is to ensure the LEDs are turned on strictly according to the load priority.

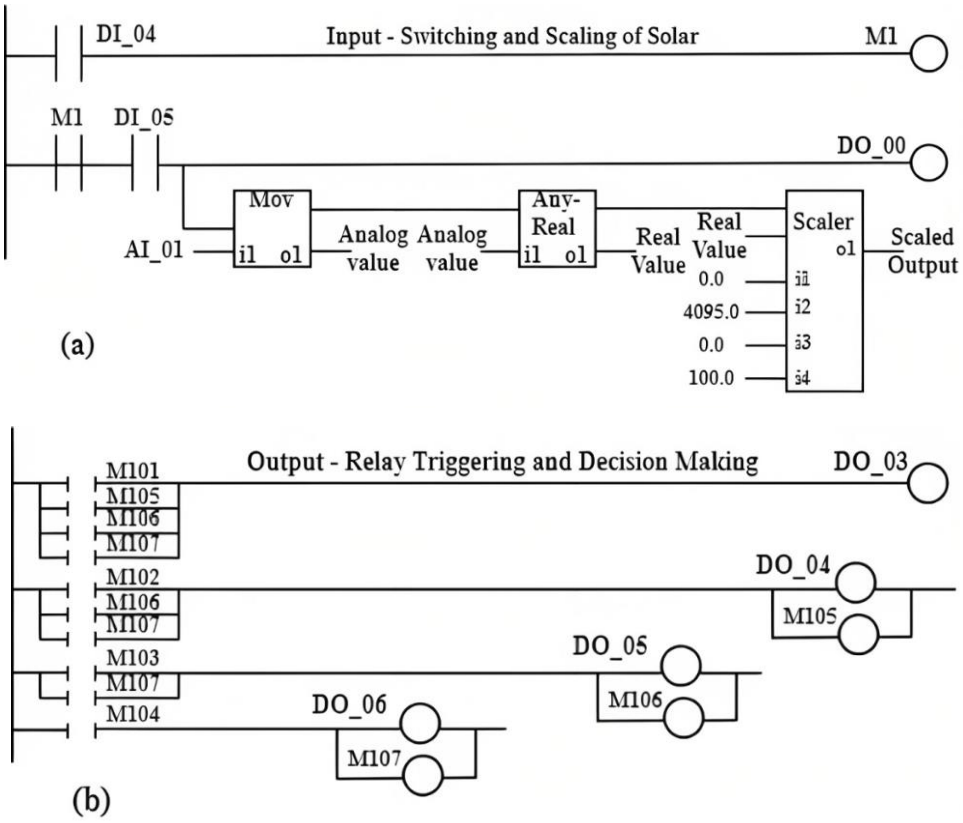

Figure 3.8. CCW software (a) Parameter Input Window (b) Output Window

For reference, Figure 3.9 shows the developed hardware test bench with key components annotated.

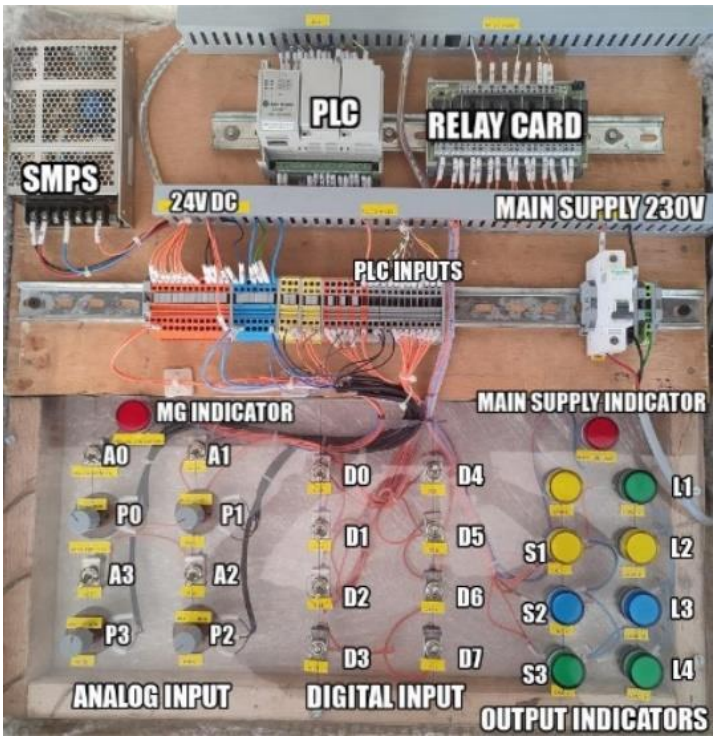

Figure 3.9. PLC-based control test bench

3.5.Design details of a Fuzzy logic controller

A fuzzy Logic Controller (FLC) is a computational paradigm adept at handling approximate reasoning, which is crucial for addressing systems steeped in inherent uncertainty or vagueness. It conceptualizes human knowledge using linguistic terms, providing a nuanced framework to navigate and control complex systems effectively. The various components of the Fuzzy Logic Controller include -

A. Fuzzifier: The fuzzifier serves as an intermediary, converting crisp inputs into fuzzy sets by assigning degrees of membership through predefined membership functions. These functions, including triangular, trapezoidal, Gaussian, and sigmoidal, are tailored to capture specific input data characteristics. For example, triangular functions offer simplicity and are well-suited for evenly distributed input values, while trapezoidal functions allow for more flexibility, accommodating asymmetrical distributions.

B. Fuzzy Inference Engine (FIE): Fuzzy Inference Engine (FIE) is defined as the core of the Fuzzy Logic Controller (FLC), responsible for processing fuzzy inputs and generating fuzzy outputs. It applies fuzzy logic rules, such as those defined in the Mamdani or Sugeno methods, to infer appropriate actions based on the given inputs. The FIE's role is to interpret the fuzzy sets generated by the fuzzifier, execute the fuzzy inference process according to the specified rules, and produce fuzzy outputs that guide the system's behavior. The decision-making engine navigates complex systems using fuzzy logic principles, providing adaptability and robustness in uncertain environments. Specifically, the Mamdani and Sugeno methods are briefly defined as:

- Mamdani Method: Named after Ebrahim Mamdani, this method employs fuzzy "if-then" rules to derive outputs, handling linguistic variables effectively and generating human-interpretable fuzzy sets.
- Sugeno Method: Resembling the Mamdani approach, the Sugeno method yields crisp output values derived from inputs via a weighted linear combination, offering computational efficiency, especially when precise numerical outputs are required.

C. Defuzzifier: Essential for decision-making, the defuzzifier converts fuzzy outputs into crisp values, typically by finding the centroid or center of gravity within the fuzzy output set.

D. Membership Functions: Membership functions are pivotal in shaping fuzzy sets and mapping input values onto linguistic variables. Triangular and trapezoidal functions offer specific advantages, such as simplicity, flexibility, and ease of interpretation. Triangular functions are particularly useful for evenly distributed input values, while trapezoidal functions accommodate asymmetrical distributions with greater flexibility [154-156].

Triangular and trapezoidal MFs have been employed in this present research, as referred to in the literature. These types of MF are easy to use and are more flexible, giving a single peak output value at the best instance. Besides, the min-max method for designing the MFS has been adopted as it provides a better platform considering the variability present in the input parameters. Mathematically, the triangular membership function can be defined as Equation 3.19.

$$f(x; a, b, c) = \max\left(min\left(\frac{x-a}{b-a}, \frac{c-x}{c-b}\right), 0\right) \tag{3.19}$$

Where x defines the input values for which membership values are calculated, and a, b, c defines the triangular membership function's first, middle, and last value. Further, as per the process mentioned above and the details, the following subsection demonstrates the design and details of the dual FLC in detail. For reference, Figure 3.10 presents a sample membership function using both trapezoidal and triangular membership functions, where x_1, x_2, x_3, and x_4 are the defining values for the variable (range). For example, considering the variable as battery state of charge, 'x' can be the percentage of the state of charge, where x_1 can be 20 %, and x_4 can be 70 % [155-156].

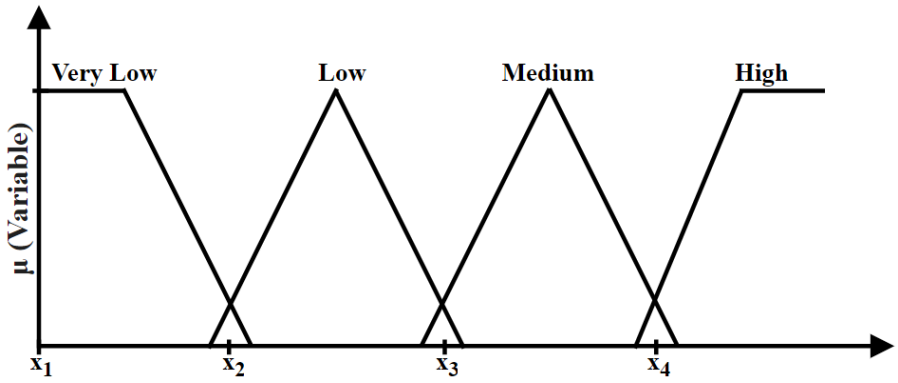

Figure 3.10. Sample membership function for a 'Variable'

Notably, the range of membership functions has been decided as per the following steps, i.e., variable understanding, defining linguistic terms, selecting membership function shapes, setting range for membership functions, selecting overlap value of membership functions, and lastly, tuning and validating the membership functions as per model testing/user observations. The brief explanation is as follows –

- Understand the Variables: Identify the input variables related to the developed microgrid system. For the present case, solar irradiance, wind speed and battery SOC have been considered and correspondingly, their min./max. values have been acknowledged.
- Define Linguistic Terms: Determine and understand the linguistic terms describing the input variables, such as best, good, poor, very poor, etc.

- Select Membership Function Shapes: Choose appropriate membership function shapes for each linguistic term. In the present work, triangular and trapezoidal shapes have been considered (explanation given above).
- Set Ranges for Membership Functions: Based on the input parameters, min./max. value and percentage of changes (depends on the context and the data distribution), the range for each membership function is selected, where data distribution includes data analysis to know where most data points lie. For example, the min./max. range of battery SOC is 0 % and 100 %, in that case, "Low" or "very poor" membership function range as 0-30 % and "Medium" or ("poor" + "Average") as 20-70 %.
- Overlap of Membership Functions: For smooth transitions and robust reasoning, 2-10 % of overlapping has been considered as a higher percentage of overlapping leads to increased ambiguity.
- Fine-tuning and validation: Lastly, the developed FLC is tested with random variable input to see the variation in output and further validation of the developed logic [157-159].

In detail, the membership functions working as the core of the proposed control approach are designed and implemented in the developed model as per the following steps.

- Investigation of each parameter's maximum/minimum value given IEEE standards system.
- Rationalize the parameters for system simplicity for better understanding and mapping per standards. For example, the voltage parameter (V) is converted into voltage deviation (%) for better understanding and mapping as per standards.
- Division of universe of discourse in sub-parts considering linguistic variables (Best, Good, …, Very poor). This division can be done in multiple sub-parts, whereas the 'number' of divisions is used to calculate the total number of fuzzy rules.
- Selection of the type of membership function according to system requirements. In the present case, triangular and trapezoidal membership functions are employed as the triangular membership function offers various advantages, such as robustness to noise and disturbances in input values, efficient computation, fast response with respect to a developed control algorithm, and adaptability with a wide range of input values. Besides, the trapezoidal membership function offers flexible and comparatively better handling of uncertain boundaries, easy and smooth computation of values, and improved accuracy for systems with an uncertain range of values.
- Development of membership functions in the FLC toolbox.

Lastly, tuning membership functions and dependent rules given applicability, feasibility, output accuracy, etc. In the present case, the tuning of membership functions (overlapping of

membership functions and rule base has been done as per the offline learning process using presumptions, simulation experience, and a literature survey [160-162].

E. Rules: Fuzzy logic rules encapsulate expert knowledge in "if-then" statements, using linguistic terms and fuzzy sets governing system behavior. For instance, "If the temperature is cold and humidity is high, then increase heating, "where cold, high, & heating are linguistic values defined by fuzzy sets on discourse temperature, humidity, & output universes.

The various advantages of the FLC are listed as follows:

- Handling Uncertainty: FLCs adeptly navigate uncertain, imprecise, or incomplete information, making them indispensable in real-world scenarios.
- Ease of Implementation: By assimilating human expertise and linguistic variables, fuzzy logic renders control systems more intuitive and development-friendly.
- Robustness: Fuzzy logic controllers exhibit resilience against noise or disturbances, ensuring consistent performance under varying conditions.
- Nonlinear Systems: Fuzzy logic's prowess extends to nonlinear systems, offering a more effective approach than traditional control methods.
- The choice between Mamdani and Sugeno methods hinges on considerations like system complexity, interpretability, and computational efficiency. While Sugeno is preferred for its numerical precision, Mamdani stands out for its interpretability and ability to handle linguistic variables effectively in various applications.

Thus, transitioning from the detailed microgrid design and modeling discussed in the current chapter, the next chapter introduces a control approach to enhance microgrid stability and performance. Particularly, Chapter 4 presents a centralized and a cascaded dual fuzzy logic controller (FLC), aiming at a stable PV/wind/battery-based microgrid system. While the centralized controller operates in multiple stages, the cascaded FLC considers both controllable and non-controllable parameters, dividing control into two FLCs for battery operation and stable microgrid operation under challenging grid conditions. The proposed controller(s) are praised for adaptability, user-friendliness, intelligence, and flexibility across different microgrid configurations and resource combinations, validating its robustness and universal applicability.

Chapter Summary

This chapter thoroughly conceptualizes microgrid design and modeling, emphasizing the integration of renewable energy sources such as solar PV, wind, and battery-based energy storage. The primary focus lies in developing a comprehensive microgrid model using the

MATLAB Simulink simulation tool, covering detailed modeling procedures for solar, wind, battery, and power converters. Additionally, the chapter delves into economic assessment using HOMER Pro software, highlighting critical factors like net present cost and renewable fraction. Furthermore, it explores the implementation of control algorithms through a PLC-based hardware test bench, offering insights into its block diagram, wiring architecture, and other details. Thus, focusing on the modeling concepts and information, the further chapters present the use of such models in validating the proposed control approaches, such as cascaded and centralized control approach, use of HOMER Pro for economic validation, and hardware test bench for implementation assessment.

CHAPTER 4
PROPOSED CENTRALIZED AND CASCADED CONTROL APPROACH FOR STABLE MICROGRID OPERATION

In a microgrid, perturbations from uncertain renewable sources and sudden load fluctuations can result in voltage, frequency deviations, and more deviations, leading to instability. Thus, this work presents an energy management system for microgrids, aiming to address instability caused by perturbations from renewable sources and load fluctuations. Firstly, the work presents a stage-wise control approach, utilizing a fuzzy logic controller with 64 rules, that focuses on stages involving managing minor perturbations and shedding non-critical loads during significant disturbances to stabilize microgrid operation. The analysis includes scenarios such as reduced renewable output and microgrid transitions. Further, the chapter presents a cascaded dual-fuzzy logic-based control approach that regulates system parameters like voltage, frequency, and DC-Link voltage. It incorporates a voltage regulator and considers nine controllable/non-controllable parameters to enhance stability. The proposed algorithm manages battery operation, microgrid mode of operation, and load management, improving stability under varied conditions. Lastly, the respective control approach is compared with existing control topologies, evaluating parameters including load voltage, frequency, and DC-Link voltage, such that the developed approaches exhibit lower deviations than existing methods, underscoring their effectiveness in achieving stable microgrid operation.

4.1.State-of-the-art work on a centralized controller

The high penetration of renewable and non-conventional energy sources (RNCESs) into existing power systems and their impacts are trending research topics. In this scenario, microgrid(s) (MGs) are independent micro-level power systems comprising different RNCES as distributed generator (DG) units, energy storage systems (ESSs), and loads interfacing the present power systems for a given electrical parameter [1, 7, 163]. These MG units are designed to provide the required voltage support for local loads and power flow control for the existing power system [164]. Among the MG types (AC, DC, and AC/DC), the AC/DC microgrid system is the most efficient, with maximum energy utilization. The AC/DC MG is a collection of interlinked renewable and conventional energy resources like photovoltaic (PV) and battery (DC source) with wind energy systems (AC source) and others such as electrolyzers and fuel cells [19]. These are connected to users (residential/commercial or others) and controlled by a controller to ensure efficient energy usage and storage. It leads to a more convenient way of interfacing the system with different categories of loads and the existing system via bi-

directional converters [13, 165]. Besides the simplicity of the AC/DC MG concept, the various issues related to its configuration, protection, uncertain output, and incredibly stable operation are of significant concern [1, 166]. It is of utmost importance that the designed system is proficient enough to cater to the electric load demand while working in the islanded mode of operation. In addition, it is also essential that the system adapts to any change while regulating the system voltage and frequency, aiming at its stable operation.

The battery storage device plays a vital role in providing ancillary support to the system and absorbing excessive power as per requirement [20-22]. However, the three control schemes have been identified in the literature, focusing on the MG system's voltage and frequency parameter regulation. These include - centralized, decentralized, and distributed control schemes. A comparative analysis for the same has been presented in [11]. However, considering the present state-of-the-art research, the centralized control scheme with fewer local controllers and the ability to handle critical operations with the least number of communication protocols can be advantageous and most influential [17, 167]. This issue can be addressed based on information and communication technology (ICT). Given the ideal central controller for low voltage and low power MG, such a technology involving high bandwidth communication, etc., is not required [168].

Converging on an islanded microgrid's voltage and frequency regulation, [169] proposed the fuzzy logic-based controller (FLC). This work considered the fuel-cell-based MG with voltage error and its derivative as the ambiguous inputs. Besides, the load disturbance is the critical parameter for validating the proposed scheme. Similarly, [96] developed the FLC for frequency and voltage regulation while aiming for MG stability. The source of disturbance has been considered in the form of fluctuating load and power generation. The outcome of this work highlights the significant performance of the storage devices in providing ancillary support to the system. Analyzing the performance of FLC for voltage control in PV-Storage MG, [161] presented a comparative study on FLC with the conventional PI controller. The work recommends using FLC over PI controller due to its fast response time and adaptive control. Like working for the frequency regulation in PV-storage-grid connected MG, [170] proposed an FLC targeting to balance renewable power and reduce grid power consumption. The work highlights the ideology of accurate power balance leading to efficient system parameter regulation. Working in an islanded mode of MG operation with a diesel generator, [14] acknowledged the FLC for MG frequency regulation. The work presents the control of battery operation, such as balancing the power demand and the MG stability. Highlighting the shortcomings of the droop controller [14], research work in [15] proposed a centralized control scheme for voltage and frequency regulation. The scheme shows the importance of storage

devices for better control and fast response to system fluctuations. Identifying the voltage and frequency deviation as critical parameters, [171] proposed a less complex FLC for stable MG. The work focuses on injecting the required power via battery storage and thus also managing its operation. Presenting the ideology of remote MG, [172] validated a fuzzy-based MG system with multiple renewable energy sources for improved voltage regulation using different real-time case studies. The simultaneous voltage and frequency regulation using FLC for islanded MG was also discussed in [173]. It validates the robust behavior of FLC under variable conditions and load fluctuation. Thus, it is evident that the researchers have explored the aspects of FLC in voltage and frequency control for stable MG operation. It highlights the significance of adaptive and robust FLCs for efficient voltage and frequency regulation.

Besides the work on fuzzy-based control for stable microgrid operation, various other control techniques have also been explored in the literature. Also, additional control techniques such as multiagent-based, model-predictive control, modified invasive weed optimization, consensus-based control, optimization-based supervisory control, metaheuristic optimization-based control, game-theoretic control, and supervisory control theory-based discrete power management strategy [174-175] are found in the literature. These control techniques serve different purposes in microgrid control, including maximum power extraction, optimal size calculation, active/reactive power management, controller parameter tuning, battery operation control, etc.

4.1.1. Microgrid Configuration and Development

The research model in this work investigates an MG system, as shown in Figure 4.1. The purpose of designing such a system is to incorporate the AC and DC power sources for the connected residential load in the presence of the uncontrolled rectifier and an inverter. The system includes a wind energy source (WES) of 40 kW capacity, a solar PV of 30 kW, and a lithium-ion-based battery energy storage system (BESS) rated at 360 V and 55 Ah. The figure shows that the power sources are connected through the AC/DC/AC converter modules with the DC link in the Perturb and Observe (P&O) based MPPT controller. Employing the P&O algorithm allows the connected converters to operate the PV panel and the wind turbine at peak power under varying conditions.

The system is designed for a total residential electrical load of 60 kW capacity, where 20 ± 5 kW is the critical load (CL), and 35 kW is the non-critical load (NCL). Notably, the capacity of different energy sources is calculated while considering various parameters, including the total load demand and efficiency of wind and solar energy sources. Wind energy system with higher efficiency (40 % - 50 %) than in comparison to solar energy (17 % to 25 %) is considered

to be of 40 kW renewable capacity, and the rest is estimated to be fulfilled by solar energy (30 kW capacity). Besides, the battery capacity has been calculated based on parameters like critical load demand (25 kW), backup time (considered as 25 – 35 minutes), battery terminal voltage (360 V), and depth of discharge (60 %) [149-150]. Further, considering the block representation of MG in Figure 4.1, the power system constraints and conditions are co-related as per Equations 3.1 to 3.3.

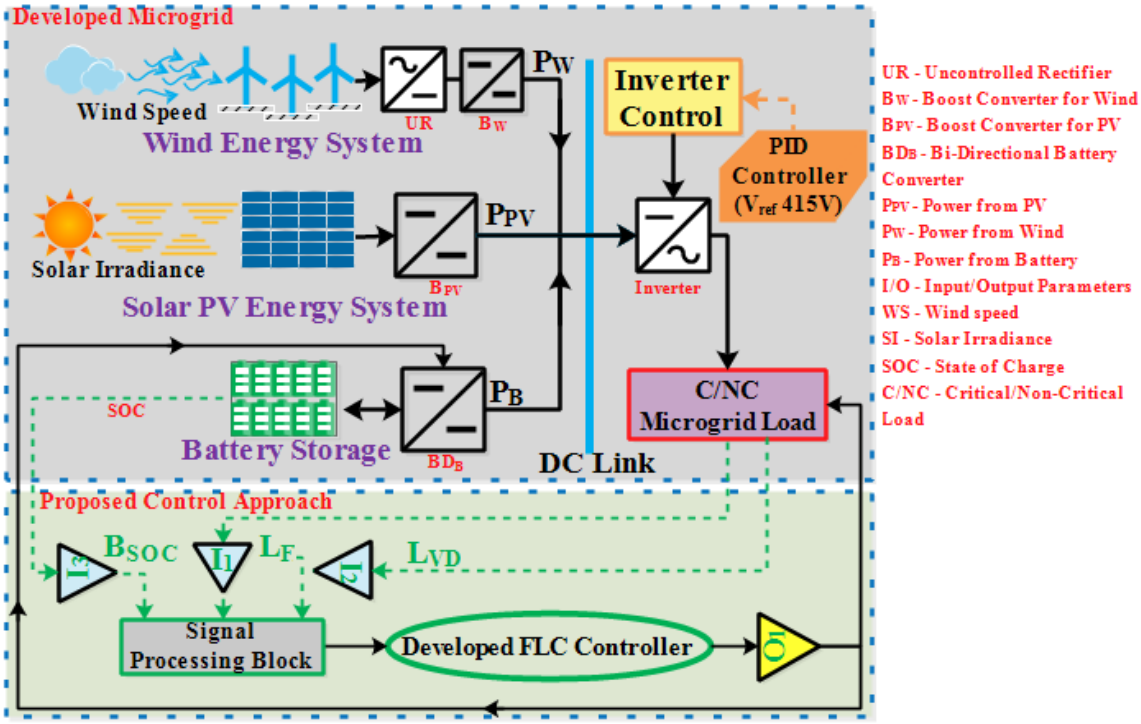

Figure 4.1. Microgrid model under investigation

Further, considering Figure 4.1 and aiming at the stable microgrid operation, I_x (x = 1 - 3) represents the various inputs like load voltage deviation (L_{VD}), load frequency (L_F), and battery SOC. However, the defuzzified output signal is represented by O_x (x = 1) as per the proposed control approach. The system configuration details used in MATLAB Simulink software and FLC details are in Table 4.1.

Table 4.1. System Simulink model configuration parameters and FLC functions

Parameter	Value
Simulation mode	Normal
Start and Stop Time	0 – 4sec.
Nominal voltage (Vrms)	415 V
Nominal frequency	50 Hz
Sample time (s)	Ts (2e-6)

Number of blocks and components	240/1245
Solver mode	Auto
Solver	ode23tb
Solver type	Variable step
Relative tolerance	1e-3
Parameter	Value
FLC	Struct
Type	Mamdani
And method	Min
Or method	Max
Defuzz method	Centroid
Imp method	Min
Agg method	Max
Input (s)	3
Output (s)	1
Rule (s)	64

4.1.2. Controller Design for Voltage and Frequency Regulation

The proposed three-stage control approach employing a fuzzy logic-based controller (FLC) has been presented in this section. The functional flowchart of the designed FLC is shown in Figure 4.2. The data from the parameter processing block is given to the designed FLC as per the figure. Sixty-four rules concerning input parameters and several linguistic variables have been developed inside the controller. The defuzzification process is based on the real-time simulation values, which deliver the crisp output value represented by the random variable '*x*'. Besides, based on the distinguished stage-wise control and aiming for simpler FLC, the decision-making has been performed using the output value of '*x*'.

From the figure, it is evident that with the value of *x* lying in the range of 0 – 1, the stage 1 control action will be initialized, followed by stage 2 action, when *x* lies in the output range of 1 – 2 and thus likewise. In addition to this discussion, the green dotted block in the figure presents the novel stage-wise control approach. It can be understood that the initial control stage is decided as per the random variable '*x'*. It depends upon the status of deviation in system parameters and battery SOC. After the initial control action has been executed, a different comparative algorithm is run, which compares the present deviation state with a feasible range of operations. If variations exceed the feasible range, the algorithm turns on to the next stage of control action. This loop is executed till maximum system stability is achieved. Because of this,

the voltage and frequency of the system are continuously measured. Also, the battery operates to stabilize these parameters along with the load-shedding algorithm.

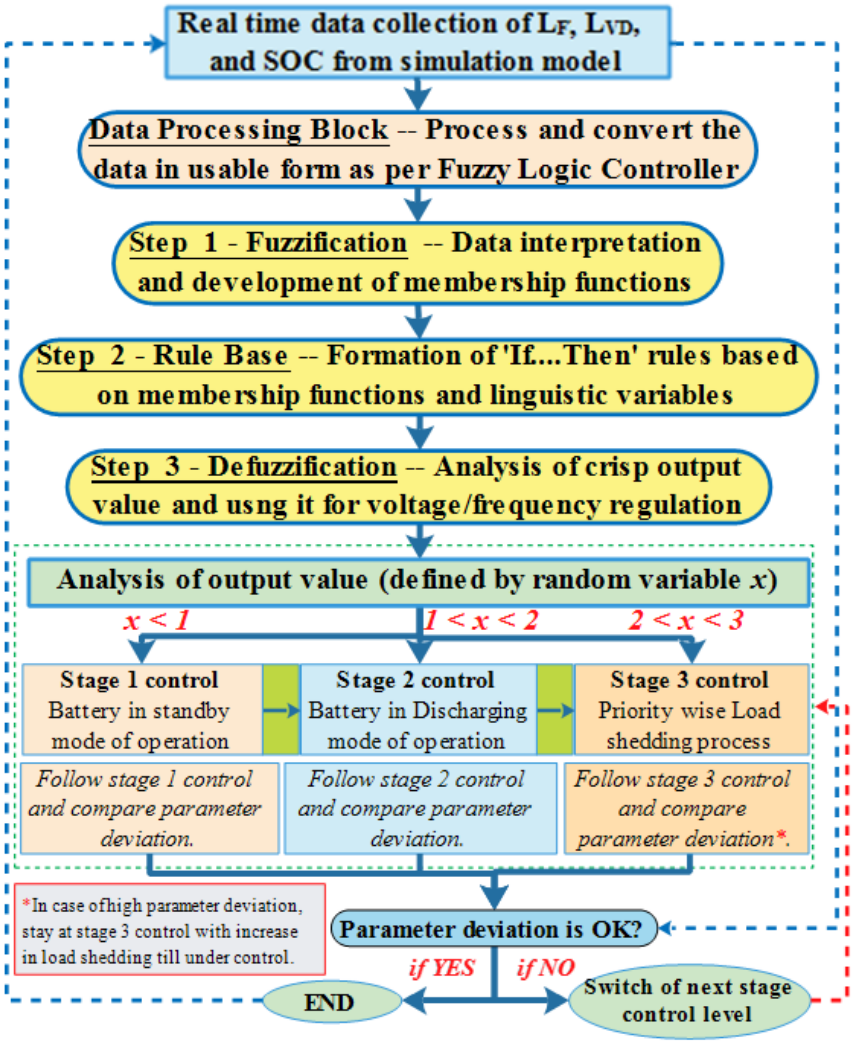

Figure 4.2. Working flowchart of proposed FLC and different control actions

A detailed discussion of the stage-wise control action can be described in the bullet points below. Notably, the key objective of the controller is to satisfy the maximum MG load demand while keeping the voltage and frequency in a feasible range of operation.

- Stage 1 – In case of unstable system conditions with a frequency lower than the standard level, the need for system parameter regulation should be fulfilled. The stage 1 control approach will focus on switching the battery from the charging mode to the standby mode of operation, thus utilizing the available power to satisfy the unmet load. Therefore, in such cases of small perturbations, the total power generated will be used optimally to balance the unmet load. Notably, in different instances where the frequency increases due to low power demand, the control approach will automatically turn the battery into a charging mode while keeping the system under stable operation. Besides, as shown in Figure 4.3, a conventional mathematical logic has been developed to send a signal to allow the sources to operate

where no power will be delivered. As per the figure, in the case of high battery SOC, low microgrid load, and high renewable energy generation, feedback in the form of battery state of charge and system frequency is sent to the comparator blocks. For SOC to be higher than 80 % and system frequency to be higher than 50.2 Hz, the comparator block sends a high signal (1) if the comparator satisfies the said range of parameters. Further, the AND gate sends a high signal for both power sources to perform the open circuit condition. If either of the parameters un-satisfies the comparator condition, the sources are connected back into the system for stable operation.

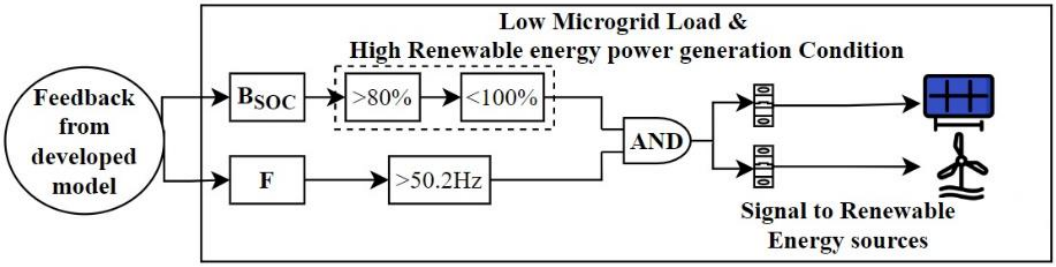

Figure 4.3. Operatable Condition

- Stage 2 – Following case 1, if the voltage/frequency fails to get regulated as per the feasible range of operation, the controller will shift its action to stage 2 control. Notably, in this stage, the battery will operate at its full potential per the system requirement to fulfill the available load demand. Thus, the system will observe the power generation via renewable sources and the battery storage (discharging mode of operation) with the 100 % load met condition as a critical constraint.
- Stage 3 – If voltage and frequency do not lie in a feasible and safe operating range, the controller will move towards the constrained solution of load curtailment. But, unlike the conventional load shedding criteria, the proposed controller will disconnect the available load as per load priority, i.e., disconnection of non-critical load step-wise (10 %, 20 %, …100 %) followed by the critical load on a priority basis if required. The process will continue until the system observes its maximum stability, when MG observes all concerning parameters in a feasible working range, and when the overall operation is stable. Mathematically, equation 4.1. represents the criteria for maximum stability (%) for the developed system. Notably, the parameters have been rationalized in percentage for the mathematical analysis. For voltage deviation parameters, - 10 % to 25 % are considered in the 0 to 100 % range. For load frequency, 49 Hz to 51 Hz have been considered in the 0 % to 100 % range, and the battery SOC has been considered in the 0 to 100 % operating range.

$$Stability_{max.} = Max.\{L_{VD(Best)\,(calculated)} + L_{F(Best)(calculated)} + SOC_{(Best)(actual)}\} \quad (4.1)$$

Concerning the sample mathematical calculation for analyzing the maximum stability (%), for example, the voltage deviation as per the system operation is approximately 2.5 %, i.e., 405 V concerning 415 V (Set system voltage), the calculated $L_{(VD(Best)(calculated))}$ for stability calculation will be 97.5 % approximately (100 % - 2.5 %). For the frequency parameter, where 49 Hz represents 0 %, and 51 Hz represents 100 % (1 Hz equivalent to 50 %), the 4 % deviation (49.92 Hz) will lead to 96 % of $L_{(F(Best)(calculated))}$. Besides, the battery SOC assumed to be 79 % is considerable in the calculation. Thus, substituting the values in equation 14 gives the considered system 97.5 % (maximum value) stability. Discoursing the FLC, the membership functions for the proposed controller are provided below in Figure 4.4, which shows the values for the Best, …., Very poor range of concerned parameters. Notably, the membership function range has been decided as per the details shared in Chapter 3 – Section 3.5.

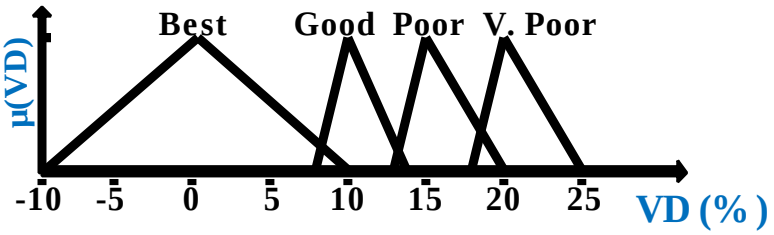

(a) Membership Function for load voltage deviation

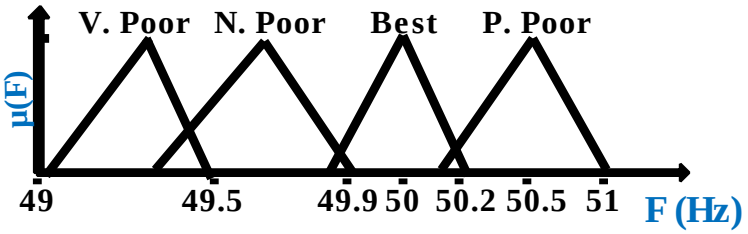

(b) Membership Function for load frequency

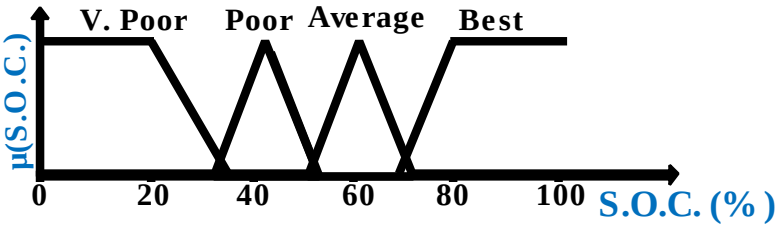

(c) Membership Function for battery SOC

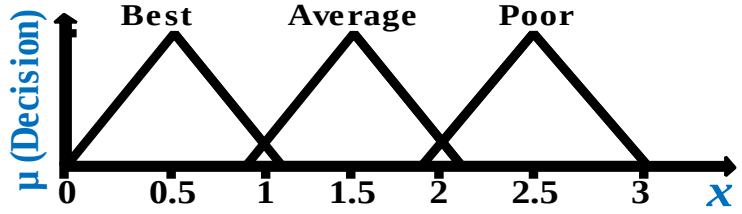

(d) Membership Function for output parameter '*x*'

Figure 4.4. Membership functions for developed FLC

Figure 4.4 presents the membership functions for the proposed FLC-based stage-wise control approach for voltage/frequency regulation and, thus, stable MG operation. In the figure, the 'x-axis represents the universe of discourse. For the given parameter, e.g., Figure 4.4(a), the universe of discourse varies from -10 % of voltage deviation to a maximum of 25 % of voltage deviation. Notably, the universe of discourse is mentioned in terms of parameter range. Likewise, for Figure 4.4(b), the universe of discourse (range) is from 49 Hz to 51 Hz. In Figure 4.4c, it varies from 0 – 100 %. The output parameter in Figure 4.4(d) ranges from 0 – 3. In detail, the membership functions working as the core of the proposed control approach have been designed and implemented in the developed model as per the details available in Chapter 3 – Section 3.5. For FLC reproducibility, the ranges of analytical values are below in Table 4.2.

Table 4.2. Details of parameter specifications for the proposed controller [176-177]

Parameter	Feasible Range and Membership Functions			
VD	Best (-10, 0, 10)	Good (8, 10, 14)	Poor (13, 15, 20)	Very Poor (18, 20, 25)
F	Very Poor (49, 49.225, 49.45)	Negative Poor (49.35, 49.65, 49.95)	Best (49.85, 50, 50.15)	Positive Poor (50.05, 50.525, 51)
SOC	Very Poor (20, 26, 32)	Poor (32, 40, 48)	Average (48, 55, 62)	Best (62, 71, 80)
Decision	Best (0, 0.55,1.1)	Good (0.9, 1.5,2.1)	Average (1.9,2.45,3)	

Where, VD is voltage deviation, F is frequency, SOC is battery state of charge, and Base Values are 415 V and 50 Hz. The best possible range for each case has been presented under the best/high membership function. Thus, summarizing the values, the permissible range of voltage deviation is ±5 %, whereas the allowable frequency deviation is ±0.2 %, with base values of 415 V_{RMS} and 50 Hz frequency. Besides, battery SOC is idealized to always lie in the high range of operation, i.e., the battery must be fully charged. It can be reconnected anytime for necessary ancillary support to the system. The three crisp decisions have been measured considering the output parameter. These decisions target the action based on specific stage control. For instance, a sample rule can be explained as follows - In case of high parameter deviations in the system, the proposed control approach will automatically take action as per stage 3. Likewise, stage one control will be initiated per the control approach, and the FLC rule base will be developed in case of minor deviations. Thus, focusing on the proposed FLC-based control scheme mentioned above, the scenarios and case studies investigated for validation are discussed in the next section. It includes scenarios such as a system with no controller, a system

with large perturbations, and a system with small perturbations. The comparative analysis with other control techniques/controllers is demonstrated in the next section.

4.1.3. Case Studies and Simulation Results

The three case studies investigated in this work on the voltage/frequency regulation via the proposed controller aiming for stable MG operation are listed below. Fluctuation in power sources has been considered in the range of 0 to 15 m/s wind speed and 0 to 1000 W/m^2 solar radiation for creating perturbations. However, for different cases, the level of fluctuation varies; like in large perturbations, the wind speed is gradually simulated to drop from 12 m/s to 3 m/s, and solar radiation is simulated to drop progressively from 850 W/m^2 to 130 W/m^2. Similar fluctuations are also assumed in the small-scale perturbations, such that partial shading, change in temperature, time of day, etc., act as critical factors [178]. Briefly, the three case studies present the following scope -

- Unstable system: The system will be investigated with a change in system parameters (Electric Load) without controller condition. The analysis will be based on how the system gets unstable and why there is a need to incorporate the proposed controller.
- Large-scale perturbation: The system is investigated under highly unstable conditions with large perturbations such that the third-level stage control is executed to balance the system operation. The situation is simulated with a decrease in renewable power generation and peak fluctuating load demand. The analysis will focus on how much the performance of the system parameters improves as per the step-wise control actions.
- Small-scale perturbation: The system will investigate medium-level stability issues like small changes in load and average renewable power generation. The analysis will focus on the battery operation and its role in balancing the system performance.

Correspondingly, the results and related discussion have been done below –

A. Results for Case Study 1 – Unstable System

The collected waveform data elucidates critical aspects of the system, such as Voltage, Frequency, DC-Link Voltage, and Total Harmonic Distortion (THD), within a perturbation scenario and without controller intervention. Figure 4.5(a) illustrates the voltage waveform, emphasizing substantial deviations that surpass the established operational range due to the lack of control input, indicating inherent instability. Similarly, Figure 4.5(b) reveals significant-frequency oscillations, emphasizing the need for robust control strategies to maintain consistent frequency accuracy. The DC-Link voltage waveform in Figure 4.5(c) demonstrates fluctuating amplitudes, highlighting the absence of stabilization mechanisms and the resultant departure

from optimal voltage levels. Figure 4.5(d) shows elevated THD levels, highlighting insufficient harmonic suppression without control. Observed parameter deviations undergo rigorous comparison against stipulated operational thresholds outlined in Table 4.2 and reference [34], emphasizing the pivotal role of control mechanisms in mitigating instability while preserving parameter fidelity. In particular, the system experiences an average 20.26 % voltage deviation, 2.68 % frequency deviation, 23.98 % DC-Link voltage deviation, and 11.21 % THD. In conclusion, this analytical exposition emphasizes the indispensability of control methodologies in reinforcing systemic equilibrium, optimizing performance profiles, and ensuring adherence to operational benchmarks.

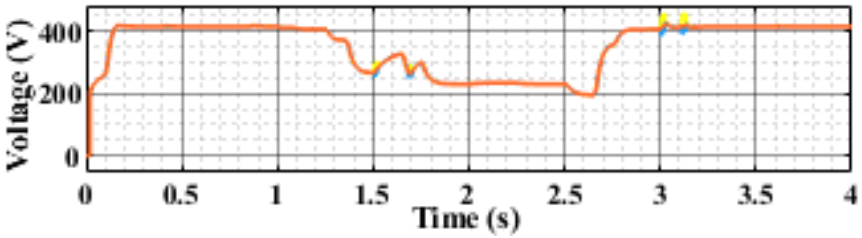

(a) Load voltage

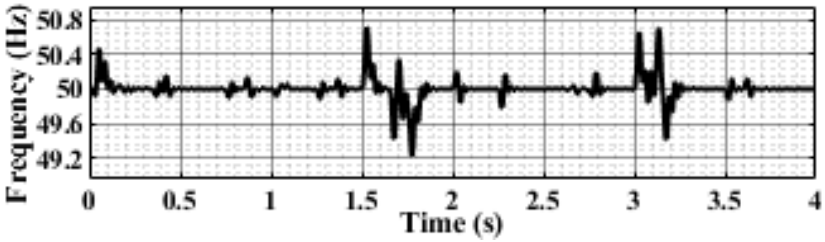

(b) Load frequency

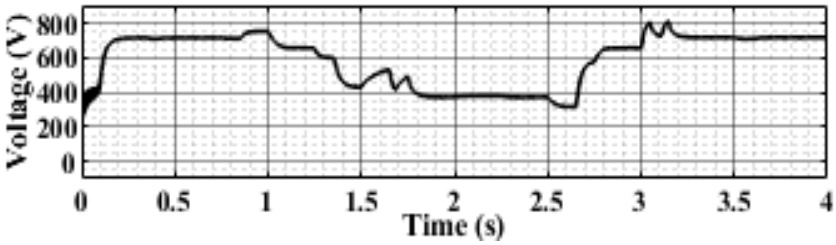

(c) DC-Link Voltage

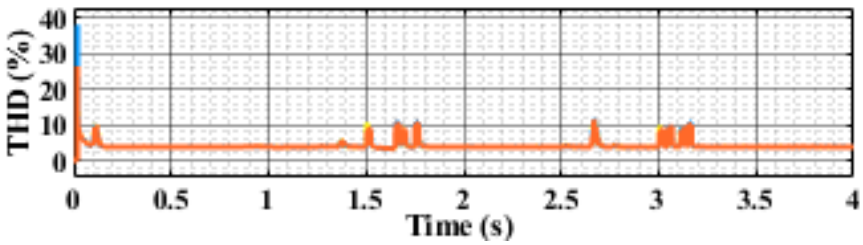

(d) Harmonics in Voltage Parameter

Figure 4.5. Results for Unstable System – Case Study 1

B. Results for Case Study 2 – Large Perturbations

The outcomes for case study 2 are graphically illustrated in Figure 4.6. The system encounters significant disturbances in this scenario, prompting the controller to assess the various system parameters. These parameters are then channeled to the proposed controller for further processing. The controller's analysis results in a definitive and precise output value, which triggers the implementation of stage-wise control strategies tailored to specific aspects of the system. The primary objective of these control strategies is to mitigate any deviations observed in the system's parameters from their intended values. Upon examining the results, it becomes evident that a particular phase, identified as stage 3 control, emerges. During this phase, a distinct behavior is observed in the battery's operational mode—it is found to be discharging. This insight is derived from the data presented in the analysis.

Further, Figure 4.6(a) illustrates the load voltage where the observed deviations are 0.72 %, Figure 4.6(b) represents load frequency for which observed deviations are 0.17 %, and likewise, 0.82 % DC-link voltage deviations and 4.11 % THD have been observed. In addition, Figure 4.6(d) illustrates net power-sharing dynamics, which portrays the interaction between different system components regarding power distribution. Notably, the reduction in the magnitude of deviations aligns with the initiation and execution of the control actions. Additionally, the results highlight the implementation of load curtailment, a strategic procedure aimed at achieving balance in system parameters. This process is visually depicted in Figure 4.7. Notably, this load curtailment is distributed based on a priority framework, with each connected load assigned a distinct level of importance within the system architecture. This prioritized approach to load curtailment aligns to ensure the system's stability and optimized performance.

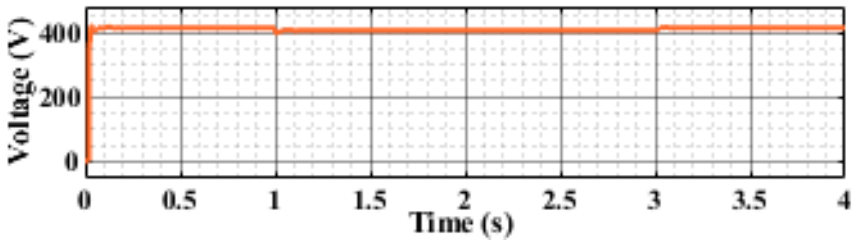

(a) Load voltage

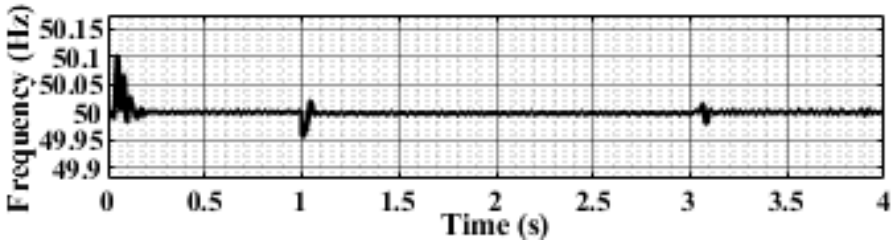

(b) Load frequency

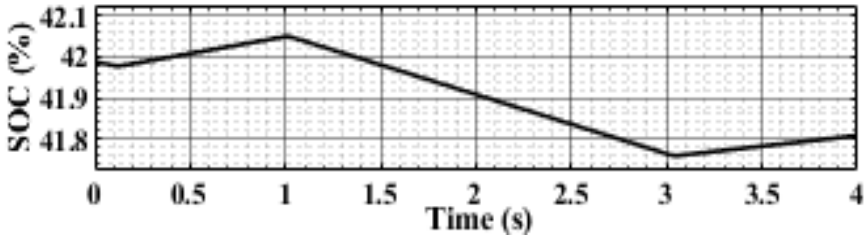

(c) Battery SOC

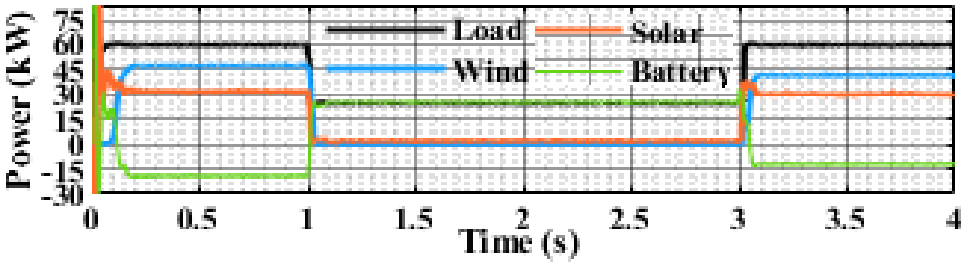

(d) Load Power sharing

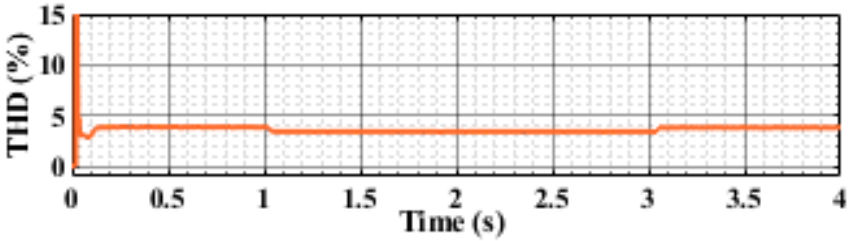

(e) Harmonics in Voltage Parameter

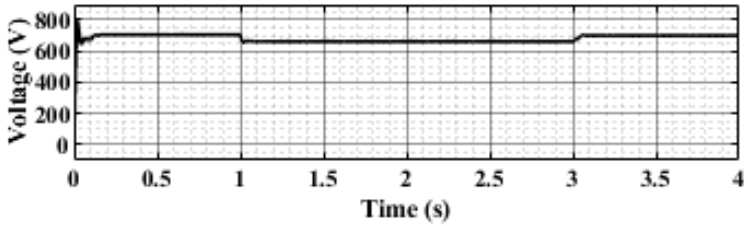

(f) DC-Link Voltage

Figure 4.6. Results for Case Study 2

C. Results for Case Study 3 – Small-scale perturbations

In the context of microgrid operation, this study delves into the prevailing scenario frequently encountered—a scenario characterized by small perturbations stemming from marginal fluctuations in power generation and the variable nature of load demand. With a specific focus on the simulation of fluctuating increases in connected load, this analysis centers on implementing stage 2 control. This strategic control approach leverages battery storage as an ancillary source to fulfill power demands while simultaneously regulating essential system parameters. The comprehensive findings, graphically represented in Figure 4.7, encompass a range of critical factors, including load voltage/frequency, battery state of charge (SOC), and other pertinent parameters.

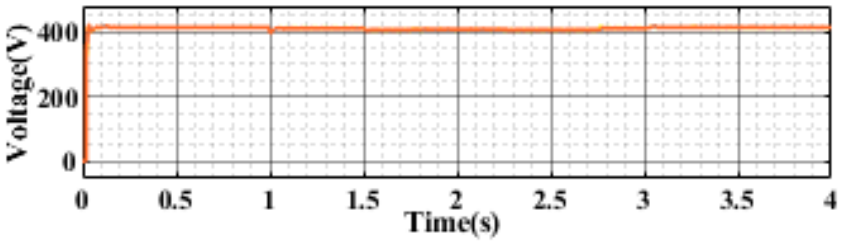

(a) Load voltage

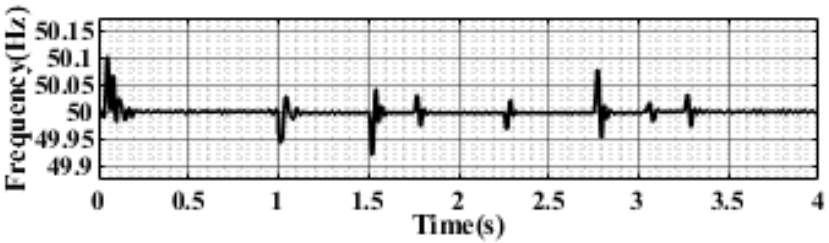

(b) Load frequency

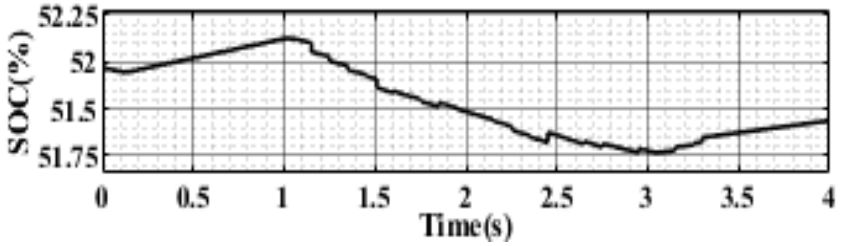

(c) Battery SOC

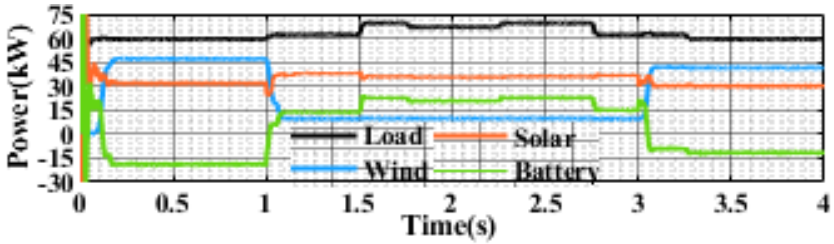

(d) Load Power sharing

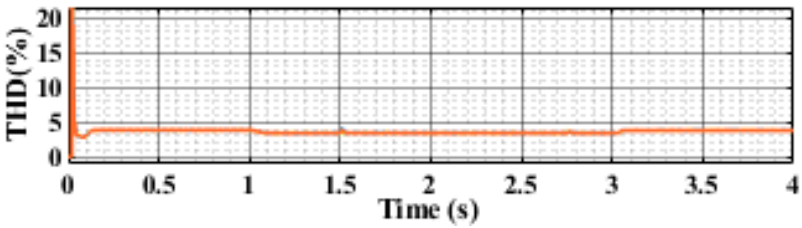

(e) Harmonics in Voltage Parameter

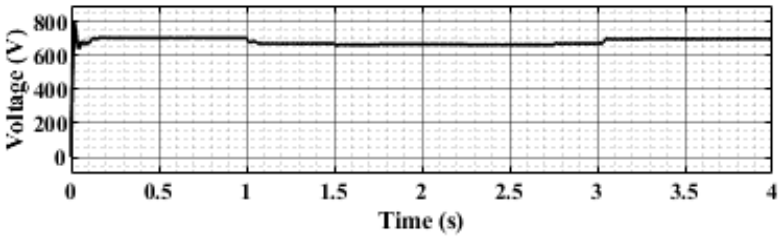

(f) DC-Link Voltage

Figure 4.7. Results for Case Study 3

As per the observations, the system experiences 0.57 % average voltage deviation, 0.14 % average frequency deviation, 0.71 % DC-Link voltage deviation, and 4.01 % average THD. Significantly, the system also experiences stable operation with accurate power sharing between different sources, and the battery acts as ancillary support. Notably, the observable fluctuations in the frequency waveform are attributed to the dynamic shifts in electrical load magnitude.

Crucially, the results emphasize the proposed controller's efficacy in promptly initiating stage 2 control by discerning deviations stemming from the subtle perturbations introduced through load augmentation. Furthermore, the battery's dynamic role emerges as a significant enabler of system stability, effectively adapting to variations in load and thereby significantly enhancing the overall operational equilibrium. Subsequent meticulous assessment emphasizes the compelling outcome that, facilitated by the devised control strategy, all pertinent parameters reflect deviations that adhere to the stringent IEEE standards, conclusively affirming the microgrid's robust and reliable operation [34].

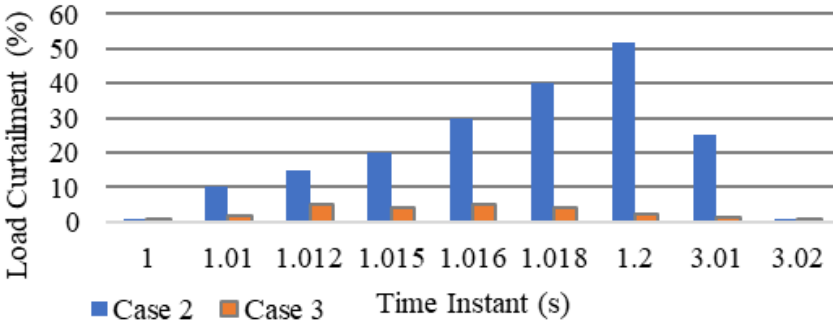

Figure 4.8. Percentage of load curtailment

Figure 4.8 shows the load curtailment percentage for cases 2 and case 3. It can be analyzed that with the required ancillary support from battery storage, the curtailment rate (%) in case study 3 is lesser than in case study 2. Further, Table 4.3 shows the tabulated data for deviations (%) present in the system parameters, i.e., Voltage, frequency, and DC-link Voltage. As per data and compared to case study 1, the developed system with the proposed controller tends to perform satisfactorily under the influence of significant perturbation.

Table 4.3. Summary of simulated results during the investigated time

Parameter / Case study	Average Voltage Deviation	Average Frequency Deviation	Average DC-Link voltage Deviation	Average THD
1	20.26 %	2.68 %	23.98 %	11.21 %
2	0.72 %	0.17 %	0.82 %	4.11 %
3	0.57 %	0.14 %	0.71 %	4.01 %

The results show that the system stability is most affected by the disturbance caused in the system for various reasons. As per the plots in Figure 4.5 – Figure 4.7, in Table 4.3, the impact of variable load and variable power generation on stability can be well analyzed. Besides, the role of battery storage in providing ancillary support to the system, such as maintaining the system's overall performance and regulating the MG parameters, can also be observed. However, the proposed FLC-based controller is the key to regulating the MG parameters and thus sustaining the system's stability. Notably, for each case demonstrated, the controller tends to stabilize the uncertainty present in the system with necessary decisions and quick action-making. Henceforth, an adaptive control approach is of utmost importance and necessary to balance such a system, aiming for its smooth and stable operation.

D. Comparative Analysis

The proposed controller has been compared with existing control topologies like the robust controller [179], the analytical approach [180], and a system without a controller under large perturbations. The parameters considered for this purpose include the electrical parameters – system voltage, frequency, and DC-link Voltage. In contrast, other parameters include decision-making time, power-sharing, and battery management efficacy. From Table 4.4, the improvement in the system performance can be observed as it experiences low deviation in the concerned parameters under the influence of the proposed stage-wise control approach.

Table 4.4. Comparative analysis with other controllers

Technique	Electrical Parameters Deviation				Other Parameters		
	Voltage (%)	Freq. (%)	DC-Link voltage (%)	THD (%)	Decision Making Time	Power Sharing Efficacy	Battery operation Efficacy
Without Controller	20.26	2.68	23.98	11.21	--	Poor	Poor
Robust Controller	2.54	0.721	2.05	4.98	Slow	Good	Average
Analytical Approach	1.34	0.64	1.78	5.012	Fast	Average	Average
Proposed Controller	0.72	0.17	0.82	4.11	Fast	Good	Good

Besides this, a similar system has been tested under the influence of a PI/PID-based controller, wherein the parameters, such as overshoot, settling time, and maximum and minimum settling value, have been analyzed. Notably, the PI and PID controllers offer simple implementation, robustness, fast response, and adaptability, making them reliable for stable microgrid control [181]. Accordingly, Table 4.5 below compares proposed fuzzy controllers with PI/PID controllers.

Table 4.5. Comparative analysis with PI/PID controller

Parameter / Controller	Overshoot (%)	Settling time (sec)	Settling max. (Hz)	Settling min. (Hz)
PI	5.63	0.46	52.815	49.271
PID	4.94	0.38	52.47	49.318
Proposed FLC	0.17	0.187	50.085	49.995

As per the table, it can be observed that the proposed FLC-based control approach outperforms the PI/PID-based controller. Regarding the overshoot, FLC shows 0.17 % overshoot, while the other controller shows 5.63 and 4.94 %, besides the other parameters proposed.

E. Sensitivity and Robustness Analysis

A sensitivity analysis for the proposed system has been done to inspect the effect of variation in input parameters (Solar Irradiance – SI, Wind Speed – WS, battery state of charge – SOC) and the dependence on initial ground conditions as large perturbations. Tables 6(a) and 6(b) present the developed system's parameter sensitivity analysis and the robustness analysis of the proposed FLC controller for stage-wise microgrid control. The input parameters, including solar irradiance, wind speed, and battery state of charge, are varied as per the respective units, i.e., W/m^2, m/s, and %, from the best value for investigation [182]. As per the observations, the developed system is susceptible without the proposed controller, so the highest variation in system parameters is observed. Significantly, with a slight change in the input value, the parameter deviates from the ideal value and thus leads to an unstable state of operation. However, in the presence of the proposed controller, the output parameters' standard deviation and relative variation (RV) concerning the change in input values are comparatively less.

Table 4.6(a). System Frequency Sensitivity Analysis

Condition	Parameter	Scope of Variation	Step	System Frequency				
				Min. Value	Max. Value	Mean Value	Standard Deviation	RV (%)
Without Controller	SI (W/m^2)	0-1000	75	49.15	50.52	49.68	0.2401	0.508
	WS (m/s)	0-15	1.5	49.12	50.67	49.56	0.2841	0.583
	SOC (%)	0-100	10	49.41	50.19	49.81	0.2101	0.400
With Controller	SI W/m^2)	0-1000	75	49.95	50.02	49.998	0.1041	0.011
	WS (m/s)	0-15	1.5	49.92	50.07	49.99	0.1042	0.051
	SOC (%)	0-100	10	49.99	50.009	49.99	0.051	0.0047

Table 4.6(b). System Voltage Sensitivity Analysis

Condition	Parameter	Scope of Variation	Step	System Voltage				
				Min. Value	Max. Value	Mean Value	Standard Deviation	RV (%)
Without Controller	SI (W/m^2)	0-1000	75	342.3	491.4	426.2	40.18	10.57
	WS (m/s)	0-15	1.5	338.1	495.1	429.1	42.65	13.96
	SOC (%)	0-100	10	367.5	464.2	421.9	9.167	2.17
With Controller	SI W/m^2)	0-1000	75	402.3	421.5	416.5	19.18	5.52
	WS (m/s)	0-15	1.5	399.8	425.8	419.4	24.65	6.96
	SOC (%)	0-100	10	409.5	416.0	411.2	5.167	0.47

In detail, as per the analysis done in Tables 4.6(a) and 4.6(b), it can be observed that the system is comparatively susceptible to the change in SI and WS values concerning battery SOC when considered under the system with no controller. For system voltage, the standard deviation is 40.18, 42.65, and 9.167. In contrast, relative variation (%) is observed to be 10.57, 13.96, and 2.17, concerning SI (observed minimum and maximum voltage: 342.3 - 491.4 V), WS (observed minimum and maximum voltage: 338.1 - 495.1 V, and SOC (observed minimum and maximum voltage: 367.5 - 464.2 V). The frequency parameter's standard deviation is also observed as 0.2401, 0.2841, and 0.2101. In contrast, relative variation is 0.508, 0.583, and 0.400 concerning similar input parameters, where the observed minimum and maximum frequency for change in SI is 49.15 - 50.52 Hz, minimum and maximum frequency for change in WS is 49.12 - 50.67 Hz, minimum and maximum frequency for change in SOC is 49.41 - 50.19 HZ.

With respect to this, the system with the controller has also been tested. The observations are as follows - for system voltage, standard deviation is observed to be 19.18, 24.65, and 5.167,

whereas relative variation (%) is observed to be 5.52, 6.96, and 0.47, with respect to SI (observed minimum and maximum voltage: 402.3 - 421.5 V), WS (observed minimum and maximum voltage: 399.8 - 425.8 V, and SOC (observed minimum and maximum voltage: 409.5 - 416.0 V). The frequency parameter's standard deviation is also observed as 0.1041, 0.1042, and 0.051. In contrast, relative variation is 0.011, 0.051, and 0.0047 with respect to similar input parameters, where the observed minimum and maximum frequency for change in SI is 49.95 - 50.02 Hz, minimum and maximum frequency for change in WS is 49.92 - 50.07 Hz, minimum and maximum frequency for change in SOC is 49.99 - 50.009 Hz.

Significantly, the developed system is characterized as moderately responsive, exceptionally stable, and resilient when confronted with fluctuations. It adeptly adjusts its system parameters in response to alterations in input conditions. This adaptiveness empowers the system to uphold its stability and dependability while remaining agile in changing dynamics.

Table 4.7. Fuzzy-based controller robustness analysis

Functional Parameters	Value		Concerned Output			
			Accuracy	Response Time	Complexity	Effectiveness
Possible number of input variables	Minimum	2	High	Low	Low	Low
	Maximum	6	High	High	High	High
	Present Case	3	High	Low	Low	High
Possible number of membership functions	Minimum	9	Low	Low	Low	Low
	Maximum	15	High	High	High	High
	Present Case	12	High	Low	Medium	High
Possible number of rules (for each parameter)	Minimum (considering 3 MFs)	27	Low	Very Low	Very Low	Low
	Maximum (considering 5 MFs)	125	High	High	Very High	High
	Present Case (considering 4 MFs)	64	High	Low	Low	High

The analysis provided in Table 4.7 showcases the resilience and effectiveness of the proposed controller when subjected to alterations in its functional parameters, employing the model-checking methodology. The assessed output factors, encompassing response time, complexity, decision-making accuracy, and more, experience fluctuations in tandem with the adjustments in the function parameters. Notably, the desired outcomes for the proposed controller consistently manifest as intended, encompassing notable accuracy, swift response times, minimal complexity, and pronounced effectiveness. This validation serves to emphasize the controller's robustness across diverse dimensions. It can be inferred that the developed system, fortified by the suggested fuzzy logic control approach, exemplifies substantial stability owing to its less sensitive and robust characteristics, even when influenced by varying parameters and functional circumstances.

4.2.State-of-the-art work on the cascaded dual fuzzy logic controller

Uncertainty conditions like the variable nature of renewable sources, fluctuating load, substandard battery storage operation, etc., affect the overall stability of MG operation. These conditions result in causing disturbances in the system in the form of parameter deviations [183]. Specifically aiming at stable MG operation, these constraints, such as uncertain conditions, maximum renewable extraction, the minimum percentage of unmet load, etc., need special attention [1, 7]. The stable MG operation signifies the proper and steady working of the system with minor fluctuations, minimum parameter deviations, etc. Such stable operation and control of the MG system require attention to the adaptive energy management system (EMS), reliable and secure MG operation, optimum use of storage devices, all parameters working in a feasible range, etc. Explicitly, the EMS should ensure the overall stability of the MG system, including decision-making like changes in the mode of operation and load management. The various features of EMS in MG control and its stable operation are well-discussed in [16, 184-185]. It mainly includes its ability to control the power flow of MG, leading to regulating system parameters for stable operation. Besides, it also leads to enhanced charging/discharging operation for storage devices. Various research studies have been published on stable MG operation and EMS, identifying electrical parameters like system voltage, frequency, DC-link voltage, and system power. These parameters have been classified into two major categories – controllable and non-controllable. Solar irradiance (SI), wind speed (WS), and likewise uncertain parameters are considered non-controllable parameters [186-187].

In contrast, DC link voltage, net power, battery state of charge, voltage, frequency, etc., are controllable parameters [33, 188-189]. The EMS for stable MG operation has been investigated in the literature, focusing on different combinations of such parameters and control strategies.

Besides, the literature highlights all the above parameters that influence the stable MG operation. However, considering the present state of research and uncertain conditions, intelligent and adaptive control techniques, especially fuzzy logic-based algorithms, need much attention due to their nature of solving complex, vague, and uncertain data-related problems. This user-friendly approach can provide a crisp and quick decision based on comprehensive data analysis of renewable sources, system parameters, etc., leading to an accurate solution to the present power system-related problem. Besides, it can be applied to any system configuration by changing the type and range of input parameters and a slight change in its rule base if required. Thus, focusing on the same, this section has reported some literature on fuzzy logic control (FLC) for MG's stable operation and EMS. An FLC with a conventional PI controller has been discussed in [158, 190] for the stable and smooth transition between the different modes of MG operation modes based on the system power, voltage, and battery state of charge. Considering the variable Photovoltaic (PV) and dependent battery storage-based hybrid system, robust FLC for improved EMS has been investigated [150]. As per the analysis, the effectiveness of the developed controller for stable MG operation has been justified, with all parameters settling in a feasible operating range. [157] employed the rate of change of energy and battery SOC as inputs for a less complex single FLC-based EMS aiming at MG stability. The system considers the uncertain conditions and the experimental setup for the system validation. Focusing on the robust FLC for EMS, [190] employed the fuzzy prediction interval model with net power and total system power as inputs and the demand side management (DSM) as the base output. This work validates the overall robustness and improved performance of the designed system with FLC while considering all the uncertainties. [159] proposes an FLC using the actual MG data, including battery SOC and fuel cell, for its stable operation. The designed approach improves the system performance but does not consider different operating conditions. [133] discussed the EMS for the hybrid MG system, focusing on applying FLC in decision-making for DSM and storage management. The work considers the net power and battery SOC as the core inputs and DSM as the output of the investigated controller. Considering DC link voltage, frequency, battery SOC, and voltage as inputs for the battery and frequency control, an adaptive FLC has been inspected in [162, 191]. However, it fails to consider system uncertainty and its impact on MG performance. The EMS aiming at the stable MG operation with RNCES power, SOC, and DC link voltage as critical inputs for FLC has been developed in [160, 192]. In addition, several other controllers and methods, such as fuzzy-based consensus control, rule-based system management, fuzzy-based energy management, adaptive neuro-fuzzy, and distributed control, have been reported in the literature, dealing with stable microgrid operation [148, 154, 193-194]. Likewise, the work in [195-199]

highlights the cascaded controllers combined with fuzzy-PID, PD-PI, optimized fuzzy, and PD-fuzzy-PID controllers for smooth operation and inverter control. A comparative analysis highlighting the different input parameters employed by various researchers while aiming at EMS and multiple decision-making for the stable MG operation is tabulated in Table 4.8.

Table 4.8. Comparison of the proposed approach with existing works

Reference No.	Input Parameters/Conditions										Output Parameters		
	V_{dc}	P_{net}	P_{mg}	SI	WS	SOC	V_{grid}	V_{mg}	F_{grid}	F_{mg}	Load management	Storage device management	Operating mode Management
[133]		✓				✓					✓	✓	
[148]						✓					✓		
[150]				✓		✓					✓		
[157]			✓			✓					✓		✓
[158]			✓				✓	✓			✓		✓
[159]						✓					✓	✓	✓
[160]		✓				✓					✓		
[162]		✓				✓		✓			✓		
[190]		✓	✓								✓		
[191]	✓									✓	✓	✓	
[192]	✓		✓			✓					✓	✓	
[193]		✓	✓			✓					✓		
[194]						✓					✓		
[195]	✓										✓		
[196]				✓	✓	✓		✓			✓	✓	
[197]								✓			✓		
[198]	✓									✓	✓		
[199]				✓	✓					✓	✓		
[200]		✓				✓					✓	✓	
Proposed Controller	✓	✓		✓	✓	✓	✓	✓	✓	✓	✓	✓	✓

Where, V_{dc} represents dc link voltage, P_{net} is net mg power, P_{mg} is total generated mg power, si represents solar irradiance, WS represents wind speed, soc represents battery state of charge, V represents voltage (grid and mg), f represents frequency (grid and mg), others include – fuel cell status, system current, PV temperature, rate of change of energy, and error derivatives, power forecast error.

4.2.1. Microgrid Configuration and Modeling

This work investigates the low-voltage MG system with a wind turbine of 40 kW rated capacity, a PV array of 30 kW, and an energy storage system formed via a lithium-ion battery pack with a rated voltage of 360 V and 55 Ah. All the power sources are connected with the DC link, followed by the conventional PI-based voltage regulator inverter circuit with a reference voltage of 415 V. Notably, the other RNCES can be connected in the present configuration to maintain the universal applicability of the developed approach. The change in respective configuration can be tested with a corresponding change in the type and range of the corresponding parameter while keeping the proposed control logic the same.

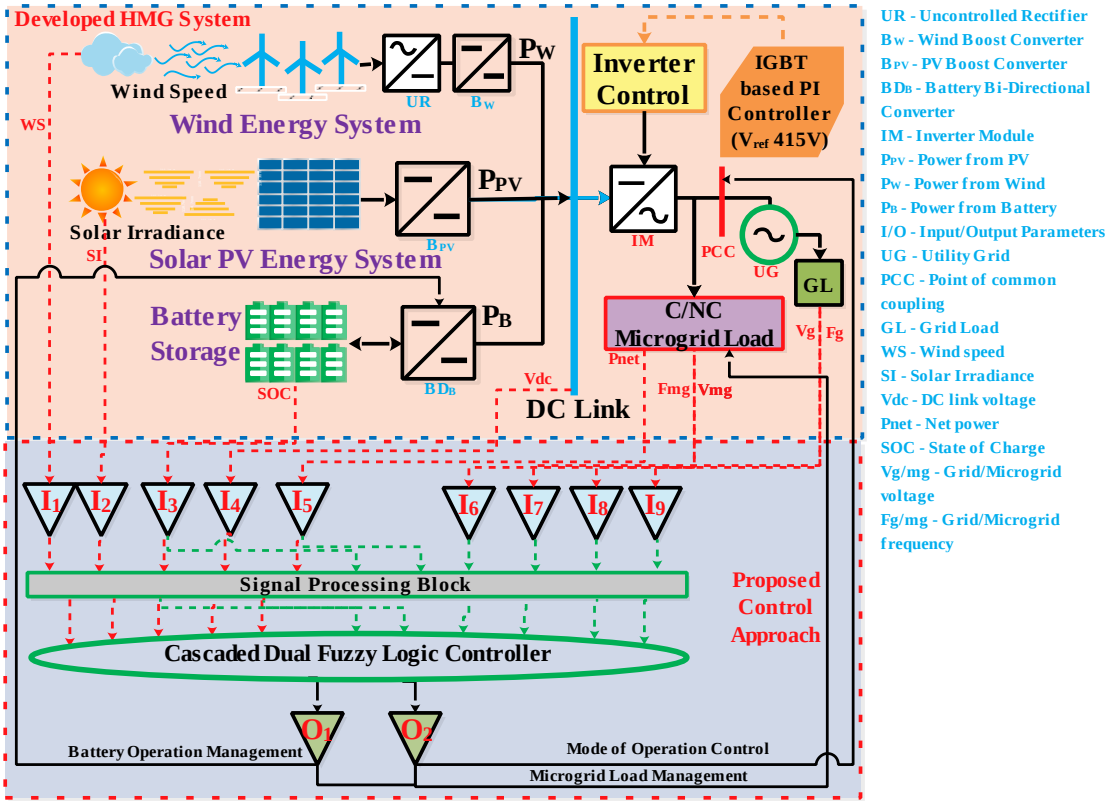

Figure 4.9. Proposed cascaded dual fuzzy logic controller-based microgrid model

A cascaded dual fuzzy logic controller has also been proposed. The nine electrical parameters as separate inputs (green and red dotted lines) and three decisions as outputs (solid black lines) have been shown in Figure 4.9. The benefit of the proposed cascaded scheme with PI-based inverter control is reflected in the system performance, which provides more robustness, adaptiveness, and flexibility in smooth operation. The proposed controller incorporates the different inputs (input signals) represented by I_x (where x = 1-9), including solar irradiance (SI), wind speed (WS), DC link voltage (V_{dc}), battery state of charge (SOC), and likewise the (output/control signals); O_x (where, x = 1 - 2) representing the defuzzified output signals for controlling the battery and related MG operation. A signal processing unit

processes the raw values of different parameters into their usable form to simplify the system configuration. For example, the input values for parameters, such as voltage, frequency, and net power shared, are applied as inputs into the signal processing block such that the values can be rationalized into a range of 0 to 1, where the rationalized value in the range of 0 – 0.5 is abnormal/negative and value in the range of 0.5 – 1 is normal/positive, respectively.

Further, these input parameters are processed into the individual FLCs where the controllers work in cascaded formation, i.e., in parallel combination to incorporate all the significant parameters leading to the appropriate decision making. The power converters have been used for appropriate conversion and synchronization of the system components. The electrical load connected to the system is classified as critical and non-critical load (CL/NCL) with a rated power of 20 ± 5 kW and 35 kW, respectively. The system configuration parameters used in MATLAB Simulink software and FLC details are tabulated in Table 4.9. The details include information such as, simulation time, sample time, solver type, number of FLC input and output parameters, number of rules, and defuzzification method.

Table 4.9. System Simulink model configuration parameters and FLC functions

Parameter	Value	Parameter	Value
Simulation mode	Normal	Consecutive ZCs steps	10*128*eps
Start and Stop Time	0 – 4 sec.	Max consecutive ZCs	1000
Nominal P-P voltage (Vrms)	415 V	FLC	Struct
Nominal frequency	50 Hz	Type	Mamdani
Sample time (s)	Ts (2e-6)	And/Or method	MinMax
Total number of blocks	240	Defuzz method	Centroid
Max/Min step	Auto/Auto	Imp method	Min
Solver/Solver mode	ode23tb /Auto	Aggregation method	Max
Solver type	Variable step	Input (s)/Output(s)	9/2
Relative tolerance	1e-3	Rule (s)	108/96

4.2.2. Proposed Cascaded Control Strategy

As shown in Figure 4.9, the designed MG model comprises three power sources, respectively. The dual-FLC has been developed to achieve smooth and stable system control. The developed control approach can also be implemented for other MG configurations. In contrast, the configuration change can be dealt with side-by-side changes in the type and range of input/output parameters to apply the proposed method for other configurations. Thus, this section discusses the proposed control scheme and its components.

A. Fuzzy Controller Design

As presented in Table 4.9, the controller block consists of a Mamdani-based inference system with the center of gravity technique for defuzzification dependent upon the number of input/output parameters and a designed set of rules. Unlike the Sugeno FIS, the Mamdani FIS has been considered because of its flexibility, accuracy, and improved results. It is important to note that the range and design of membership functions and the rules mapping are based on the offline learning process using presumptions, simulation experience, and literature survey. A detailed architecture of the proposed controller where the processed system signals and related decisions for stable MG operation and control have been showcased are presented in Figure 4.10. Following the signal processing unit, Figure 4.11 illustrates the membership functions used for the proposed dual fuzzy logic controller. In contrast, Figure 4.11(a) illustrates the MF for V_{dc}, V_{grid}, V_{mg}, F_{grid}, and F_{mg}. Figure 4.11(b) presents the net power (P_{net}) shared within the system following equation 2, Figures 4.11(c) and 4.11(d) represent the MF for SI in W/m^2 and WS in m/s for the MG system, and Figure 4.11(e) presents the battery SOC in percentage. Figures 4.11(f) and 4.11(g) represent the proposed system's output MFs.

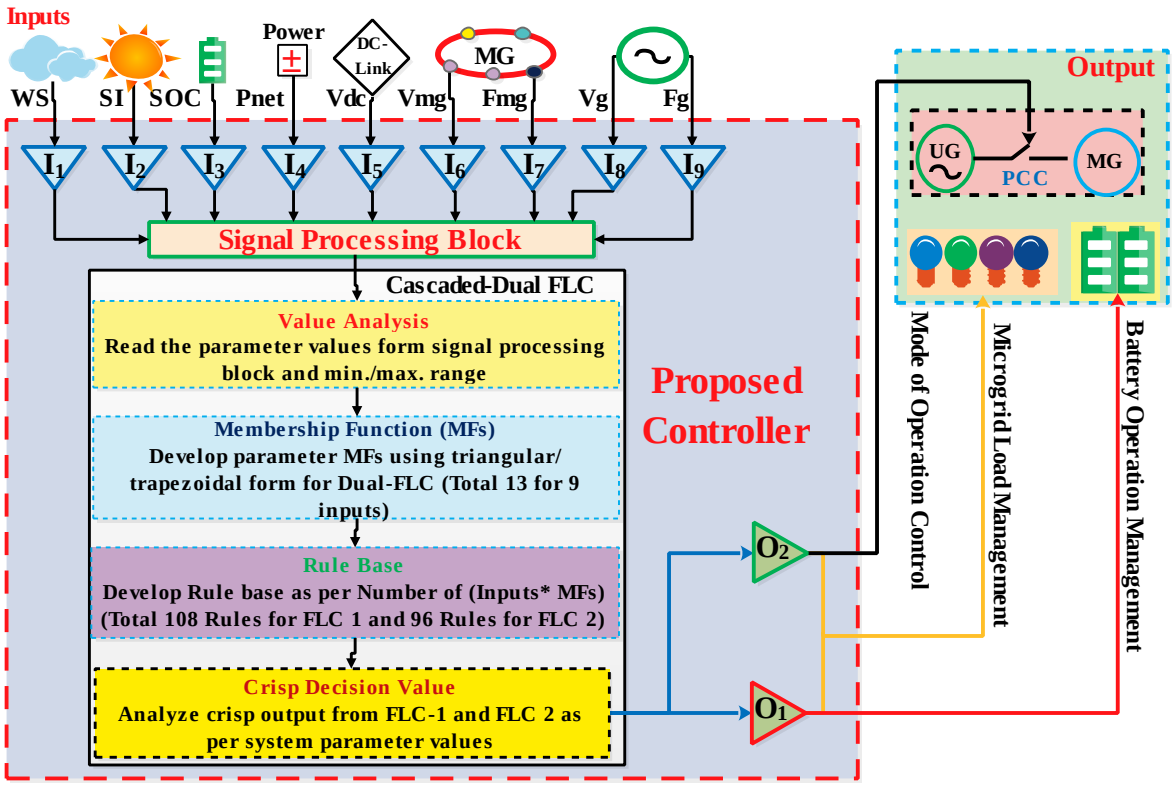

Figure 4.10. Detailed architecture of the proposed controller

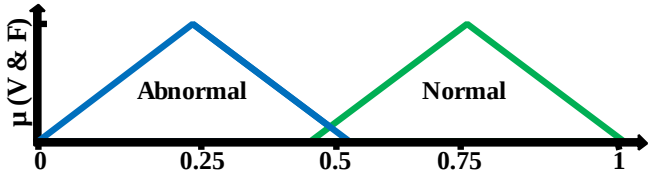

(a) Membership function for V_{dc}, V_{grid}, V_{mg}, F_{grid}, F_{mg}

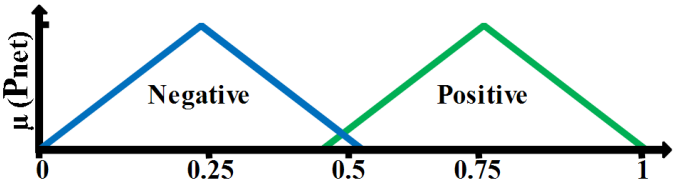

(b) Membership function for Net power shared

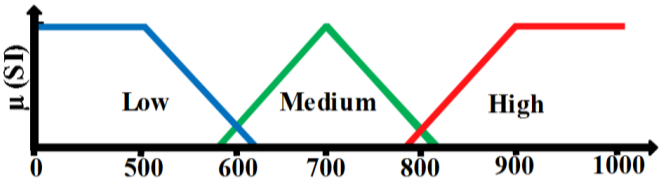

(c) Membership function for solar irradiance

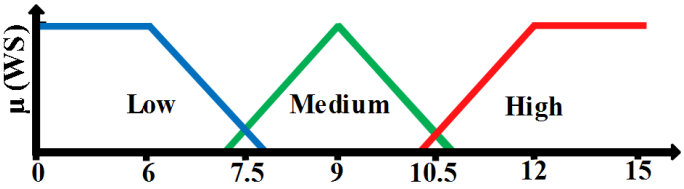

(d) Membership function for wind speed

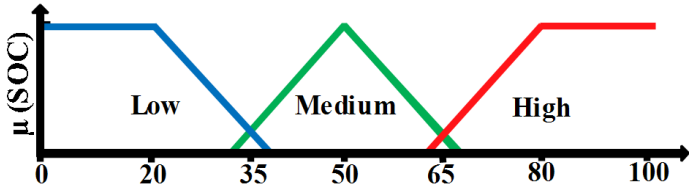

(e) Membership function for battery state of charge

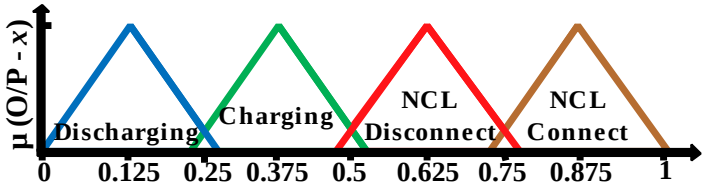

(f) Membership function for output – FLC 1

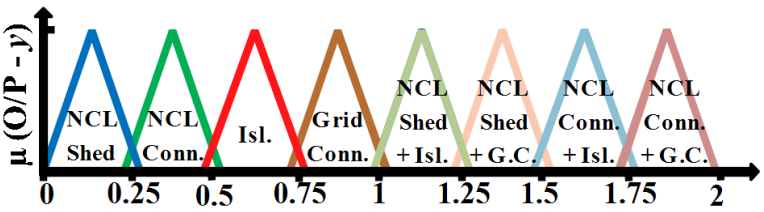

(g) Membership function for output - FLC 2

Figure 4.11. Input and output membership functions for FLC (1&2)

4.2.3. Developed Cascaded Dual-fuzzy logic-based controllers

As discussed before, the proposed dual FLC (1&2) has been presented in this subsection. Considering the proposed FLC-1 for battery operation and its management, Figure 4.12 illustrates its working flowchart, where the inputs to the controller include V_{dc}, P_{net}, SI, WS, and the battery SOC. The output is the decision for battery operation and load management (NCL) depending upon the condition of the input mentioned above parameters. This control's key objectives and novelty include – (i) charging/discharging battery storage and (ii) connection/Disconnecting of the NCL. As per the figure, the input parameters are processed to the Mamdani-based fuzzy inference system (FIS), resulting in the crisp output value further divided into sub-values/ranges considering the total number of decisions required.

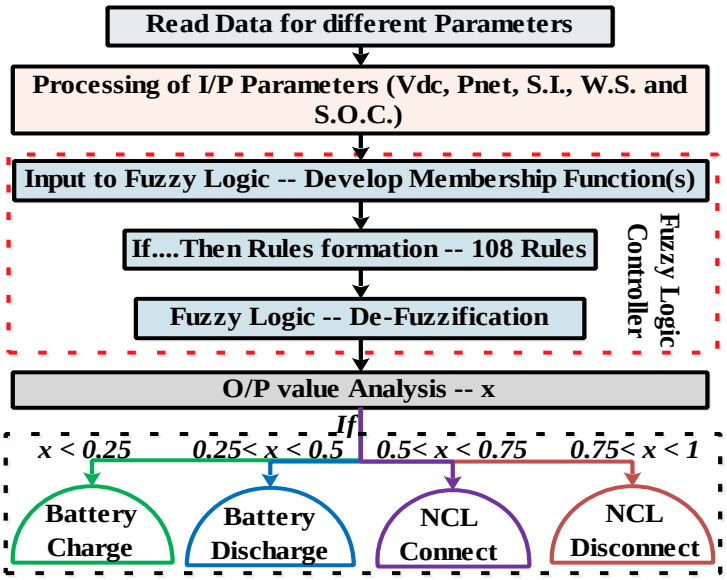

Figure 4.12 Flow diagram for battery management in microgrid

Likewise, the FLC-2 for improved load management and decision on the operating mode of microgrid operation based on different grid and MG parameters has been presented in Figure 4.13. As per the figure, input to the controller includes V_{grid}, V_{mg}, F_{grid}, F_{mg}, P_{net}, and battery SOC. The related outputs are the individual and a combination of various decisions like shedding/connecting of NCL and islanding/grid-connected mode of MG depending upon the condition of the input parameters as mentioned above. Notably, the frequency parameter plays a vital role in considering the connection and disconnection of NCL from the system. For maintaining the stable microgrid operation, fuzzy-based load shedding to stabilize the system has been considered one of the most dominant solutions in literature [5, 156, 201-203]. The objectives and novelty of this control scheme are in the combination of the mentioned criteria – (i) microgrid load management and (ii) decision on the operating mode of MG operation, i.e., smooth transition between grid-connected and islanded mode.

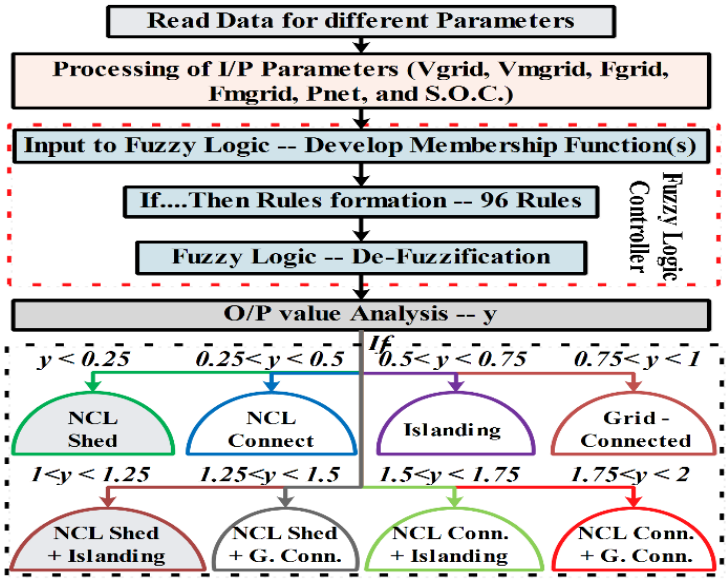

Figure 4.13. Flow diagram for load management in microgrid

The most important aspects of designing FLC are the membership function and matching rule base. Figure 4.12 presents the MFs for the proposed controller, whereas Table 4.10 and Table 4.11 present the sample set of rules for the proposed cascaded dual fuzzy logic controllers, where Isl. represents islanding, GC represents grid-connected**,** Dis. Ch. represents Discharging, L. Sh. represents Load Shedding, LC. represents Load Connected.

Table 4.10. Sample rules for FLC – 1

Rule No.	V_{dc}	P_{net}	SI	WS	SOC	Decision
12	Abnormal	Negative	Medium	Low	High	Dis. Ch.
31	Abnormal	Positive	Low	Medium	Low	Charging
55	Normal	Negative	Low	Low	Low	L. Sh.
72	Normal	Negative	Medium	High	High	Dis. Ch.
108	Normal	Positive	High	High	High	LC.

Table 4.11. Sample rules for FLC – 2

Rule No.	V_g	F_g	V_{mg}	F_{mg}	P_{net}	SOC	Decision
19	Abnormal	Abnormal	Normal	Normal	Negative	Low	Isl. + L. Sh.
48	Abnormal	Normal	Normal	Normal	Positive	High	Isl. + LC.
60	Normal	Abnormal	Abnormal	Normal	Positive	High	Isl.
80	Normal	Normal	Abnormal	Normal	Negative	Med.	GC + L. Sh.
88	Normal	Normal	Normal	Abnor.	Positive	Low	G.C
96	Normal	Normal	Normal	Normal	Positive	High	G.C. + LC.

For the FLC, as mentioned above (1&2), the range and base value of the different parameters for the present research and other details are tabulated in Table 4.12.

Table 4.12. Design details for developed membership functions

Parameter Type	Parameter	Base value	Mapped value	Best feasible range
Input	V_{grid}	415 V	0 – 1	395 - 435
	V_{mg}	415 V	0 – 1	395 - 435
	V_{dc}	700 V	0 – 1	665 - 735
	F_{grid}	50 Hz	0 – 1	49 – 50.5
	F_{mg}	50 Hz	0 – 1	49 – 50.5
	P_{net}	0	(-)1 – 1	As per eq. (2)
	SOC	50 %	20 - 80	0 - 100
	SI	750 W/m^2	500 – 1000	600 - 1000
	WS	9 m/s	6 - 15	7.5 - 15
Output	FLC-1	0.5	0 - 1	0 - 1
	FLC-2	1	0 - 2	0 - 2

As per the table and design logic, the base value has been selected for different parameters processed to the signal processing block as the reference value. Notably, the parameters are chosen based on the feasible operating range, i.e., ±5 % for voltage parameters and likewise. As per the standard guidelines and specific set of relations, the signal processing block compares the actual value with the reference value and converts the same in the normal or abnormal range. For example, the system frequency is fed to the processing block, compared with the reference values. If the actual value lies in the feasible range of operation (49.5 – 50.2 Hz), the output signal falls in the normal range, whereas if the value is less than 49.5 or greater than 50.2 Hz, it is considered an abnormal frequency value.

A similar process is followed for other parameters, whereas SOC, SI, and WS are fed directly to the FLC. The P_{net} is calculated and processed to the controller as per equation 2, where the positive value of P_{net} is favorable. Thus, for the stable MG operation comprising of P.V./wind/battery storage power sources and the critical and non-critical load, the dual-FLC (1 & 2) has been developed. The total number of rules for the FLCs are 108 and 96, respectively, whereas all MG parameters have been considered for specific control operations.

4.2.4. Results and Discussions

The simulation results for 6 case studies covering all the possible and feasible conditions have been showcased in this section. It is noteworthy that the key parameters, including F_{mg}, V_{mg} (RMS), V_{dc}, $P_{net,}$ and battery SOC, are observed under different conditions to validate the proposed dual-FLC performance. For the simulation purpose, the considered perturbations are represented in Figure 4.14, where for 0 – 0.5 secs. and 3.5 – 4 sec., the graph shows the ideal state of resources, and from 0.5 – 3.5 sec., the graph shows the degraded value of both resources, such that uncertainty given large and small perturbations can be observed. Notably, under large perturbations, the wind speed drops as low as 3.2 m/s, and solar irradiance drops to 260 W/m^2, and for small perturbations, these values range higher, i.e., 6.5 m/s and 560 W/m2, respectively.

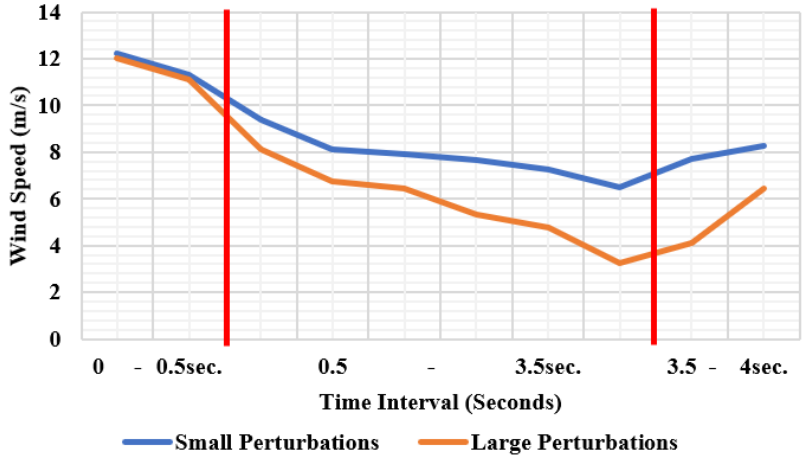

Wind

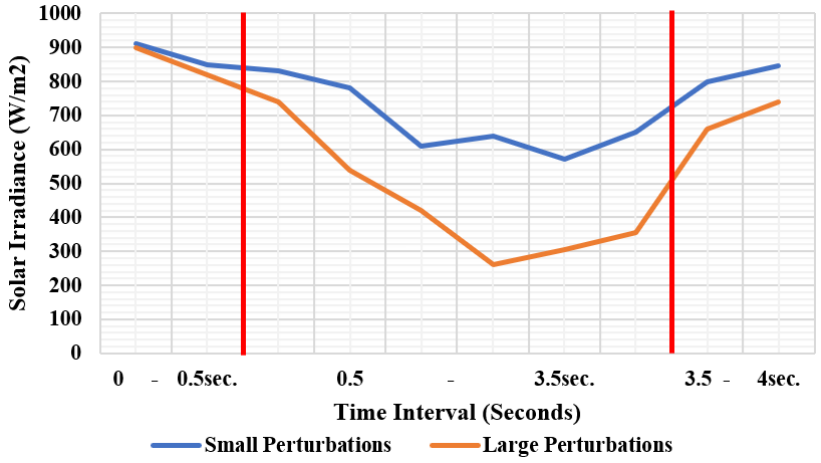

Solar

Figure 4.14. Considered perturbations in Wind and Solar

Further, Figure 4.15 represents the professional square process chart illustrating the different case studies. Likewise, the line diagram of the simulated system concerning different case studies has been presented in Figure 4.16.

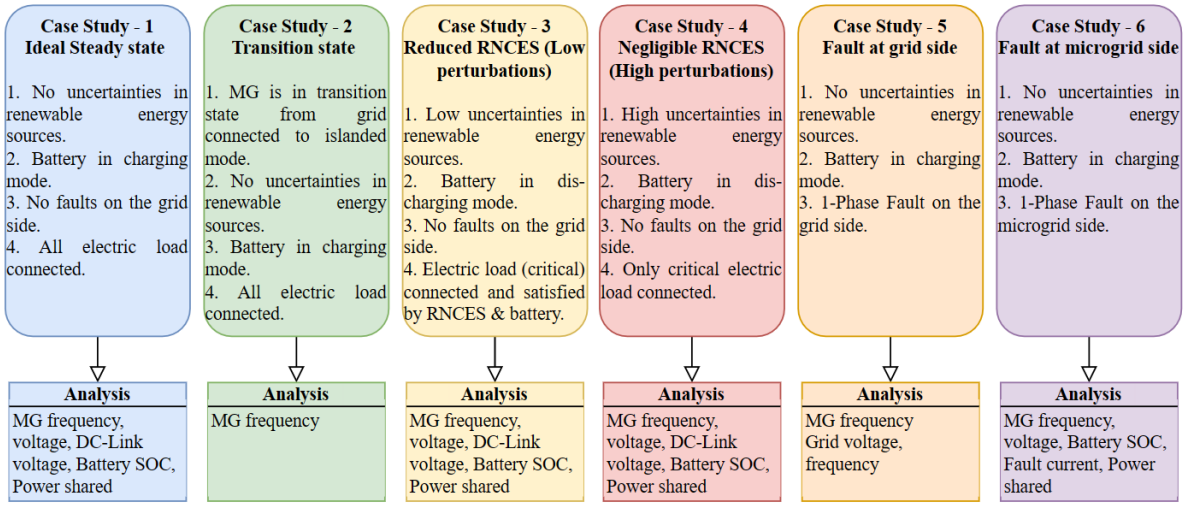

Figure 4.15. Square process chart representing the performed case studies

In detail, Figure 4.16(a) discloses the ideal state of an MG, such that all the input parameters (for example, solar irradiance and wind speed) for the simulated model are considered ideal. Further, Figure 4.16(b) discloses the transition state, i.e., the state where the MG parameters are analyzed under the effect of change in the mode of operation from grid-connected mode to islanded mode. Furthermore, Figure 4.16(c) presents conditions where the RNCES are reduced in nature, i.e., reduced solar irradiance and wind speed with battery SOC as a medium. Further, Figure 4.16(d) presents the system with almost negligible RNCES, i.e., the MG relies on the battery as the primary power source. Furthermore, Figure 4.16(e) presents the case study, including the MG analysis considering a fault in the utility grid (UG). Lastly, Figure 4.16(f) presents the case study incorporating the effects of a fault on the MG side. Considerably, in the figures, the green color highlights the positive nature of all the components (with respect to the ideal conditions), the red color highlights the harmful nature of the components, and "F" represents the fault location. Notably, the analysis for all parameters considered in the afore-mentioned case studies is as per the CERC Staff Paper March 2011 under the Indian Electricity Grid Code (IEGC) and recommended IEEE standards 1547 and 2030 [176, 204-205].

In the figure, the healthy state of the system is represented by green color and vice versa; red color represents the unhealthy component of the system. For PCC, red indicates the breaker is normally open, whereas the arrow indicates the transition mode condition for PCC. Besides this, the down arrows in the Figures 4.16(c) and 4.16(d) represent the state of reduced RNCES output and Negligible RNCES output, respectively.

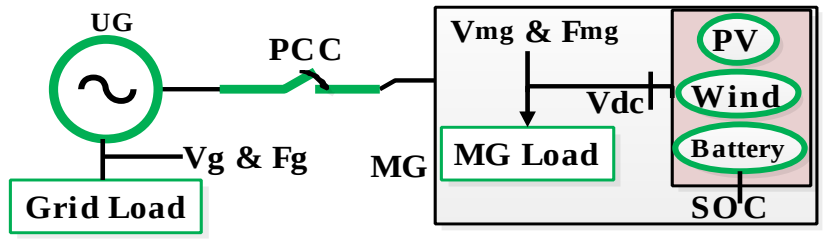

(a) Ideal state case study

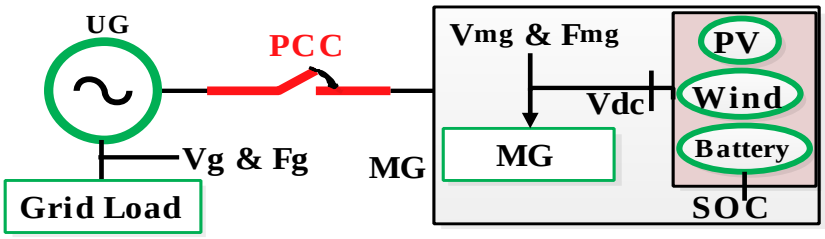

(b) Transition State case study

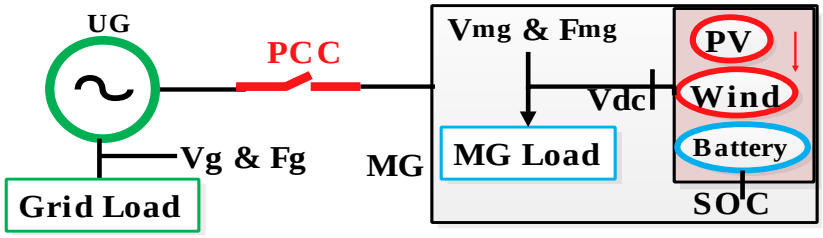

(c) Reduced RNCES output case study

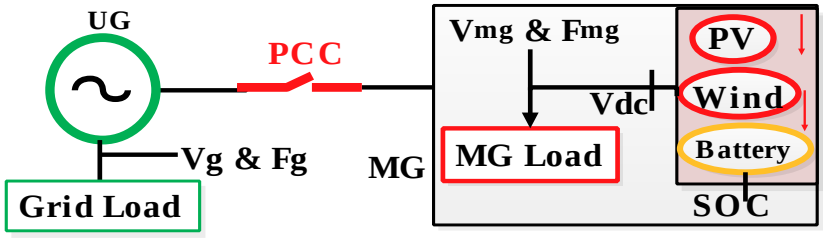

(d) Negligible RNCES output case study

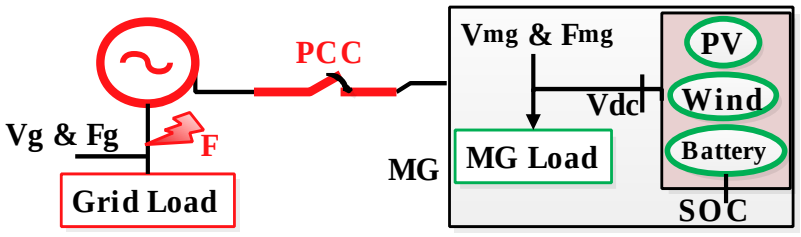

(e) Fault at grid end case study

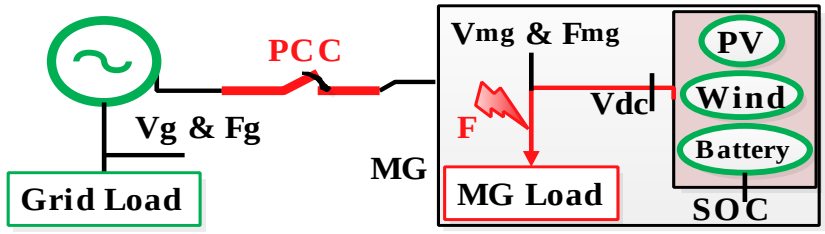

(f) Fault at MG end case study

Figure 4.16. System Line/block diagram under consideration for different case studies

A. Case Study-1: Ideal steady-state condition

This case presents the ideal MG operation, i.e., grid-connected with all power sources working in healthy condition and all CL/NCL connected. The results for this case are presented in Figure 4.17. Notably, P_{net} is positive, and the all-electric load of the MG system is fulfilled. Also, the battery storage will be in charge mode.

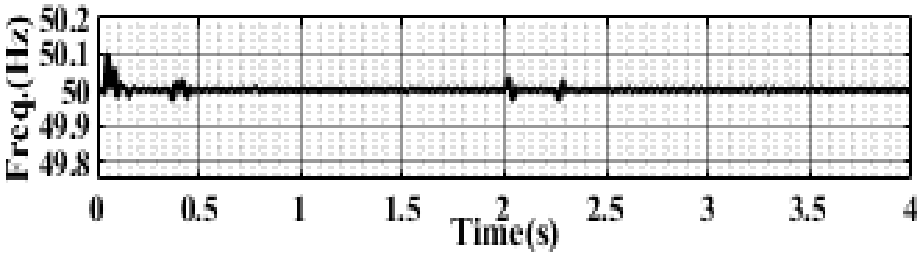

(a) Load frequency with the proposed controller

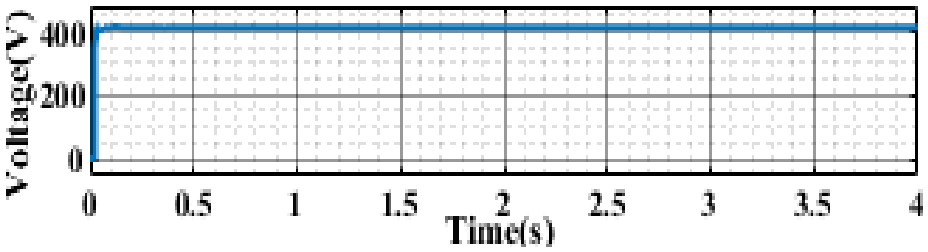

(b) Load Voltage with the proposed controller

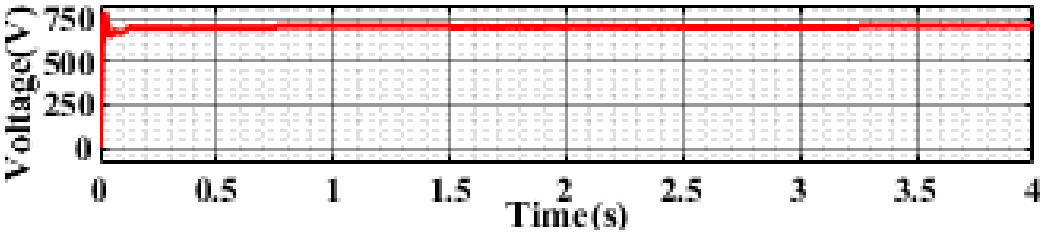

(c) DC-link voltage with proposed controller

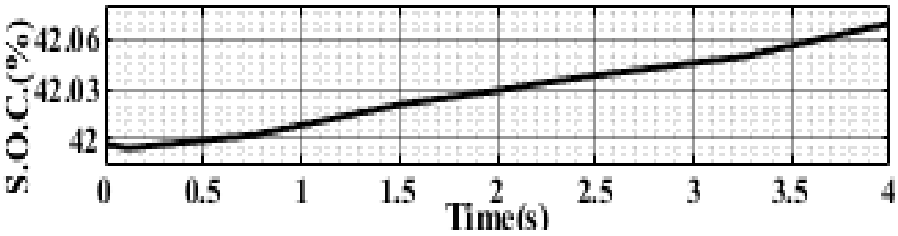

(d) Battery SOC with the proposed controller

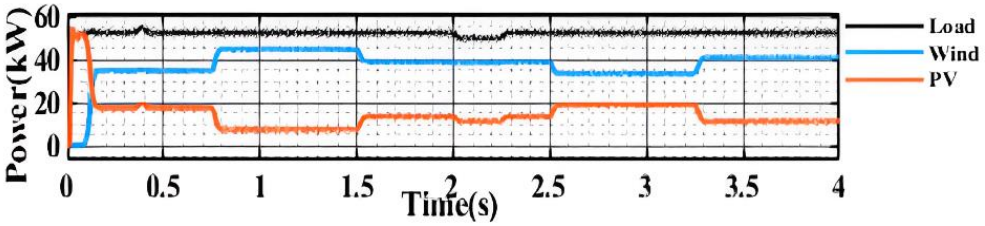

(e) Net power Shared with the proposed controller

Figure 4.17. Results for Case Study - 1

Figure 4.17(a) presents the F_{mg} with a nominal value of 50 Hz ranging from 49.99 Hz to 50.084 Hz. It considerably shows the system frequency with the proposed controller. Likewise, Figure 4.17(b) illustrates the RMS value of V_{mg} where the nominal value is 415 V. Figure 4.17(c) presents the $V_{dc,}$ which is maintained stable under variable WS and SI with a nominal value of 700 V along with 0.845 as the inverter modulation index value. Similar to system frequency, slight deviations can be observed in V_{mg} and V_{dc}. Notably, the level of deviations is not as high as the ideal conditions observed in this case. Figure 4.17(d) presents the battery SOC under the controller conditions. The figure shows the battery in charging mode under controlled conditions, which is valid for ideal operating conditions. Figure 4.17(e) illustrates the P_{net} shared in the system. The variation in power generated results from variable input to the system (WS and SI). With all parameters lying in the feasible range of operation, the MG is healthy and stable.

B. Case 2: Transition from grid-connected – islanded – grid-connected mode of operation under ideal conditions

Similar to case 1, the impact of the mode of operation on the system parameters has been presented in case 2. As per the literature, MG frequency (F_{mg}) has been considered the most critical parameter and is represented in Figure 4.18. The figure shows the instant change in the operation mode from grid-connected to islanded mode at 1 sec. And back to the grid-connected mode of operation at 3.5 sec. of total simulation time. With the change in the mode of operation, the system without a controller observes more frequency deviation than a controller. Thus, considering the transition condition, the FLC controller performs satisfactorily. Besides, it is noteworthy that all other results follow a trend similar to case 1, as all other conditions have been considered ideal and healthy.

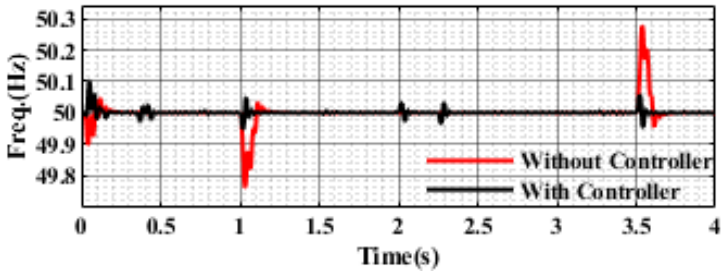

Figure 4.18. Microgrid - Load frequency in the transition period with/without the proposed controller

C. Case 3: Reduced RNCES output (Small Perturbations)

In this case, the natural and practical environmental conditions, i.e., randomly varying solar and wind profiles (uncertainty in the RNCES), have been considered. The performance

assessment under reduced RNCES can be observed in the islanded MG operation. Notably, Pnet is negative in this case, i.e., $P_{PV}+ P_W< P_D$. Therefore, the NCL will be disconnected to balance the system, and the battery will be in the discharging mode of operation. Figure 4.19 shows the various parameters for this case. Notably, the system works in ideal conditions for T = 0 – 1 sec. At T = 1 - 1.5 sec. The system performance starts deteriorating rapidly such that wind/PV attempts to balance the system with the battery in discharging mode (Power sharing P_b shown in green). Whereas, at T = 1.5 – 3 sec., the P_{net} by RNCES reduces such that the NCL is disconnected and the battery goes into discharging mode to balance the entire system. The proposed controller system performance has been compared with those without a controller for better analysis. As per the observations, the proposed controller balances the system parameters within the feasible range of operation and thus performs satisfactorily.

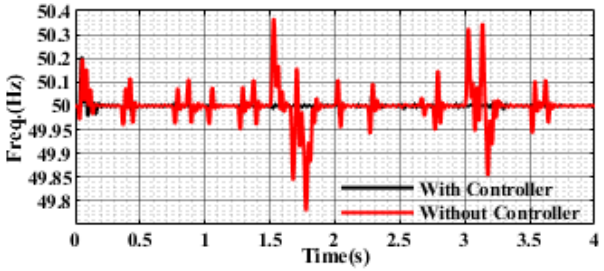

(a) Load frequency with/without the proposed controller

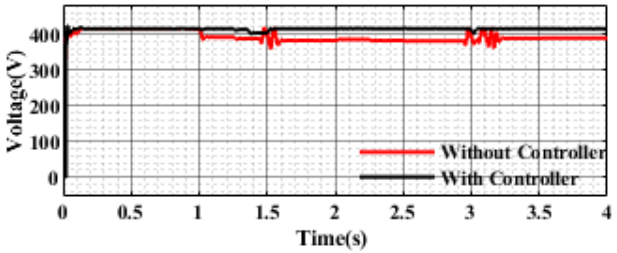

(b) Load Voltage with/without the proposed controller

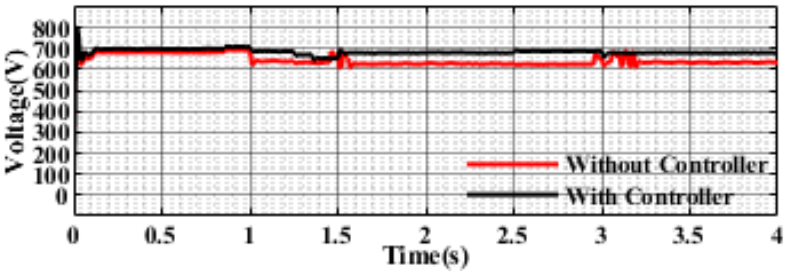

(c) DC-link voltage with/without the proposed controller

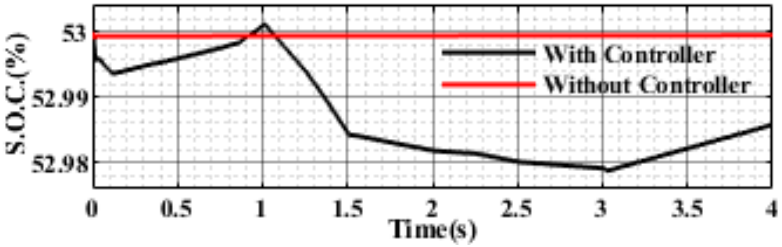

(d) Battery SOC with/without proposed controller

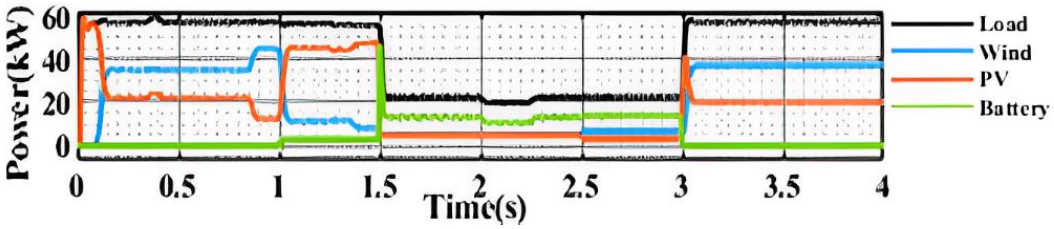

(e) Net power Shared with the proposed controller

Figure 4.19. Results for Case Study - 3

D. Case 4: Minimum RNCES output (Large perturbations)

In case 4, the absence of the grid and the uncertainty in RNCES have been considered with RNCES power output ≈ 0, i.e., $P_{PV} = P_W \approx 0$. Likewise, in case 3, the same time intervals to analyze the condition have been considered. Load curtailment by the proposed dual FLC under the EMS strategy will be done, along with the battery working in a discharging mode for stable operation. The results are shown in Figure 4.20.

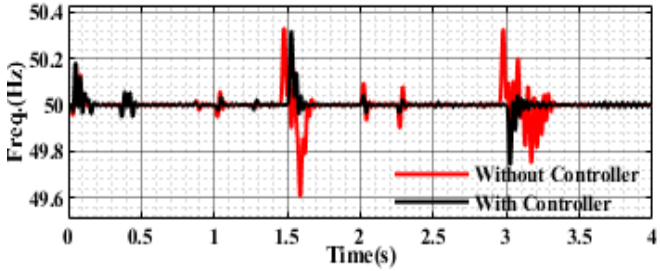

(a) Load frequency with/without the proposed controller

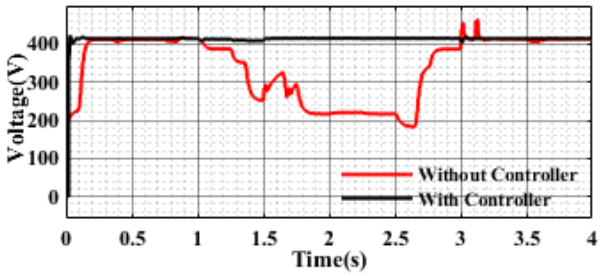

(b) Load Voltage with/without the proposed controller

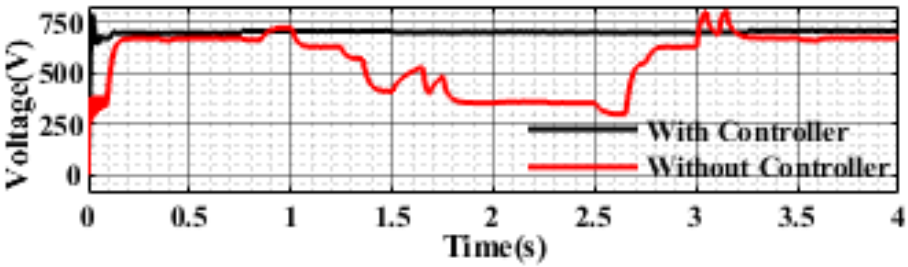

(c) DC-link voltage with/without the proposed controller

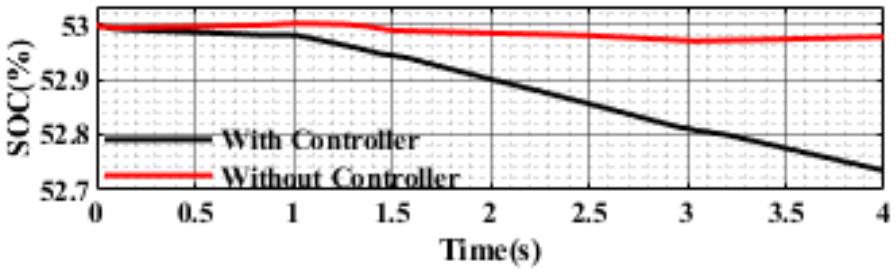

(d) Battery SOC with/without proposed controller

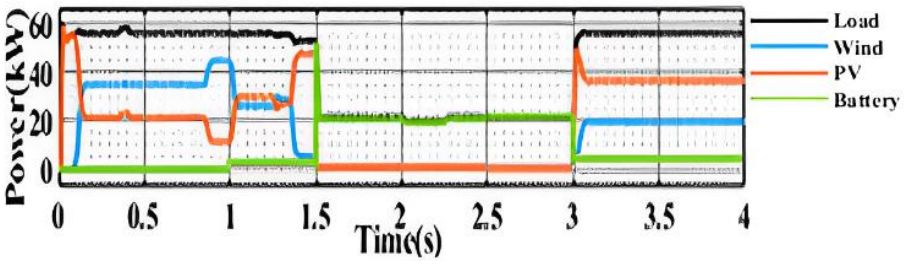

(e) Net Power Shared

Figure 4.20. Results for Case Study - 4

The results show that when the RNCES drops, i.e., maximum dip in the solar/wind profiles, there is a significant change in battery SOC and power-sharing plots. Thus, because of the RNCES unavailability, the load demand is shifted from full load to only critical load conditions as per the decision given by the proposed dual FLC controller, leading all the other parameters in a feasible operating range [176, 204-205]. Besides, the deviation in every parameter can be observed under the no controller condition. As per the recommended standards, the parameters are not in the feasible working range for such cases. Thus, the system tends to be in an unstable state of operation.

E. Case 5: Fault at the Grid End

This case presents the response of the proposed controller in case of unhealthy grid voltage (due to the occurrence of a Line-Ground fault). Based on grid voltage/ frequency properties, the controller isolates the MG system and changes its mode of operation from grid-connected to islanded mode. Figure 4.21 shows the crucial role of the proposed dual FLC in maintaining the F_{mg} and the other parameters even at the 1-phase fault on the grid side. Notably, under the no controller condition, the system experiences deviations much higher than the nominal value of frequency and voltage under the controller condition. Besides, the system resumes the feasible operation much faster when considering the proposed controller.

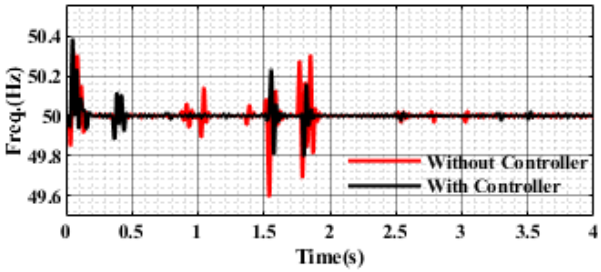

(a) MG frequency with/without the proposed controller

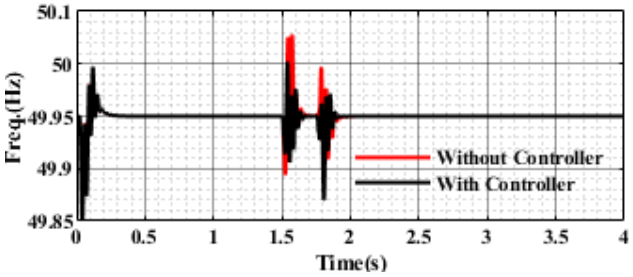

(b) Grid Frequency with/without the proposed controller

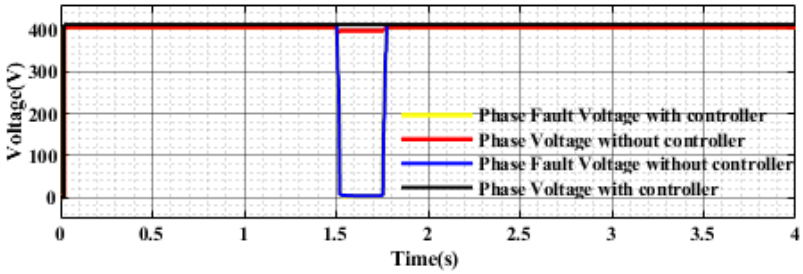

(c) Grid Voltage

Figure 4.21. Results for Case Study - 5

F. Case 6: Fault in Microgrid

In this case, the transition from grid-connected to the islanded mode of operation has been carried out due to MG's unhealthy conditions (Line-Ground fault in MG). Thus, the system is examined under such conditions. Following the protection ideology and general practice, the system is isolated as per the decision made by the proposed controller while sensing the concerned parameters. Figure 4.22(a) shows the simulation's frequency instability at 1.5 and 1.75 sec. Notably, during the fault duration and considering the protection aspects, the MG system operates in the islanded mode under the influence of the proposed dual FLC. Sensing the system parameters, the controller isolates the complete electric load of the system. However, this operation is not present in the vice-versa case of the system without the controller. In addition, the battery operates in charging mode to balance the excessive power of the system as per the command given by dual FLC; otherwise, it discharges to maintain the system parameters, as shown in Figure 4.22(c). However, it can be observed that the system operation is exploited when it is considered without the proposed controller, which validates its importance and significance.

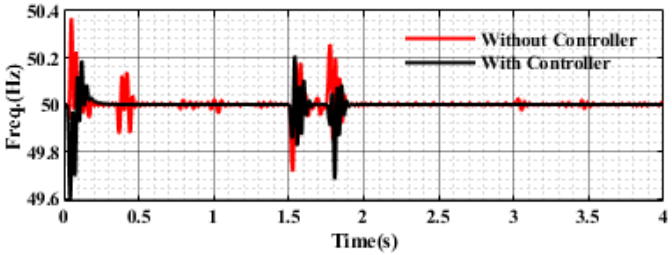

(a) MG frequency with/without proposed controller

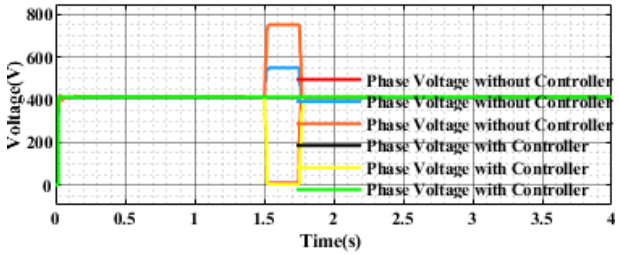

(b) MG Voltage

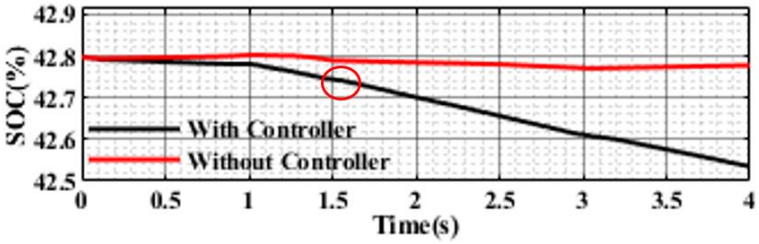

(c) Battery SOC with/without proposed controller

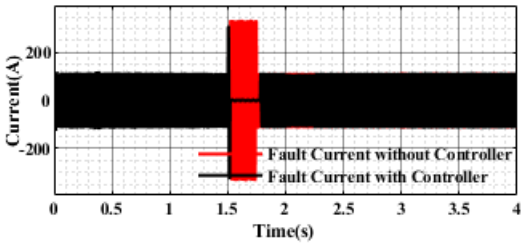

(d) Fault current with/without proposed controller

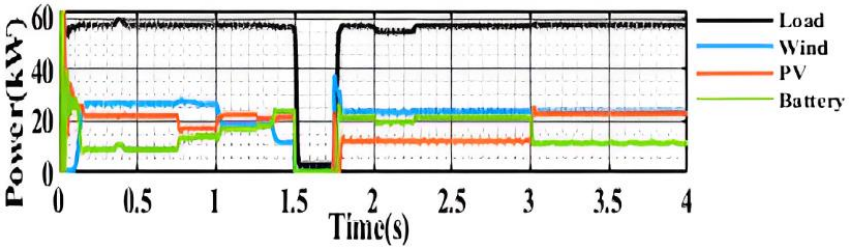

(e) Net Power Shared

Figure 4.22. Results for Case Study - 6

Hence, it is evident that the controller performs satisfactorily under all the feasible test conditions to maintain the stable system operation, i.e., all the parameters lie in the feasible range per recommended standards [176, 204-205]. Also, it is essential to note that the power sources balance the system load demand in all cases. In the case of low RNCES output, the

battery operates in the discharging mode to supply the critical load. Also, with the inclusion of FLC as the central controller, the system response time improves due to the quick decision-making process. Compared to the initial cause of an unstable system, the MG observes minimum variation in voltage, frequency, and a mismatch in the system's net power. Therefore, the proposed approach can be a better solution for maintaining a stable system operation and balanced EMS under uncertain conditions. Table 4.13 presents a brief comparison between the results from the present work and existing literature.

Table 4.13. Comparison of results with existing literature

Sr. No.	Reference	Voltage deviation (%)	Frequency deviation (%)	DC link voltage deviation (%)
1.	Without Controller	16.1	1.21	18.94
2.	[7]	0.894	0.667	1.06
3.	[22]	1.37	1.26	1.68
4.	[192]	0.68	0.88	0.91
5.	[206]	0.857	0.91	1.44
6.	Proposed Controller	0.57	0.25	0.877

From the table, the other controllers simulated in the present MG configuration, i.e., droop control [7], ideal fuzzy logic control [22], coordinated control [192], and robust autonomous control [206], show a comparatively high percentage of deviation for the considered parameters. These controllers consider the system voltage and frequency as the primary input parameters for the operation and control of the developed MG. Notably, the concerned output parameter is the aspect of load curtailment to obtain stable operation. Research has been carried out for different MG configurations and modifications in developed control techniques to analyze the deviation in the system parameters like system frequency, load voltage, and DC-link voltage. The observations under uncertain conditions have been tabulated in Table 4.13 for the system without a controller, a system with reference controllers, and the proposed cascaded dual FLC. As per observations, the deviation in the frequency parameter of the designed system without the proposed controller is 1.21 %. However, for a similar system and in the presence of the proposed controller, the deviation is 0.25 %, i.e., 0.96 % less. Likewise, the deviation in voltage parameter without the proposed controller is 16.1 %, and in the presence of the proposed controller is 0.57 %, i.e., 15.53 % less. Similarly, the deviation in the DC-link voltage parameter without the proposed controller is 18.94 %, and in the presence of the proposed controller is 0.877 %, i.e., 15.53 % less. Further, the difference between state-of-the-art controllers and

proposed controllers has been observed. Significantly, a system with the proposed controller shows 0.324 %, 0.11 %, 0.8 %, and 0.287 % less voltage deviation while simulated under uncertain renewable conditions. Likewise, considering the frequency parameter, the proposed cascaded dual-FLC shows a reduced level of deviations, i.e., 0.417 %, 0.63 %, 1.01 %, and 0.66 %, respectively. Besides, the proposed controller is also valuable for the DC-Link voltage as it significantly reduces deviations. As observed, the proposed controller in the developed MG system shows 0.183 %, 0.033 %, 0.803 %, and 0.563 %, which are lower deviations than the other controllers available in the literature. Henceforth, the difference in the level of deviation can be analyzed, which validates the quality and performance of the proposed controller.
Thus, it is evident that considering the various scenarios with controllable/non-controllable input parameters, the proposed dual FLC proves to be significantly better. Henceforth, it can be explored with other parameters and MG configurations for better applicability in the future. Besides, it is also important to highlight that the relevance and capability of accounting for several parameters can only be performed while employing the proposed control approach, making this research contribution more novel.

Building the foundation of centralized and cascaded dual FLC, the next Chapter presents a comprehensive study on PLC configuration and test bench development for real-time controller implementation in microgrid technology. It introduces a hardware test bench prototype using a reconfigurable Allen-Bradley Micro820/2080-LC20-20QBB PLC, enabling analysis of load management with variable renewable sources like solar, wind, and battery. The prototype showcases quick decision-making and load-switching capabilities crucial for stable microgrid operation under uncertain conditions. Additionally, CCW software validates real-time program performance, while MATLAB simulations confirm the control approach, ensuring stable microgrid operation within IEEE standards.

Chapter Summary

A centralized and a cascaded dual fuzzy logic controller (FLC) are introduced for a stable PV/wind/battery-based microgrid system. Conclusively, the centralized controller operates in multiple stages while the cascaded dual FLC operates considers both controllable and non-controllable parameters, dividing control into two FLCs with FLC 1 related to battery operation and FLC 2 related to stable microgrid operation under challenging grid conditions. The controllers work cohesively to balance load demand, maintaining electrical parameters within a feasible range and minimizing uncertainties. The system demonstrates improved voltage and frequency regulation under various microgrid conditions. Despite a

limitation in handling overlapping conditions, the controller reduces voltage, frequency, and DC-link voltage deviations. The proposed controller(s) are praised for its adaptability, user-friendliness, intelligence, and flexibility across different microgrid configurations and resource combinations, validating its robustness and universal applicability.

CHAPTER 5
DEVELOPMENT OF PLC-BASED HARDWARE TEST-BENCH PROTOTYPE FOR CONTROL ALGORITHM VALIDATION

Programmable Logic Controllers (PLCs) are gaining traction in microgrid operation due to their real-time deployment, reliable and robust operation, and fast response, even in harsh environments. Recognizing the critical need for robust and reconfigurable microgrid control and operation, this part of the research presents a hardware test bench prototype using the Reconfigurable Allen-Bradley - Micro820/2080-LC20-20QBB PLC to demonstrate control algorithms aiming for efficient control, energy management, and resilient microgrid automation. The design and construction of a prototype controller test bench, along with the PLC configuration, wiring diagrams, and control logic, constitute the significant contributions of this research. The proposed controller test bench's performance is evaluated through similar condition simulations in the presence of disturbances induced by the reduced contributions of renewable energy sources, such as solar and wind. The results illustrate the effectiveness of the developed control algorithm implemented in the proposed controller, ensuring the stable operation of the microgrid. Consequently, this work advances the simulation-based validation of microgrid control algorithms and provides insights into the practical application of a PLC-based hardware test bench under various environmental conditions.

5.1.Introduction and background

An independent network that connects critical and non-critical loads, integrating renewable and non-conventional energy sources (RNCES), is widely termed a microgrid (MG). It offers benefits by optimizing energy production and load consumption in a specific region [204]. However, ensuring control and stability under uncertain conditions is a significant challenge. Different controllers have been proposed to address this issue [1]. While stability parameters like voltage and frequency have been the focus, maintaining a proper power balance and power-sharing within the system is crucial. An efficient energy management system (EMS) that is practical, adaptive, and intelligent plays a vital role in achieving this [12, 207-208]. Energy management involves collecting data on various energy sources, such as solar PV, wind energy systems, battery storage, and peak load usage. Battery storage systems have the advantage of being able to both charge and discharge, providing dual functionality. When the battery's state of charge is low and there is excess power generation, it charges.

Conversely, when the power generated by the Renewable Non-Conventional Energy Sources (RNCES) is insufficient to meet the load demand, the battery discharges and acts as a

power source [209]. However, considering the limitations of the battery, a non-critical load-shedding strategy was implemented to ensure system stability. In detail, for an efficient Energy Management System (EMS), two controllers are proposed: an adaptive and intelligent controller mentioned in [210] and a fuzzy logic controller (FLC) mentioned in [211].

The real-time application of a microgrid (MG) system in real-world conditions is crucial for its practical implementation. This involves validating and implementing a proposed control scheme using the MG central controller (MGCC), which is responsible for quick decision-making and connecting essential parameters. Existing literature suggests various hardware setups, platforms, and toolboxes for validating simulated microgrid systems under uncertain conditions. These include Power Systems Computer Aided Design (PSCAD), Electromagnetic Transient Simulation Engine (EMTDC), TRNSYS, Hybrid Optimization of Multiple Energy Resources ((HOMER) or (HOMER Pro)), Real-time Structured Computer-Aided Design (RSCAD), and Hardware in Loop (HIL) simulations [212-217]. However, these tools and test benches are primarily suited for laboratory environments and lack practical applicability in real-world settings due to constraints and challenging environmental conditions. This study suggests adopting an industrial programmable logic-based automated controller (PLC) to resolve this problem and provide real-time stability in microgrid control. PLCs are programming-based controllers known for their robustness, reliability, flexibility, and efficient decision-making capabilities in diverse engineering fields [218]. Numerous examples in the literature demonstrate the wide range of PLC applications [219-227]. The subsequent section will explore significant studies in this area.

Several studies have demonstrated the effectiveness of PLCs in microgrid (MG) systems. A PLC-based MG testbed was used to showcase how a PLC with a controllable load ensures stable MG operation by balancing energy requirements [219]. Similarly, [220] used an emulator in the lab to test frequency-based logic for reliable performance in a small-scale hydropower system. Using programming logic and signals, [221] implemented PLC-based DC drive control for low-cost three-phase MG development, achieving balanced line voltages and steady operation. Likewise, [222] explored PLC applications and security, networking, and communication limitations, addressing concerns with unauthentic protocols. Further, the authors in [223] extensively discussed ladder logic, the widely adopted programming platform for PLC logic design, highlighting its features and importance.

Ladder logic is presented in this work as a viable solution to address potential error margins in PLC input/output signals. Modern PLCs are frequently used for actual automation applications despite these drawbacks. This assertion is supported by the concepts and analyses of virtual PLCs presented in [224] and [225] and the use, benefits, and comparison of PLCs and

FPGAs. PLCs surpass FPGAs in the performance tests carried out for this study, indicating their more comprehensive range and applicability. Further investigation into PLC-based battery control is also done [226-227] by replicating real-time circumstances with potentiometers. These results urge the authors to create a fully functional microgrid prototype to test the effectiveness of the control algorithm under variable conditions. A crucial aspect of PLCs is the development of a real-time implementable test bench. This entails a comprehensive understanding of electrical wiring, component operation, connection procedures, and coordinated and parallel operation. As mentioned earlier, there are research gaps concerning the MG test bench prototype, particularly in the intricate planning and creation of an automated version.

Further research is necessary to deploy industrial PLCs and achieve reliable MG operation while accounting for uncertainties. It is essential to investigate how the performance of the controller and MG is affected by disturbances such as cloud movement and shadowing. Additionally, the validation procedure for an adaptive and automated MG central controller, particularly in real-time practical applications, needs to be explored using a PLC prototype. Further, Table 5.1 presents the comparative analysis between the existing literature and the proposed work concerning the PLC details and configuration, along with the key insights/remarks related to the work [228-231].

Table 5.1 Summary of existing work in the Indian scenario

Reference	PLC Details/ Configuration	Brief Details	Remarks
[228]	GP-Pro EX V4	• Demonstration of open platform PLC software. • Basic PLC functionalities disclosed.	• Discussion on PLC implementation is not disclosed. • Information related to PLC configuration has not been disclosed. • Microgrid configuration and respective implementation of PLC are not disclosed. • Details for hardware implementation are not available. • Information related to system/control approach reproducibility is deficient.

[229]	Not Disclosed	• Case study on implementing PLC for DG sets synchronization in a microgrid. • Use of ETAP software for generator synchronization.	• Information related to PLC is not disclosed. • Discussion on PLC implementation is not disclosed. • Discussion related to the role of PLC in microgrids, considering renewable sources or uncertainties, is not available. • A solution/methodology for hardware implementation is not available. • Microgrid configuration and respective implementation of PLC are not disclosed. • Information related to system/control approach reproducibility is deficient.
[230]	Schneider Safety PLC (Configuration details not available)	• Multiple softwares are disclosed for the developed system. • The developed system demonstrates PSCAD-based Simulation results.	• Information related to PLC configuration has not been disclosed. • Discussion related to the role of PLC in microgrids, considering uncertainties in renewable energy sources, is not available. • Explicit details for hardware implementation are not available. • Microgrid configuration and respective implementation of PLC are not disclosed. • Simulation results are showcased to validate the methodology. • Information related to system/control approach reproducibility is deficient.

[231]	PLC CD-24 V DC CROUZET	• Solar-based system integrated with PLC is disclosed.	• Information related to PLC configuration has not been disclosed. • Discussion related to the role of PLC in microgrids, considering uncertainties in renewable energy sources, is not available. • A solution/methodology for hardware implementation is not available. • Hardware results (validation) are not available. • Information related to system/control approach reproducibility is deficient.
Developed system	Reconfigurable Allen-Bradley - Micro820/2080-LC20-20QBB	• Control approach for a stable microgrid (solar-wind-battery) operation. • Fuzzy-based control approach for developed system (simulated using MATLAB Simulink) • A PLC-based hardware test bench has validated the proposed control approach.	• Details of the PLC-based test bench prototype are disclosed, including PLC configuration, wiring diagrams, etc. • Information about system/control approach reproducibility is well presented and explained. • Simulation and hardware results concerning solar-wind-battery-based microgrid and considering the real-time renewable sources uncertainties are presented. • The energy management system for stable microgrid operation is validated using simulations and a hardware test bench.

The tabulated details show that the scope of the PLC-based control approach in microgrids is of high potential. Remarkably, the previous state-of-the-art literature did not disclose

different details, such as PLC configuration, the role of PLC in microgrids, and wiring details related to system reproducibility. Besides, the knowledge gap remains in using PLCs in varying load conditions and intermittent renewable energy generation. Hence, motivated by the role of PLCs in offering advanced control capabilities, optimal utilization in decision-making, reliable development and validation of control logic, quick real-time decision-making and action-taking, this research aims to address the challenges by investigating a hardware test bench microgrid prototype with a reconfigurable PLC to validate control strategy for stable microgrid operation. Considering this, the critical contributions of the present work include a comprehensive study to build, design, and implement a reconfigurable PLC-based hardware test bench prototype for stable microgrid operation, where PLC (programmable logic controller) is an industrial controller. Further, validate an adaptive and robust energy management system (EMS) using the developed hardware test bench prototype considering the uncertain and, therefore, variable renewable sources, such as low solar irradiance, variable wind speed, etc. Lastly, a comparative study concerning the developed hardware PLC-based test bench will be performed in view of the MATLAB simulation platform to validate the performance and control approach for stable microgrid (MG) operation.

5.2.Proposed Methodology

This section focuses on the proposed methodology for the energy management system (EMS) to ensure the stable operation of the microgrid (MG). The discussion begins with a brief overview of the FLC (Fuzzy Logic Controller) concept, followed by a detailed flowchart illustrating how the hardware test bench works. Additionally, as mentioned earlier, a load priority chart, which provides clear visual guidance, is presented in Figure 5.1.

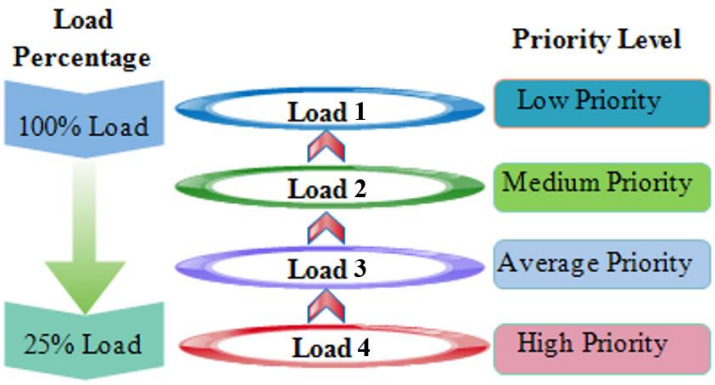

Figure 5.1. Load Priority chart

Figure 5.1 illustrates a priority-based distribution of electrical load, comprising four distinct loads represented as Load 1 - Load 4, such that each load's weightage is 25 % of the total load. Further, as shown in the figure, priority levels are assigned to each load based on the load

criticality i.e., Load 1 is designated as the highest priority, and Load 4 is the minimum priority. Load 1, representing the highest criticality (critical load), receives the share of power resources at the highest priority to ensure uninterrupted operation. In contrast, Load 4 (less critical or non-critical load) receives the lowest priority. This dynamic and adaptable approach allows the system to efficiently manage varying conditions and power distribution to meet specific needs by ensuring consistent power supply to critical and non-critical loads.

Further, Section 3 introduces the FLC-based adaptive EMS controller in detail as a method for effective energy management in microgrid operations, specifically in subsection 3.1. The PLC-based hardware test bench is described in subsection 3.4 of the work as a helpful tool for validating and evaluating the performance of the suggested controller. Specifically, the control algorithm is implemented and evaluated using this test bench in real-time, ensuring its usefulness in real-world microgrid applications.

5.2.1. Fuzzy Logic Controller-based control strategy

The operation of the fuzzy logic controller (FLC) within the microgrid (MG) system is shown in the flowchart in Figure 5.2.

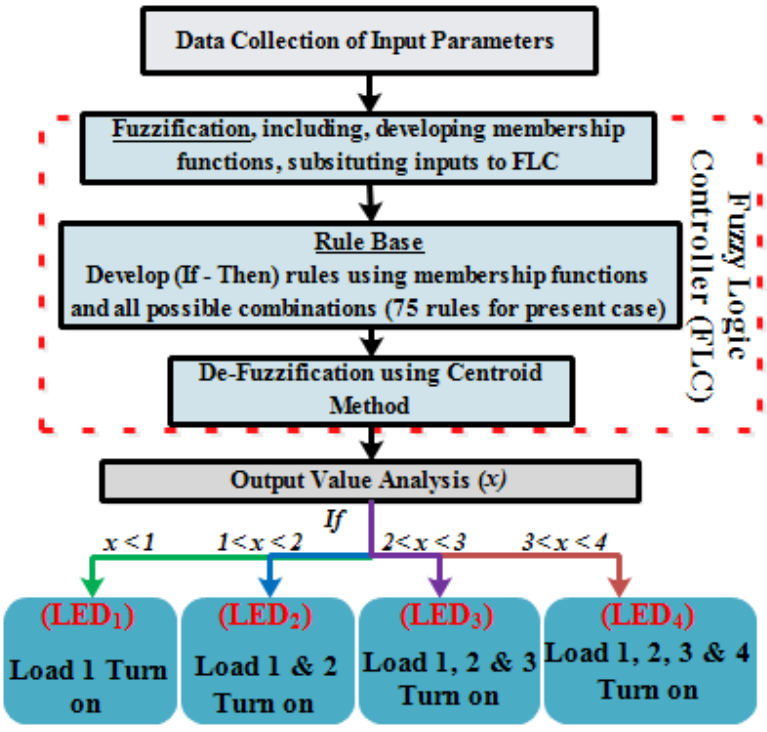

Figure 5.2. Designed FLC approach for simulated MG aiming EMS

As illustrated in the diagram, this FLC system gets three crucial input parameters: solar irradiation, wind speed, and battery state of charge (SOC). A set of 75 rules has been meticulously created to guarantee smooth and effective load connection or disconnection in the MG system. The required parameter ranges for solar irradiation, wind speed, and battery SOC

are 0 - 1000 W/m^2 (Watts/metre^2), 0 - 15 m/s (meter/second), and 0 % – 100 %, respectively. The FLC can decide on load curtailment within these specified load categories by dividing the load into 4 categories based on the value of "x". This categorization ensures the load is managed effectively and optimally within the microgrid system.

Table 5.2. Membership functions for different inputs

Input/Output	MFs (%)	Range (%)				
Input	SI (0 to 100)	Very Low (0 to 22)	Low (18 to 42)	Medium (38 to 62)	High (58 to 82)	Very High (82 to 100)
	WS (0 to 100)	Very Low (0 to 22)	Low (18 to 42)	Medium (38 to 62)	High (58 to 82)	Very High (82 to 100)
	Battery SOC (0 to 100)	Low (0 to 37.5)		Medium (32.5 to 67.5)	High (62.5 to 100)	
Output	Decision (0 to 4)	$Load_1$ (0 to 1.05)	$Load_2$ (0.95 to 2.05)	$Load_3$ (1.95 to 3.05)	$Load_4$ (2.95 to 4)	

Table 5.2 provides the range of various parameters considered in the present work. The membership functions of the developed fuzzy logic controller (FLC) are used to generate the set of rules as tabulated in Table 5.3 (sample set of rules). Based on the current status of the power sources, the FLC produces a crisp output, and the adaptive energy management system (EMS) decision-making process is implemented accordingly.

Table 5.3. Sample rules for developed controller

Rule No.	Solar Irradiance (SI)	Wind Speed (WS)	Battery SOC	Decision
1	Very Low (VL)	Very Low (VL)	Low (L)	Poor
12	Very Low (VL)	High (H)	High (H)	Average
38	Medium (M)	Medium (M)	Medium (M)	Good
75	Very High (VH)	Very High (VH)	High (H)	Very Good

Rule 12 is based on the system's inputs, specifically the solar irradiance (SI), wind speed (WS), and battery state of charge (SOC). Accordingly, the power sources should only supply 25 to 50 percent of the total load, considering at least one source is low, i.e., very low solar irradiance. However, the status of other sources, i.e., wind speed and battery state of charge

(SOC), is high. This indicates that, given the criticality of the loads, the system prioritizes depending on other sources rather than utilizing all available power sources. This allows the microgrid system's load management optimization and ensures effective resource use.

5.2.2. Operation of PLC

Figure 5.3 shows the operational flowchart for examining the energy management system (EMS) within the simulated microgrid (MG) system connected to the established PLC test bench.

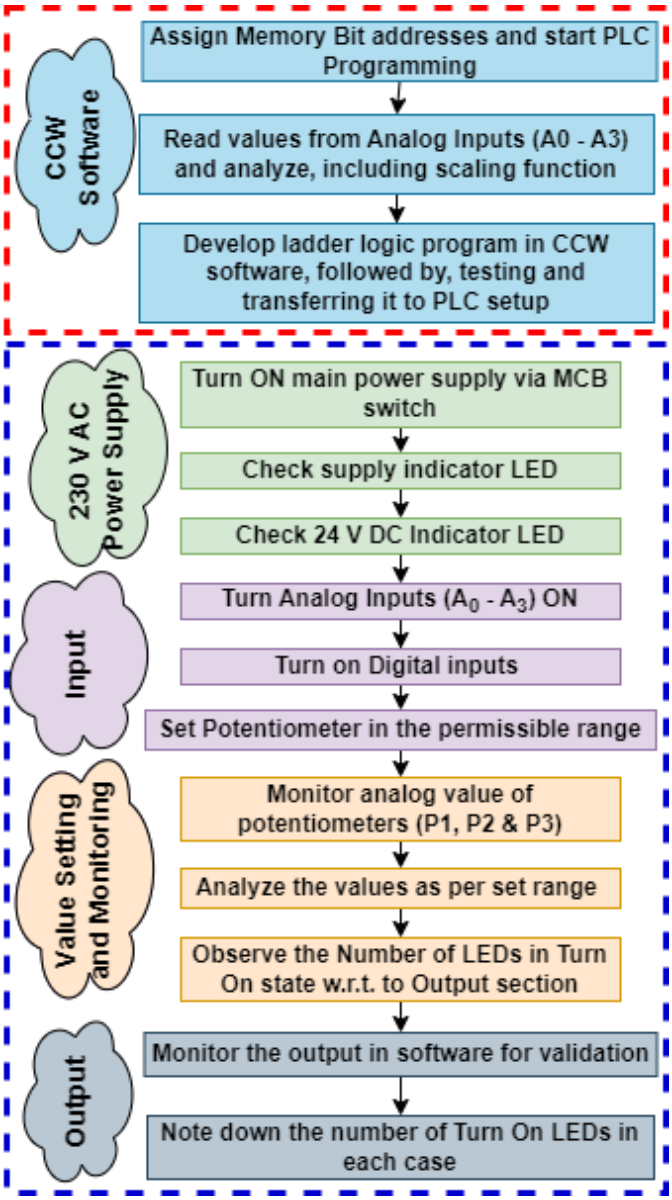

Figure 5.3. PLC approach for simulated MG aiming EMS

The first step entails using the CCW program to set up the fundamental logic stages. The power supply component, which includes the switch-mode power supply (SMPS), is turned on at the following stage. The analog and digital pins are turned on during stage three to simulate

the erratic behavior of power sources. Ladder logic is being created concurrently for the adaptive EMS in the PV-Wind-Battery-based MG. Stage four concludes with calibrating the potentiometers within their specified range and monitoring their performance using the CCW software. The results are assessed when the LED load lamps are on during the last phase. The programmed EMS logic chooses the number of lit LEDs based on the resources. The automatic EMS logic will turn on all load LEDs with high PV and wind power availability and generate enough power to satisfy the power balance calculation. The online CCW program also makes it possible to check and keep track of the status of all parts and LEDs.

5.3. Results and Discussions

This section presents the findings of various case studies conducted to evaluate the performance of the PLC-based test bench. Three different test cases were performed, and the state of the load in the test bench was analyzed for each case. In addition to validating the results in the simulation setup, graphical representations have been provided to enhance the understanding and visualization of the outcomes.

5.3.1. Case study 1 - Low Solar Irradiance (SI), Wind Speed (WS), and Medium Battery SOC

The worst-case scenario (case study 1) for a microgrid (MG) functioning in this instance is low RNCES (renewable sources) and medium battery SOC. A large amount of load shedding must be performed when evaluating essential and non-critical loads, particularly in percentage. Figure 5.4 illustrates the hardware and simulation findings by this.

Accordingly, Figure 5.4(a) presents the distribution of net power among various sources, and the battery, acting as an ancillary support to the system, is demonstrated to meet the demands of the connected load. However, due to the low RNCES, a swift non-critical load shedding occurs and can be analyzed in 1-3 seconds. Notably, during this period, the battery serves as a critical support to the system, particularly evident during scenarios where the output of renewable energy sources plummets to a minimum level, i.e., the RNCES (solar and wind) output is considered negligible. In such an instance, it can be observed that the battery discharges within a mere 2 seconds of simulation, witnessing a minor reduction in State of Charge (SOC) from 51.02 % to 50.94 % (demonstrated by the green color in Figure 5.4(a) and 5.4(b)). Notably, before and after dedicated simulation time, i.e., between 0-1 second and 3-4 seconds, the battery is in charging mode, whereas the reduction is observed during the period of 1-3 seconds. This rapid response is crucial in maintaining system stability and ensuring the critical load receives a continuous power supply. Furthermore, Figure 5.4(c) showcases the

hardware test bench where only one LED (L4 representing critical load) is activated, aligning with simulation results. The Programmable Logic Controller (PLC) precisely orchestrates the deactivation of non-critical loads under analogous input conditions, dedicating power solely to the critical load. This underscores the PLC's capability to promptly analyze input variations and execute rapid load switching, with the battery playing a pivotal role as an essential ancillary support during critical load scenarios.

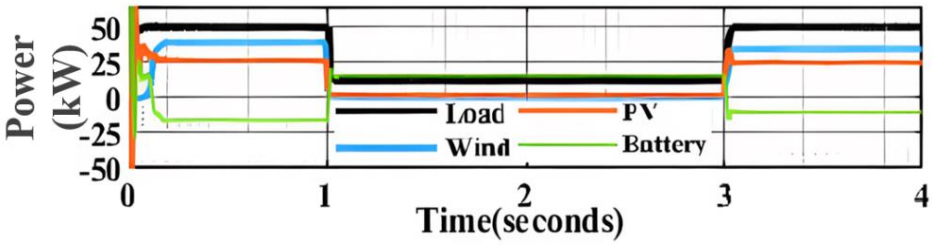

(a) Net Power Sharing

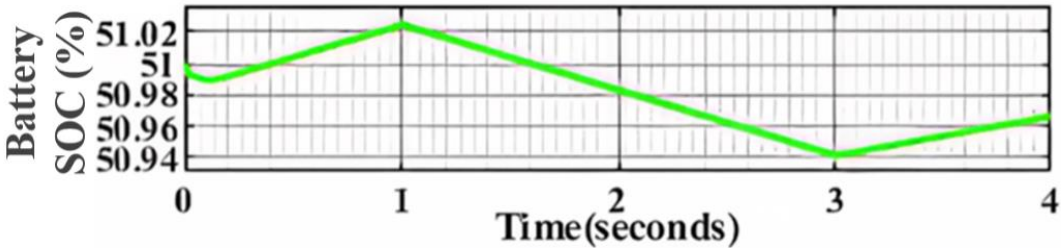

(b) Battery SOC

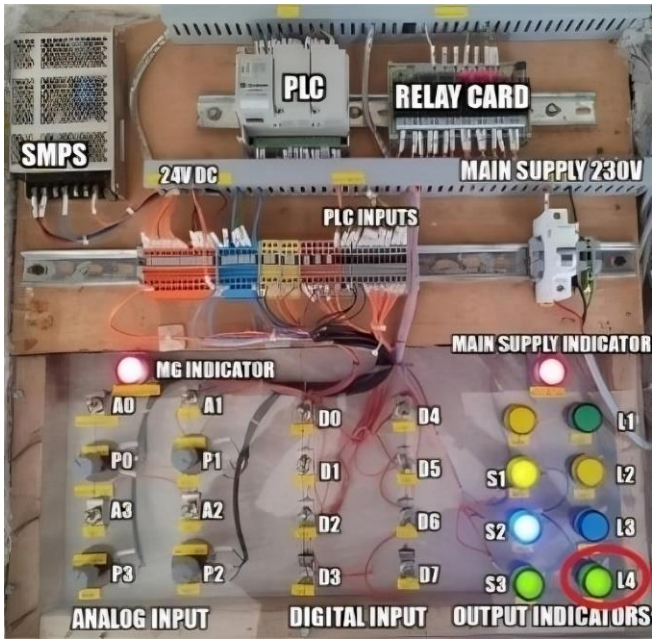

(c) Hardware test bench with L4 turned ON

Figure 5.4. Simulation and hardware results for Low Solar Irradiance & Wind Speed (non-ideal values) and Medium Battery SOC

5.3.2. Case Study 2 - High Solar Irradiance (SI), Wind Speed (WS), and Medium Battery SOC

The outcomes are shown in Figure 5.5 when the best-case scenario for microgrid (MG) operation is taken into account, which includes high output from the Renewable Non-Conventional Energy Sources (RNCES) and the battery functioning in a charging condition. The performance and results related to this specific case are analyzed in these figures.

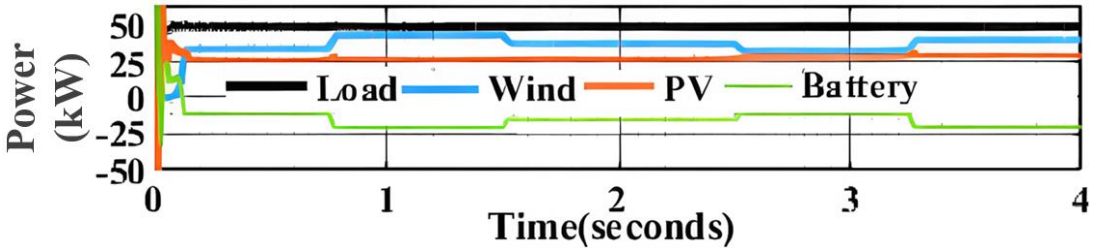

(a) Net Power Sharing

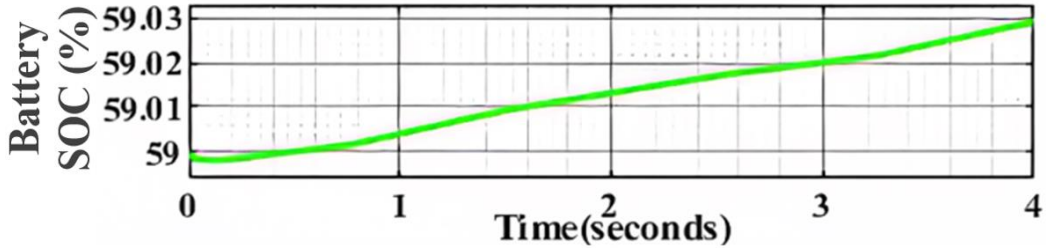

(b) Battery SOC

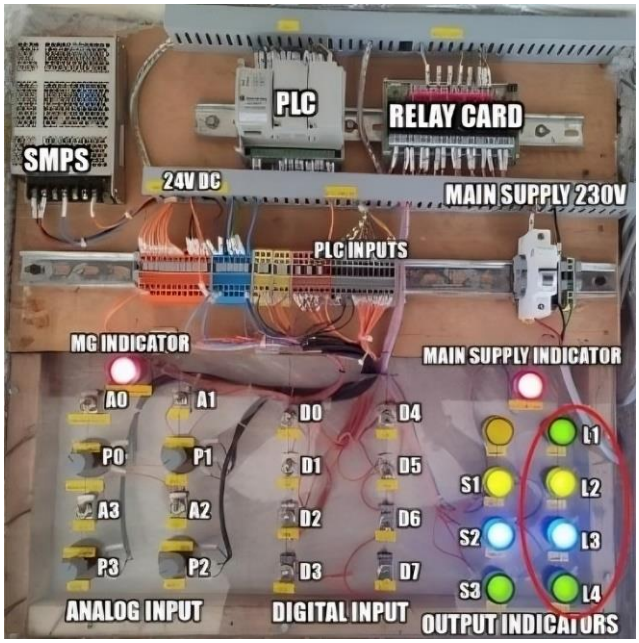

(c) Hardware test bench with L1 – L4 turned ON

Figure 5.5 Simulation and hardware results for High Solar Irradiance & Wind Speed (ideal values) and Medium Battery SOC

Accordingly, Figure 5.5(a) presents the net power distribution among different sources, highlighting the absence of load shedding, as the system operates under the ideal RNCES

conditions, i.e., the output of renewable sources is significant to fulfill the connected electrical load (0 % load shedding) even when subjected to slight variations in wind speed. This is a crucial distinction, emphasizing the system's ability to maintain 100 % load fulfillment without resorting to load-shedding practices. Concurrently, in Figure 5.5(b), the battery's role is highlighted as it operates in a charging mode, where the level of SOC increases from 58.99 % to 59.03 %. This is evident from the negative net sharing of power for the battery, demonstrating its capability to recharge while consuming any extra generated power at all instances of operation, as shown in Figures 5.5(a) and 5.5(b). Moreover, Figure 5.5(c) provides insights from the hardware test bench, mirroring the simulation results. All load LEDs (L1, L2, L3, and L4) are illuminated, representing an ideal scenario with 0 % load shedding. This comprehensive alignment between simulation and hardware results signifies the system's robustness under optimal conditions. It showcases its ability to fulfill 100 % of the load without resorting to load shedding while efficiently putting the battery in charging mode. Notably, the complete load has been satisfied by the generated power output. As shown in Table 5.4, all pertinent parameters are within a practicable range of operation as per the IEEE standards, such that results show that the MG system is optimally operating and achieving the intended performance [204, 232].

5.3.3. Case Study 3 - Medium Solar Irradiance (SI), Low Wind Speed (WS), and Medium Battery SOC

The production of low to moderate amounts of renewable non-conventional energy source (RNCES) output is a typical microgrid (MG) operation scenario. Figure 5.6 depicts the predicted outcomes and the output of the PLC test bench. The results show how the MG system performs in these circumstances, showing the role of ancillary support in conditions of decreased RNCES production. Similar to Figure 5.5, Figure 5.6(a) illustrates the net power distribution among various sources. However, under medium-level renewable sources inputs, i.e., a slight drop in wind and a significant drop in solar power output, a change in the percentage of load fulfilled can be observed. Under such circumstances, 50 % of the load is fulfilled, whereas the rest of the non-critical load is shed to maintain the stable microgrid operation. In response to such a drop in RNCES, the battery transitions from a charging mode to a discharging mode, as observed in Figure 5.6(b), where the battery SOC drops from 40.991 % to 40.952 %. This shift is crucial for ensuring maximum load satisfaction within the microgrid. Notably, in the event of a significant RNCES decrease and with a strategic 50 % load shedding implemented to maintain a stable microgrid operation, all microgrid parameters, such as voltage and frequency, are maintained within a feasible and operational range. Reducing frequency and voltage deviation is crucial for maximum load fulfillment and stable microgrid operation. The

tabulated values in Table 5.4 confirm deviations within the permissible range [204, 232], signifying system stability. Further, Figure 5.6(c) displays hardware test bench results, validating the MATLAB Simulink simulation outcomes. In this scenario, 50 % of the load is turned on, with LEDs representing loads L3 and L4 (whereas L4 is the most critical load and L3 is the second most critical load per the load priority chart presented in Figure 5.1) illuminated while others are off. This aligns with the simulated 50 % load shedding, highlighting the consistency between the hardware test bench and simulation results.

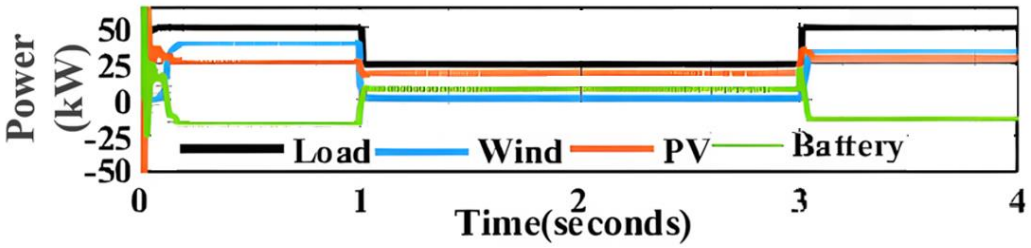

(a) Net Power Sharing

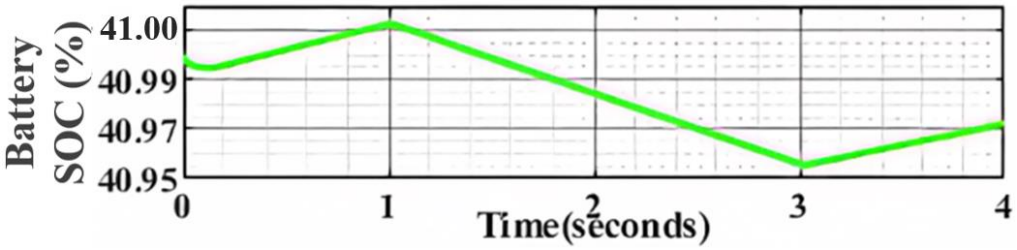

(b) Battery SOC

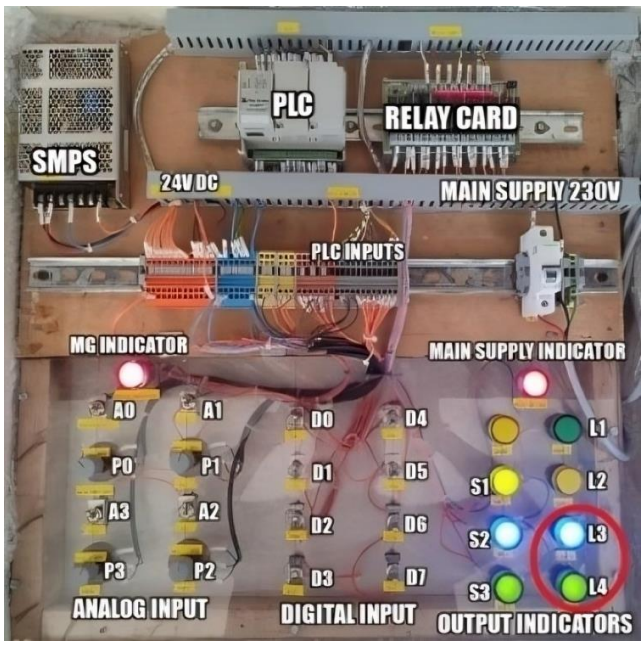

(c) Hardware test bench with L3 and L4 turned ON

Figure 5.6. Simulation and hardware results for Medium Solar Irradiance, Low Wind Speed (average values), and Medium Battery SOC

5.4.Result Analysis

Concerning the presented results in sections 5.1, 5.2, and 5.3, the developed control logic, i.e., FLC-based energy management using MATLAB Simulation and PLC-based hardware test bench aiming for stable microgrid operation, has been validated. Specifically, the results presented in Figures 5.4(c), 5.5(c), and 5.6(c) show the applicability of the proposed PLC-based hardware test bench in controlling and switching the electrical load under various uncertainties. Besides the graphical results from the simulation model and hardware test bench, Tables 5 and 6 present the tabulated analysis to discuss the outcomes in detail. It includes an analysis tabulated in Table 5.3, which presents the voltage and frequency deviation analysis, battery SOC, and power-sharing status in different simulated case studies. In contrast, Table 5.4 highlights the performance of the hardware test bench. Lastly, Table 5.5 presents the performance of the hardware test bench in view of power quality and load status, considering different levels of disturbances and noise.

Table 5.6 shows the deviation data for various parameters observed during the MATLAB simulation. This includes voltage and frequency deviation for all the simulated case studies, the level of power-sharing, and the battery state of charge. Specifically, as observed in cases 1 and 3, the system experiences comparatively high voltage and frequency deviations due to the uncertainty in RNCES. Besides, the battery is in discharging mode (represented by a negative state of charge). However, considering the ideal case scenario (case 2), the deviations are comparatively less, i.e., V_d is -0.18 %, and F_d is -0.08 %; additionally, the battery is in charging mode. The RNCES output is considerably high and sufficient to fulfill the load demand. Notably, in all the 3 cases, the deviations are in the permissible range of operation, i.e., the controller works in an ideal manner to balance the generation and load demand, such as to achieve a stable microgrid operation [204, 232].

Table 5.4. Simulation results including parameter deviation data

Case Study	Time Interval (1 – 3 seconds)			
	Parameter 1 - V_d (%)	Parameter 2 - F_d (%)	Parameter 3 - SOC (%)	PS (%)
1.	-0.85	-0.2	-50.98	+0.39
2.	-0.18	-0.08	+59.03	+0.61
3.	-0.45	-0.24	-40.985	+0.33

Where, V_d & F_d represents a deviation in respective Parameter 1 (Voltage), and Parameter 2 (Frequency), PS (%) represents the status of power-sharing (in percentage). The sign (=/-) associated with each tabulated value indicates the positive or negative inclination of the

parameter or charging/discharging with respect to the connected battery.

Similar situations to the simulated case studies have been replicated in the hardware test bench, taking solar, wind, and battery input into account, as shown in Table 5.4. As observed, in cases 1 and 3, the analog input voltage is in the low range; therefore, the load percentage met is 25 % and 50 %, respectively. This is similar to the reason for low RNCES; therefore, the battery acts as an ancillary support to satisfy the critical load. However, in case 2, the RNCES contribution is comparatively high, i.e., the analog input voltage is in the high range, and therefore, 100 % load fulfillment can be observed.

In addition, Figure 5.7 presents the visual observations of the hardware test bench under voltages from various power sources during operation. The figure presents the load status analysis for different case studies. In case 1, specific voltage values are assigned to the PV source, WT, and BS, resulting in load configurations where Load 4 is activated while Load 1 to Load 3 is deactivated based on the designed logic. This load status is represented by the binary sequence (0, 0, 0, 1), and it is noteworthy that Load 4 remains active unless there are shutdowns or faults, reflecting its critical priority in the system. From this analysis presented in Figures 5.4, 5.5, 5.6 and Tables 5.4 and 5.5, it is evident that the developed control approach considering FLC and PLC worked in an appropriate manner such that under the uncertain RNCES conditions, the controller(s) performs energy management effectively such that the system operates in the stable state.

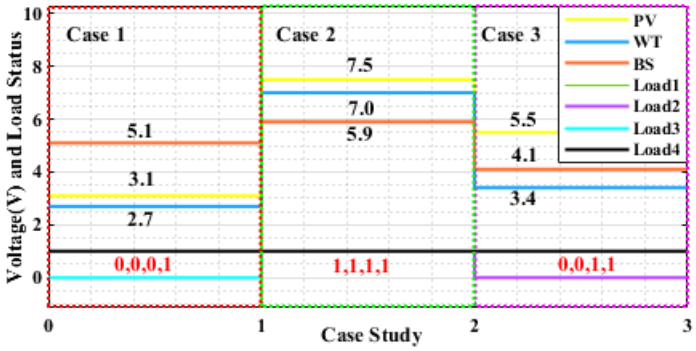

Figure 5.7. Graphical Plot corresponding to Table 5.4

Besides, the tabulated result involving the disturbances using a random function block in the analog input of the hardware test bench is presented below. With the disturbance level specified as a percentage, the disturbances cause random fluctuations, specifically a decrease in effective voltage. This approach allows the evaluation of the impact of external disturbances on the system performance, especially on the overall system output, including the effects of disturbances on voltage levels and signal quality drops in the system. The results of this experiment, including power quality assessment categorized as “Good” or “Average”, are summarized in Table 5.5.

Table 5.5. Hardware results including the percentage of load fulfilled

Case Study	Analog Input Voltage			Output Status				
	PV	WT	BS	Load Output (L1)	Load Output (L2)	Load Output (L3)	Load Output (L4)	Load Percentage
	(in terms of voltage)							
1.	Low 3.1 V	Low 2.7 V	Medium 5.1 V	0	0	0	1	25 %
2.	High 7.5 V	High 7 V	Medium 5.9 V	1	1	1	1	100 %
3.	Medium 5.5 V	Low 3.4 V	Medium 4.1 V	0	0	1	1	50 %
*0 and 1 represent the On and Off state of the connected load.								

Table 5.6. Hardware results considering disturbances

Case Study	Disturbances	Analog Input Voltage (PV)	Analog input Voltage (WT)	Analog Input Voltage (BESS)	Power Quality	Load status
		(in terms of voltage)				
1.	Low Level (5-10 %)	Low: 2.85 V	Low: 2.49 V	Medium: 4.76 V	Good	(0,0,0,1)
2.	High Level (20-35 %)	High: 6.12 V	High/ 5.81 V	Medium: 4.27 V	Average	(**0**,1,1,1)
3.	Medium Level (10-20 %)	Medium: 4.15 V	Low: 2.31 V	Medium: 3.13 V	Good	(0,0,1,1)

As per the tabulated results shown above, the voltage drops across all the resources concerning the intensity of disturbances, i.e., with the increase in the level of disturbances (in percentage), the voltage realized across the PLC terminal drops, causing variation in the output. In detail, considering case 2, it can be observed that power quality degrades as the level of disturbances increases, and besides, the percentage of load supplied also decreases from 100 %, i.e., (1,1,1,1) to 75 %, i.e., (0,1,1,1). Henceforth, it has been observed that the developed control logic concerning the simulated model and hardware test bench parameters manages and satisfies the system requirements, i.e., to achieve stable microgrid operation.

On the foundation of Chapter 5 and aiming for a comprehensive assessment, Chapter 6 focuses on implementing a microgrid in the Kibber region of India to address rural electrification using solar and wind energy. Technical and economic analysis has been presented to emphasize the need for location-specific assessments and provide guidelines for planning microgrids in remote areas.

Chapter Summary

The chapter presents a comprehensive study on PLC configuration and test-bench development for real-time controller implementation in microgrid technology. It discloses a hardware test bench prototype using a reconfigurable Allen-Bradley - Micro820/2080-LC20-20QBB PLC, enabling analysis of load management while considering variable renewable sources like solar, wind, and battery. Further, the prototype demonstrates quick decision-making and load-switching capabilities, which are crucial for stable microgrid operation under uncertain conditions. Further, the CCW software validates real-time program performance, while MATLAB simulation validates the control approach, ensuring stable microgrid operation within IEEE standards. The future scope of this work includes integrating real-time Renewable and Non-Conventional Energy Sources, exploring fault diagnostics, and implementing a cascaded control approach for enhanced decision-making in microgrid systems.

CHAPTER 6
TECHNO-ECONOMIC ASSESSMENT OF DEVELOPED MICROGRID SYSTEM

Rural and remote electrification stands as a formidable challenge globally, prompting the exploration of viable solutions to address this critical issue. In response, well-planned and cost-effective microgrids, seamlessly integrating renewable energy sources, have emerged as promising remedies. Despite their potential, the stable operation and future deployment of microgrids face substantial challenges, influenced by perturbations arising from uncertainties in renewable sources, dependency on the battery state of charge, and fluctuations in load.

Recognizing the multifaceted concerns that impact the planning and development of microgrids in diverse regions, this chapter introduces a research initiative proposing a comprehensive performance assessment. Focused on a residential microgrid, the study centers on the Kibber village in Himachal Pradesh, India, leveraging a carefully constructed load model.

The proposed approach is structured into three phases, each contributing to optimal microgrid planning. First, employing the technical prowess of MATLAB–Simulink software, a meticulous analysis of system performance is conducted under perturbations, considering the variability of available renewable sources. Second, an economic evaluation facilitated by HOMER Pro software delves into the cost-effectiveness of the envisioned microgrid model. This includes a simulation of electrical loads specific to Kibber village, factoring in the dynamic nature of renewable resources. Validation of the proposed controller encompasses critical parameters such as system voltage, frequency, power distribution, percentage of load met, energy cost, and available renewable energy resources. The resulting comprehensive assessment of the microgrid model is designed to be reproducible, offering adaptability for application in varied geographical locations.

6.1.Introduction and background for comprehensive assessment

Rural and remote region electrification is integral to poverty mitigation, rural growth, and socioeconomic development, especially in India. It supports the region’s growth by providing reliable and continuous electricity for residential and commercial needs [233-234]. Given this, MG for rural and remote areas is a favorable solution with technological development and the capacity to integrate renewable energy sources (RESs). However, the critical concern related to rural area electrification via MG includes its optimal design, planning, and assessment considering the available resources and consumer demand [235-236]. Under such a concern,

the techno-economic feasibility analysis has been coined as a favorable solution in the literature [236]. This analysis uses various factors to calculate the possible combination of resources for the given location while considering the system cost, available resources type, total load demand, type of integrated storage, and mode of MG operation.

Previously, several pieces of research around the globe have been carried out for MG system feasibility analysis. A detailed investigation based on a single RES with ESS has been done for the developed system, considering the percentage of renewable penetration, cost of energy (COE), and carbon emissions as effective parameters [237]. Besides, the design optimization and feasibility analysis of the PV-fuel cell-based MG model developed using HOMER (hybrid optimization model for multiple energy resources) Pro software are presented in [238]. The investigation includes the effect of ESS's presence on MG economics. The impact of optimal resource sizing on islanded MG's financial and sensitivity analysis has been discussed in [239]. A feasibility analysis of PV-diesel generator-flywheel-based MG for the remote location of Saudi Arabia has been presented in [240]. Using the HOMER Pro software, the impact of ESS on the system economics and the effect of diesel generators (in coordination with RESs) on the environment have been investigated. A biomass-gasifier-based MG system has been studied using HOMER software [241], aiming at a minimum (0 %) unmet load condition. The analysis shows a high reduction in environmental impact but a hike in capital investment and COE.

Similarly, a PV and biomass-based MG model with an agricultural farm and a residential community load has been investigated in [241]. The off-grid MG model is analyzed based on per-unit cost and payback period. Multiple MG models and combinations have been studied in [242]. The work presents (PV)/battery and PV/battery/fuel cell (FC) power-based models, where the analysis is done per the initial cost, operating cost, and COE. The HOMER Pro software has analyzed the PV/hydro/diesel and battery-based systems [243]. The work presents different scenarios where the system's performance assessment and sensitivity analysis have been done. A summary of previous research articles discussing HOMER Pro software's assessment aspects and application for different RES combinations in the Indian locations are tabulated in Table 6.1.

Table 6.1. Summary of existing work in the Indian scenario

System Design	Location	Assessment Aspects	Remarks
PV-Battery-Grid [214]	Punjab, India	• Economic Feasibility	• High renewable potential in northern India. • An inverse relationship exists between the renewable energy output level and the designed system's COE.

Wind-PV-Battery-Grid [251]	Haryana, India	• Economic Feasibility	• Economic analysis of proposed MG for a given geographical area. • A technical assessment using MATLAB was done to share power between different sources.
PV-Wind-Diesel-Battery [252]	Punjab, India	• Economic Feasibility	• Assessment of multiple locations in Punjab for comparative analysis. • Comparison between different combinations of sources, from which the significance of PV in the northern region of India has been highlighted. • Consideration of 1.3 kW telecommunication load as critical load.
PV-Battery-Grid [253]	Uttar Pradesh, India	• Economic Feasibility • CO_2 Emissions • Technical Assessment with DSM	• Impact of grid availability on COE. • RES Optimization is needed to satisfy the daily load demand. • DSM of developed MG with NCL shed/shifted towards available solar or battery energy sources (grid satisfying critical load)
PV-Wind-Biomass-Battery [254]	Pondicherry, India	• Techno-Economic Analysis • Net Present Cost (NPC) analysis • Load Growth Assessment	• Predicted load growth using the ANN-LM technique. • Islanded MG as a cost-effective solution for rural electrification. • Reduced system emission and optimized system with ANN-LM • Biomass is a critical contributor to renewable Fraction (f_{ren}) and reliable power supply.
PV-Wind-Biomass [255]	Madras, India	• Economic Feasibility • Optimal component sizing	• HOMER Pro tool for techno-economic analysis and MG planning. • Review on HOMER Pro for MG design and simulation. • Effective use of available RESs for electrification. • COE is a significant parameter in overall system analysis.
PV-Wind-Hydro-Gen.-Battery [256]	Gujarat, India	• Economic Feasibility • Reduced Carbon emissions • Urban Electrification	• High renewable contribution for optimal MG planning. • Economical results with a higher number of RESs with reduced emissions. • Higher capital cost leads to an overall increase in other economic parameters.

PV-Wind-Hydro-Biomass-Battery [257]	Uttarakhand, India	• Economic Feasibility • Reliability analysis • Technical Assessment with DSM	• Islanded MG is used for remote and rural region electrification, with wind as the dominant resource. • Economic assessment and DSM analysis for the designed MG system. • Biomass as a reliable RES can only be used for high-availability locations, which increases system economics.
PV-Wind-Hydro-Battery [258]	Tamil Nadu, India	• Techno-Economic Feasibility • Environmental Aspect	• Hydropower sources are significant but constrained to the high amount of water resource availability and specific geographical location. • The wind is a significant RES in coastal regions for higher power generation. • Higher RES contribution leads to minimizing carbon emissions.
PV-Wind-Hydro-Bio. Battery [152]	Puducherry, India	• Techno-Economic Feasibility • Resource Assessment	• A higher value of f_{ren} leads to a minimum unmet load percentage. • Islanded MG as a favorable solution for rural and remote villages. • An abundance of solar and wind energy reduces COE for more than 90 % of load hours.
PV-Wind-Hydro-Bio. Battery [259]	Chhattisgarh, India.	• Techno-Economic Feasibility • Resource Assessment • Financial and Business Aspects	• The application and combination of different RESs satisfy multiple types of electric loads. • The dependency of component sizing is based on the peak load demand of the day. • Discussion on financing challenges, business models, and tariff issues.
PV-Wind-Battery-Grid [260]	Haryana, India	• Techno-Economic Feasibility	• Solar and wind-based RESs have a higher potential for satisfying multiple types of electric loads. • The excessive potential of solar energy in northern India. • Reduced CO_2 emissions due to higher renewable contribution.
Grid-PV-Wind-Diesel Generator [261]	Tamil Nadu, India	• Techno-Economic Feasibility	• However, using a diesel generator to enhance system reliability is unsuitable given environmental constraints. • A significant impact of only RESs-based system on CO_2 emissions and overall system cost.

			• An abundance of RESs leads to reduced COE and overall gas emissions.
PV-Wind-Battery-Grid [262]	Rajasthan, India	• Techno-Economic Feasibility	• Application of RESs to cater to environmental pollution. • Cost-effective solution for increasing power demand in India. • Applicability of high solar potential for high system efficiency and low dependency on the grid.

From the observation, the critical parameters identified for the MG's overall planning and feasibility analysis include the availability of RESs, different storage options, load conditions, and specific geographical locations. The other aspects of comprehensive MG assessment include technical simulation and control algorithm validation of the planned MG model using various simulation tools and laboratory-based hardware setups. These aspects are essential from the validation point of view. In the case of MG deployment, simulation validation plays a crucial role in understanding the system's behavior under uncertain conditions [244-246]. For this purpose, the MATLAB Simulation-based platform proves advantageous where the MG system can be simulated under standard and uncertain test conditions. Herein, the MATLAB Simulink platform offers the advantage of simulating the planned MG model to perform technical analysis. It allows for the simulation of the system under uncertain conditions and in the presence of a controller, wherein the performance can be assessed [247-248].

Further, the decision to stabilize MG's operation relies on technical performance analysis, including the system's electrical parameters, for example, system voltage, frequency, power-sharing between resources, etc. [249-250]. In continuation, the other shortcoming in the previous state-of-the-art research is the implementation assessment of the planned MG model. In the case of MG deployment, testing the planned MG and its behavior analysis in the presence of the actual controller is of utmost importance. It tests the control logic designed for the planned MG and allows for the analysis of the performance of the actual controller in real-time.

6.2.Methodology

This section presents this research's proposed methodology, including location information, load profile assessment, resource assessment, simulation and optimization tools, and the functional flowchart.

6.2.1. Location and Site Background

Figure 6.1 shows the site considered in this work, i.e., Kibber village in Spiti Valley,

Himachal Pradesh state, India, at a Longitude of 78°0’36.95 “E and Latitude of 32°19’57.58 “N at an altitude of 4135 m / 13566 feet above the sea level. The main reason for selecting such a region is the mass availability of RESs and the high cost of electricity transmission. It is relevant to mention that the authors did not physically visit this location. However, selecting remote sites using HOMER Pro and satellite imagery information has been used for academic research to investigate the MG feasibility in a remote location. This pre-planning assessment approach of MG’s technical and economic feasibility is deemed acceptable as it reduces the R&D cost before the site visit.

According to Census 2011 information on this site, approximately 366 people lived in 77 families/households with 4-7 persons in each house [263]. The main occupations of this 465-hectare village are agriculture and small businesses. In addition, this site is considered one of the last motorable villages with low or negligible communication facilities. Maintaining an uninterrupted power supply is a significant challenge because of the high altitude, rough terrain, and limited transportation facilities. Therefore, under the Rural Electrification Act, which aims toward electrical development, an MG system at this site must be proposed to meet the load demand and deliver a reliable power supply.

Figure 6.1. Geographical view of the investigated site

6.2.2. Load Profile Assessment

The load demand requirement of the Kibber village has been estimated by considering the number of households and the number of people [263]. It includes various domestic, commercial, and agricultural loads over 24 hours. The input of estimated load data, considering the number of households and essential electrical appliances, is given to HOMER Pro software [263-264]. The scaled value of the annual average load per day (kWh/d) is considered. Also, HOMER Pro software evaluates hourly electrical load values by using an hourly load profile and incorporating random variability factors. It can be observed that the load demand is

maximum during the morning and evening hours of the day. The load has been categorized as Load#1 (Domestic load) and Load#2 (commercial + agricultural load) for the developed model. The data analysis has identified that the peak and daily load demand of Load#1 nursed in HOMER Pro are 18.52 kW and 89.15 kWh/d, respectively. As analyzed, the combined peak load and daily load demand of Load#2 are 6.53 kW and 41.88 kWh/d, respectively. Figures 6.2(a) and 6.2(b) depict the daily, seasonal, and yearly load profiles.

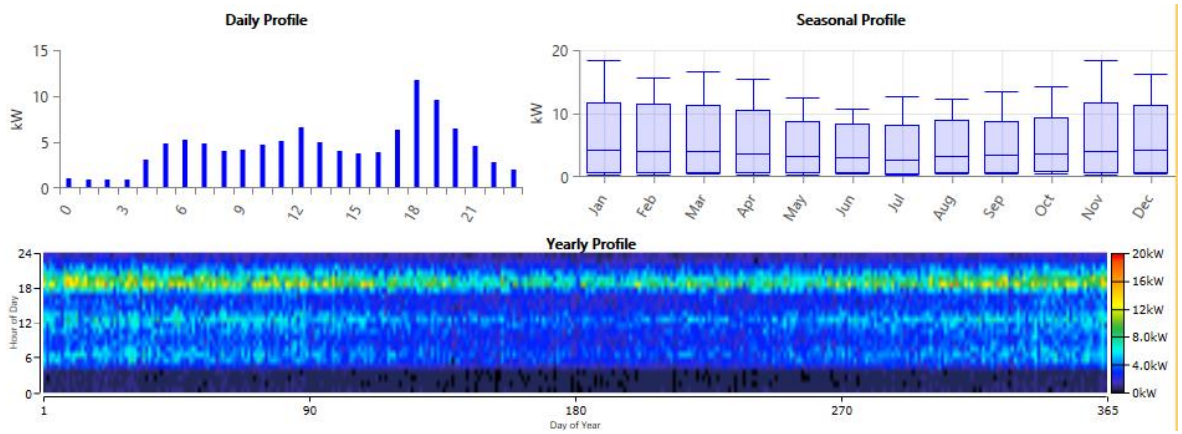

Average Load = 89 kWh/d Peak Load = 18.52 kW

(a) Plots for Domestic load profile (Load#1)

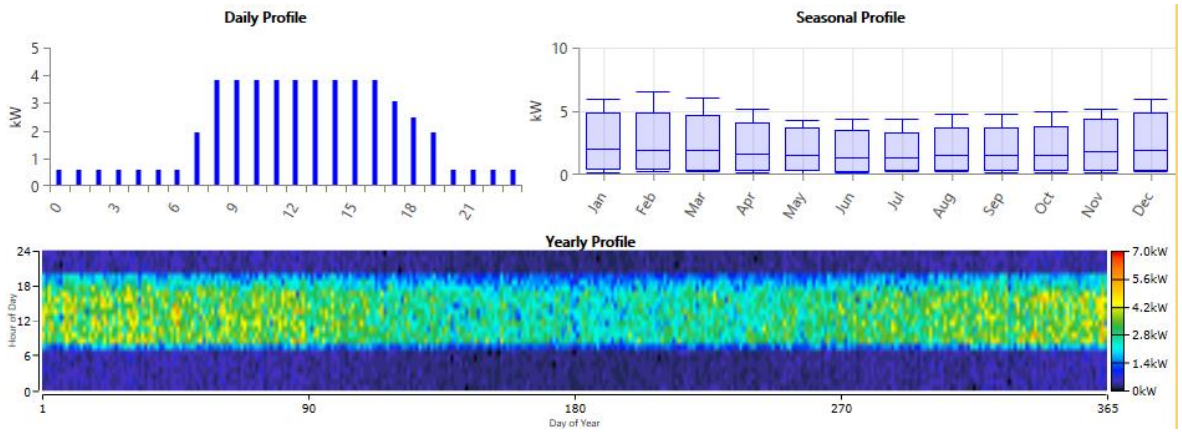

Average Load = 41.88 kWh/d Peak Load = 6.53 kW

(b) Plots for Commercial and Agricultural load profile (Load#2)

Figure 6.2. Plots for investigated load profiles

6.2.3. Resource Assessment

This work considers solar and wind-based RESs and the battery energy storage system for designing the MG model. The data for the site, i.e., Kibber village in Himachal Pradesh, was obtained from the NASA Surface Meteorology and Solar Energy database and NREL (National Renewable Energy Laboratory).

A. Solar Photovoltaic Resource

Solar resource potential is very high at the given location of Kibber, especially in summer. Due to the high altitude, the location experiences a high sky clearness index (CI) and, thus, high solar radiation. The solar PV data from NREL for both CI and daily radiation in kWh/m^2/day has been tabulated in Table 6.2 with other details. Besides, the annual average value of solar irradiance is also mentioned as a part of tabulated data. As per analysis, the CI varies from 0.538 to 0.699, and Global Horizontal Irradiance (GHI) varies from 2.990 to 7.020 kWh/m^2/day. Lastly, the scaled annual average value of GHI is 5.10 kWh/m^2/day.

Table 6.2. Tabulated Data for Solar Photovoltaic Energy Resource

Solar Radiation data

Month	CI	Solar Radiation (kWh/m^2/day)	Month	CI	Solar Radiation (kWh/m^2/day)
January	0.573	3.170	July	0.592	6.670
February	0.567	3.860	August	0.589	6.150
March	0.547	4.660	September	0.644	5.820
April	0.538	5.440	October	0.699	5.100
May	0.578	6.420	November	0.663	3.850
June	0.611	7.020	December	0.583	2.990
Minimum: 2.990, Maximum: 7.020			Annual average value: 5.10		

Technical and Economic Data

Parameter	Value	Parameter	Value
Pmax	350 W	Capital cost	725 $/kW
Derating factor	88 %	Replacement cost	725 $/kW
Efficiency	18.90 %	O&M cost	10 $/kW/y
Lifetime	25 Years	Operating Temperature	≈+85°C
Technology	Monocrystalline (Mono)	Operating current	10.52 A
Temperature coefficient	-0.390	Operating voltage	33.3 V
Open circuit voltage	40 V	Short circuit current	11.28 A

B. Wind Energy Resource

Analogous to solar photovoltaic, wind resource for the considered location has a high potential. With an approximate altitude of 4000 m, wind availability is very high and can be utilized as a potential resource. The mathematical expression related to the real power of the wind energy system for each instant of time depends on various parameters. These factors

include - wind density, wind speed, turbine sweep area, and power coefficient. Table 6.3 below shows the monthly average wind speed data, which varies from 5.350 to 8.290 m/s with an annual average wind speed of 7.110 m/s. Notably, the height considered for measuring the wind speed using an anemometer is 50 m. Also, the effects of wind speed variation on system performance can be investigated by performing the sensitivity analysis, depending on the variation in values.

Table 6.3. Tabulated Data for Wind Energy Resource

Wind Speed data

Month	Wind Speed (m/s)	Month	Wind Speed (m/s)
January	7.960	July	5.600
February	7.890	August	5.350
March	7.580	September	6.090
April	7.010	October	7.440
May	7.200	November	7.970
June	6.900	December	8.290
Minimum: 5.350, Maximum: 8.290		Annual average value: 7.110	

Technical and Economic Data

Parameter	Value	Parameter	Value
Manufacturer	Generic	Rated capacity (kW)	10
Lifetime (y)	22	Rotor diameter (m)	22
Hub height (m)	24	Tower height (m)	50
Capital cost	$44500	Swept area (m^2)	2300
Replacement cost	$40500	Number of blades	3
O & M cost/year	$400	Cut-in-speed (m/s)	3
Rated wind speed (m/s)	10	Cut-out-speed (m/s)	21

C. Other Components

- Battery Energy Storage System (BESS)

The power produced by the RESs may not be utilized at every time of the day. Thus, storing the excess energy from the RESs in a BESS is highly significant. In HOMER Pro software, various storage units are available, including a Li-ion battery, flywheel, and fuel cell. The details of BESS employed in this work are given in Table 6.4. The prime aim of adding a storage unit into the system is to use it as ancillary support, such as to increase the system's reliability.

Table 6.4. Tabulated Data for Battery Energy Storage System

Parameter	Value	Parameter	Value
Manufacturer	Discover Innovative battery solutions	Minimum/Maximum SOC	20 % to 80 %
Efficiency	80 %	Nominal voltage	12 V
Capital cost	$400	Nominal capacity	3.11 kWh
Replacement cost	$330	Initial SOC	100 %
O&M cost/year	$7	Electrolyte	1.255 SG
Maximum charge current	43 A	Height	410 mm
Internal resistance	5 mω	Weight	60.8 kg
Short circuit	2150 A	Maximum capacity	260 Ah
Self-discharge	5 %/month	Lifetime throughput	3581.60 kWh

- Power Converters/Inverters

AC/DC, DC/AC converters, and inverters are the most critical components for designing an MG with different power sources. With such components, all the resources and different types of loads can be interconnected, aiming for smooth integration between resource and load. The converter forms a two-way bus system, resulting in the bidirectional power flow. The AC power can be converted into DC for battery charging (as required), and DC power can be converted into AC (acting as an inverter) for the connected electrical load. The configuration details of the power converter used in the present research are tabulated in Table 6.5.

Table 6.5. Tabulated Data for Power Converter

Parameter	Value	Parameter	Value
Type	AC-DC-AC	Replacement cost ($)	350
Capital cost ($)	600	O &M cost ($)	5/year
Lifetime (years)	18	Efficiency	95 %

6.3.System Configuration and Description

6.3.1. MATLAB-Simulink model

Focusing on the technical grounds of MG feasibility, the electrical parameters identified in the literature include voltage, frequency, and power-sharing [1, 148]. As per the IEEE standards and CERC Staff Paper March 2011, the feasible frequency range under the Indian Electricity Grid Code (IEGC) must be 49.5 Hz to 50.2 Hz and ±5 % of the standard voltage [176, 204-205].

The proposed model of the residential MG is shown in Figure 6.3. The system includes a wind energy source (WES) of 25 kW capacity, a solar PV of 15 kW, and a lithium-ion-based battery energy storage system (BESS) with a rated capacity of 360 V and 55 Ah. The figure shows that the power sources are connected through the converter modules with the DC link. The conventional PID-based voltage regulator further controls and regulates the inverter output. The system is designed for a total peak electrical load of approximately 25 kW capacity, where 7.5 ± 2.5 kW is the critical load (CL), and the remaining is the non-critical load (NCL). Table 6.6 below presents the data employed to develop the simulation model using the MATLAB Simulink software, version 2019b. The tabulated data represents the information related to the simulated system, system design, and fuzzy logic controller design.

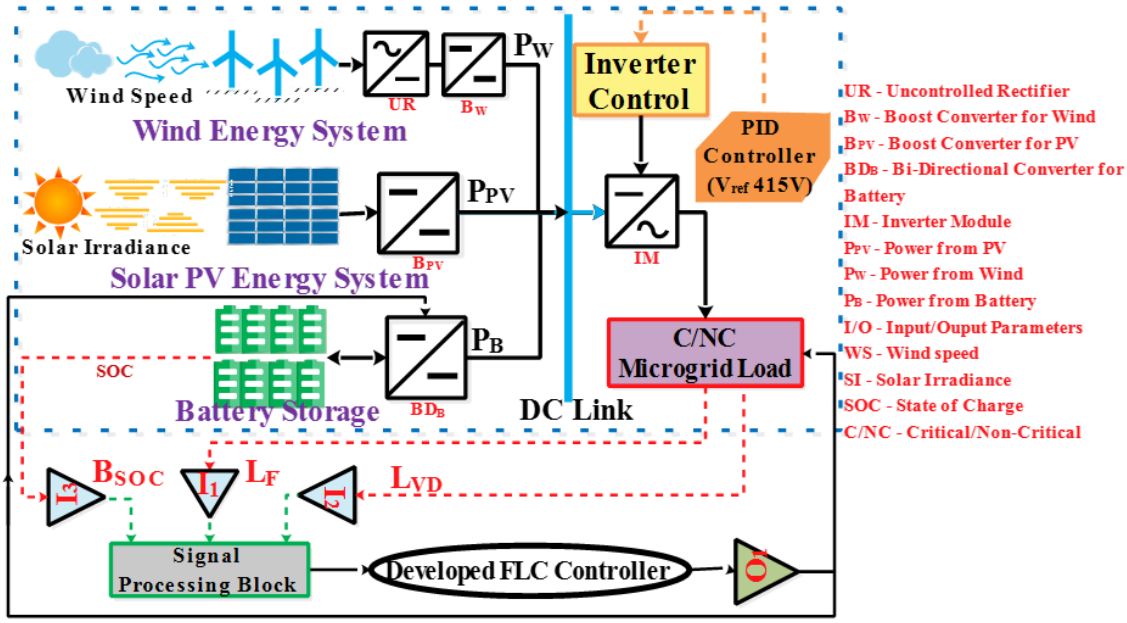

Figure 6.3. MG model under investigation

Table 6.6. Tabulated data for the simulation model

Parameter	Value	Parameter	Value
Simulation mode	Normal	PV rating	15 kW
Start and Stop Time	0 – 4 sec.	Wind rating	25 kW
Nominal P-P voltage (Vrms)	415 V	Battery rating	360 V/55 Ah
Nominal frequency	50 Hz	Solar STC	1000 W/m^2
Sample time (s)	Ts (2e-6)	Load Value`	25 kW
Number of blocks and components	240/1245	FLC	Struct
Max/Min step	Auto/Auto	Type	Mamdani
Solver/Solver mode	ode23tb /Auto	And/Or method	MinMax
Solver type	Variable step	Defuzz method	Centroid

Relative tolerance	1e-3	Imp method	Min
Consecutive ZCs step rel tol	10*128*eps	Agg method	Max
Max consecutive ZCs	1000	Input & Output	3/1
Base Wind speed	7.2 m/s	Rule (s)	75
Pitch Angle	0^0	Tip Ratio	8.152

6.3.2. HOMER Pro Model

The developed system incorporates power sources, including a solar PV module, a wind energy module, and a battery energy storage system. Designing such a system combines two or more renewable sources to improve operating characteristics, reliability, and performance. The sources are connected using the converter module, as shown in Figure 6.4, whereas the related data is tabulated in Table 6.2 to Table 6.5.

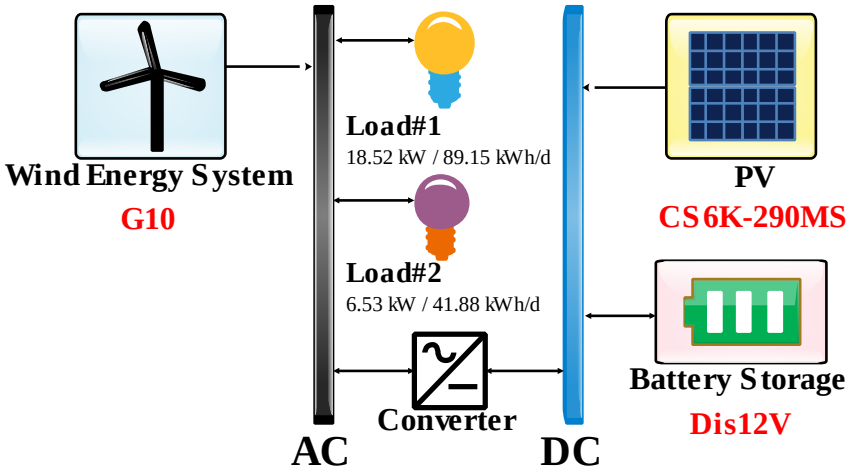

Figure 6.4. MG Layout in HOMER Pro Software

6.4.Working Flowchart for Proposed Methodology

This section presents the functional and comprehensive flowchart of the proposed methodology while aiming at the complete assessment of the developed MG. The flowchart illustrates the different aspects of assessment done in this work to validate the proposed MG structure's novel performance. Besides, the step-by-step details of the flowchart shown in Figure 6.5 have also been organized. In the figure, a comprehensive layout of the proposed methodology has been presented. The flowchart can be explained in 2 steps, as discussed below:

Step 1 – Technical Assessment: Considering the aspects of technical assessment of the developed MG, the MATLAB – Simulink platform has been employed. The variable and uncertain renewable output as critical conditions have been considered to validate system performance. Significant parameters, including the system voltage, frequency, accuracy in

power-sharing, and the DC-link voltage, have been considered for the analysis. For this purpose, the different standards and regulations passed by the Electricity Board of India have been considered to validate the system's feasibility. It is noteworthy that such case studies must be simulated before the practical realization of the existing system. This way, through simulations, the technical assessment can be analyzed.

Step 2 – Economic Assessment: Considering the given configuration, it is crucial to assess the economic aspects of the MG. The present research focuses on the key parameters, like COE, O&M Cost, etc. The other important part of such analysis is the set constraints, including the minimized unmet load percentage, maximum renewable extraction, and minimum carbon emissions. Thus, employing the HOMER Pro software, the economic analysis of the developed system can be done for several resource combinations, out of which the most feasible and optimized solution can be attained.

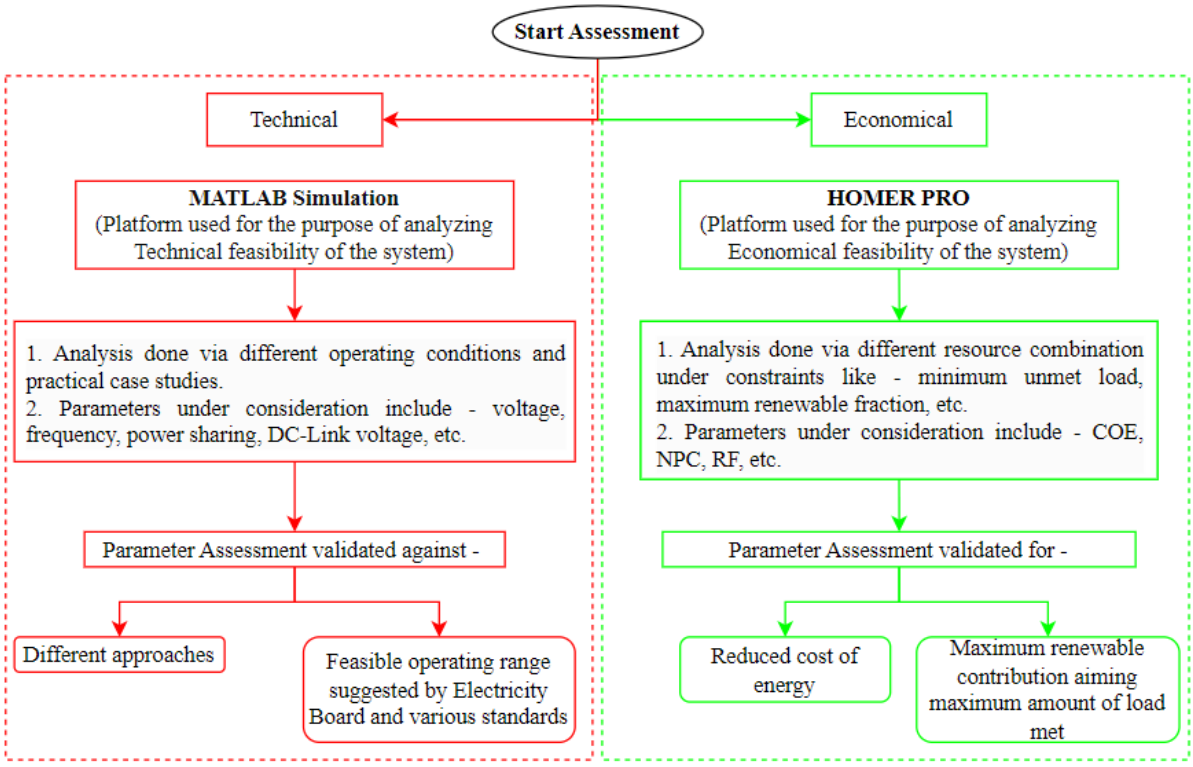

Figure 6.5. The layout of the proposed methodology

6.5.Results and Discussion

6.5.1. Technical Simulation Results

Following Figure 6.3 and Figure 6.5, the simulation results for developed MG using MATLAB Simulink software are presented below in Figures 6.6(a) to 6.6(d). The aforementioned key parameters, i.e., voltage, frequency, and power-sharing, have been showcased under the ideal and non-ideal scenarios.

Figure 6.6(a) presents the system RMS voltage under ideal conditions (415 V). Figure 6.6(b) presents the system frequency observed across the connected load. Figure 6.6(d) presents the power-sharing among renewable sources while fulfilling the total load demand. It is worth analyzing that the frequency and voltage parameters lie in the feasible range of operation, i.e., the permissible range (49.5 Hz to 50.2 Hz) as per the Indian Electricity Grid Code (IEGC), and the obtained value shown in Figure 6.6(b) is minimum 49.97 Hz and maximum 50.05 Hz [176, 204-205]. Besides, the battery associated with the developed MG can be observed to be in the charging mode of operation considering the ideal conditions and sufficient renewable output, as shown in Figure 6.6(c). Compared to the ideal conditions, the MG feasibility and operation have also been analyzed under non-ideal conditions. Considering the small village load and islanded MG condition in remote regions, the drop in renewable output has been seen as one of the significant concerns in MG stability [148]. Henceforth, a similar condition has been simulated in this work for the feasibility and response analysis of the proposed MG.

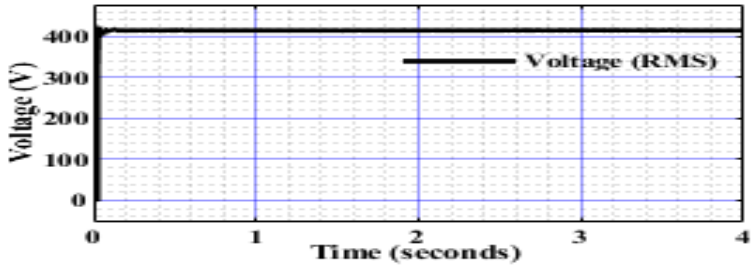

(a) MG Voltage Parameter

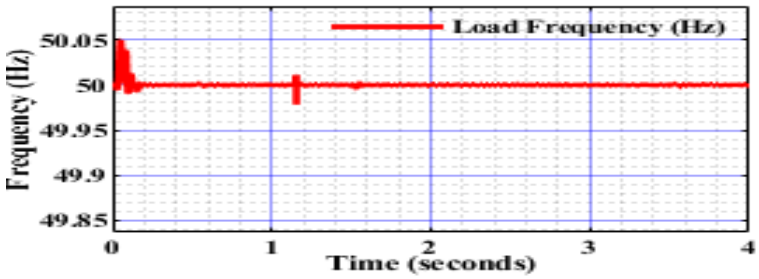

(b) MG Frequency Parameter

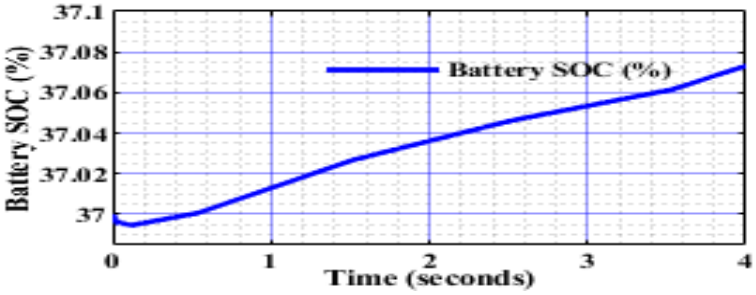

(c) Battery SOC

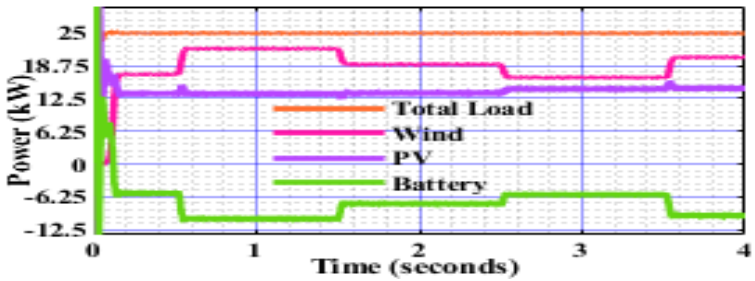

(d) MG Power Sharing

Figure 6.6. Technical feasibility analysis results – Ideal Conditions

In Figure 6.7, the fluctuation due to small perturbations in the simulation can be observed where the renewable output is supposed to drop. Figures 6.7(a) and 6.7(b) show that the voltage and frequency parameter deviation can be observed during this period. In the presence of a developed FLC controller, this fluctuation is balanced and strained within the permissible limits, i.e., 49.5 Hz to 50.2 Hz as per the Indian Electricity Grid Code (IEGC), and the obtained value shown in Figure 6.7(b) is the minimum 49.935 Hz and maximum 50.1 Hz [176, 204-205]. From Figure 6.7(c), the battery SOC can be observed to be in discharging mode once the renewable output drops due to the small perturbations. Notably, under small perturbations, the battery with a high SOC can feed the village's critical and non-critical load for a given period, after which load shedding according to load priority shall be performed. However, the battery will discharge significantly in large perturbations caused by a significant solar and wind energy drop. Henceforth, the considerable role of providing ancillary support to the islanded system is well suited and taken by the battery ESS, as shown in Figure 6.7(d).

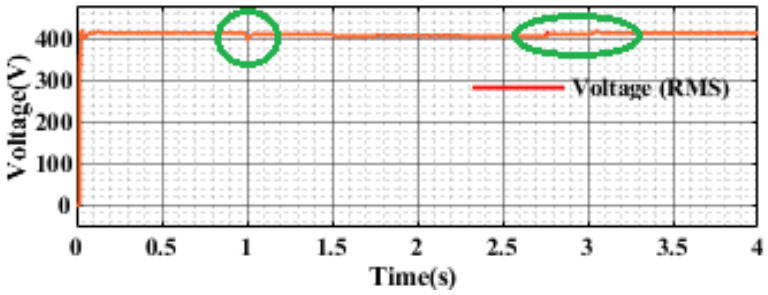

(a) MG Voltage Parameter

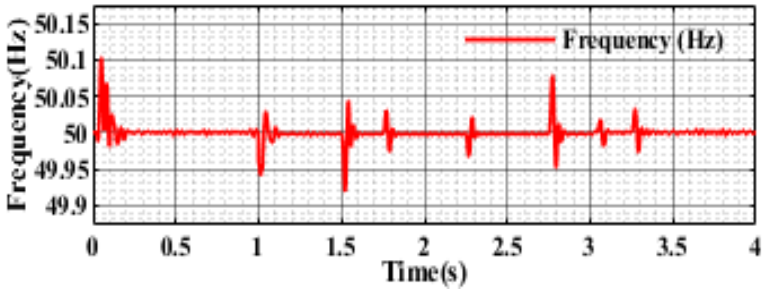

(b) MG Frequency Parameter

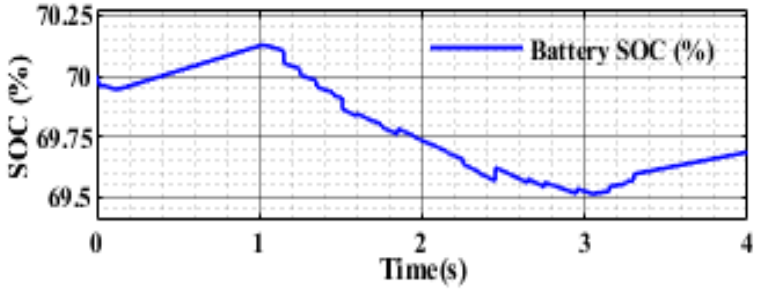

(c) Battery SOC

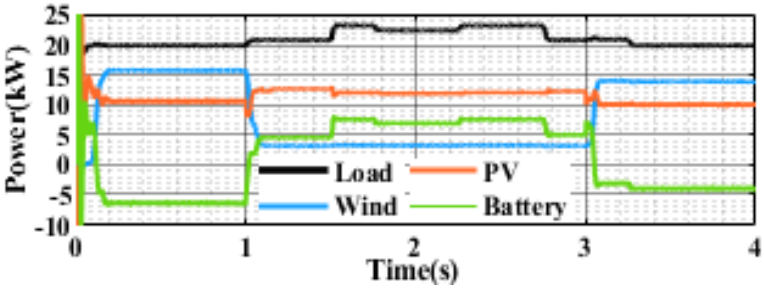

(d) MG Power Sharing

Figure 6.7. Technical Feasibility Analysis Results – Non-Ideal Conditions

6.5.2. Economic Assessment Results

For an economic assessment of the proposed MG architecture for the Kibber region, Himachal Pradesh, the HOMER Pro software has been used in this research. As discussed, the software allows the optimal combination of resources for the said location from a techno-economic viewpoint. In addition, a separate sensitivity analysis has been performed to analyze the system response regarding the change in average values of RESs. The comprehensive details and results for the developed MG for the most feasible combinations have been tabulated in Table 6.7. Notably, the cost for various components and parameters has been considered in US Dollars ($), which in Indian Rupee (INR) is equal to Rs. 75/- approximately $1 as of January 25, 2022 [265].

Table 6.7. Comparison of the different optimized configurations

Sr. No.	Classification	Parameter	Configuration		
			PV + Battery	PV + Wind + Battery	Wind + battery
1.	Architecture	Architecture/CS6K-290MS (kW)	54	47.25	--
2.		Architecture/G10	0	1	13
3.		Architecture/Dis12V	183	177	213
4.		Architecture/Converter (kW)	25.729	26.916	24.657
5.		Architecture/Dispatch	CC	CC	CC
6.	Cost	Cost/COE ($)	0.127	0.171	0.277

7.		Cost/NPC ($)	248966.1	282958.1	818979.3
8.		Cost/Operating cost ($/yr)	3749.477	4148.756	10867.12
9.		Cost/Initial capital ($)	20049.6	229325	678494.4
10.		Cost/Fuel cost ($/yr)	0	0	0
11.		Cost/O&M ($/yr)	2952.503	3123.583	6814.287
12.		CS6K-290MS/Capital Cost ($)	111857.1	97875	--
13.		G10/Capital Cost ($)	--	44500	578500
14.		G10/O&M cost ($)	--	400	5200
15.	System Component(s)	System/Ren Frac (%)	100	100	100
16.		System/Total Fuel (L/yr)	0	0	0
17.		System/Cap Short (%)	0.09759784	0.000764332	0.0985902
18.		System/Excess Elec (%)	36.56232	39.48045	66.7873
19.		System/Unmet load (%)	0.02102028	2.20E-15	0.05702304
20.		System/Unmet load (kWh/yr)	12.37111	1.29E-12	33.55989
21.		System/CO_2 (kg/yr)	0	0	0
22.		CS6K-290MS/Production (kWh/yr)	104196.7	91172.15	--
23.		G10/Production (kWh/yr)	--	15099.26	196290.4
24.		Dis12V/Autonomy (hr)	67.86707	65.64193	78.99283
25.		Dis12V/Annual Throughput (kWh/yr)	19737.41	13697.71	19485.57
26.		Dis12V/Nominal Capacity (kWh)	569.9479	551.2612	663.3821
27.		Dis12V/Usable Nominal Capacity (kWh)	455.9584	441.0089	530.7056

The analysis shows that the PV + Battery combination with a COE of $0.127 is the best configuration for the given location. This configuration is followed by the PV + Wind + Battery combination with a COE of $0.171. This increase in COE value is due to the high operating cost, O&M cost, etc., which are higher in the other two cases. However, with the high COE and other cost parameters, the wind + battery combination stands last as the most feasible solution. The other observations made from the analysis include –

- Negligible or deficient unmet load percentage with the value of 0.021020 %, 2.20E-15 %, and 0.057023 %, respectively, along with 100 % f_{ren}. It validates the maximum renewable extraction for the minimum unmet load percentage.
- Islanded MG system that eliminates the CO_2 emissions from the concerned site.

- Without any generator set, the system's fuel consumption is nonexistent, which validates minimum environmental damage.
- In the case of future developments concerning net metering, the scope of excess electricity that can be supplied back to the grid or utilized for other purposes is high. For each case, the excess electricity percentage varies from 36.56232 %, 39.48045 %, and 66.7873 %, respectively.
- PV and Battery combination is a viable option given the COE, system operating cost, and O&M costs. Furthermore, in this combination, the PV unit can supply the electric load for most hours, covering the peak load with the battery acting as ancillary support during the off hours. However, with significantly less difference in the COE, the other combination of (PV + Wind + Battery) can also be preferred, bearing in mind the renewable uncertainty.

Besides the above observations, sensitivity analysis was performed to understand the system's behavior by considering key input parameters. These parameters include load fluctuation, uncertainty in solar radiation, and wind speed database. The observations are listed below:

- As the domestic load is considered dynamic, thus a variation in load has been considered. It is worth noting that with the increase in the total load demand, more PV modules must be installed. This has led to an approximate rise of 14.5 % in NPC. This increase in the number of PV modules analytically leads to a slight decrease in the COE from $0.127 to $0.123.
- The average solar radiation database varies from 4.50 kWh/m2/day to 5.50 kWh/m2/day, keeping other parameters fixed. Remarkably, with the increase in solar radiation, the PV power output increases and thus leads to a drop in COE from $0.127 to $0.124. However, the COE increases to $0.130 when the solar radiation is dropped down to a 4.5 kWh/m2/day value.
- Likewise, the wind speed data for solar radiation varies from 6.5 m/s to 7.5 m/s value. It has been observed that the number of wind units remains the same while the wind speed is varied, though the COE varies significantly. For an increase in wind speed, the COE for the most feasible case drops from $0.171 to $0.164. Simultaneously, it increases to $0.175 for the drop in wind speed. Notably, the NPC also varies with the variation in RES data.
- Lastly, with the variation in the capital cost of ESS, the COE and other cost parameters vary significantly. When the capital cost of the battery is reduced from $400 to $350, the NPC of the system drops by 10-15 %, and COE drops to a minimum value of $0.111. However, if the capital cost is increased to $450, a considerable increase in the COE and NPC has

been observed. Thus, a drop in ESS price leads to a more economical and feasible MG architecture.

6.6.Strategic Initiatives

Considering the present state of rural and remote electrification in India, several initiatives can be idealized to enhance existing policies. Traditionally, policies like the Pradhan Mantri Gramodaya Yojna (PMGY), Kutir Jyoti Program (KJP), Minimum Needs Program (MNP), Accelerated Rural Electrification Program (AREP), Rural Electricity Supply Technology Mission (REST), and Rajiv Gandhi Grameen Vidyutikaran Yojna have primarily focused on the availability of electricity. However, with advancements in renewable technology, the focus should shift towards providing more reliable and continuous electricity. This particularly includes leveraging renewable energy sources to their fullest potential. Besides, the new policies should be based on microgrids' power quality and stability index to ensure secure and reliable connections. Additionally, the cost of ancillary support, especially battery and other equipment should be subsidized or reduced to enhance affordability. Lastly, a thorough assessment, including technical simulations, economic analysis, and controller testing, is essential to ensure security, stability, and proper control before deployment.

Thus, transitioning from implementing a microgrid, as detailed in Chapter 6, Chapter 7 presents a methodology for continuously measuring key parameters for assessing microgrid stability using a microgrid stability index (MGSI).

Chapter Summary

This chapter focuses on implementing a microgrid (MG) in the Kibber region of Himachal Pradesh, India, to address rural electrification using solar and wind energy. Technical analysis using MATLAB Simulink demonstrates the MG's reliable performance in power-sharing and response under uncertain conditions. Economic analysis, conducted with HOMER Pro software, determines optimal generating units, cost of energy (COE), and net present cost (NPC), showcasing the system's efficiency. The study emphasizes the need for location-specific assessments and provides guidelines for planning MGs in remote areas. Future plans include on-site assessments in Kibber Village, considering factors like insurance and battery damage, and exploring alternatives for battery storage in a multidimensional approach.

CHAPTER 7
METHODOLOGY FOR DETERMINATION OF MICROGRID STABILITY INDEX BASED ON MAMDANI-FIS

The operational stability of microgrids (MGs) presents significant challenges for engineers and researchers, encompassing issues related to energy management, power quality maintenance, and the impact of perturbations. To address such challenges, this chapter introduces a novel decision-making methodology to determine the Microgrid Stability Index (MGSI), providing a comprehensive measure of MG stability. The proposed index continuously monitors fundamental MG parameters, such as voltage, frequency, battery state of charge (SOC), and total harmonic distortion. A Mamdani-based fuzzy inference system incorporating 256 rules assesses the influence of these parameters on system stability.

Motivated by the need for a robust stability assessment tool, this chapter evaluates the proposed methodology through seven case studies. These scenarios encompass diverse modes of MG operation, various load types, and different power source availabilities, simulated using MATLAB Simulink software. Results reveal discernible variations in MGSI across different scenarios, highlighting the superior performance of a grid-connected MG system with high renewable output, elevated battery SOC, and a mix of critical and non-critical loads. Conversely, an islanded MG system with low renewable output, depleted battery SOC, and an inductive load demonstrate the least MGSI.

In addition to showcasing the effectiveness of the fuzzy-based controller in complex decision-making, the chapter conducts a comparative analysis with the analytic hierarchy process as part of the multi-criteria decision-making technique. The study includes sensitivity analysis, illustrating the system's responsiveness to various input sources, and a robustness analysis of the controller. Through these comprehensive evaluations, the chapter contributes to the understanding and enhancement of MG stability assessment methodologies.

7.1.Background for comprehensive assessment

Global energy consumption has observed a drastic change in the trends and highest peaks over the past decade. This peak results from increasing residential, industrial, and commercial loads in the current power system. The critical loads have been considered significant among all the residential and commercial loads. Besides this, the increasing demand from the building and retail industries is also the leading cause of ever-increasing societal emissions [266-267]. As per International Energy Agency (IEA), World Energy Outlook, and Ministry of New and Renewable Energy, India (MNRE) reports, the rate of energy consumption from such sectors

is expected to increase up to 1.5–2 % in the next 15 years [268-270]. Following a similar trend but with a higher slope, the residential load is expected to increase the consumption rate by 13 – 15 % in the coming 15 years [271]. To cope with such a rise in demand and environmental concerns, like high CO2 emissions, the favorable solution for researchers and industrialists has shifted from conventional sources to renewable and non-conventional energy sources (RNCES). The inclusion and increased penetration of renewable sources have led the traditional power system to transform into an active and advanced solution in the form of MGs. This transformation has been very well adapted and works to decarbonize power systems in modern society. A microgrid (MG) is a self-sustaining energy model that will create an advanced power system with minimum or zero carbon emissions and environmental threats. Besides, the key advantage of such an advanced system is its ability to generate, distribute, and fulfill the daily energy demands within the infinitesimal operation boundary in a well-controlled manner. Considering numerous advantages, the intelligent microgrid (MG) system is the most trending type of MG. It incorporates energy resources like solar photovoltaic (PV), wind turbines, fuel cells, battery storage (including Electric vehicles (EV) occupied with batteries as ancillary support), biomass, geothermal, tidal power, etc., both AC/DC loads, and advanced monitoring and measuring units. Out of all the sources above, PV and wind turbine-based power sources offer several benefits considering different loads and conditions, like rural and remote locations. However, the uncertainty and variability present in these resources limit the system's performance and make it unstable [272-274].

Thus, MG stability is considered the most significant among all the challenges and constraints. The variable nature of the resources and load tends to alter the system's stability on the negative side and thus needs to be specially measured and monitored [1]. Besides, some critical issues include MG's dynamic and unpredictable nature, application of power electronic converters, etc., leading to voltage fluctuations, poor frequency regulations, and system shutdown in the worst case [275-276]. Hereafter, it is concluded that integrating various RNCES gives an advantage to the hybrid MG system but also leads to a concerning issue related to its stability.

Thus, MGs' stability and measurement are significant concerns. It is explained as the ability to maintain all the system parameters, including voltage, frequency, total harmonic distortion (THD), net power shared in the system (power balance), etc., within their feasible range [1, 275-277]. Notably, the measurement and continuous monitoring of other components and parameters like the battery state of charge (SOC), DC link voltage, solar irradiance level, wind speed, etc., also play an essential role in system stability. Such a highly advantageous mini-power system aiming at the best stability level at all instants of operation is desirable. It

becomes the responsibility of the researchers, system operators, and industry persons to enhance the working and feasibility of the designed MG system because of continuous parameter measurements, system monitoring, and decision-making.

The literature review reveals various control techniques for measuring and monitoring MG stability, categorized as conventional, intelligent, and hybrid control techniques [1]. Intelligent control techniques, including neural networks, fuzzy logic, neuro-fuzzy control, etc., have been highlighted in the literature. These control techniques use multiple measurement units and data related to multiple parameters for enhanced control and stable MG operation. Focusing on this, the researchers in [7, 278] consider the measured data of different electrical parameters affecting MG stability, especially voltage, frequency, and the system's net power. Notably, based on the superior value of these parameters and their possible range of operation, the stability of the designed MG has been established and validated. [279] addressed the MG framework, which explains various challenges present in MG design and its stability. The survey concluded that the core issue related to MG stability is its mode of operation, i.e., islanding and grid-connected, along with the variation in the energy resources, the battery SOC, point of measurement, and related decision-making. Further, [94, 102, 103, 280-281] discussed the various control techniques working in a centralized, decentralized, and distributed manner aiming at the voltage parameter. Notably, the work focused on maintaining the voltage balance for stable MG operation. The conditions and variables in the literature include measuring and monitoring DC-Link voltage, power management, temporary transients, etc. Also, focusing on the other parameters and related literature, [108, 113, 282] discussed the operation and control of frequency parameters and their influence on MG stability. The various issues and conditions considered by the researchers included the load fluctuations and variability in the RNCES, especially while working in the islanded mode of operation. Besides, previous research has shown the significance of power balance and its efficient management in maintaining a stable operation. As per literature [122, 127, 131, 283-284], various control schemes have been proposed to measure the instability caused by the fluctuations in the system. The researchers discussed the importance of power control, its continuous measurement, and monitoring to maintain a stable MG operation.

In addition to these parameters and control approaches, the fuzzy logic controller is highly significant because of its various advantages. These are adaptive nature, intelligent control, adaptability to multiple parameters, allowable permittable range, etc. Converging on this, [71, 285] discussed the various applications and work related to a fuzzy logic controller and stable MG operation. Likewise, [286] presents the application of a fuzzy logic controller in the load

frequency control (LFC) of a wind-based system. Significantly, the work highlights the role of an optimized fuzzy controller in maintaining stable MG operation under various perturbations.

Similarly, [287-288] presents the significance of an optimized fuzzy controller in stable system operation under load variations, changes in weather patterns, the collapse of power generation units, etc. It evaluates individual Microgrid (MG) parameters, like voltage and frequency stability. Besides the risk evaluation of MG based on system stability and reliability, controllers for MG stability in an islanded mode of operation under various scenarios have been explored [289-291]. Additionally, controllers for multi-microgrid systems, including fuzzy logic, have been studied, highlighting the importance of fuzzy logic and significant MG stability [37-38]. Likewise, stability assessment for DC MGs, distributed control approach for regulating system voltage and frequency of AC/DC MGs, the effect of electric vehicles on the system performance, especially voltage and frequency regulation, and overall stability have been well explored [292-296]. However, a notable lack of significant literature comprehensively addresses the stability assessment of the entire MG system, considering its key parameters, uncertain conditions, and diverse electric loads [297-298]. While conventional power system stability and multi-area criteria control methodologies have been explored, they fail to provide a comprehensive approach for calculating and evaluating the overall system stability index. Instead, these methods often emphasize stability under smooth integration scenarios, which may not accurately represent the complexities and challenges of microgrid operations. Hence, there is a pressing need to develop specialized methodologies tailored to microgrids' unique characteristics to establish a more accurate and relevant stability index to enhance microgrid control and management.

Considering the absence of a comprehensive methodology for calculating and evaluating Microgrid (MG) stability highlights the critical need for such an approach. Current research primarily focuses on assessing individual MG parameters, leaving a gap in understanding the overall system stability under diverse operating conditions. A well-established system stability index that considers factors such as parameter measurement, uncertainty in power generation, variability in electrical load, and uncontrollable conditions is essential to address this. The significance of the Microgrid Stability Index (MGSI) lies in its ability to provide a holistic view of the system's stability. The MGSI offers valuable insights into the microgrid's performance and reliability by considering multiple parameters and uncertainties. This comprehensive assessment is vital for modern microgrids, which increasingly integrate renewable energy sources and power electronic converters, adding complexity and challenges to their operation. With a well-defined MGSI, operators and managers can effectively monitor and control the microgrid to ensure stability. This empowers them to take proactive measures in response to

fluctuations in renewable energy generation, dynamic changes in electrical load demand, and other unpredictable factors that may impact the microgrid's stability.

Moreover, a reliable MGSI can be a decision-making tool for optimizing microgrid control strategies, resource allocation, and operational planning. By understanding the system's stability, stakeholders can make informed choices to enhance efficiency, reduce downtime, and improve the microgrid's resilience to various disruptions. Ultimately, developing and implementing a comprehensive MGSI paves the way for more efficient, sustainable, and reliable microgrid operation. As microgrids play an increasingly critical role in the future of energy distribution, having a robust stability index becomes essential to their successful integration into the broader energy landscape.

7.2.Microgrid Description and Modeling

This section presents the MG description and its modeling. The first part discusses the configuration details of the MG system developed using MATLAB Simulink Software v2019b. The latter part of the section presents the details and mathematical modeling of the system's key components. It is noteworthy that the proposed MG model is novel, considering its design, configuration, and methodology.

7.2.1. Microgrid Configuration

This subsection discusses the design and configuration of the proposed hybrid MG model. The designed system integrates the wind energy system where WS represents the variable wind speed, a solar photovoltaic-based renewable source with variable solar irradiance (SI), and a lithium-ion-based battery storage device. The power components are connected at the common DC link through various AC/DC/AC converters. As discussed above, the system design was developed using blocks and mathematical modeling of the components in MATLAB Simulink software 2019b. Furthermore, parameters such as solar irradiance, wind speed, battery state of charge, DC-Link voltage, etc., are all measured and considered in the developed model.

As shown in Figure 7.1, the RNCES, like solar PV and wind energy systems with variable raw resources (SI and WS), have been considered the system's primary power sources. In addition, the battery energy storage system has also been connected as ancillary support to stabilize the system under uncertain conditions. The primary purpose of connecting the battery energy storage system is to supply the amount of energy required by the system in various instances like the partial or complete absence of RNCES, islanding conditions with a fluctuating load, etc. [299] A typical DC-link configuration has been considered for integrating the resources and necessary synchronization. Considering the low voltage residential/commercial

MG with system voltage and frequency ratings of 415 V and 50 Hz, the wind turbine of 40 kW rated capacity, a PV array of 30 kW, and the lithium-ion battery pack with a rated voltage of 360 V and 55 Ah are present in the system with the critical load of 15 kW and a non-critical load of 35 kW. Following this, the PI-controller DC/AC IGBT-based inverter module has been connected to the system to supply constant AC per the set reference to the MG system. The modulation index is measured to vary between 0.81 and 0.86 per the uncertain conditions of RNCES considering inverter control [5].

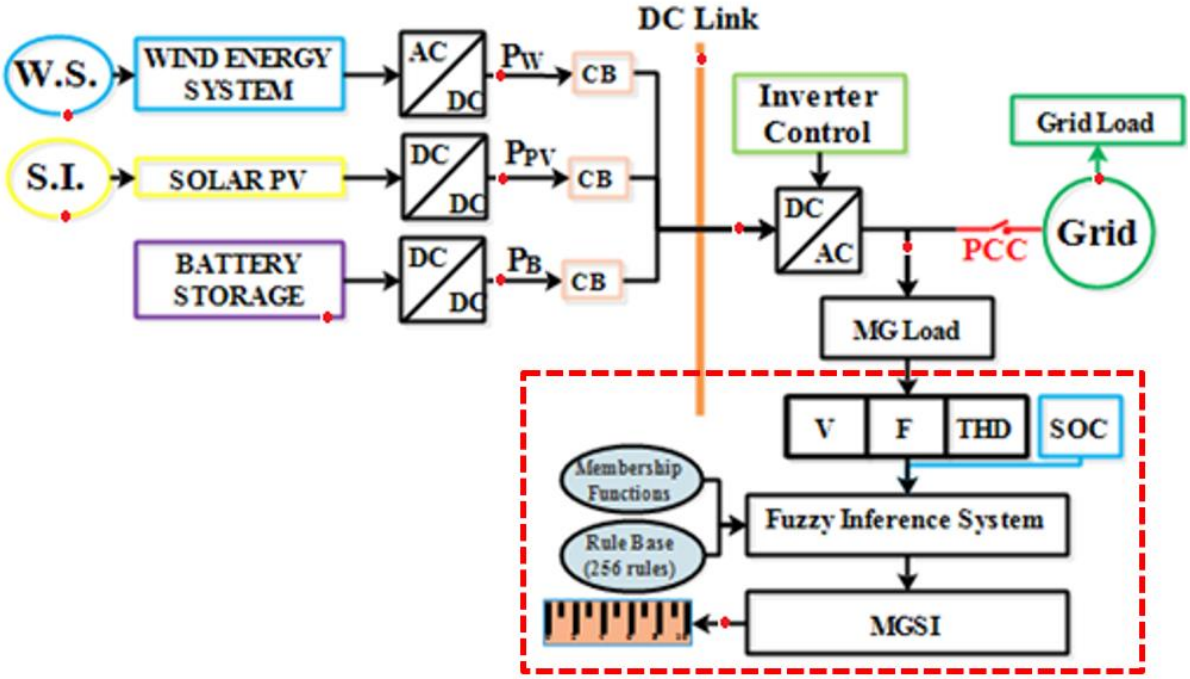

Figure 7.1. Proposed microgrid design

Following the design and configuration details, Figure 7.1 presents the proposed methodology, where different components and several measuring units (marked as a red dot) concerning the components are showcased. Considering the MG load, the critical input parameters for calculating the MGSI are voltage, frequency, and THD across the load conditions. It is important to note that with battery storage integrated into the system, the battery SOC plays a crucial role in analyzing the MG stability. Thus, it has been considered the fourth input parameter, as shown in the red dotted box. Based on the developed membership functions and rule base, the MGSI value for various conditions and case studies is calculated and interpreted using the MGSI scale. The detailed proposed methodology, along with the interpretation of the scale, is presented in section 7.3.

7.3.Proposed Methodology

This section discusses the proposed methodology of this research. It includes a detailed working flowchart focusing on designing a fuzzy logic-based assessment of MGSI followed by

the category-wise interpretation of MGSI. Further, the various membership functions involved in designing and developing fuzzy inference systems have been presented. Finally, the comprehensive information on different membership functions, minimum-maximum working range, etc., have been discussed in this section's latter part.

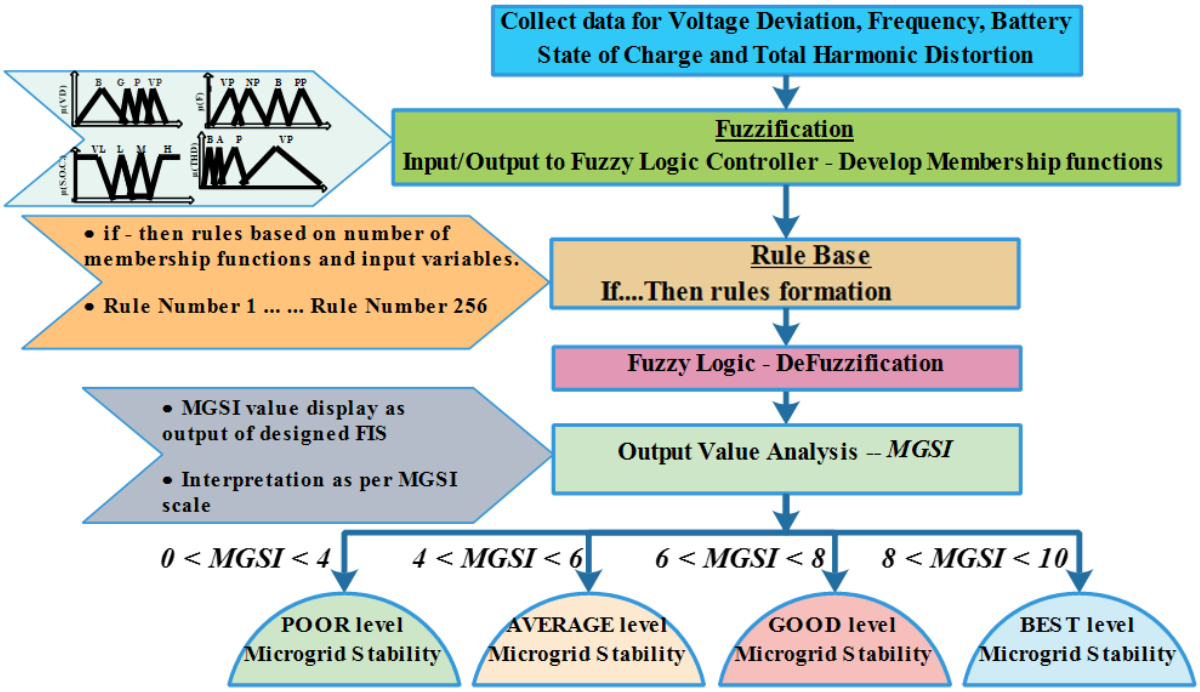

Figure 7.2. Flowchart of the proposed methodology

The working flowchart for the proposed state-of-the-art research is illustrated in Figure 7.2. The evaluation of the Microgrid Stability Index (MGSI) begins with the assessment of voltage deviation, frequency, Total Harmonic Distortion (THD), and battery State of Charge (SOC). These parameters serve as the inputs for the proposed Fuzzy Inference System (FIS), as depicted in Figure 7.3, where membership functions for all input and output parameters are designed and developed based on the minimum and maximum measured values. The details of membership functions for the designed system are available in Table 7.1. The next step involves the creation of rules in the FIS, which are determined by the number of membership functions and parameters. In the present research, the total number of rules amounts to 256. These rules encompass the decision-making process and enable the system to compute the appropriate MGSI value based on system parameters and testing conditions. The defuzzification process follows, which converts the fuzzy output into a crisp value, resulting in the final display of the output—the MGSI value. This value represents the comprehensive assessment of the Microgrid's stability under the given operating conditions. By following this flowchart, the proposed methodology effectively quantifies the MGSI, providing valuable insights into the stability and performance of the Microgrid. The Fuzzy Inference System allows for a robust

evaluation that considers various parameters and conditions, contributing to the advancement of microgrid control and optimization strategies.

Table 7.1. Details of membership functions for designed controller

MFs	Range(s)			
VD (- 10 to 25) %	Best (-10, 0, 10)	Good (8, 10, 14)	Poor (13, 15, 20)	V. Poor (18, 20, 25)
F (47 to 52) Hz	Very Poor (47, 48, 48.5)	Negative Poor (48, 48.7, 49.6)	Best (49.5, 50, 50.25)	Positive Poor (50.15, 51, 52)
SOC (20 to 80) %	Very Low (0, 20, 37.5)	Low (32.5, 42.5, 52.5)	Medium (47.5, 60, 72.5)	High (70, 80, 100)
THD (0 to 115) %	Best (0, 2.5, 5.8)	Average (5, 7.5, 10)	Poor (9, 25, 35)	V. Poor (30, 75, 115)
MGSI (0 to 10)	Poor (0, 2.125, 4.25)	Average (3.75, 5, 6.25)	Good (5.75, 7.125, 8.5)	Best (8, 9, 10)

It is important to note that, when considering the multiple parameters for MGSI evaluation, the parameters considered for the variation in system conditions and scenarios include solar irradiance (SI), wind speed (WS), and battery SOC. Notably, the range of the variable parameters is 0-1000W/m^2, 0-15m/s, and 0-100 %, respectively. Following the above details related to the proposed methodology, the membership functions for the designed fuzzy logic are given in Figure 7.3.

In Figures 7.3(a) to 7.3(e), the membership function for four input parameters, such as voltage deviation (VD), MG system frequency (F), battery SOC, and total harmonic distortion (THD), are presented. These membership functions are used to assess and evaluate the MG stability index (MGSI), which is the core output of the system. The triangular membership functions have been used judiciously for parameters with fixed range and trapezoidal values outside the range, as shown in Figure 7.3(c) for SOC. Remarkably, the triangular membership function offers various advantages, such as robustness to noise and disturbances in input values, efficient computation, fast response concerning a developed control algorithm, and adaptability with a wide range of input values. Besides, the trapezoidal membership function offers flexible and comparatively better handling of uncertain boundaries, easy and smooth computation of values, and improved accuracy for systems with an uncertain range of values.

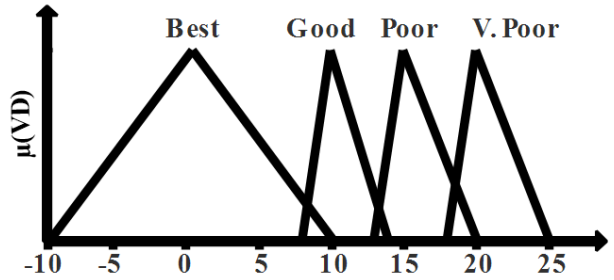

(a) Voltage Deviation

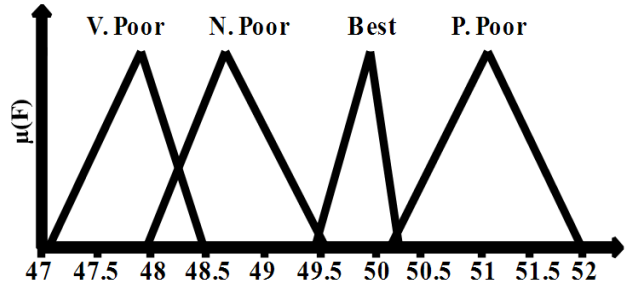

(b) Frequency

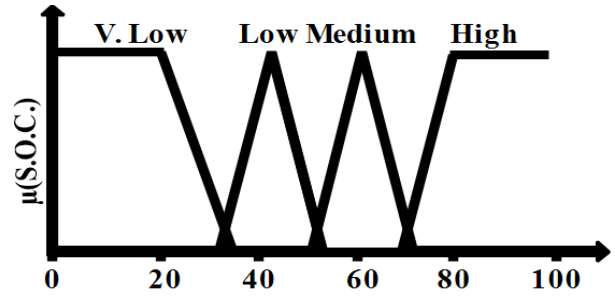

(c) Battery SOC

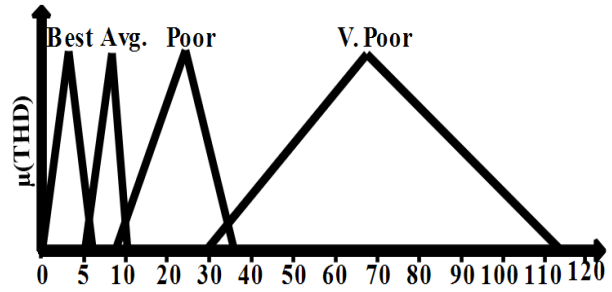

(d) Total Harmonic Distortion (THD)

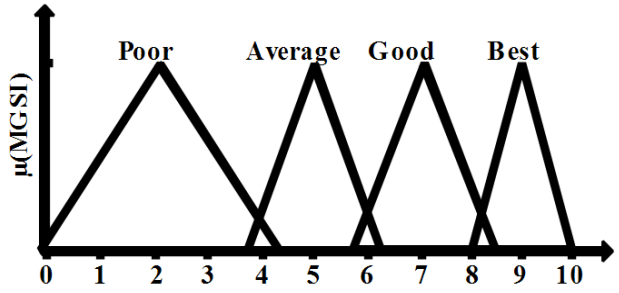

(e) Microgrid Stability Index (MGSI)

Figure 7.3. Membership functions for designed FIS

In Figure 7.3(a), membership function VD has been presented in the best range of ±10 % of the nominal value of 415 V. Other membership functions, namely – Good, Poor, and Very Poor, have been designed based on the literature survey and observations from the developed MG system under different case studies [177]. Figure 7.3(b) presents the membership function for the frequency parameter where the best range lies between 49.5 to 50.2 Hz as per the CERC Staff Paper March 2011 under the Indian Electricity Grid Code (IEGC). In contrast, the range selection for other membership functions, namely – very poor, negative poor, and positive poor, is done based on the observations from the designed MG system [176]. The third input parameter is the battery SOC, which plays a crucial role in MG design and development. The battery storage device works as the backup power source to the system and, in the absence of main power contributors, fulfills the system load and maintains system stability. In the present research, the membership function for SOC lies between the safe zone of battery operation, i.e., 20 – 80 %, as shown in Figure 7.3(c). Based on previous research in battery control, the membership functions have been designed to be above 70 % SOC; the battery is considered in the best state.

Further, considering the different types of loads and their effects on the power quality of the MG, THD has been considered an essential parameter governing MG stability [277]. The membership function considered in the present research is per IEEE Std. 519-2014. Thus, the best range of THD lies within 5 % of the actual value, as shown in Figure 7.3(d). The other membership functions are assumed based on the system observations, i.e., in the case of the islanded condition, THD increases, leading to an impact on power quality and, thus, MG stability [300]. The "output value analyses" subdivided into four categories can be better understood through Figures 7.3(e) and 7.4, respectively.

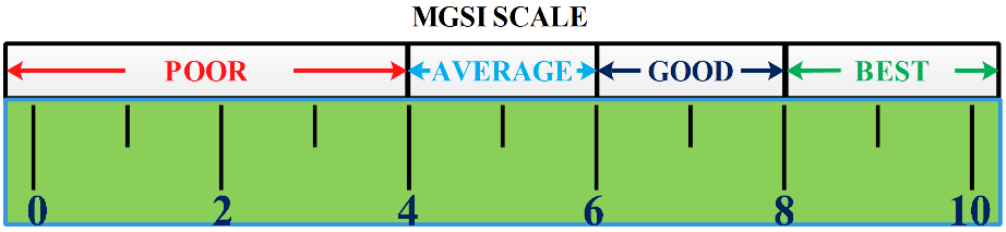

Figure 7.4. MGSI Scale

As presented in Figure 7.4, the different MGSI value ranges vary from 1 (minimum) to 10 (maximum) (values selected as a normalized scale range), subdivided into four categories: poor, average, good, and best. The detailed analysis and interpretation of the MGSI value for different categories are given below:

- Category 1 – Poor: The range for this category lies within 0 to 4 on the 10-point scale, which means that based on the system input parameters and conditions, the MG system is poorly

stable in between this range. Also, it is realized and understood that if the value on the stability index is 3.2, it means in terms of percentage (0 -100 %) that the system is only 32 % stable.

- Category 2 – Average: The range for this category lies above 4 and 6 on a 10-point scale. If the system stability lies in this range, the system, as per the stability scale, will be averagely stable. Besides, in terms of percentage, the system will be stable from 40 % to 60 %.
- Category 3 – Good: The stability of the MG system under various conditions and scenarios will be considered in the good category when it lies in the range of 60 % to 80 % or as per the MGSI scale measured between 6 to 8 values.
- Category 4 – Best: In the ideal conditions and best range values of input parameters, the MGSI value on the scale appears in this stability category, i.e., in between the range of 80 % to 100 % stable system. It is noteworthy that when the system's power balance or energy management is at the best level, and the system in terms of power generation and consumption is ideally balanced, the system stability lies within this range. Ideally, the MGs are developed based on their feasibility and reliability (mainly regarding the availability of RNCES), and MG stability analysis should fall in this category.

Thus, this section discussed the various details and explanations related to the design and development of the FIS-based MGSI. This section also discusses the MGSI scale, presenting the concept of poor and best levels of MG stability under various conditions. In addition to this, the advantage of the proposed method can be extended towards the other MG configurations, like – solar/wind/biomass/storage, solar/diesel/storage, etc., as it primarily focuses on the electrical parameters of the designed system and is independent of the resources. Thus, making the proposed methodology robust and reproducible. The various case studies and subsequent results showcasing the variation in MGSI value based on conditions and input parameters are discussed in the next section.

7.4.Results and Discussions

This section presents a comprehensive discussion of the various case studies in the present research. The uncertainties, practical scenarios, and other observed issues in the literature have been considered for testing and validating the proposed MGSI. The various effectual conditions influencing the MG stability and, thus, MGSI has been diagrammatically presented in Figure 7.5.

In detail, the various possible and feasible combinations simulated in the present work focus on the real-time scenarios of microgrids. Therefore, assessing the microgrid stability index

becomes essential to take appropriate measures, such as load shedding, etc., based on the index. Focusing on the different conditions and their respective combinations, the section below examines the impact of the same on MGSI.

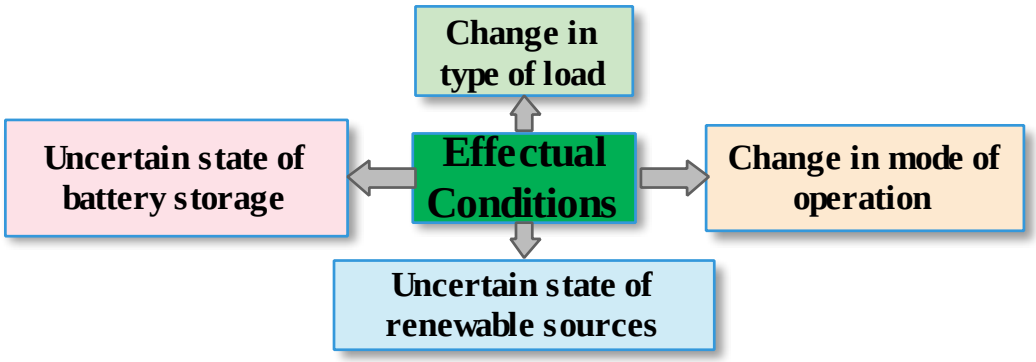

Figure 7.5. Different effectual conditions assumed in the present work

A. Results for combination – 1: Grid-Connected, High renewable output, High battery SOC, and critical/non-critical (full load)

This combination assumes a grid-connected MG system with high renewable power output, high battery SOC (75 %), and two types of loads connected. It is also considered the ideal operating conditions of MG, where all the conditions are favorable. The results are presented in Table 7.2 and Figure 7.6 below.

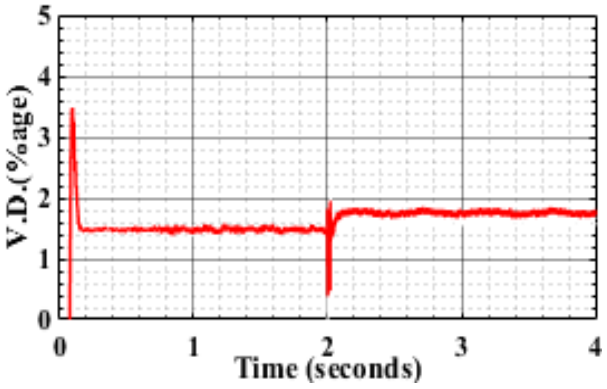

(a) Voltage Deviation

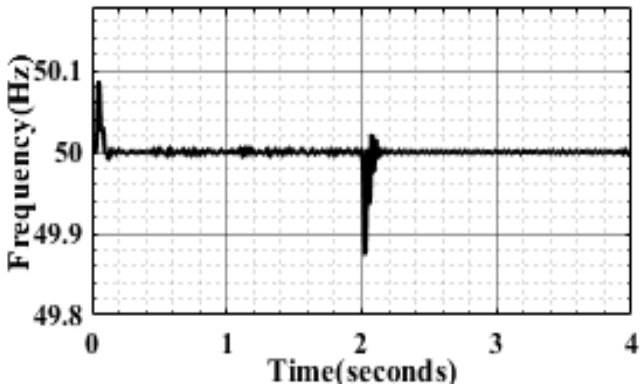

(b) Frequency

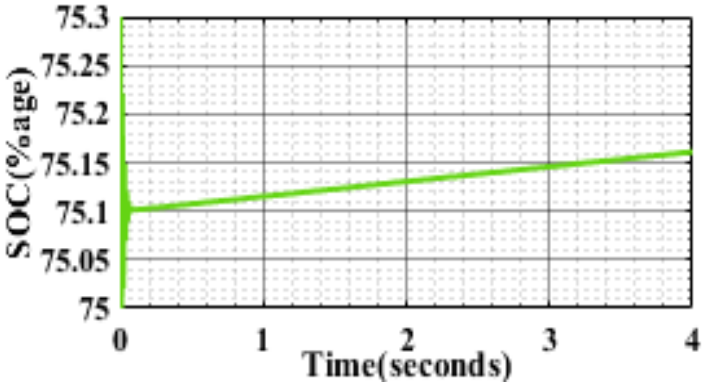

(c) SOC

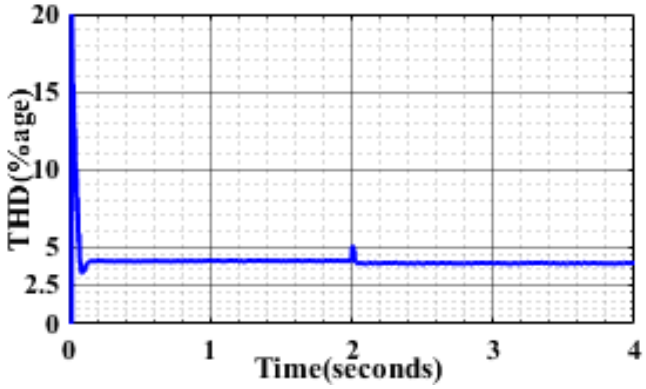

(d) THD

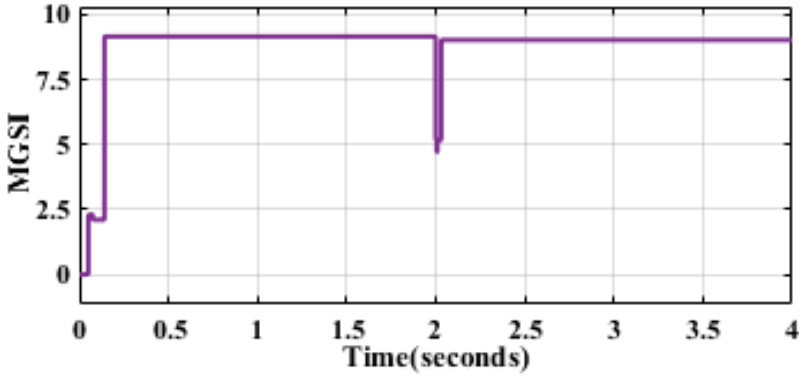

(e) MGSI

Figure 7.6. Microgrid Parameters for Combination 1

Table 7.2 Microgrid parameters and MGSI for combination 1

Type(s) of load	Transition interval (s)	VD (%age)	THD (%age)	Frequency (Hz)	SOC (%age)	MGSI scale value
Only Critical Load	0 - 2	1.51	4.05	49.99 – 50.05	75.12	9.15
Full Load (Non–Critical)	2 - 4	1.89	3.93	49.88 – 50.01	75.149	9.02

As shown in Table 7.2, the total simulation time is subdivided into two major categories where the load has been switched between two different types. It is observed that while working in these operating conditions, the MG parameters, like percentage voltage deviation for critical

and non-critical or full load conditions, are 1.51 % and 1.89 %, which fall in the best range category. Like this, the frequency is 49.88 Hz to 50.05 Hz during the simulation process and is in the most feasible working range. Notably, it is understood that considering the nearly ideal conditions, such as high renewable output, grid connection, and high battery SOC, the system experiences an ideal operating state, i.e., stable microgrid operation. As per the graphical results obtained from a simulation of a Microgrid (MG) system, Figures 7.6(a) – 7.6(d) display the performance of various parameters throughout the simulation period. The voltage deviation remains below 2 % for the entire duration, indicating that the system operates within the best operating range, as defined by the standards.

Additionally, the system frequency closely matches the nominal value of 50 Hz, and the Total Harmonic Distortion (THD) stays within an acceptable range of operation. Furthermore, the battery state of charge (SOC) is observed to be in charging mode, which suggests that the MG system efficiently manages its energy storage during the simulation. Based on these observations, the Microgrid Stability Index (MGSI) is calculated from the simulation results. The MGSI is 9.15 for a critical load condition, while for a full load or non-critical load condition, it is 9.02. Both values fall within the best range of 8-10 on the MGSI scale, indicating that the MG system functions ideally under the given conditions and parameter values. Thus, the simulation results demonstrate that the Microgrid system operates optimally, maintains stable voltage and frequency levels, manages battery SOC effectively, and achieves a high MGSI score within the best range. This indicates the system is in ideal working condition, ensuring reliable and efficient performance for critical and non-critical load conditions.

B. Results for combination – 2: Grid-Connected, Low renewable output, High battery SOC, and critical/non-critical (full load)

In this subsection, the grid-connected system but with drop-in renewable output has been considered. All the other conditions are assumed to be ideal as per subsection 4.1, but the impact of low renewable output on MGSI is showcased in this case study. The results are given in Figure 7.7 and Table 7.3. As in the previous case, the total simulation time is subdivided into two categories based on loads. Further, the observations from Figures 7.7(a) – 7.7(d) indicate that when the MG operates with low or no RNCES, its performance experiences a significant drop. Still, it remains relatively smooth and well-supported in grid-connected mode.

Consequently, the Microgrid Stability Index (MGSI) value decreases slightly compared to the previous results. Still, it falls within the best range, indicating that the MG system maintains an acceptable level of performance under these conditions. However, it is essential to note that the decrease in RNCES reduces the battery's charge rate, impacting various MG parameters.

The percentage voltage deviation is observed as 1.8 % and 2.3 %, while the frequency varies between 49.87 Hz to 50.92 Hz, and Total Harmonic Distortion (THD) ranges between 3.89 % and 4.01 %. Despite the variations in these parameters, the system's overall stability is sustained to a certain level, especially with grid connection support. The graphical analysis reveals that the MG system experiences a slight voltage deviation increase and variation in other parameters due to its dependency on connected renewable sources. The MGSI values from Figure 7.7(e) are 8.99 and 8.85 under the specific load conditions. However, it is emphasized that the MGSI value can significantly decrease in the event of grid failure or fault in the grid, leading to low RNCES availability. In such scenarios, the stability of the MG system may be influenced by the status of the battery's State of Charge (SOC). The battery can serve as a backup power source for the system, mitigating the impact of reduced RNCES availability.

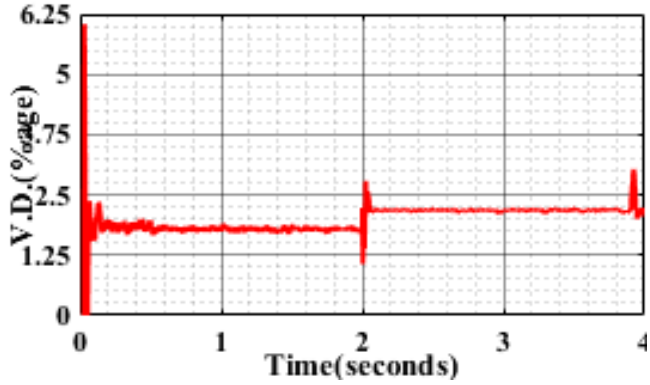

(a) Voltage Deviation

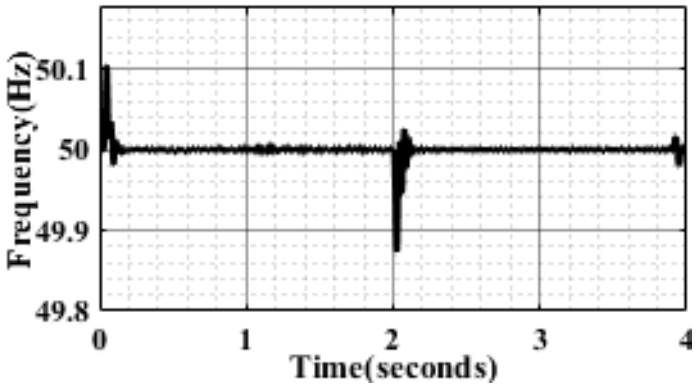

(b) Frequency

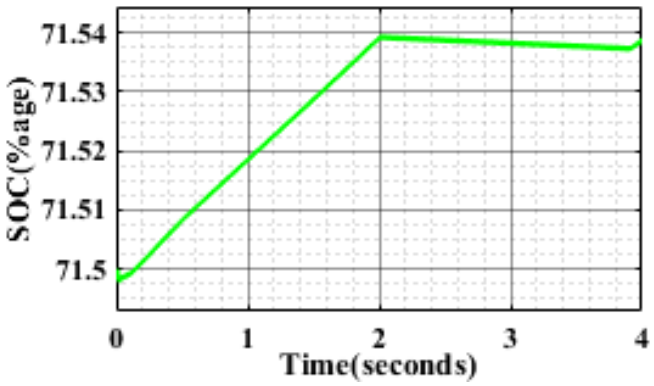

(c) SOC

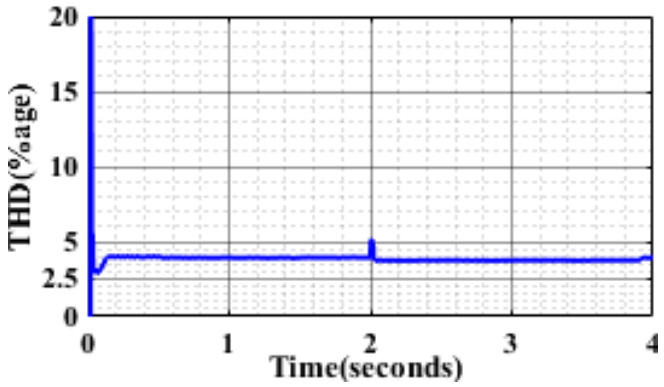

(d) THD

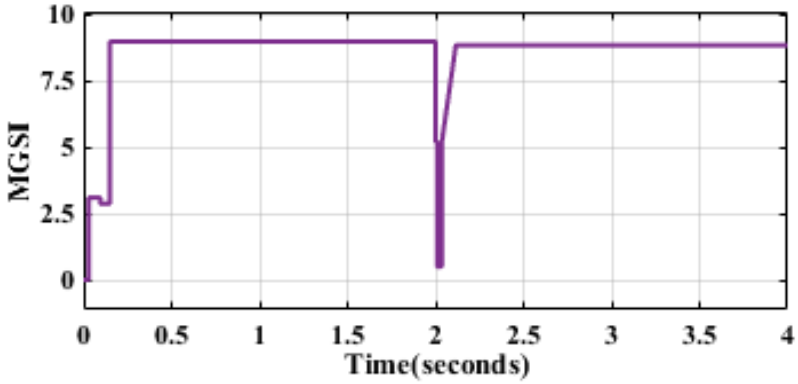

(E) MGSI

Figure 7.7. Microgrid Parameters for Combination 2

Table 7.3 Microgrid parameters and MGSI for combination 2

Type(s) of load	Transition interval (s)	VD (%age)	THD (%age)	Frequency (Hz)	SOC (%age)	MGSI scale value
Only Critical Load	0 – 2	1.8	4.01	49.997 – 50.092	71.52	8.99
Full Load (Non–Critical)	2- 4	2.3	3.89	49.87 – 50.019	71.538	8.85

In summary, the simulation results highlight the importance of RNCES in enhancing the performance and stability of the MG system. Grid-connected mode provides additional reliability and security, ensuring sustained stability to a certain extent. However, low RNCES availability can lead to fluctuations in MG parameters and potentially influence system stability, with the battery SOC status playing a crucial role as a backup power source.

C. Results for combination – 3: Grid-Connected, Medium renewable output, Very Low battery SOC, and critical/non-critical (full load)

In this subsection, the grid-connected system with average renewable output is considered. Notably, the battery SOC has been considered very low (25 %); thus, the extensive battery charging and its influence on MGSI have been much focused. The results are given in Table

7.4 and Figure 7.8. In this scenario, the Microgrid (MG) system operates with a grid connection and with average Renewable Non-Conventional Energy Sources (RNCES). However, due to a low State of Charge (SOC) in the battery (25 %), the Microgrid Stability Index (MGSI) experiences a dip to a good range, as depicted in Figures 7.8(a) and 7.8(b). In such a situation, the main challenge arises from the uncertainty in both the renewable power output and grid connection, as these factors are highly dynamic and can be affected by faults and load changes. The system becomes susceptible to major stability-related issues with a low SOC battery, especially if any power source fails to operate at a particular time. In this case, the drop in MGSI value highlights the importance of maintaining an adequate battery SOC and efficiently diverting renewable power to charge the battery. To ensure the system's stability, it becomes crucial to manage the allocation of renewable power, prioritizing charging the battery to maintain its SOC. The remaining available power from renewable fractions and utility grids can then be utilized to meet the total MG load, balancing the energy distribution effectively. Overall, the MGSI dip serves as a valuable indicator of the significance of battery SOC management in ensuring the overall stability and reliability of the MG system, especially in situations without grid connection and where renewable power output and grid availability are uncertain and subject to fluctuations. Proper battery SOC management will be instrumental in ensuring the microgrid's ability to function optimally and deliver a consistent power supply to its loads.

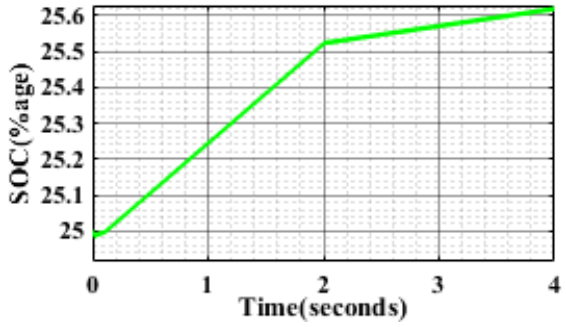

(a) SOC

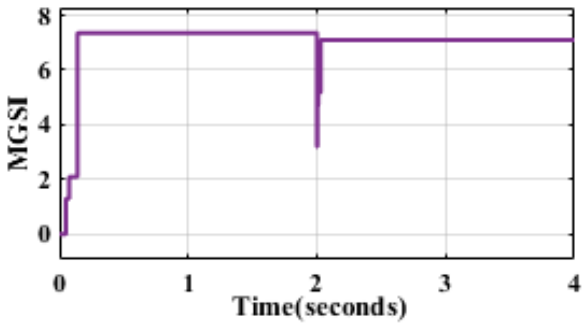

(b) MGSI

Figure 7.8. Microgrid Parameters for Combination 3

Table 7.4 Microgrid parameters and MGSI for combination 3

Type(s) of load	Transition interval (s)	VD (%age)	THD (%age)	Frequency (Hz)	SOC (%age)	MGSI scale value
Only Critical Load	0 - 2	1.74	4	49.99 – 50.052	25.25	7.36
Full Load (Non–Critical)	2 - 4	2.76	3.79	49.89 – 50.023	25.56	7.1

D. Results for combination – 4: Islanded, Low renewable output, high battery SOC, and critical/non-critical (full load)

This case study primarily focuses on the islanded mode, one of the most critical conditions of the Microgrid (MG) system, where the battery plays a crucial role in stabilizing the system and supplying the critical load. The variation in system parameters and battery State of Charge (SOC) are presented in Table 7.5 and Figure 7.9, respectively. From the observations in Figure 7.9(a) - Figure 7.9(d), it is evident that the voltage deviations are higher compared to previous cases, accompanied by a notable error margin in other parameters. The system frequency settles at a lower value of 49.8 Hz, and the Total Harmonic Distortion (THD) increases by over 10 %. Consequently, the Microgrid Stability Index (MGSI) value decreases accordingly to 7.36 and 7.1, as depicted in Figure 7.9(e).

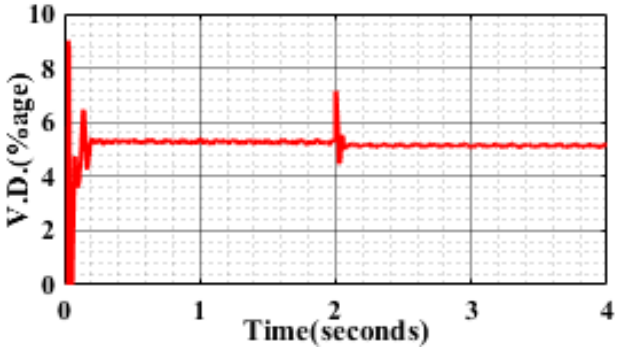

(a) Voltage Deviation

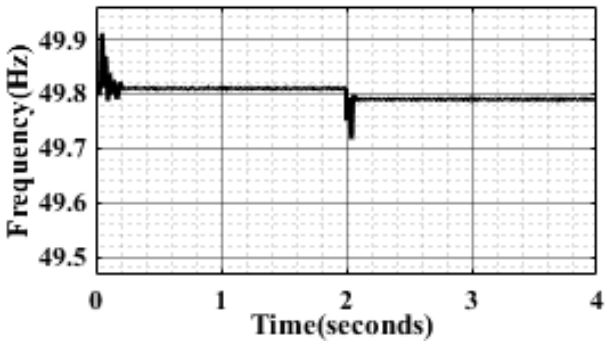

(b) Frequency

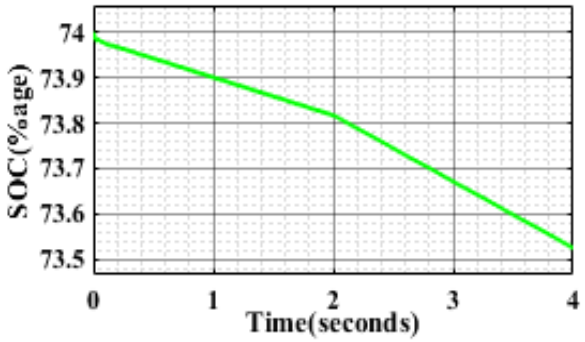

(c) SOC

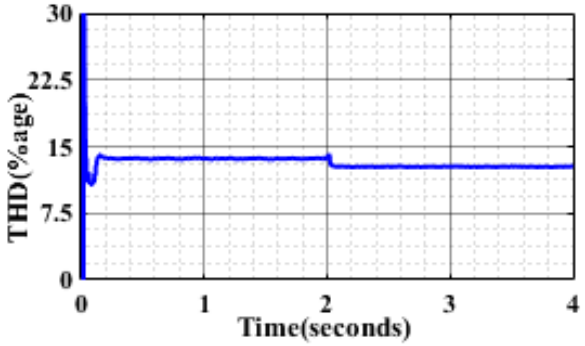

(d) THD

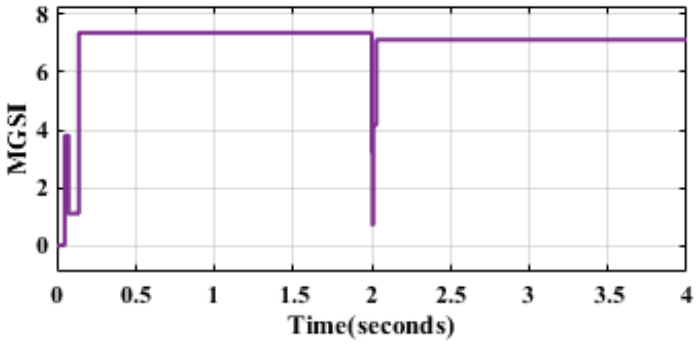

(e) MGSI

Figure 7.9. Microgrid Parameters for Combination 4

Table 7.5 Microgrid parameters and MGSI for combination 4

Type(s) of load	Transition interval (s)	VD (%age)	THD (%age)	Frequency (Hz)	SOC (%age)	MGSI scale value
Only Critical Load	0 - 2	5.62	14.02	49.81 – 49.91	73.9	7.36
Full Load (Non–Critical)	2 - 4	5.56	13.76	49.72 - 49.78	73.68	7.1

Considering the complete electrical load of the MG system, the MGSI experiences a significant drop, as all parameters, including voltage deviation, frequency, and THD, are affected due to the battery storage's inefficiency in catering to the total load with 100 %

smoothness. Despite the dip, MGSI still falls within the good range when the MG operates at full load, as the battery SOC is initially very high and can supply the load temporarily but for a short period. However, it should be anticipated that the MGSI will gradually decrease after a specific instant due to a rapid decline in battery SOC and increasing fluctuations. These fluctuations and lower SOC levels pose challenges to the stability of the MG system over time (This has been thoroughly discussed in subsection 4.6, where simulations and analyses were conducted to understand the MG system's behavior under the islanded mode, explicitly focusing on the role of the battery in ensuring system stability and supplying critical loads).

E. Results for combination – 5: Islanded, Medium renewable output, Low battery SOC, and critical/non-critical (full load)

This case study aims to demonstrate the dynamic nature and self-sufficiency of Microgrids (MGs) in operating independently without relying on the grid while also being responsible for charging backup power devices. The Microgrid Stability Index (MGSI) is a crucial metric in this case, as it needs to be monitored to take necessary actions, such as discontinuing battery charging or shedding the extra load if the MGSI value falls below a certain threshold. The variations in MGSI and other result analyses are presented in Table 7.6 and Figure 7.10, respectively. As observed from Figure 7.10(a) - Figure 7.10(d), under the notable changes in system parameters, i.e., voltage deviation increases from 6.27 % to 6.81 %, THD varies from 7.8 to 7.95 and frequency varies in the range of 49.75 Hz to 50.12 Hz, the MGSI values fall within the average range, i.e., 7.70 and 7.42, respectively. Further, the graphical analysis reveals an interesting behavior of the battery storage device. The battery stops charging instantly when a non-critical load is added to the system. This occurs because the available power was consumed earlier for the charging operation. However, with the addition of a non-critical load, the battery dynamically adjusts and starts delivering the required power to the system, aiming at a balanced power-sharing approach. The graph also indicates the discharging operation of the battery, but the slope of the graph varies depending on the system loading. In summary, the study emphasizes MGs' dynamic nature, ability to operate independently without grid dependency, and the battery's intelligent behavior in adapting to changing load conditions to maintain system stability and optimal power sharing.

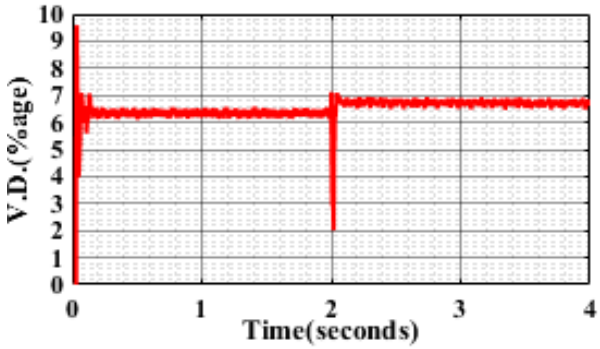

(a) Voltage Deviation

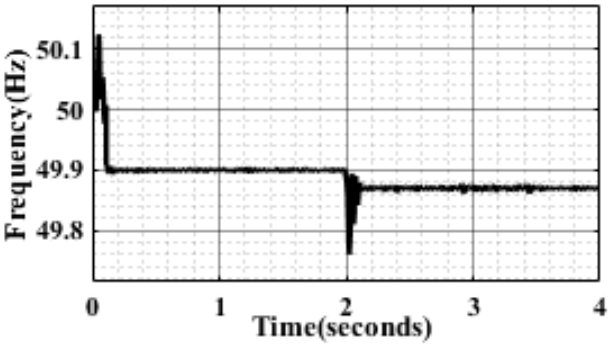

(b) Frequency

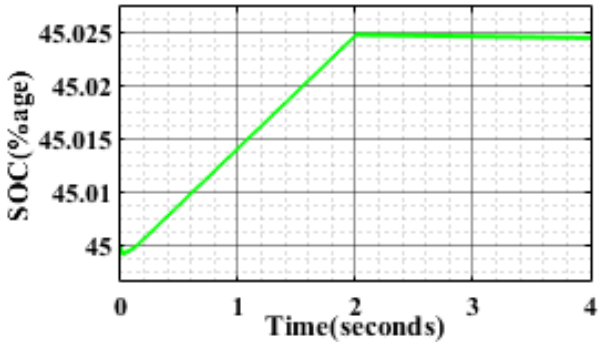

(c) SOC

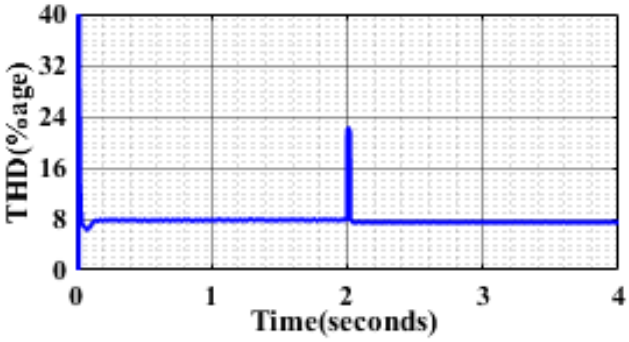

(d) THD

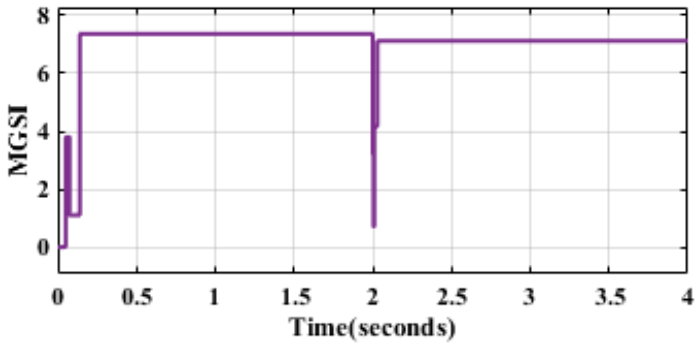

(e) MGSI

Figure 7.10. Microgrid Parameters for Combination 5

Table 7.6 Microgrid parameters and MGSI for combination 5

Type(s) of load	Transition interval (s)	VD (%age)	THD (%age)	Frequency (Hz)	SOC (%age)	MGSI scale value
Only Critical Load	0 - 2	6.27	7.95	49.89-50.12	45.015	7.70
Full Load (Non–Critical)	2 - 4	6.81	7.8	49.75-49.87	45.025	7.42

F. Results for combination – 6: Islanded, Low renewable output, Very Low battery SOC, and critical/non-critical (full load)

This sub-section focuses on the islanded mode of operation with low renewable energy participation and a low battery State of Charge (SOC) in the Microgrid (MG) system. Such conditions represent the worst working scenario for the MG due to the draining nature of power sources, including limited renewable energy availability and a depleted battery. The study investigates the Microgrid Stability Index (MGSI) under these challenging conditions, aiming to assess MG stability and identify areas for improvement. The variation in MGSI and other result analyses for this case are presented in Table 7.7 and Figure 7.11.

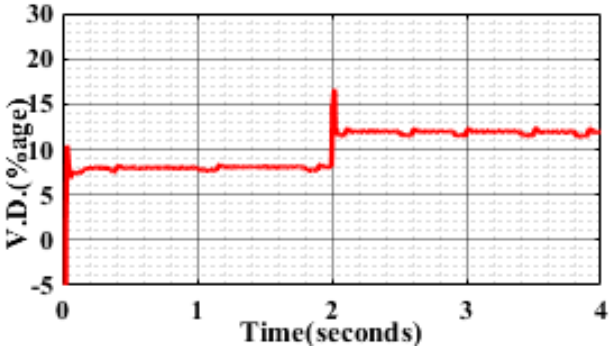

(a) Voltage Deviation

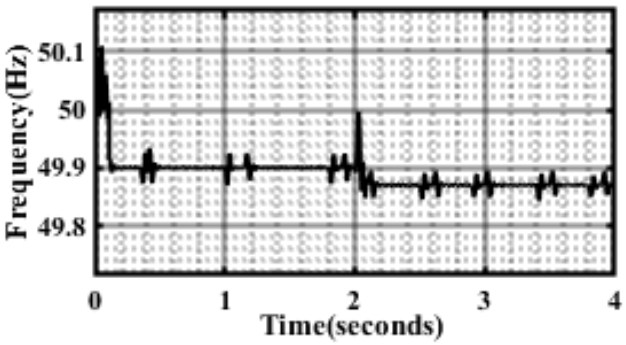

(b) Frequency

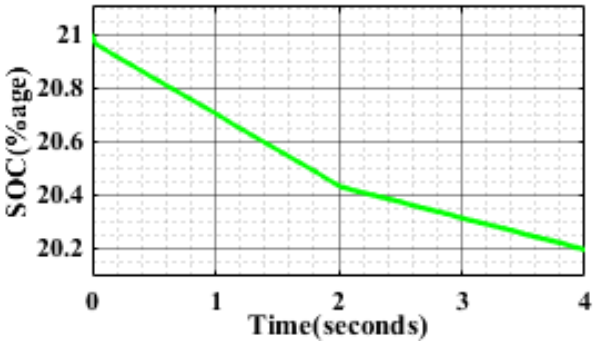

(c) SOC

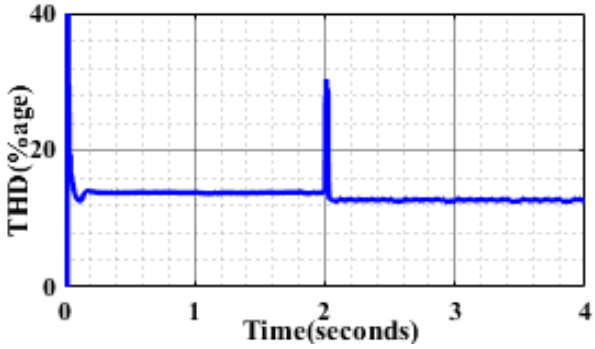

(d) THD

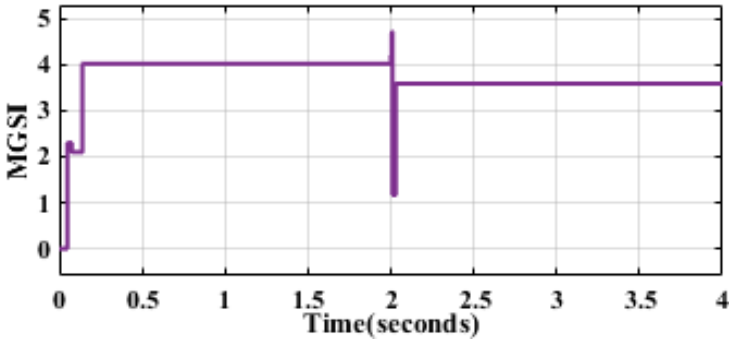

(e) MGSI

Figure 7.11. Microgrid Parameters for Combination 6

The result analysis from Figure 7.11(a) – 7.11(d) highlights poor MG stability, as all parameters show maximum deviations and error margins. The deviation in voltage parameter reaches 8.12 % and 12.03 %, and the system frequency fluctuates from 49.88 Hz to 49.92 Hz.

The Total Harmonic Distortion (THD) is significantly high, ranging from 13.9 % to 14.24 %. Moreover, the battery SOC remains low, resulting in an MGSI range of 3.59 to 4.02, as illustrated in Figure 7.11(e).

Table 7.7 Microgrid parameters and MGSI for combination 6

Type(s) of load	Transition interval (s)	VD (%age)	THD (%age)	Frequency (Hz)	SOC (%age)	MGSI scale value
Only Critical Load	0 - 2	8.12	14.24	49.92 – 50.11	20.7	4.02
Full Load (Non–Critical)	2 - 4	12.03	13.94	49.88 – 49.92	20.32	3.59

The results indicate that the MGSI value is considerably lower than in previous cases, signifying an urgent need to improve the MG system's stability under these conditions. The graphical presentation in Figure 7.11 provides further insight into the impact of challenging conditions on system parameters. Deviations and disturbances in various parameters are notably higher than observed in previous cases, corroborating the adverse effects of low renewable energy participation and a depleted battery. Continuous discharging operation of the battery and the inability of other power sources to cope with the load contribute to the even worse level of MG stability observed in this scenario. In conclusion, the study sheds light on the critical significance of renewable energy participation and maintaining an adequate battery SOC to ensure microgrid stability.

G. Results for combination – 7: Grid-connected/Islanded, High/Low renewable output, medium battery SOC, and Resistive/Inductive type of load

This case study analyzes the Microgrid Stability Index (MGSI) in two different configurations, considering both resistive (critical load value) and 15 kW of inductive (R-L) load connected to the system. In this case, the battery State of Charge (SOC) is constrained to operate in a medium range. The MGSI is assessed based on input values to demonstrate the grouping of different parameters with resistive and inductive types of loads. The results depicted in Figure 7.12 exhibit fluctuations in voltage, frequency, and Total Harmonic Distortion (THD) parameters, along with the MGSI value.

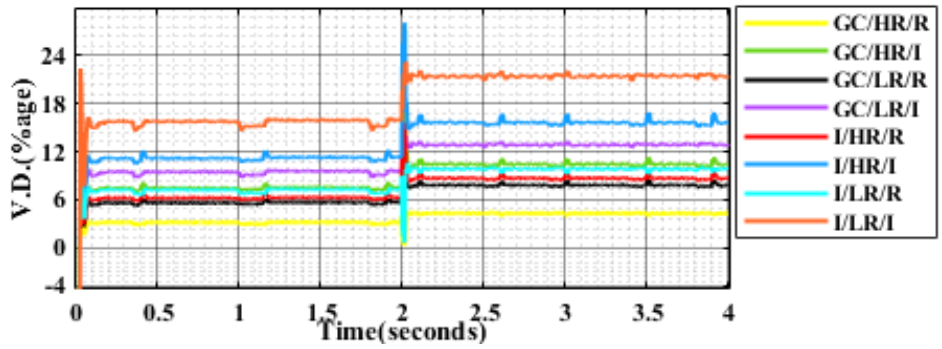

(a) Voltage Deviation

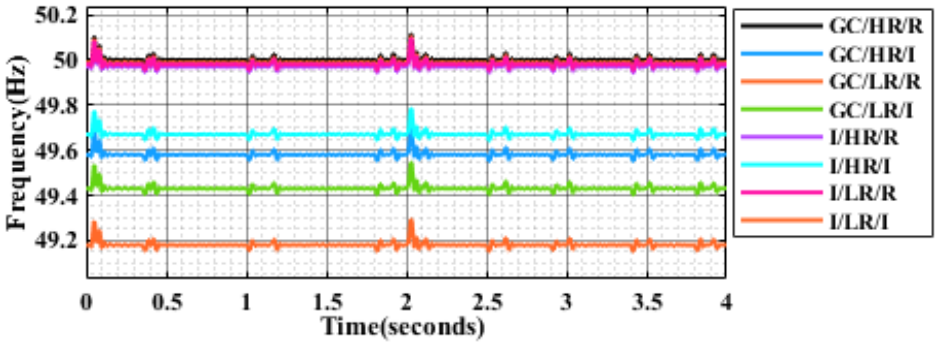

(b) Frequency

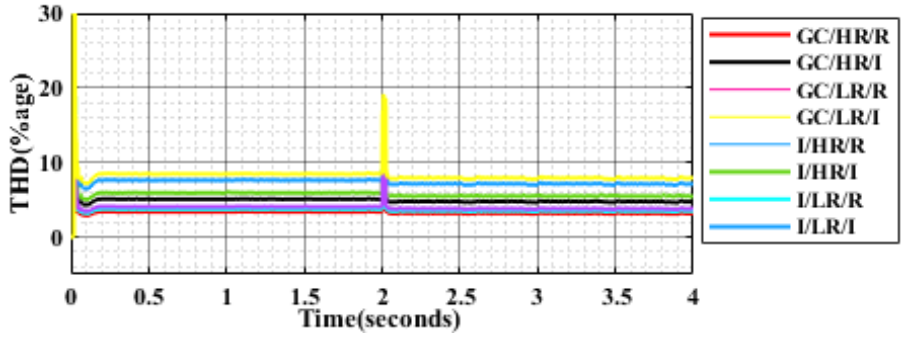

(c) THD

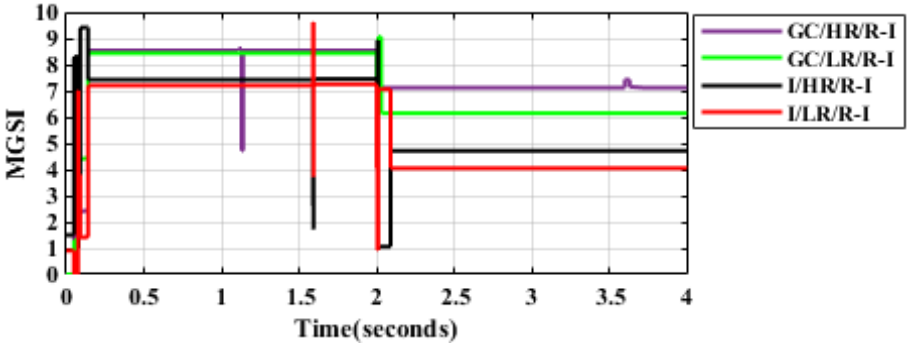

(d) MGSI

Figure 7.12. Microgrid Parameters for Combination 7

Analysis from Figure 7.12(a) - Figure 7.12(d) and Table 7.8 reveals that the presence of inductive loads introduces instability in the system to a greater extent, demanding specific attention, particularly in the islanded mode of operation. The tabulated values indicate a lower

MGSI value and an unstable MG system when combining islanded and inductive load conditions, especially with lower renewable energy sources. In the figures, the legends represent different modes of operation, levels of renewable input, and types of loads. For instance, “GC/LR/I” signifies a grid-connected mode of operation with low renewable input and an inductive type of load. It is observed that the introduction of inductive load, particularly in the islanded mode of operation, leads to increased fluctuations and deviations in each parameter, resulting in a decrease in the MGSI. Specifically, Figure 7.12(d) shows that the difference between MGSI for resistive and inductive loads connected in either mode of operation is evident, as the MGSI drops to a poor range of operation, indicated by the value of 4.05 on the MGSI scale. The study validates the Fuzzy Inference System (FIS)-based MGSI, as demonstrated in Figure 7.6 to Figure 7.12, along with tabulated results from Tables 7.2 to 7.8.

Table 7.8 Microgrid parameters and MGSI for combination 7

Mode of Operation	Type(s) of load	Transition interval (s)	VD (%age)	THD (%age)	SOC (%age)	Frequency (Hz)	MGSI scale value
Grid Connected with high renewable output	Resistive Load	0 - 2	2.6 – 4.21	1.82	65	50.01	8.54
	Inductive Load	2 - 4	7.1 – 10.11	5.01	65	49.59	7.12
Grid Connected with low renewable output	Resistive Load	0 - 2	4.9 – 6.82	2.94	65	49.88	8.43
	Inductive Load	2 - 4	9.4 – 12.95	9.42	65	49.44	6.145
Islanded with high renewable output	Resistive Load	0 - 2	5.81 – 7.91	2.23	65	49.96	7.42
	Inductive Load	2 - 4	10.91 – 15.8	5.91	65	49.67	4.71
Islanded with low renewable output	Resistive Load	0 - 2	6.89 – 9.1	4.96	65	49.98	7.2
	Inductive Load	2 - 4	16.05 – 21.02	8.94	65	49.15	4.05

The combinations and MGSI assessments were developed under specific experimental conditions and scenarios. However, the proposed controller's applicability is adaptable to any MG configuration and set of input parameters, making it a more approachable and versatile solution. The study emphasizes the significant impact of inductive loads on MG stability and performance, particularly in the islanded mode.

Further, considering the other analytical methodology, like Analytic Hierarchy Process (AHP) under the multi-criteria-decision-making technique, a comparative analysis has been done in subsection 4.8.

H. Comparative Analysis

The Analytic Hierarchy Process (AHP) is a multi-criteria decision-making technique that systematically evaluates and prioritizes alternatives based on multiple criteria. The process involves five significant steps aiming at a well-informed decision. The details related to each step are as follows:

Step 1: Develop an unstructured problem and the AHP hierarchy - In this step, the decision problem is defined and broken down into a hierarchical structure. The hierarchy comprises multiple levels, starting from the primary goal or objective at the top and then dividing into various criteria and sub-criteria contributing to achieving the goal. This hierarchical representation helps organize and understand complex decision-making.

Step 2: Pair-wise comparison and analysis of the criteria using Saaty's scale - In this step, the decision-maker performs pair-wise comparisons of the criteria and sub-criteria to determine their relative importance concerning the higher-level elements in the hierarchy. The comparisons use Saaty's numerical scale, allowing the decision-maker to express their preference for one criterion over another. The scale typically ranges from 1 (equally important) to 9 (extremely more important), with intermediate values reflecting intermediate levels of preference.

Step 3: Guesstimating and calculating the relative weights - Based on the pair-wise comparisons, a matrix is constructed, known as the pair-wise comparison matrix, which represents the relative importance of each criterion compared to others. Using mathematical algorithms, the relative weights or priority vectors for the criteria are derived from this matrix. These priority vectors show the importance of each criterion in achieving the overall goal.

Step 4: Checking the consistency ratio of the parameters - In significant decision problems, inconsistency in pair-wise comparisons may arise due to subjective judgments. The AHP process includes a consistency check to ensure the analysis's quality and reliability. The

consistency ratio is calculated to assess the degree of consistency in pair-wise comparisons. If the consistency ratio exceeds a predetermined threshold, a review and revision in pair-wise comparisons is required to make the analysis more reliable.

Step 5: Generation of the resulting overall AHP indices - Once the relative weights are obtained and the consistency of the comparisons is verified, the AHP process generates overall AHP indices for each alternative. These indices represent the performance or suitability of each alternative concerning the decision criteria. The alternative with the highest AHP index is considered the most favorable option based on the decision criteria [301-302].

In summary, the AHP process helps decision-makers structure complex problems, evaluate criteria through pair-wise comparisons, calculate relative weights, ensure consistency, and generate overall indices to systematically and rationally make well-informed decisions. The process provides a clear and logical framework for addressing multi-criteria decision-making challenges across various domains and industries [303-304].

Notably, considering the nominal voltage tolerance is 10 %, nominal frequency is 50 Hz, THD is 5 %, and SOC is an average of 20-80 %, the fuzzy variable of voltage, frequency and THD are mathematically represented in equations 7.1 to 7.4 [176-177, 272, 300] –

$$\mu(VD) = \begin{cases} 0, & V \leq (85)\% \\ \frac{1}{0.05}, (V - 0.85); & (85 \leq v \leq 90)\% \\ 1, & (90 \leq v \leq 100)\% \end{cases} \quad (7.1)$$

$$\mu(F) = \begin{cases} 0, & F \leq (96)\% \\ \frac{1}{0.055}, (F - 0.96); & (96 \leq F \leq 99.5)\% \\ 1, & (99.5 \leq F \leq 100)\% \end{cases} \quad (7.2)$$

$$\mu(THD) = \begin{cases} 0, & THD \leq (95)\% \\ \frac{1}{0.04}, (THD - 0.95); & (95 \leq THD \leq 99)\% \\ 1, & (99 \leq THD \leq 100)\% \end{cases} \quad (7.3)$$

$$\mu(SOC) = \begin{cases} 0, & SOC \leq (20)\% \\ \frac{1}{0.05}, (SOC - 0.20); & (20 \leq SOC \leq 80)\% \\ 1, & (80 \leq SOC \leq 100)\% \end{cases} \quad (7.4)$$

Considering the AHP process and as per [305-306], the pair-wise comparison matrix for the four input parameters uses the relative importance scale and is tabulated in Table 7.9, where the value for voltage deviation is 1, frequency is 5, THD is 5, and SOC is 3 (notably, these values may vary as per parameter assessment and input parameters).

Table 7.9. Pair-wise comparison matrix (Saaty's Matrix) for FIS-based MGSI assessment

Input Variable	VD	F	THD	SOC
VD	1	5	5	3
F	1/5	1	3	3
THD	1/5	1/3	1	3
SOC	1/3	1/3	1/3	1
Σ (Variable)	1.73	6.666	9.333	10

Considerably, the net variable value is calculated as voltage deviation 1.73, Frequency 6.666, THD 9.333, and SOC 10. For the normalized pair-wise matrix, each tabulated value is divided by the summation value for each variable as shown in Table 7.10. These values (tabulated in Table 7.10) further lead to the calculation of criteria weights, the sum of which should be 1 [303-304].

Table 7.10. Normalized Pair-wise matrix

Input Variable	VD	F	THD	SOC	Criteria Weight (*w*)
VD	1/1.73	5/6.666	5/9.333	3/10	0.5409
F	0.2/1.73	1/6.666	3/9.333	3/10	0.2217
THD	0.2/1.73	0.33/6.666	1/9.333	3/10	0.1430
SOC	0.33/1.73	0.33/6.666	0.33/9.333	1/10	0.0940
Σ (Variable)	1.73	6.666	9.333	10	1

Based on criteria weight *w* and equation 7.5, the MGSI value is analyzed.

$$MGSI = \min[\mu(VD)^{w1}, \mu(F)^{w2}, \mu(THD)^{w3}, \mu(SOC)^{w4}] \quad (7.5)$$

As per the standards referred to in section 3, μ(VD) is assumed as 0.78, μ(F) is taken as 0.754, μ(THD) is 0.55, and μ(SOC) is taken as 0.65. Thus, substituting the values in equation 7.5 and concerning criteria weights, MGSI is calculated as min [$0.78^{0.5409}$, $0.754^{0.2217}$, $0.55^{0.1430}$, $0.65^{0.0940}$], which is min [0.8742, 0.9394, 0.9180, 0.9603] = 0.8742. Comparing the values assumed above as per Table 7.1, the MGSI is reflected in the average window, whereas according to the calculation based on the criteria weights (AHP Process), the MGSI falls in the best range window. It is important to note that the MGSI should be in an Average region ranging from 5.75 – 8.5, as shown in Table 7.1, designed per the standards. However, the multi-criteria decision approach gives an inexact range of MGSI, even considering relative ideal values.

Henceforth, considering the present work and both the technique, i.e., AHP and fuzzy-based technique for calculating MGSI, the comparison summarized as –

(a) FIS-based MGSI provides a user-friendly MATLAB-Simulink platform for calculation and assessment. This approach uses fuzzy logic and predefined rules to compute MGSI based on input parameters and membership functions. In particular, fuzzy logic offers several advantages over the analytical hierarchy process (AHP). Firstly, it excels in handling uncertainty and vagueness in decision-making, allowing for the representation of partial truths and intermediate states, making it suitable for dealing with imprecise data and subjective judgments. Fuzzy logic can incorporate linguistic variables and fuzzy sets, enabling decision-makers to express preferences in natural language, enhancing the process's intuition and user-friendliness. It also simplifies model development, particularly when expert knowledge or if-then rules are utilized, making it advantageous for complex problems requiring a more intuitive and less formal approach. Moreover, fuzzy logic can handle non-linear relationships between variables, offering more flexible modeling of real-world systems while providing continuous value representation for smoother state transitions. Its adaptability to diverse domains demonstrates its versatility, whereas AHP may be better suited for structured decision problems.

(b) The multi-criteria decision-making approach for MGSI assessment involves complex mathematical calculations and numerous parameters to reach the final value. This complexity may hinder the accuracy and user-friendliness of the method. The parameters include complexity and subjectivity, handling uncertainty, linear relationships, and limited representation of qualitative data.

(c) The FIS-based system includes of rules due to the high number of input parameters and respective membership functions. While this may enable accurate monitoring and assessment of MGSI, it could lead to increased complexity in managing and maintaining the system. However, in the case of the AHP technique, the complexity and ability to handle complex, variable database problems affect the performance, accuracy to handle complex, variable database problems affect the performance, accuracy, and overall decision-making. Thus, considering the facts and literature, the proposed methodology is more precise and straightforward for assessing the MGSI value.

I. Sensitivity and Robustness Analysis

Sensitivity analysis for the proposed system has been done to inspect the effect of variation in input parameters (Solar Irradiance – SI, Wind Speed – WS, battery state of charge – SOC) and dependency on initial ground conditions as small perturbations. Tables 11 and 12 present

the investigation done under the test system's parameter sensitivity analysis and the robustness analysis of the proposed controller. The input parameters are varied by sample percentage from the best value for investigation [307]. Analysis done in Table 7.11 shows that the developed system is susceptible without the proposed controller. With a slight change in the input value, the parameter deviates from the ideal value and thus leads to an unstable state of operation. In the controller's presence, the output parameters' standard deviation and relative variation (RV) concerning the change in input values are comparatively more minor.

Table 7.11. Parameter Sensitivity Analysis

System Frequency							
Parameter	Variation range	Step	Min. and Max. Value		Mean	Std. Dev.	RV (%)
SI (W/m^2)	0-1000	75	49.15	50.12	49.88	0.2031	0.408
WS (m/s)	0-15	1.5	49.15	50.11	49.86	0.2011	0.403
SOC (%)	0-100	10	49.45	50.095	49.90	0.1901	0.380
System Voltage							
Parameter	Variation range	Step	Min. and Max. Value		Mean	Std. Dev.	RV (%)
SI (W/m^2)	0-1000	75	356.3	465.11	411.2	39.18	9.52
WS (m/s)	0-15	1.5	348.1	481.2	409.1	36.65	8.96
SOC (%)	0-100	10	397.5	444.6	417.9	6.167	1.47

Thus, considering the analysis done in Table 7.11, it can be observed that the system is comparatively more sensitive to the change in SI and WS values, with respect to, battery SOC. Particularly, the standard deviation for system voltage is 39.18, 36.65, and 6.167. In contrast, relative variation (%) is observed to be 9.52, 8.96, and 1.47, in respect to SI (observed minimum and maximum voltage: 356.3 V - 465.11 V), WS (observed minimum and maximum voltage: 348.1 V - 481.2 V), and SOC (observed minimum and maximum voltage: 397.5 V - 444.6 V). The frequency parameter's standard deviation is also observed as 0.2031, 0.2011, and 0.1901. In contrast, relative variation is 9.52, 8.96, and 1.47 concerning to concerning similar input parameters, where the observed minimum and maximum frequency for change in SI is 49.15 Hz - 50.12 Hz, minimum and maximum frequency for change in WS is 49.15 Hz - 50.11 Hz, minimum and maximum frequency for change in SOC is 49.45 Hz - 50.095 Hz. The designed system is considered moderately sensitive, highly stable, and robust regarding variations. It effectively responds to changes in input parameters by modifying the system parameters

accordingly. This adaptability allows the system to maintain stability and reliability while responding to dynamic conditions. However, it is noteworthy that the lease (minimum) value for respective parameters is observed in the non-ideal scenario, i.e., low renewable sources output or low battery SOC.

Table 7.12. Fuzzy-based controller robustness analysis

Functional Parameters	Value		Concerned Output			
			Accuracy	Response Time	Complexity	Effectiveness
Possible number of input variables	Minimum	3	High	Low	Low	Low
	Maximum	6	High	High	High	High
	Present Case	4	High	Low	Low	High
Possible number of membership functions	Minimum	12	Low	Low	Low	Low
	Maximum	20	High	High	High	High
	Present Case	16	High	Low	Medium	High
Possible number of rules (considering 3 - 5 MFs for each parameter)	Minimum	81	Low	Very Low	Very Low	Low
	Maximum	625	High	High	Very High	High
	Present Case	256	High	Low	Low	High

The analysis presented in Table 7.12 demonstrates the robustness and effectiveness of the proposed controller against changes in its functional parameters, utilizing the model-checking approach. The considered output conditions, such as response time, complexity, decision-making accuracy, etc., vary as the function parameters are altered. However, the desired outcomes for the proposed controller are consistently achieved, including high accuracy, low response time, low complexity, and high effectiveness. This validation confirms the robustness of the controller across various aspects. It can be interpreted that the developed system, supported by the proposed fuzzy logic control approach, exhibits high stability due to its less sensitive and robust nature under the influence of variable parameters and functional conditions.

Thus, transitioning from the comprehensive strategy for measuring the Microgrid Stability Index (MGSI) presented in Chapter 7, the next chapter synthesizes the findings from the preceding chapters, highlighting the study's key contributions and overarching insights. Specifically, it underscores the importance of integrating renewable energy sources, employing

advanced control strategies, and developing precise stability assessment tools to ensure the reliable operation of microgrids.

Chapter Summary

This chapter presented a comprehensive strategy for measuring the Microgrid Stability Index (MGSI) in a PV/Wind/Battery-based hybrid microgrid system. The methodology continuously measures key parameters - voltage, frequency, battery state of charge (SOC), and total harmonic distortion (THD) - crucial for assessing MG stability. Seven case studies validate the proposed MGSI under diverse scenarios, demonstrating its effectiveness in evaluating stable microgrid performance. An adaptive Mamdani-based fuzzy inference system (FIS) with 256 rules facilitates the calculation process, offering accurate and versatile results across different MG configurations. The research contributes significantly to enhancing microgrid stability, providing valuable insights for decision-making processes. Future work involves validating and optimizing the methodology while exploring advanced fuzzy systems, and considering additional parameters like net power, faults, and hardware implementation using programmable logic controllers (PLCs).

CHAPTER 8
CONCLUSIONS

Microgrid stability is crucial in modern power systems, especially with the rise of renewable and distributed energy resources. Ensuring microgrid stability is vital for uninterrupted power supply and enhancing grid resilience against external disturbances and fluctuations in renewable energy generation. Thus, this research thoroughly examined stable microgrid operation, covering the theoretical basics and practical needs for stable performance considering real-world situations. The work explored the critical aspects of microgrid stability, including small-signal, transient, and voltage stability, to understand the complex dynamics that ensure reliable microgrid operation. This includes explicitly various challenges that threaten microgrid stability, such as variability of renewable energy, load demand fluctuations, and disturbances from the main grid, which pose significant risks. By examining these challenges, this research lays the foundation for developing strategies to mitigate their impact and strengthen microgrid resilience. This work first presented the identified gaps and opportunities for innovation in microgrid control strategies through a thorough review of existing controllers and algorithms. Fuzzy logic controllers, in particular, show promise for handling the complex and uncertain conditions typical of microgrids. Following the Fuzzy Logic Controller based multiple control strategies, including cascaded and centralized, this research presented the methodology for using hardware controllers like programmable logic controllers (PLCs) essential for validating control algorithms in the real world. Testing control strategies in physical microgrid systems with PLCs provide valuable insights into practical stability challenges and helps refine approaches. In addition, the third work presents a comprehensive assessment of the economic and technical aspects of Homer Pro and MATLAB Simulink software, respectively. Lastly, the work presented a microgrid stability index that quantitatively assesses microgrid stability levels. By including various system parameters into one metric, this index supports decision-making and optimization of microgrid operations, enhancing future power systems' resilience and reliability.

In detail, chapter 2 presented an in-depth state-of-the-art literature survey on microgrid stability, encompassing small-signal, transient, and voltage stability. This chapter examined key factors affecting stability, such as uncertain load, power generation capacity limitations, feedback delays, and the impact of large disturbances, including losses in Distributed Energy Resources (DERs), islanding modes, load shedding, and faults. By delving into these aspects, the study highlighted the necessity of precise control mechanisms and effective mitigation strategies to manage the multifaceted challenges of maintaining stability in diverse operational

scenarios. Additionally, comparing centralized, decentralized, and hierarchical/distributed control schemes and exploring advanced control techniques like fuzzy logic provided valuable insights into enhancing microgrid stability. The significance of this lies in its detailed examination of stability improvement features and future directions for microgrid systems. The study identified critical technologies such as load and resource balancing and adaptive controllers that are essential for ensuring reliable microgrid operation.

Following the comprehensive literature survey, chapter 3 presented the design and modeling of microgrids, emphasizing integrating renewable energy sources like solar PV, wind, and battery-based energy storage. The key objective was to develop an extensive microgrid model using MATLAB Simulink, detailing the modeling processes for solar, wind, battery, and power converters. Additionally, the chapter presented details and information related to software and model designing regarding the economic assessment using HOMER Pro software, focusing on key metrics such as net present cost and renewable fraction. Further, the chapter also presented the implementation of control algorithms via a PLC-based hardware test bench, providing detailed insights into its block diagram, wiring architecture, and other technical aspects. By focusing on these modeling concepts and procedures, the subsequent chapters demonstrated the application of these models in validating proposed control strategies, including cascaded and centralized control approaches, utilizing HOMER Pro for economic validation, and assessing implementation through the hardware test bench. Thus, it is evident from the chapter that the tools for designing a microgrid model and concerning stable microgrid operation are sufficient, especially given MATLAB Simulink, HOMER Pro, and a reconfigurable PLC test bench.

Further, chapter 4 focused on addressing the perturbations in microgrid systems caused by uncertain renewable sources and sudden load fluctuations, which lead to deviations in system voltage, frequency, and DC-Link voltage, resulting in instability. To address these challenges, the chapter presented two control approaches: a cascaded dual fuzzy logic-based control approach and a centralized stage-wise control scheme for regulating frequency and voltage in islanded microgrids. The cascaded control approach employs an intelligent fuzzy logic controller (FLC) where the system also incorporates an auto-tuned PI-based voltage regulator with a reference voltage of 415 V for inverter control and nine controllable and non-controllable system parameters for the proposed cascaded control approach. This algorithm effectively controls battery operation, microgrid mode, and load management to improve stability. The proposed method was analyzed under experimental conditions, including reduced renewable output, microgrid transition, and unhealthy grid/microgrid conditions, and compared with existing control topologies by assessing load voltage, frequency, and DC-Link voltage.

Validation using MATLAB software showed that the proposed approach maintains deviations within 0.25 % for frequency, 0.57 % for voltage, and 0.877 % for DC-Link voltage, which are within acceptable limits according to IEEE 1547, IEEE 2030, and Indian standard CERC 2011.

In addition to this, the chapter also presented a novel centralized, communication-less, stage-wise control approach to ensure stable operation in islanded microgrids, addressing the critical issues of voltage and frequency regulation amid perturbations from uncertain renewable sources and sudden load fluctuations. It employs an intelligent fuzzy logic controller (FLC) with 64 rules to effectively manage the microgrid's parameters. The control strategy is divided into three stages. Stage 1 addresses minor perturbations by regulating all system parameters within a feasible operating range, utilizing a battery for ancillary support. In stages 2 and 3, non-critical loads are percentage-wise shed during significant perturbations to stabilize the system. This load-shedding process is continued until the system parameters return to an acceptable range, ensuring minimal disruption to the overall system. The proposed approach was rigorously validated using MATLAB software, demonstrating its superiority over existing topologies. The results highlighted significantly lower deviations in voltage and frequency under both small and large perturbations, adhering to recommended standards. Specifically, the system exhibited voltage deviations of 0.57 % and 0.72 % and frequency deviations of 0.14 % and 0.17 % under small and large perturbations, respectively. Compared to traditional demand-side management techniques, this novel control scheme prioritizes load satisfaction while maintaining simplicity and efficiency through stage-wise control. Load curtailment is reserved as a last resort and is employed only when power generation is low and ancillary support from storage units is minimal. The system's performance without the controller showed stark contrasts, with significantly higher deviations, underscoring the effectiveness of the proposed method.

Following the fuzzy-based controllers, chapter 5 presents the innovative use of programmable logic controllers (PLCs) for validating microgrid control algorithms, emphasizing their real-time deployability, reliability, robustness, and swift response to inputs. In detail, the reconfigurable PLCs can validate control algorithms under diverse geographic and environmental conditions. Concerning this, this research proposed a PLC-based hardware test bench prototype designed to enhance the validation process of control algorithms focusing on energy management and resilient microgrid automation. As presented, the significant contribution of this research is the design and construction of the prototype controller test bench. This bench integrates a fuzzy logic-based controller developed in MATLAB Simulink, forming an essential part of the microgrid's energy management system. The prototype's performance was rigorously assessed under disturbances caused by the declining contributions

of renewable energy sources, demonstrating the effectiveness of the implemented control algorithm in maintaining stable microgrid operations. Besides, the hardware test bench facilitates the analysis of load management in microgrid systems, considering variables such as solar radiation, wind speed, and battery charge. It offers flexibility and reconfigurability, allowing the evaluation of various power source arrangements. Utilizing CCW software, the performance of the control programs can be validated and monitored in real-time. The results indicate the PLC's ability to make rapid decisions and switch loads efficiently in response to minute input changes, adhering to IEEE standards. Particularly, from the analysis, the PLC test bench performed satisfactorily, i.e., with 3.1 V as PV input, 2.7 V of wind input, and 5.1 V of battery input, only 25 % of the load was fulfilled, indicating insufficient power.

In contrast, with 7.5 V PV input, 7 V wind input, and 5.9 V battery input, 100 % load was fulfilled, reflecting optimal conditions. These results underlined the critical impact of input voltage levels on load fulfillment and overall efficiency of the PLC test bench. In addition to this, considering the impact of disturbances on power quality and load status under varying analog input voltages, the test bench performed satisfactorily well, i.e., with 5-10 % disturbances and PV input as 2.85 V, wind input as 2.49 V, and battery input as 4.76 V, the result was equivalent to as desired. However, in contrast, with 20-35 % disturbances, the system presented 25 % less load fulfillment, indicating instability. Thus, highlighting the impact of disturbance levels on the power quality.

Concerning the economic and technical assessment of an islanded microgrid system, chapter 6 has addressed the critical issue of rural and remote area electrification by proposing a comprehensive performance assessment of a hybrid residential microgrid based on the load model of Kibber village in Himachal Pradesh, India. As the demand for energy in such regions increases, microgrids integrating renewable energy sources emerge as effective solutions. However, these microgrids' stable operation and future deployment are challenged by perturbations arising from uncertainty in renewable sources, battery state of charge dependency, and load variation. The proposed approach is structured into two parts to ensure optimal planning and development of microgrids. Firstly, technical analysis using MATLAB–Simulink software assesses system performance under perturbations, considering available renewable sources, and secondly, economic analysis via HOMER Pro software evaluates the cost-effectiveness of the microgrid model by simulating electrical loads for Kibber village. Parameters such as system voltage, frequency, power sharing, load percentage met, energy cost, and available renewable energy resources are assessed. The study focuses on Himachal Pradesh, India, where solar and wind energy resources are abundant, making it an ideal location for reliable rural electrification. The technical analysis reveals that the developed microgrid

performs well under uncertain conditions, maintaining key electrical parameters within feasible operating ranges. Economic analysis indicates the accuracy and performance of the system in meeting the village's load requirements while minimizing initial investment and renewable energy loss. The findings underscore the importance of a comprehensive assessment tailored to specific geographical locations for successful microgrid deployment. Besides, this work provides guidelines and a systematic approach for such assessments, facilitating researchers in planning and executing comprehensive evaluations for microgrids in rural and remote locations. Key findings from the analysis indicate that an increase in total load demand necessitates more PV modules, resulting in a 14.5 % rise in Net Present Cost. Besides, this increase in PV modules leads to a slight decrease in the Cost of Energy from $0.127 to $0.123, highlighting the dynamic nature of load management.

Moreover, variations in solar radiation directly impact PV power output and subsequently affect COE, i.e., an increase in solar radiation leads to a decrease in COE from $0.127 to $0.124 and vice versa, increased to $0.130 with a decrease in radiation, showcasing the sensitivity of COE to solar radiation fluctuations. Likewise, wind speed variations also significantly influence COE, with higher wind speeds reducing COE and vice versa, emphasizing the importance of wind speed in determining system feasibility. Additionally, changes in the capital cost of Energy Storage Systems notably affect COE and other cost parameters, with lower costs enhancing the economic viability of microgrid architectures, i.e., a 10-15 % drop in NPC. Conversely, higher ESS costs result in a considerable rise in COE and NPC, highlighting the importance of cost optimization strategies for system feasibility. Lastly, the results also depicted solar, wind, and battery as the most suitable combination as it led to reduced costs & increased power generation, i.e., with an excess electricity percentage of 66.7873 %.

Lastly, chapter 7 presented a decision-making methodology for determining the MG stability index (MGSI) to comprehensively measure the MG stability level. The presented index is based on continuous measurements of fundamental MG parameters, including voltage, frequency, battery state of charge (SOC), and total harmonic distortion (THD), incorporating 256 rules in a Mamdani-based fuzzy inference system. The proposed methodology's efficacy is evaluated through seven case studies simulating different modes of MG operation, load types, and power source availability using MATLAB Simulink software. Results demonstrate varying MGSI values across different scenarios, highlighting the impact of parameters such as renewable output, battery SOC, and load characteristics on MG stability. A grid-connected MG system with high renewable output and battery SOC exhibits superior MGSI compared to an islanded MG system with low renewable output, low battery SOC, and inductive loads. In addition, a comparative analysis with the analytic hierarchy process under the multi-criteria

decision-making technique validates the credibility of the fuzzy-based controller in complex decision-making. Sensitivity analysis reflects the system's responsiveness to different input sources, while robustness analysis of the controller underscores its reliability in various operational conditions. From the analysis, it has been validated that for the Grid-connected, high renewable output, high battery SOC, and critical/non-critical (full load) system, MGSI is above 9 point on the scale, i.e., best range. In contrast, for the other case, Islanded, low renewable output, high battery SOC, and critical/non-critical (full load), MGSI drops down to the range of 7, which is Good. However, in other case studies, MGSI drops down to 4 due to non-ideal conditions, such as low renewable output, islanded operation, critical and non-critical load, etc. Besides, the MGSI value also varies considering the type of load, i.e., resistive load and/or inductive load. Concerning such cases, the MGSI drops to 4.05, i.e., islanded microgrid with low renewable output and inductive load. The parameter sensitivity analysis shows that solar irradiance and wind speed significantly impact system voltage with relative variations of 9.52 % and 8.96 %, respectively, while their effect on system frequency is minimal, i.e., relative variation of 0.408 and 0.403. Besides, the standard deviation for frequency varies from 0.2011 to 0.2031, whereas for voltage, it varies from 36.65 to 39.18, w.r.t. solar radiation and wind speed.

The insights gained from the present work provide a foundation for future research, emphasizing the need for continued innovation in microgrid technology. Thus, the future scope of this work involves several key areas for further development. Firstly, validation and optimization through real-world microgrid (MG) implementations will be conducted to enhance the practical applicability of the proposed methodologies across diverse MG configurations and operating conditions. The application and performance of advanced fuzzy systems, such as Sugeno-Fuzzy Inference Systems (FIS) and type-2 fuzzy systems, will be explored, along with parameters like net power sharing and fault management within MGs to improve system resilience and efficiency. Thirdly, the methodology will be implemented using programmable logic controllers (PLC) to enable more reliable and scalable control solutions within microgrids. Additionally, integration with real-time renewable energy sources such as photovoltaic (PV) and wind power, along with the incorporation of electric vehicle (EV) characteristics, will be pursued to enhance the system's adaptability and sustainability. Moreover, hybrid energy storage systems will be considered to balance supply and demand dynamics. Finally, decision-making algorithms will be improved by considering additional parameters like power factor, further refining the system's operational efficiency and performance. Additionally, developing advanced monitoring and diagnostic tools will be essential to predict and mitigate potential issues in real time.

REFERENCES

[1] S. Mehta and P. Basak, “A comprehensive review on control techniques for stability improvement in microgrids,” in Int. Trans. Electr. Energy Syst., vol. 31, no. 4, pp. 1–28, 2021.

[2] S. Mehta and P. Basak, “A centralized stage-wise control approach for frequency and voltage regulation in PV–wind–storage based islanded microgrid,” in Electric Power Components and Systems, 2023. Available: 10.1080/15325008.2023.2276829.

[3] S. Mehta and P. Basak, “Determination of microgrid stability index based on measured electrical parameters and Mamdani fuzzy inference system,” in Electr Eng, 2023. Available: https://doi.org/10.1007/s00202-023-02002-2.

[4] S. Mehta and P. Basak, “Cascaded dual fuzzy logic controller for stable microgrid operation mitigating effects of natural uncertainty in solar and wind energy sources,” in e-Prime - Advances in Electrical Engineering, Electronics and Energy, vol. 5, 2023. Available: https://doi.org/10.1016/j.prime.2023.100215.

[5] S. Mehta and P. Basak, “A Novel Design, Economic Assessment, and Fuzzy-Based Technical Validation of an Islanded Microgrid: A Case Study on Load Model of Kibber Village in Himachal Pradesh,” in ITEES, 2022. Available: https://doi.org/10.1155/2022/9639253.

[6] N. Hatziargyriou, H. Asano, R. Iravani, and C. Marnay, “Microgrids,” in IEEE Power and Energy Magazine, vol. 5, no. 4, pp. 78-94, Jul./Aug. 2007. Available: 10.1109/MPAE.2007.376583.

[7] M. Farrokhabadi et al., “Microgrid Stability Definitions, Analysis, and Examples,” in IEEE Transactions on Power Systems, vol. 35, no. 1, pp. 13-29, Jan. 2020. Available: 10.1109/TPWRS.2019.2925703.

[8] A. Rosini, D. Mestriner, A. Labella, A. Bonfiglio, and R. Procopio, “A decentralized approach for frequency and voltage regulation in islanded PV-Storage microgrids,” in Electric Power Systems Research, vol. 193, pp. 1-16, Jan. 2021.

[9] N. Kanwar, N. Gupta, K. R. Niazi, and A. Swarnkar, “Optimal distributed resource planning for microgrids under uncertain environment,” in IET Renewable Power Generation, vol. 12, no. 2, pp. 133-265, Feb. 2018.

[10] H. Han, X. Hou, J. Yang, J. Wu, M. Su, and J. M. Guerrero, “Review of Power Sharing Control Strategies for Islanding Operation of AC Microgrids,” in IEEE Transactions on Smart Grid, vol. 7, no. 1, pp. 200-215, Jan. 2016. Available: 10.1109/TSG.2015.2434849.

[11] A. Kaur, J. Kaushal, and P. Basak, “A review on microgrid central controller,” in Renewable and Sustainable Energy Reviews, vol. 55, pp. 338-345, Mar. 2016.

[12] S. K. Rathor and D. Saxena, “Energy management system for smart grid: An overview and key issues,” in International Journal of Energy Research, pp. 1-43, 2020.

[13] R. Maurya, S. Prakash, and A. K. Singh, “Challenges, Configuration, Control, and Scope of DC Microgrid Systems: A Review,” in Journal of Electrical Engineering & Technology, 2022. Available: https://doi.org/10.1007/s42835-022-01304-y.

[14] P. Manjarres and O. Malik, “Frequency regulation by fuzzy and binary control in a hybrid islanded microgrid,” in Journal of Modern Power Systems and Clean Energy, vol. 3, no. 3, pp. 429-439, Jul. 2015.

[15] H. Bevrani and S. Shokoohi, “An Intelligent Droop Control for Simultaneous Voltage and Frequency Regulation in Islanded Microgrids,” in IEEE Transactions on Smart Grid, vol. 4, no. 3, pp. 1505-1513, Sept. 2013. Available: 10.1109/TSG.2013.2258947.

[16] F. Nejabatkhah and Y. W. Li, “Overview of power management strategies of hybrid AC/DC microgrid,” in IEEE Trans. Power Electron., vol. 30, no. 12, pp. 7072-7089, Dec. 2015. Available: 10.1109/TPEL.2014.2384999.

[17] G. Shahgholian, “A brief review on microgrids: Operation, applications, modeling, and control,” in Int. Trans. Electr. Energy Syst., vol. 31, pp. 1–28, 2021. Available: 10.1002/2050-7038.12885.

[18] S. Sen and V. Kumar, “Microgrid control: A comprehensive survey,” in Annu. Rev. Control, vol. 45, pp. 118–151, Apr. 2018. Available: 10.1016/j.arcontrol.2018.04.012.

[19] C. Pradhan, M. K. Senapati, S. G. Malla, P. K. Nayak, and T. Gjengedal, “Coordinated power management and control of standalone PV-hybrid system with modified IWO-based MPPT,” in IEEE Syst. J., vol. 15, no. 3, pp. 3585-3596, 2021.

[20] T. Caldognetto, S. Buso, P. Tenti, and D. I. Brandao, “Power-based control of low-voltage microgrids,” in IEEE J. Emerg. Sel. Topics Power Electron., vol. 3, no. 4, pp. 1056-1066, 2015. Available: 10.1109/JESTPE.2015.2413361.

[21] K. Mansiri, S. Sukchai, and C. Sirisamphanwong, “Fuzzy control algorithm for battery storage and demand side power management for economic operation of the smart grid system at Naresuan University, Thailand,” in IEEE Access, vol. 6, pp. 32440-32449, 2018. Available: 10.1109/ACCESS.2018.2838581.

[22] L. Xu and D. Chen, “Control and operation of a DC microgrid with variable generation and energy storage,” in IEEE Trans. Power Delivery, vol. 26, no. 4, pp. 2513-2522, 2011.

[23] J. Solano, J. M. Rey, J. D. Bastidas-Rodríguez, and A. I. Hernández, “Microgrids Design and Implementation” in Cham, Switzerland: Springer Nature, 2019, pp. 287-310.

[24] R. Singh and M. Kirar, “Transient stability analysis and improvement in microgrid,” presented at Int. Conf. Electr. Power Energy Syst. (ICEPES), 2016, pp. 239–245.

[25] M. Geberslassie and B. Bitzer, “Future SCADA systems for decentralized distribution systems,” in Proc. Univ. Power Eng. Conf., 2010, pp. 1–4.

[26] H. Hatta and H. Kobayashi, “Demonstration study on centralized voltage control system for distribution line with sudden voltage fluctuations,” in Proc. IET Sem. Dig. 2008, 2008, pp. 23–34.

[27] L. Meng, Q. Shafiee, G. F. Trecate, et al., “Review on control of DC microgrids and multiple microgrid clusters,” in IEEE J. Emerg. Sel. Top. Power Electron., vol. 5, no. 3, pp. 928-948, Sep. 2017.

[28] A. G. Tsikalakis and N. D. Hatziargyriou, “Centralized control for optimizing microgrids operation,” in IEEE Trans. Power Energy Soc., vol. 23, no. 1, pp. 1-8, Jan. 2011.

[29] J. Y. Kim, J. H. Jeon, S. K. Kim, et al., “Cooperative control strategy of energy storage system and microsources for stabilizing the microgrid during islanded operation,” in IEEE Trans. Power Electron., vol. 25, no. 12, pp. 3037-3048, Dec. 2010.

[30] C. X. Dou and B. Liu, “Multi-agent based hierarchical hybrid control for smart microgrid,” in IEEE Trans. Smart Grid, vol. 4, no. 2, pp. 771-778, Jun. 2013.

[31] A. Hirsch, Y. Parag, and J. Guerrero, “Microgrids: A review of technologies, key drivers and outstanding issues,” in Renew. Sustain. Energy Rev., vol. 90, no. 9, pp. 402–411, Jan. 2018.

[32] M. A. Jirdehi, V. S. Tabar, S. Ghassemzadeh, and S. Tohidi, “Different aspects of microgrid management: A comprehensive review,” in J. Energy Storage, vol. 30, 101457, Aug. 2020. Available: https://doi.org/10.1016/j.est.2020.101457.

[33] S. Pannala, N. Patari, A. K. Srivastava, and N. P. Padhy, “Effective Control and Management Scheme for Isolated and Grid Connected DC Microgrid,” in IEEE Trans. Ind. Appl., vol. 56, no. 6, pp. 6767-6780, Nov.-Dec. 2020. Available: 10.1109/TIA.2020.3015819.

[34] V. V. S. N. Murty and A. Kumar, “Multi-objective energy management in microgrids with hybrid energy sources and battery energy storage systems,” in Prot. Control Mod. Power Syst., vol. 5, no. 2, 2020. Available: https://doi.org/10.1186/s41601-019-0147-z.

[35] S. Garip, M. Bilgen, N. Altin, S. Ozdemir, and I. Sefa, “Reliability Analysis of Microgrids: Evaluation of Centralized and Decentralized Control Approaches,” in Electr. Power Compon. Syst., vol. 51, no. 19, pp. 2319-2338, 2023. Available: 10.1080/15325008.2023.2227174.

[36] D. Lakshmi Satya Nagasri and R. Marimuthu, “Review on advanced control techniques for microgrids,” in Energy Reports, vol. 10, pp. 3054-3072, Nov. 2023. Available: https://doi.org/10.1016/j.egyr.2023.09.162.

[37] M. Uddin, H. Mo, D. Dong, S. Elsawah, J. Zhu, and J. M. Guerrero, “Microgrids: A review, outstanding issues and future trends,” in Energy Strategy Rev., vol. 49, 101127, Sep. 2023. Available: https://doi.org/10.1016/j.esr.2023.101127.

[38] D. Saha, N. Bazmohammadi, J. C. Vasquez, and J. M. Guerrero, “Multiple Microgrids: A Review of Architectures and Operation and Control Strategies,” in Energies, vol. 16, no. 600, 2023. Available: https://doi.org/10.3390/en16020600.

[39] E. Hossain, E. Kabalci, R. Bayindir, and R. Perez, “A comprehensive study on microgrid technology,” in Int. J. Renew. Energy Res., vol. 4, no. 4, pp. 1094–1104, 2014.

[40] Y. Zahraoui, I. Alhamrouni, S. Mekhilef, M. R. Basir Khan, M. Seyedmahmoudian, A. Stojcevski, and B. Horan, “Energy Management System in Microgrids: A Comprehensive Review,” in Sustainability, vol. 13, no. 10492, 2021. Available: https://doi.org/10.3390/su131910492.

[41] S. L. Chartier, V. K. Venkiteswaran, S. S. Rangarajan, E. R. Collins, and T. Senjyu, “Microgrid Emergence, Integration, and Influence on the Future Energy Generation Equilibrium—A Review,” in Electronics, vol. 11, no. 791, 2022. Available: https://doi.org/10.3390/electronics11050791.

[42] I. Ahmed, M. Rehan, A. Basit, et al., “Review on microgrids design and monitoring approaches for sustainable green energy networks,” in Sci. Rep., vol. 13, 21663, 2023. Available: https://doi.org/10.1038/s41598-023-48985-7.

[43] M. U. Safder, M. J. Sanjari, A. Hamza, R. Garmabdari, M. A. Hossain, and J. Lu, “Enhancing Microgrid Stability and Energy Management: Techniques, Challenges, and Future Directions,” in Energies, vol. 16, no. 6417, 2023. Available: https://doi.org/10.3390/en16186417.

[44] N. Mohammed, L. Callegaro, M. Ciobotaru, and J. M. Guerrero, “Accurate power sharing for islanded DC microgrids considering mismatched feeder resistances,” in Appl. Energy, vol. 340, 121060, Jun. 2023. Available: https://doi.org/10.1016/j.apenergy.2023.121060.

[45] R. K. Chauhan, K. Chauhan, B. R. Subrahmanyam, A. G. Singh, and M. M. Garg, “Distributed and centralized autonomous DC microgrid for residential buildings: A case study,” in J. Build. Eng., vol. 27, 100978, Jan. 2020. Available: https://doi.org/10.1016/j.jobe.2019.100978.

[46] M. Shirkhani, J. Tavoosi, S. Danyali, A. Khosravi Sarvenoee, A. Abdali, A. Mohammadzadeh, and C. Zhang, “A review on microgrid decentralized energy/voltage control structures and methods,” in Energy Reports, vol. 10, pp. 368-380, Nov. 2023. Available: https://doi.org/10.1016/j.egyr.2023.06.022.

[47] R. G. Allwyn, A. Al-Hinai, and V. Margaret, “A comprehensive review on energy management strategy of microgrids,” in Energy Reports, vol. 9, pp. 5565-5591, Dec. 2023. Available: https://doi.org/10.1016/j.egyr.2023.09.162.

[48] M. Talaat, M. H. Elkholy, A. Alblawi, et al., “Artificial intelligence applications for microgrids integration and management of hybrid renewable energy sources,” in Artif. Intell. Rev., vol. 56, pp. 10557–10611, 2023. Available: https://doi.org/10.1007/s10462-023-10410-w.

[49] F. S. Al-Ismail, “DC Microgrid Planning, Operation, and Control: A Comprehensive Review,” in IEEE Access, vol. 9, pp. 36154-36172, 2021. Available: 10.1109/ACCESS.2021.3062840.

[50] H. Ji, C. Wang, P. Li, J. Zhao, G. Song, F. Ding, et al., “A centralized-based method to determine the local voltage control strategies of distributed generator operation in active distribution networks,” in Appl. Energy, vol. 228, pp. 2024–2036, 2018.

[51] Fahad Saleh Al-Ismail, “A Critical Review on DC Microgrids Voltage Control and Power Management”, IEEE Access, vol.12, pp.30345-30361, 2024.

[52] A. R. Singh, D. K. Raju, L. P. Raghav, and R. S. Kumar, “State-of-the-art review on energy management and control of networked microgrids,” in Sustain. Energy Technol. Assess., vol. 57, 103248, Jun. 2023. Available: https://doi.org/10.1016/j.seta.2023.103248.

[53] C. L. Bhattar and M. A. Chaudhari, “Centralized Energy Management Scheme for Grid Connected DC Microgrid,” in IEEE Systems Journal, vol. 17, no. 3, pp. 3741-3751, Sep. 2023. Available: 10.1109/JSYST.2022.3231898.

[54] Xin Lin, Ramon Zamora, Avy Sheina, “A Comprehensive Review in DC microgrids: Topologies, Controls and Future Trends”, 2023 IEEE International Conference on Energy Technologies for Future Grids (ETFG), pp.1-6, 2023.

[55] Q. Jiang, M. Xue, and G. Geng, “Energy Management of Microgrid in Grid-Connected and Stand-Alone Modes,” in IEEE Trans. Power Syst., vol. 28, no. 3, pp. 3380–3389, 2013.

[56] P. V. Nithara and R. Anand, “Comparative analysis of different control strategies in Microgrid,” Int. J. Green Energy, vol. 18, no. 12, pp. 1249-1262, 2021. Available: 10.1080/15435075.2021.1897830.

[57] P. A. V. Prasad and C. Dhanamjayulu, “An Overview on Multi-Level Inverter Topologies for Grid-Tied PV System,” in Hindawi ITEES, vol. 2023, Article ID 9690344. Available: https://doi.org/10.1155/2023/9690344.

[58] J. Kim, J. Hong, and H. Kim, “Improved Direct Deadbeat Voltage Control with an Actively Damped Inductor-Capacitor Plant Model in an Islanded AC Microgrid,” in Energies, vol. 9, pp. 1–15, 2016.

[59] W. Song, J. Ma, L. Zhou, and X. Feng, “Deadbeat Predictive Power Control of Single-Phase Using Space-Vector Modulation for Electric,” in IEEE Trans. Power Electron., vol. 31, no. 1, pp. 721–732, 2016.

[60] J. Hu et al., “Economic Model Predictive Control for Microgrid Optimization: A Review,” in IEEE Trans. Smart Grid, vol. 15, no. 1, pp. 472–484, Jan. 2024. Available: 10.1109/TSG.2023.3266253.

[61] J. Hu, J. Zhu, and D. G. Dorrell, “Model-Predictive Control of Grid-Connected Inverters for PV Systems with Flexible Power Regulation and Switching Frequency Reduction,” in 2013 IEEE Energy Convers Congr Expo, 2013, pp. 540–546.

[62] P. Cortés et al., “Predictive Control in Power Electronics and Drives,” in IEEE Trans. Ind. Electron., vol. 55, no. 12, pp. 4312–4324, 2008.

[63] N. Krismadinata, A. Rahim, and J. Selvaraj, “Implementation of Hysteresis Current Control for Single-Phase Grid Connected Inverter,” in PEDS 2007, 2007, pp. 1097–1101.

[64] N. Prabhakar and M. K. Mishra, “Dynamic Hysteresis Current Control to Minimize Switching for Three-Phase Four-Leg V.S.I. Topology to Compensate Nonlinear Load,” in IEEE Trans. Power Electron., vol. 25, no. 8, pp. 1935–1942, 2010.

[65] G. Weiss, Q. Zhong, T. C. Green, and J. Liang, “H∞ Repetitive Control of DC-AC Converters in Microgrids,” in IEEE Trans. Power Electron., vol. 19, no. 1, pp. 219–230, 2004.

[66] Q. Zhao, K. Liu, and H. Li, “A Fractional-Order Multi-Rate Repetitive Controller for Single-Phase Grid-Connected Inverters,” in Electronics, vol. 12, p. 1021, 2023. Available: 10.3390/electronics12041021.

[67] S. Hara, Y. Yamamoto, T. Omata, and M. Nakano, “Repetitive Control System: A New Type Servo System for Periodic Exogenous Signals,” in IEEE Trans. Autom. Control, vol. 33, no. 7.

[68] Y. L. Wei Jin, G. Sun, and L. Bu, “H ∞ Repetitive Control Based on Active Damping with Reduced Computation Delay for LCL-Type,” in Energies, 2017.

[69] T. Liu and D. Wang, “Parallel Structure Fractional Repetitive Control for PWM Inverters,” in IEEE Transactions on Industrial Electronics, vol. 62, no. 8, pp. 5045-5054, Aug. 2015. Available: 10.1109/TIE.2015.2402117.

[70] M. A. Sharaf, H. Armghan, N. Ali, A. Yousef, Y. S. Abdalla, A. R. Boudabbous, H. Mehdi, and A. Armghan, “Hybrid Control of the DC Microgrid Using Deep Neural Networks and Global Terminal Sliding Mode Control with the Exponential Reaching Law,” in Sensors, vol. 23, p. 9342, 2023. Available: 10.3390/s23239342.

[71] L. Suganthi, S. Iniyan, and A. A. Samuel, “Applications of fuzzy logic in renewable energy systems – A review,” in Renew. Sustain. Energy Rev., vol. 48, pp. 585–607, 2015.

[72] M. Rodriguez, D. Arcos-Aviles, and F. Guinjoan, “Simple fuzzy logic-based energy management for power exchange in isolated multi-microgrid systems: A case study in a remote community in the Amazon region of Ecuador,” in Applied Energy, vol. 357, Mar. 2024, p. 122522.

[73] I. Sefa, N. Altin, S. Ozdemir, and O. Kaplan, “Fuzzy PI controlled inverter for grid interactive renewable energy systems,” in IET Renew. Power Gener., vol. 9, pp. 729–738, 2015.

[74] Z. Chen, A. Luo, H. Wang, Y. Chen, M. Li, and Y. Huang, “Adaptive sliding-mode voltage control for inverter operating in islanded mode in microgrid,” in Int. J. Electr. Power Energy Syst., vol. 66, pp. 133–143, 2015.

[75] A. Esmaeli, “Stability analysis and control of microgrids by sliding mode control,” in Int. J. Electr. Power Energy Syst., vol. 78, no. 11, pp. 22–28, 2016.

[76] K. H. Ahmed, A. M. Massoud, S. J. Finney and B. W. Williams, “Optimum selection of state feedback variables PWM inverters control,” 2008 4th IET Conference on Power Electronics, Machines and Drives, York, 2008, pp. 125-129.

[77] S. Pa, M. B. Yakoob, M. Seetharaman, J. D. Victor, K. Arumugam, and S. Muthukumaran, “Linear Quadratic Gaussian Design in a Grid-Connected and Islanded Microgrid System for Stability Enrichment,” in Eng. Proc., vol. 37, p. 65, 2023. Available: 10.3390/ECP2023-14672.

[78] R. S. Mohankumar, N. Selvaganesan, M. Jayakumar, and P. Sathishkumar, “Centralised fractional order LQI controller design for quadruple tank process — An optimisation approach,” in Results Control Optimization, vol. 10, Mar. 2023, p. 100202. Available: 10.1016/j.rico.2023.100202.

[79] C. Jaen, J. Pou, R. Pindado, V. Sala, and J. Zaragoza, “A Linear-Quadratic Regulator with Integral Action Applied to PWM DC-DC Converters,” in IECON 2006 - 32nd Annu. Conf. IEEE Ind. Electron., 2006, pp. 2280–2285.

[80] R. K. Chauhan, B. S. Rajpurohit, R. E. Hebner, S. N. Singh, and F. M. G. Longatt, “Design and analysis of PID and fuzzy-PID controller for voltage control of DC microgrid,” in Proc 2015 IEEE Innov Smart Grid Technol - Asia, ISGT ASIA 2015., 2015.

[81] Y. Allahvirdizadeh, H. Shayanfar, and M. Parsa Moghaddam, “A comparative study of PI, fuzzy-PI, and sliding mode control strategy for battery bank SOC control in a standalone hybrid renewable system,” in Int Trans Electr Energy Syst., vol. 30, no. 2, pp. 1-23, 2020.

[82] A. Singh and Sathans, “ANFIS based control strategy for frequency regulation in AC microgrid,” in Proc. 5th Int. Conf. Eco-Friendly Comput. Commun. Syst. (ICECCS), 2016, pp. 38-42.

[83] S. Kaur, T. Kaur, and R. Khanna, “ANFIS Based Frequency Control in an Autonomous Microgrid Integrated with PV and Battery Storage,” in 9th Int. Conf. Power Energy Syst. (ICPES), 2019, pp. 6-9.

[84] M. Dashtdar, A. Flah, S. M. S. Hosseinimoghadam et al., “Frequency control of the islanded microgrid including energy storage using soft computing,” in Sci Rep, vol. 12, p. 20409, 2022. Available: 10.1038/s41598-022-24758-6.

[85] M. Rahimi and S. Ghadiriyan, “A generalized droop-based compensator for addressing the issues raised in a DC microgrid comprising hybrid wind-battery-back up generation sources,” in Int Trans Electr Energy Syst, vol. 29, pp. 1–20, 2019.

[86] F. Zishan, E. Akbari, O. D. Montoya, D. A. Giral-Ramírez, and A. Molina-Cabrera, “Efficient P.I.D. Control Design for Frequency Regulation in an Independent Microgrid Based on the Hybrid PSO-GSA Algorithm,” in Electronics, vol. 11, p. 3886, 2022. Available: 10.3390/electronics11233886.

[87] P. N. Rekha and P. Kanakasabapathy, “PR controller-based droop control strategy for AC microgrid using Ant Lion Optimization technique,” in Energy Reports, vol. 9, pp. 6189–6198, Dec. 2023. Available: 10.1016/j.egyr.2023.05.220.

[88] R. Majumder, “Some aspects of stability in microgrids,” in IEEE Trans. Power Syst., vol. 28, no. 3, pp. 3243–3252, 2013.

[89] P. C. Sekhar, S. Mishra, and R. Sharma, “Data analytics based neuro-fuzzy controller for diesel-photovoltaic hybrid AC microgrid,” in IET Gen. Tran. Distr., vol. 9, no. 2, pp. 193–207, 2015.

[90] F. Asghar, M. Talha, and S. H. Kim, “Robust frequency and voltage stability control strategy for standalone AC/DC hybrid microgrid,” in Energies, vol. 10, no. 6, pp. 1–20, 2017.

[91] T. Tricarico, G. Gontijo, M. Neves, M. Soares, M. Aredes, and J. M. Guerrero, “Control design, stability analysis and experimental validation of new application of an interleaved converter operating as a power interface in hybrid microgrids,” in Energies, vol. 12, no. 3, pp. 1–23, 2019.

[92] M. Ahmed, A. Vahidnia, M. Datta, and L. Meegahapola, “An Adaptive Power Oscillation Damping Controller for a Hybrid AC/DC Microgrid,” in IEEE Access, vol. 8, pp. 69482-69495, 2020. Available: 10.1109/ACCESS.2020.2985978.

[93] S. Kotra and M. K. Mishra, “Design and stability analysis of DC microgrid with hybrid energy storage system,” in IEEE Trans. Sustain. Energy, vol. 10, pp. 1603–1612, 2019.

[94] R. K. Chauhan, K. Chauhan, and J. M. Guerrero, “Controller design and stability analysis of grid connected DC microgrid,” in J. Renew. Sustain. Energy, vol. 10, no. 3, pp. 1–10, 2018.

[95] W. Issa, S. Sharkh, and M. Abusara, “Hybrid Generators-based AC Microgrid Performance Assessment in Island Mode,” in IET Power Electron., 2019, pp. 1–10.

[96] F. Asghar, M. Talha, and S. H. Kim, “Fuzzy logic-based intelligent frequency and voltage stability control system for standalone microgrid,” in Int Trans Electr Energy Syst, vol. 28, pp. 1–14, 2018.

[97] S. Hoseinnia, M. Akhbari, M. Hamzeh, and J. M. Guerrero, “A control scheme for voltage unbalance compensation in an islanded microgrid,” in Electr. Power Syst. Res., vol. 177, p. 106016, 2019.

[98] A. M. M. Nour, A. A. Helal, M. M. El-Saadawi et al., “Voltage imbalance mitigation in an active distribution network using decentralized current control,” in Prot Control Mod Power Syst, vol. 8, p. 20, 2023. Available: 10.1186/s41601-023-00293-y.

[99] M. Nabatirad, R. Razzaghi, and B. Bahrani, “Decentralized Energy Management and Voltage Regulation in Islanded DC Microgrids,” in IEEE Systems Journal, vol. 16, no. 4, pp. 5835–5844, Dec. 2022. Available: 10.1109/JSYST.2022.3190279.

[100] M. Nabatirad, B. Bahrani, and R. Razzaghi, “Decentralized secondary controller in islanded dc microgrids to enhance voltage regulation and load sharing accuracy,” in Proc IEEE Int Conf Ind Technol, 2019, pp. 1692–1697.

[101] X. Lu, J. M. Guerrero, K. Sun, J. C. Vasquez, R. Teodorescu, and L. Huang, “Hierarchical control of parallel AC-DC converter interfaces for hybrid microgrids,” in IEEE Trans Smart Grid, vol. 5, no. 2, pp. 683–692, 2014.

[102] A. Navarro-Rodriguez, P. Garcia, R. Georgious, and J. Garcia, “Adaptive active power sharing techniques for DC and AC voltage control in a hybrid DC/AC microgrid,” in IEEE Trans Ind Appl, vol. 55, no. 2, pp. 1106–1116, 2019.

[103] M. Dong, L. Li, Y. Nie, D. Song, and J. Yang, “Stability analysis of a novel distributed secondary control considering communication delay in DC microgrids,” in IEEE Trans Smart Grid, vol. 10, pp. 6690–6700, 2019.

[104] M. Ghazzali and M. Haloua, “Distributed voltage and frequency control of islanded AC microgrids,” in Proc. 2018 6th Int. Renew. Sustain. Energy Conf. (IRSEC 2018), 2018, pp. 1–6.

[105] Y. Awda, M. Alowaifeer, and M. A. Abido, “Hierarchical Fuzzy Logic Controller for Islanded DC Microgrids with HESS,” in Proc. 2022 IEEE PES 14th Asia-Pacific Power and Energy Engineering Conference (APPEEC), Melbourne, Australia, 2022, pp. 1-6.

[106] Q. Xu, X. Hu, P. Wang, J. Xiao, P. Tu, C. Wen, et al., “A Decentralized Dynamic Power Sharing Strategy for Hybrid Energy Storage System in Autonomous DC Microgrid,” in IEEE Transactions on Industrial Electronics, vol. 64, no. 7, pp. 5930–5941, 2017.

[107] T. Srikanth and S. Chitra Selvi, “A Review of Microgrid Energy Management and Control Strategies,” in IEEE Access, vol. 11, pp. 21729-21757, 2023.

[108] S. Kayalvizhi and D. M. Vinod Kumar, “Load frequency control of an isolated micro grid using fuzzy adaptive model predictive control,” in IEEE Access, vol. 5, pp. 16241–16251, 2017.

[109] J. Pahasa and I. Ngamroo, “Coordinated PHEV, PV, and ESS for Microgrid Frequency Regulation Using Centralized Model Predictive Control Considering Variation of PHEV Number,” in IEEE Access, vol. 6, pp. 69151–69161, 2018.

[110] K. Zuo and L. Wu, “A review of decentralized and distributed control approaches for islanded microgrids: Novel designs, current trends, and emerging challenges,” in The Electricity Journal, vol. 35, no. 5, 107138, 2022. Available: https://doi.org/10.1016/j.tej.2022.107138.

[111] Y. Khayat et al., “Decentralized Frequency Control of AC Microgrids: An Estimation-Based Consensus Approach,” in IEEE Journal of Emerging and Selected Topics in Power Electronics, vol. 9, no. 5, pp. 5183-5191, 2021.

[112] S. Jena, N. P. Padhy, and J. M. Guerrero, “Decentralized Primary and Distributed Secondary Control for Current Sharing and Voltage Regulation in DC Microgrid Clusters with HESS,” in Proc. 2020 IEEE International Conference on Power Electronics, Drives and Energy Systems (PEDES), Jaipur, India, 2020, pp. 1-7.

[113] G. Agundis-Tinajero, J. Segundo-Ramírez, N. Visairo-Cruz, M. Savaghebi, J. M. Guerrero, and E. Barocio, “Power flow modeling of islanded AC microgrids with hierarchical control,” in International Journal of Electrical Power & Energy Systems, vol. 105, pp. 28–36, 2019.

[114] I. Serban, “Frequency restoration in microgrids by means of distributed control with minimum communication requirements,” in Proc. IEEE International Symposium on Industrial Electronics (ISIE), 2014, pp. 2590–2595.

[115] M. S. Toularoud, M. K. Rudposhti, S. Bagheri, and A. H. Salemi, “A hierarchical control approach to improve the voltage and frequency stability for hybrid microgrids-based distributed energy resources,” in Energy Reports, vol. 10, pp. 2693–2709, 2023.

[116] A. Calpbinici, E. Irmak, E. Kabalcı, and R. Bayındır, “Design of an Energy Management System for AC/DC Microgrid,” in Proc. 2021 3rd Global Power, Energy and Communication Conference (GPECOM), 2021, pp. 184-189.

[117] Y. Wang, X. Zhang, H. Iu, T. Fernando, and M. Ujjal, “Energy Management Strategy of Islanded Hybrid DC/AC Microgrid with Energy Storage System,” in Proc. 2021 31st Australasian Universities Power Engineering Conference (AUPEC), 2021, pp. 1-6.

[118] Q. Sun, Q. Sun, and D. Qin, “Adaptive fuzzy droop control for optimized power sharing in an islanded microgrid,” in Energies, vol. 12, no. 2, pp. 1–23, 2019.

[119] N. Vafamand, M. H. Khooban, T. Dragicevic, F. Blaabjerg, and J. Boudjadar, “Robust non-fragile fuzzy control of uncertain DC microgrids feeding constant power loads,” in IEEE Transactions on Power Electronics, vol. 34, pp. 11300–11308, 2019.

[120] Z. Shuai, Y. Peng, J. M. Guerrero, Y. Li, and Z. J. Shen, “Transient Response Analysis of Inverter-Based Microgrids under Unbalanced Conditions Using a Dynamic Phasor Model,” in IEEE Transactions on Industrial Electronics, vol. 66, no. 4, pp. 2868–2879, 2019.

[121] S. D. Dwivedi and P. K. Ray, “Energy Management and control of Grid-connected Microgrid integrated with HESS,” in Proc. 2022 International Conference on Intelligent Controller and Computing for Smart Power (ICICCSP), 2022, pp. 1-6.

[122] N. R. Tummuru, U. Manandhar, A. Ukil, H. B. Gooi, S. K. Kollimalla, and S. Naidu, “Control strategy for AC-DC microgrid with hybrid energy storage under different operating modes,” in International Journal of Electrical Power & Energy Systems, vol. 104, pp. 807–816, 2019.

[123] M. M. Iqbal, S. Kumar, C. Lal, et al., “Energy management system for a small-scale microgrid,” in Journal of Electrical Systems and Information Technology, vol. 9, no. 5, 2022. Available: https://doi.org/10.1186/s43067-022-00046-1.

[124] R. Gugulothu, B. Nagu, and D. Pullaguram, “Energy management strategy for standalone DC microgrid system with photovoltaic/fuel cell/battery storage,” in Journal of Energy Storage, vol. 57, 106274, 2023. Available: https://doi.org/10.1016/j.est.2022.106274.

[125] H. Abouobaida, L. de Oliveira-Assis, E. P. P. Soares-Ramos, H. Mahmoudi, J. M. Guerrero, and M. Jamil, “Energy management and control strategy of DC microgrid based hybrid storage system,” in Simulation Modelling Practice and Theory, vol. 124, 102726, 2023. Available: https://doi.org/10.1016/j.simpat.2023.102726.

[126] M. Abbes, H. Jmii, and S. Chebbi, “Centralized Control of Distributed Generation Sources in AC Microgrids for Reactive Power Provision,” in Proc. Int. Conf. Adv. Syst. Emerg. Technol. (IC_ASET 2019), pp. 273–278, 2019.

[127] M. Hamzeh, H. Mokhtari, and H. Karimi, “A decentralized self-adjusting control strategy for reactive power management in an islanded multi-bus MV microgrid,” in Canadian Journal of Electrical and Computer Engineering, vol. 36, no. 1, pp. 18–25, 2013.

[128] H. R. Baghaee, M. Mirsalim, G. B. Gharehpetian, and H. A. Talebi, “A Decentralized Power Management and Sliding Mode Control Strategy for Hybrid AC/DC Microgrids including Renewable Energy Resources,” in IEEE Transactions on Industrial Informatics, vol. 3203, no. 3, pp. 1–10, 2017.

[129] R. Zhao, X. He, H. Xin, Z. Wang, and K. P. Wong, “A decentralized and hierarchical reactive power sharing control strategy for DGs parallel operation in an islanded microgrid,” in IET Semin. Dig., 2015.

[130] S. Khongkhachat and S. Khomfoi, “Hierarchical control strategies in AC microgrids,” in Proc. 2015 12th International Conference on Electrical Engineering/Electronics, Computer, Telecommunications and Information Technology (ECTI-CON), pp. 5–10, 2015.

[131] Y. Guan, J. C. Vasquez, J. M. Guerrero, Y. Wang, and W. Feng, “Frequency Stability of Hierarchically Controlled Hybrid Photovoltaic-Battery-Hydropower Microgrids,” in IEEE Transactions on Industry Applications, vol. 51, no. 6, pp. 4729–4742, 2015.

[132] A. Kahrobaeian and Mohamed Yari, “Networked-based hybrid distributed power sharing and control for islanded microgrid systems,” in IEEE Transactions on Power Electronics, vol. 30, no. 2, pp. 603–617, 2015.

[133] F. R. Salmasi and M. Hosseinzadeh, “Power management of an isolated hybrid AC/DC micro-grid with fuzzy control of battery banks,” in I.E.T. Renewable Power Generation, vol. 9, no. 5, pp. 484–493, 2015. Available:10.1049/iet-rpg.2014.0271.

[134] J. Hu, Y. Shan, Y. Xu, and J. M. Guerrero, “A coordinated control of hybrid ac/dc microgrids with PV-wind-battery under variable generation and load conditions,” in International Journal of Electrical Power and Energy Systems, vol. 104, pp. 583–592, 2019.

[135] S. M. Ashabani and Mohamed Yari, “A flexible control strategy for grid-connected and islanded microgrids with enhanced stability using nonlinear microgrid stabilizer,” in IEEE Transactions on Smart Grid, vol. 3, no. 3, pp. 1291–1301, 2012.

[136] A. Saim, A. Houari, J. M. Guerrero, A. Djerioui, M. Machmoum, and M. A. Ahmed, “Stability analysis and robust damping of multiresonances in distributed-generation-based islanded microgrids,” in IEEE Transactions on Industrial Electronics, vol. 66, pp. 8958–8970, 2019.

[137] IEEE Standard for DC Microgrids for Rural and Remote Electricity Access Applications, IEEE Power and Energy Society, IEEE Std 2030.10™-2021, pp. 1-47.

[138] M. S. S. Danish, H. Matayoshi, H. R. Howlader, S. Chakraborty, P. Mandal and T. Senjyu, “Microgrid Planning and Design: Resilience to Sustainability,” 2019 IEEE PES GTD Grand International Conference and Exposition Asia (GTD Asia), Bangkok, Thailand, 2019, pp. 253-258. Available: 10.1109/GTDAsia.2019.8716010.

[139] N. Zhang, Z. Hu, B. Shen, G. He, and Y. Zheng, “An integrated source-grid-load planning model at the macro level: Case study for China’s power sector,” in Energy, vol. 126, pp. 231-246, May 2017. Available: 10.1016/j.energy.2017.03.026.

[140] H. Sun, X. Cui, and H. Latifi, “Optimal management of microgrid energy by considering demand side management plan and maintenance cost with developed particle swarm algorithm,” in Electric Power Systems Research, vol. 231, p. 110312, Jun. 2024. Available: 10.1016/j.epsr.2024.110312.

[141] D. M. Teferra, L. M. H. Ngoo, and G. N. Nyakoe, “Fuzzy-based prediction of solar PV and wind power generation for microgrid modeling using particle swarm optimization,” in Heliyon, vol. 9, no. 1, p. e12802, Jan. 2023. Available: 10.1016/j.heliyon.2023.e12802.

[142] M. Mohamed, F. E. Mahmood, M. A. Abd, A. Chandra and B. Singh, “Dynamic Forecasting of Solar Energy Microgrid Systems Using Feature Engineering,” in IEEE Transactions on Industry Applications, vol. 58, no. 6, pp. 7857-7869, Nov.-Dec. 2022. Available: 10.1109/TIA.2022.3199182.

[143] J. Wang, J. Yan, Y. Xu, and K. Huang, “Power flow calculation method for isolated microgrid considering the influence of harmonic power,” in The Journal of Engineering, vol. 2017, pp. 2615-2621, 2017. Available: 10.1049/joe.2017.0844.

[144] H. Wang, Z. Yan, X. Xu, and K. He, “Probabilistic power flow analysis of microgrid with renewable energy,” International Journal of Electrical Power & Energy Systems, vol. 114, p. 105393, Jan. 2020. Available: 10.1016/j.ijepes.2019.105393.

[145] S. Shendryk, V. Shendryk, Y. Parfenenko, O. Drozdenko and S. Tymchuk, “Decision Support System for Efficient Energy Management of MicroGrid with Renewable Energy Sources,” 2021 11th IEEE International Conference on Intelligent Data Acquisition and Advanced Computing Systems: Technology and Applications (IDAACS), Cracow, Poland, 2021, pp. 225-230. Available: 10.1109/IDAACS53288.2021.9660966.

[146] M. Hasan, Z. Mifta, N. A. Salsabil, S. J. Papiya, M. Hossain, P. Roy, N.-U.-R. Chowdhury, and O. Farrok, “A critical review on control mechanisms, supporting measures, and monitoring systems of microgrids considering large scale integration of renewable energy sources,” in Energy Reports, vol. 10, pp. 4582-4603, Nov. 2023. Available: 10.1016/j.egyr.2023.11.025.

[147] N. M. Tabatabaei, E. Kabalci, and N. Bizon, “Microgrid Planning and Modeling,” in Microgrid Architectures, Control and Protection Methods, Springer, 2020, pp. 27-64. Available: 10.1007/978-3-030-23723-3_2.

[148] A. K. Roy, G. R. Biswal, and P. Basak, “An integrated rule-based power management and dynamic feed-forward low voltage ride through scheme for a grid-connected hybrid energy system,” in Journal of Renewable and Sustainable Energy, vol. 12, no. 5, pp. 1–18, 2020. Available:10.1063/5.0019254.

[149] T. Vigneysh and N. Kumarappan, “Autonomous operation and control of photovoltaic/solid oxide fuel cell/battery energy storage based microgrid using fuzzy logic controller,” International Journal of Hydrogen Energy, vol. 41, no. 3, pp. 1877–1891, 2016.

[150] A. Mohammadzadeh and S. Rathinasamy, “Energy management in photovoltaic battery hybrid systems: A novel type-2 fuzzy control,” in International Journal of Hydrogen Energy, vol. 45, no. 41, pp. 20970–20982, 2020. Available:10.1016/j.ijhydene.2020.05.187.

[151] M. K. Senapati, C. Pradhan, and R. K. Calay, “A computational intelligence based maximum power point tracking for photovoltaic power generation system with small-signal analysis,” Optimal Control Applications and Methods, vol. 32, no. 2, pp. 617–636, 2021.

[152] S. Jeyasudha et al., “Techno economic performance analysis of hybrid renewable electrification system for remote villages of India,” in Int. Trans. Electr. Energy Syst., vol. 31, no. 10, pp. 1–18, 2021. Available: 10.1002/2050-7038.12515.

[153] Available at: https://support.ul-renewables.com/homer-manuals-pro/controller.html (accessed on March 25, 2024).

[154] D. Arcos-Aviles, D. Pacheco, D. Pereira, et al., “A comparison of fuzzy-based energy management systems adjusted by nature-inspired algorithms,” in Applied Sciences, vol. 11, no. 4, pp. 1–22, 2021. Available:10.3390/app11041663.

[155] M. Y. Worku, M. A. Hassan, and M. A. Abido, “Power Management, Voltage Control and Grid Synchronization of Microgrids in Real Time,” in Arabian Journal for Science and Engineering, vol. 46, pp. 1411–1429, 2021. https://doi.org/10.1007/s13369-020-05062-9.

[156] S. M. S. Kalajahi, H. Seyedi, and K. Zare, “Under-frequency load shedding in isolated multi-microgrids,” in Sustainable Energy, Grids and Networks, vol. 27, 100494, 2021. Available:10.1016/j.segan.2021.100494.

[157] D. Arcos-Aviles, J. Pascual, L. Marroyo, P. Sanchis, and F. Guinjoan, “Fuzzy logic-based energy management system design for residential grid-connected microgrids,” in IEEE Transactions on Smart Grid, vol. 9, no. 2, pp. 530–543, 2018. Available:10.1109/TSG.2016.2555245.

[158] J. Hmad, A. Houari, H. Trabelsi, and M. Machmoum, “Fuzzy logic approach for smooth transition between grid-connected and stand-alone modes of three-phase DG-inverter,” in Electric Power Systems Research, vol. 175, pp. 105892, 2019. Available:10.1016/j.epsr.2019.105892.

[159] M. Jafari, Z. Malekjamshidi, J. Zhu, and M. H. Khooban, “A Novel Predictive Fuzzy Logic-Based Energy Management System for Grid-Connected and Off-Grid Operation of Residential Smart Microgrids,” in IEEE Journal of Emerging and Selected Topics in Power Electronics, vol. 8, no. 2, pp. 1391–1404, 2020. Available:10.1109/JESTPE.2018.2882509.

[160] J. C. Pena-Aguirre, A. I. Barranco-Gutierrez, J. A. Padilla-Medina, A. Espinosa-Calderon, and F. J. Perez-Pinal, “Fuzzy Logic Power Management Strategy for a Residential DC-Microgrid,” in IEEE Access, vol. 8, pp. 116733–116743, 2020. Available:10.1109/ACCESS.2020.3004611.

[161] A. Kaysal and R. Bayindir, “Design and Analysis of Fuzzy Logic Controllers for Microgrid Voltage Control,” in 2018 2nd International Symposium on Multidisciplinary Studies and Innovative Technologies (ISMSIT), pp. 1–6, 2018.

[162] S. K. Sahoo and N. K. Kishore, “Battery state-of-charge-based control and frequency regulation in the mmg system using fuzzy logic,” in IET Generation, Transmission & Distribution, vol. 14, no. 14, pp. 2698–2709, 2020. Available:10.1049/iet-gtd.2019.1638.

[163] I. U. Salam, M. Yousif, M. Numan, and M. Billah, “Addressing the Challenge of Climate Change: The Role of Microgrids in Fostering a Sustainable Future - A Comprehensive Review,” Renewable Energy Focus, vol. 48, p. 100538, Mar. 2024. Available: https://doi.org/10.1016/j.ref.2024.100538.

[164] A. K. Barik, D. Tripathy, D. L. Das, and S. C. Sahoo, “Optimal Load-Frequency Regulation of Demand Response Supported Isolated Hybrid Microgrid Using Fuzzy PD+I Controller,” in Intelligent Techniques and Applications in Science and Technology, ICIMSAT 2019, Learning and Analytics in Intelligent Systems, vol. 12, pp. 798-806, 2020.

[165] J. Kaur and A. Khosla, “Simulation and harmonic analysis of hybrid distributed energy generation based microgrid system using intelligent technique,” Indonesian Journal of Electrical Engineering and Computer Science, vol. 30, no. 3, pp. 1287-1296, 2023.

[166] M. K. Senapati, C. Pradhan, P. K. Nayak, and S. R. Samantaray, “Lagrange interpolating polynomial-based deloading control scheme for variable speed wind turbines,” International Transactions on Electrical Energy Systems, vol. 29, no. 5, pp. 1-17, 2019.

[167] B. Vadlamudi and T. Anuradha, “Review of islanding detection using advanced signal processing techniques,” Electrical Engineering, vol. 106, pp. 181-202, 2024. Available: https://doi.org/10.1007/s00202-023-01967-4.

[168] W. Issa, S. Sharkh, and M. Abusara, “A review of recent control techniques of drooped inverter-based AC microgrids,” Energy Science & Engineering, vol. 12, pp. 1792-1814, 2024. Available: 10.1002/ese3.1670.

[169] E. S. Roudbari, M. T. H. Beheshti, and S. M. Rakhtala, “Voltage and frequency regulation in an islanded microgrid with PEM fuel cell based on a fuzzy logic voltage control and adaptive droop control,” IET Power Electron., vol. 13, no. 1, pp. 78–85, 2020.

[170] M. Habib, A. A. Ladjici, and A. Harrag, “Microgrid management using hybrid inverter fuzzy-based control,” Neural Comput. Appl., vol. 32, no. 13, pp. 9093–9111, 2020.

[171] H. Zhao, M. Hong, W. Lin, and K. A. Loparo, “Voltage and Frequency Regulation of Microgrid with Battery Energy Storage Systems,” IEEE Transactions on Smart Grid, vol. 10, no. 1, pp. 414-424, 2019. Available: 10.1109/TSG.2017.2741668.

[172] D. J. Petrović, M. M. Lazić, B. V. Jovanović Lazić, B. D. Blanuša, and S. O. Aleksić, “Hybrid Power Supply System with Fuzzy Logic Controller: Power Control Algorithm, Main Properties, and Applications,” Journal of Modern Power Systems and Clean Energy, vol. 10, no. 4, pp. 923-931, 2022.

[173] D. Kumar, H. D. Mathur, S. Bhanot, and R. C. Bansal, “Frequency regulation in islanded microgrid considering stochastic model of wind and PV,” Int. Trans. Electr. Energy Syst., vol. 29, no. 9, pp. 1–17, 2019.

[174] S. K. Sahoo, A. K. Sinha, and N. K. Kishore, “Control Techniques in AC, DC, and Hybrid AC–DC Microgrid: A Review,” IEEE Journal of Emerging and Selected Topics in Power Electronics, vol. 6, no. 2, pp. 738-759, 2018. Available: 10.1109/JESTPE.2017.2786588.

[175] A. Ghasaei, Z. J. Zhang, W. M. Wonham, and R. Iravani, “A Discrete-Event Supervisory Control for the AC Microgrid,” IEEE Transactions on Power Delivery, vol. 36, no. 2, pp. 663-675, 2021. Available: 10.1109/TPWRD.2020.2988687.

[176] “Central Electricity Regulatory Commission (CERC) - Staff Paper, New Delhi,” Available at: http://www.cercind.gov.in/, 2011 (accessed on December 25, 2022).

[177] “IEEE Guide for Identifying and Improving Voltage Quality in Power Systems,” in IEEE Std 1250-2011 (Revision of IEEE Std 1250-1995), 1-70, 31 March 2011 (accessed on December 26, 2022).

[178] A. Grover, A. Khosla, D. Joshi, and V. Vimal, “Implementation of Soft Computing Techniques to Evade Partial Shading Effects for PV Based Off-Grid System,” in 13th IEEE PES Asia Pacific Power & Energy Engineering Conference (APPEEC), Thiruvananthapuram, India, pp. 1-6, 2021. Available: 10.1109/APPEEC50844.2021.9687716.

[179] N. Tephiruk, W. Kanokbannakorn, T. Kerdphol, Y. Mitani, and K. Hongesombut, “Fuzzy Logic Control of a Battery Energy Storage System for Stability Improvement in an Islanded Microgrid,” Sustainability, vol. 10, no. 5, pp. 1-16, 2018.

[180] B. Madaci, R. Chenni, E. Kurt, and K. E. Hemsas, “Design and Control of a Stand-alone Hybrid Power System,” International Journal of Hydrogen Energy, vol. 41, no. 29, pp. 12485-12496, 2016.

[181] N. Hakimuddin, A. Khosla, and J. K. Garg, “Comparative Performance Investigation of Genetic Algorithms (GAs), Particle Swarm Optimization (PSO) and Bacteria Foraging

Algorithm (BFA) Based Automatic Generation Control (AGC) with Multi Source Power Plants (MSPPs),” Electric Power Components and Systems, vol. 49, no. 20, pp. 1513-1524, 2022.

[182] M. Bhuyan, D. C. Das, A. K. Barik, and S. C. Sahoo, “Performance Assessment of Novel Solar Thermal-Based Dual Hybrid Microgrid System Using CBOA Optimized Cascaded PI-TID Controller,” IETE Journal of Research, vol. 1, pp. 1-19, 2022. Available: 10.1080/03772063.2022.2083026.

[183] X. Liu, P. Wang, and P. C. Loh, “A Hybrid AC/DC Microgrid and Its Coordination Control,” IEEE Transactions on Smart Grid, vol. 2, no. 2, pp. 278-286, 2011. Available:10.1109/TSG.2011.2116162.

[184] A. C. Luna, L. Meng, N. L. Diaz, M. Graells, J. C. Vasquez, and J. M. Guerrero, “Online Energy Management Systems for Microgrids: Experimental Validation and Assessment Framework,” IEEE Transactions on Power Electronics, vol. 33, no. 3, pp. 2201-2215, 2018. Available:10.1109/TPEL.2017.2700083.

[185] B. Zhao, X. Wang, D. Lin, et al., “Energy management of multiple microgrids based on a system of systems architecture,” IEEE Transactions on Power Systems, vol. 33, no. 6, pp. 6410-6421, 2018. Available:10.1109/TPWRS.2018.2840055.

[186] C. Wang, P. Yang, C. Ye, Y. Wang, and Z. Xu, “Voltage control strategy for three/single phase hybrid multimicrogrid,” IEEE Transactions on Energy Conversion, vol. 31, no. 4, pp. 1498-1509, 2016. Available:10.1109/TEC.2016.2595860.

[187] A. A. A. Moussavou, M. Adonis, and A. K. Raji, “Microgrid energy management system control strategy,” in Proceedings of the Conference on Industrial and Commercial Use of Energy (ICUE), 2015, pp. 147-154. Available:10.1109/ICUE.2015.7280261.

[188] L. I. Minchala-Avila, L. Garza-Castanon, Y. Zhang, and H. J. A. Ferrer, “Optimal Energy Management for Stable Operation of an Islanded Microgrid,” IEEE Transactions on Industrial Informatics, vol. 12, no. 4, pp. 1361-1370, 2016. Available:10.1109/TII.2016.2569525.

[189] R. Roofegari Nejad and S. M. Moghaddas Tafreshi, “Operation Planning of a Smart Microgrid Including Controllable Loads and Intermittent Energy Resources by Considering Uncertainties,” Arabian Journal for Science and Engineering, vol. 39, pp. 6297–6315, 2014. Available:10.1007/s13369-014-1267-4.

[190] F. Valencia, J. Collado, D. Sáez, and L. G. Marín, “Robust Energy Management System for a Microgrid Based on a Fuzzy Prediction Interval Model,” IEEE Transactions on Smart Grid, vol. 7, no. 3, pp. 1486–1494, 2016. Available:10.1109/TSG.2015.2463079.

[191] Z. Lv, Y. Zhang, M. Yu, Y. Xia, and W. Wei, “Decentralised coordinated energy management for hybrid AC/DC microgrid by using fuzzy control strategy,” IET Renewable Power Generation, vol. 14, no. 14, pp. 2649–2656, 2020. Available:10.1049/iet-rpg.2019.1281.

[192] M. K. Senapati, C. Pradhan, S. R. Samantaray, and P. K. Nayak, “Improved power management control strategy for renewable energy-based DC micro-grid with energy storage integration,” IET Generation, Transmission & Distribution, vol. 13, no. 6, pp. 838–849, 2019. Available:10.1049/iet-gtd.2018.5019.

[193] M. Eskandari, L. Li, and M. H. Moradi, “Improving power sharing in islanded networked microgrids using fuzzy-based consensus control,” Sustainable Energy, Grids and Networks, vol. 16, pp. 259–269, 2018. Available:10.1016/j.segan.2018.09.001.

[194] J. Preetha Roselyn, A. Ravi, D. Devaraj, R. Venkatesan, M. Sadees, and K. Vijayakumar, “Intelligent coordinated control for improved voltage and frequency regulation with smooth switchover operation in LV microgrid,” Sustainable Energy, Grids and Networks, vol. 22, p. 100356, 2020. Available:10.1016/j.segan.2020.100356.

[195] Shivam and R. Dahiya, “Intelligent Distributed Control Techniques for Effective Current Sharing and Voltage Regulation in DC Distributed Systems,” Arabian Journal for Science and Engineering, vol. 42, pp. 5071–5081, 2017. Available: https://doi.org/10.1007/s13369-017-2576-1.

[196] B. Khokhar, S. Dahiya, and K. P. Singh Parmar, “A Robust Cascade Controller for Load Frequency Control of a Standalone Microgrid Incorporating Electric Vehicles,” Electric Power Components and Systems, vol. 48, pp. 711–726, 2020. Available: https://doi.org/10.1080/15325008.2020.1797936.

[197] O. M. Salim, A. Aboraya, and S. I. Arafa, “Cascaded controller for a standalone microgrid-connected inverter based on tripleaction controller and particle swarm optimisation,” IET Generation, Transmission & Distribution, vol. 14, pp. 3389–3399, 2020. Available: https://doi.org/10.1049/iet-gtd.2019.1641.

[198] M. K. Debnath, T. Jena, and R. K. Mallick, “Optimal design of PD-Fuzzy-PID cascaded controller for automatic generation control,” Cogent Engineering, vol. 4, pp. 1–27, 2017. Available: https://doi.org/10.1080/23311916.2017.1416535.

[199] A. Annamraju, L. Bhukya, and S. Nandiraju, “Robust frequency control in a standalone microgrid: An adaptive fuzzy based fractional order cascade PD-PI approach,” Advances in Control and Applied Informatics, vol. 3, pp. 1–18, 2021. Available: https://doi.org/10.1002/adc2.72.

[200] B. Benlahbib, N. Bouarroudj, S. Mekhilef, et al., “Experimental investigation of power management and control of a PV/wind/fuel cell/battery hybrid energy system microgrid,”

International Journal of Hydrogen Energy, vol. 45, no. 53, pp. 29110-29122, 2020. Available:10.1016/j.ijhydene.2020.07.251.

[201] P. Bhowmik, S. Chandak, and P. K. Rout, “State of charge and state of power management of the hybrid energy storage system in an architecture of microgrid,” Journal of Renewable and Sustainable Energy, vol. 11, no. 1, pp. 1–21, 2019. Available:10.1063/1.5053567.

[202] A. S. Alahmed and M. M. Al-Muhaini, “An intelligent load priority list–based integrated energy management system in microgrids,” Electric Power Systems Research, vol. 185, p. 106404, 2020. Available: https://doi.org/10.1016/j.epsr.2020.106404.

[203] M. Kheshti, X. Kang, and Y. Jiarula, “Smooth Integration of Gansu Wind Farm into the Grid Using the Stator Flux-Oriented Vector Method and Fuzzy Logic Control,” Arabian Journal for Science and Engineering, vol. 42, pp. 5059–5069, 2017. Available: https://doi.org/10.1007/s13369-017-2596-x.

[204] “IEEE Standard for Interconnection and Interoperability of Distributed Energy Resources with Associated Electric Power Systems Interfaces,” in IEEE Std 1547-2018 (Revision of IEEE Std 1547-2003), vol., no., pp.1-138, 6 April 2018. Available: 10.1109/IEEESTD.2018.8332112.

[205] “IEEE Guide for Smart Grid Interoperability of Energy Technology and Information Technology Operation with the Electric Power System (EPS), End-Use Applications, and Loads,” in IEEE Std 2030-2011, vol., no., pp.1-126, 10 Sept. 2011. Available: 10.1109/IEEESTD.2011.6018239.

[206] D. Chen, L. Xu, and L. Yao, “DC voltage variation based autonomous control of DC microgrids,” IEEE Transactions on Power Delivery, vol. 28, no. 2, pp. 637-648, 2013. Available: 10.1109/TPWRD.2013.2241083.

[207] Y. E. G. Vera, R. Dufo-López, and J. L. Bernal-Agustín, “Energy management in microgrids with renewable energy sources: A literature review,” Applied Sciences, vol. 9, no. 18, pp. 1–28, 2019.

[208] S. K. Rangu, P. R. Lolla, K. R. Dhenuvakonda, and A. R. Singh, “Recent trends in power management strategies for optimal operation of distributed energy resources in microgrids: A comprehensive review,” International Journal of Energy Research, vol. 44, no. 13, pp. 9889–9911, 2020.

[209] N. Mohammed and A. M. Saif, “Programmable logic controller based lithium-ion battery management system for accurate state of charge estimation,” Computers & Electrical Engineering, vol. 93, pp. 107301-107306, 2021.

[210] R. Deshmukh, M. S. Ballal, and H. M. Suryawanshi, “A Fuzzy Logic Based Supervisory Control for Power Management in Multibus DC Microgrid,” IEEE Transactions on Industry Applications, vol. 56, no. 6, pp. 6174-6185, 2020.

[211] P. B. Nempu and N. S. Jayalakshmi, “Coordinated Power Management of the Subgrids in a Hybrid AC–DC Microgrid with Multiple Renewable Sources,” IETE Journal of Research, vol. 68, no. 4, pp. 2790-2800, 2022.

[212] J. B. Almada, R. P. S. Leão, R. F. Sampaio, and G. C. Barroso, “A centralized and heuristic approach for energy management of an AC microgrid,” Renewable and Sustainable Energy Reviews, vol. 60, pp. 1396–1404, 2016.

[213] S. Mehta and P. Basak, “Development of PLC-Based Hardware Test-Bench Prototype for Solar-Wind-Battery-Based Microgrid System’s Control Algorithm Validation”, in Electric Power Components and Systems, 2024. Available: https://doi.org/10.1080/15325008.2024.2329326.

[214] S. Mehta and P. Basak, “A Case Study on PV Assisted Microgrid Using HOMER Pro for Variation of Solar Irradiance Affecting Cost of Energy,” in 2020 IEEE 9th Power India International Conference (PIICON), pp. 1-6, 2020.

[215] R. S. Netto et al., “Real-Time framework for energy management system of a smart microgrid using multiagent systems,” Energies, vol. 11, no. 3, pp. 1–17, 2018.

[216] A. H. Etemadi, E. J. Davison, and R. Iravani, “A Generalized Decentralized Robust Control of Islanded Microgrids,” IEEE Transactions on Power Systems, vol. 29, no. 6, pp. 3102-3113, 2014.

[217] S. Nigam, O. Ajala, A. D. Domínguez-García, and P. W. Sauer, “Controller hardware in the loop testing of microgrid secondary frequency control schemes,” Electrical Power Systems Research, vol. 190, pp. 1-7, 2021.

[218] K. T. Erickson, “Programmable logic controllers,” IEEE Potentials, vol. 15, no. 1, pp. 14-17, 1996. Available: 10.1109/45.481370.

[219] I. Billas, J. Konstantaras, E. Tsambasis, C. Elias, A. Ktena, and C. Manasis, “Smart Load for a Hybrid Microgrid Testbed,” in 2019 8th Mediterranean Conference on Embedded Computing (MECO), pp. 1-5, 2019.

[220] M. Kabalan, D. Tamir, and P. Singh, “Electrical load controller for rural micro-hydroelectric systems using a programmable logic controller,” in 2015 IEEE Canada International Humanitarian Technology Conference (IHTC2015), pp. 1-4, 2015.

[221] A. Zia, Q. Malik, A. Saeed, N. Ahmad, and Z. A. Javed, “Operational Control of Three Phase MicroGrid using Programmable Logic Controller,” in 2019 IEEE Conference on

Sustainable Utilization and Development in Engineering and Technologies (CSUDET), pp. 214-218, 2019.

[222] D. Formby and R. Beyah, “Temporal Execution Behavior for Host Anomaly Detection in Programmable Logic Controllers,” IEEE Transactions on Information Forensics and Security, vol. 15, pp. 1455-1469, 2020.

[223] H. Zhang, Y. Jiang, W. N. N. Hung, X. Song, M. Gu, and J. Sun, “Symbolic Analysis of Programmable Logic Controllers,” IEEE Transactions on Computers, vol. 63, no. 10, pp. 2563-2575, 2014.

[224] T. Cruz, P. Simões, and E. Monteiro, “Virtualizing Programmable Logic Controllers: Toward a Convergent Approach,” IEEE Embedded Systems Letters, vol. 8, no. 4, pp. 69-72, 2016.

[225] Z. Hajduk, B. Trybus, and J. Sadolewski, “Architecture of FPGA Embedded Multiprocessor Programmable Controller,” IEEE Transactions on Industrial Electronics, vol. 62, no. 5, pp. 2952-2961, 2015.

[226] J. E. Wilson and F. Bried, “Application of programmable logic controllers for pipeline local and remote control,” IEEE Transactions on Industry Applications, vol. 24, no. 6, pp. 1082-1088, 1988.

[227] J. J. Sammarco, “Programmable Electronic and Hardwired Emergency Shut-down Systems: A Quantified Safety Analysis,” IEEE Transactions on Industry Applications, vol. 43, no. 4, pp. 1061-1068, 2007.

[228] H. Sheila, M. Abhishek, C. N. Neelalochana, P. Swetha, and G. Pragathi, “PLC based Microgrid Controller for Power management during Disaster,” International Journal of Innovative Research in Technology, vol. 9, no. 10, pp. 406-409, 2023.

[229] O. V. Gnana Swathika, K. Karthikeyan, S. Hemamalini, and R. Balakrishnan, “PLC based LV-DG Synchronization in Real-Time Microgrid Network,” ARPN Journal of Engineering and Applied Sciences, vol. 11, no. 5, pp. 3193-3197, 2016.

[230] V. Mukherjee and S. Khatua, “Application of PLC based smart microgrid controller for sequential load restoration during station blackout of nuclear power plants,” Annals of Nuclear Energy, vol. 151, pp. 1-16, 2021.

[231] G. Madhan, S. Muruganand, and N. Sureshkumar, “PLC Based ON-Grid System for Home Appliances,” Journal of NanoScience and NanoTechnology, vol. 2, no. 2, pp. 120-124, 2014.

[232] J. Sheeba Jeba Malar, A. Bisharathu Beevi, and M. Jayaraju, “Efficient Power Flow Management in Hybrid Renewable Energy Systems,” IETE Journal of Research, vol. 69, no. 2, pp. 1088-1100, 2021. Available: 10.1080/03772063.2020.1853617.

[233] S. Goel and R. Sharma, “Performance evaluation of stand alone, grid connected and hybrid renewable energy systems for rural application: A comparative review,” Renew. Sustain. Energy Rev., vol. 78, no. October 2016, pp. 1378–1389, 2017.

[234] G. Rohani and M. Nour, “Techno-economical analysis of stand-alone hybrid renewable power system for Ras Musherib in United Arab Emirates,” energy, vol. 64, pp. 828–841, 2014.

[235] S. Marais, K. Kusakana, and S. P. Koko, “Techno-economic feasibility analysis of a grid-interactive solar PV system for South African residential load,” IEEE clean energy, 2019 Int. Conf. Domest. Use Energy, pp. 163–168, 2016.

[236] M. Hossain, S. Mekhilef, and L. Olatomiwa, “Performance evaluation of a stand-alone PV-wind-diesel-battery hybrid system feasible for a large resort center in South China Sea,” Sustain. Cities Soc., vol. 28, pp. 358–366, 2017.

[237] E. I. Ã. Zoulias and N. Lymberopoulos, “Techno-economic analysis of the integration of hydrogen energy technologies in renewable energy-based stand-alone power systems,” vol. 32, pp. 680–696, 2007.

[238] A. Singh, P. Baredar, and B. Gupta, “Techno-economic feasibility analysis of hydrogen fuel cell and solar photovoltaic hybrid renewable energy system for academic research building,” Energy Conversion and Management, vol. 145, pp. 398-414, Aug. 2017. AVAILABLE: https://doi.org/10.1016/j.enconman.2017.05.014.

[239] T. Ma, H. Yang, and L. Lu, “A feasibility study of a stand-alone hybrid solar – wind – battery system for a remote island,” Appl. Energy, vol. 121, pp. 149–158, 2014.

[240] M. A. M. Ramli, A. Hiendro, and S. Twaha, “Economic analysis of PV / diesel hybrid system with flywheel energy storage,” Renew. Energy, vol. 78, pp. 398–405, 2015.

[241] M. K. Shahzad, A. Zahid, T. Rashid, M. A. Rehan, M. Ali, and M. Ahmad, “Techno-economic feasibility analysis of a solar-biomass off grid system for the electrification of remote rural areas in Pakistan using HOMER software,” Renew. Energy, vol. 106, pp. 264–273, 2017.

[242] Li, “Environmental Effects Techno-economic study of off-grid hybrid photovoltaic / battery and photovoltaic / battery / fuel cell power systems in Kunming, China,” Energy Sources, Part A Recover. Util. Environ. Eff., vol. 41, no. 13, pp. 1588–1604, 2019.

[243] M. Saleh, N. Faridun, M. Tajuddin, A. Ra, A. Azmi, and M. A. M. Ramli, “Optimization and sensitivity analysis of standalone hybrid energy systems for rural electrification: A case study of Iraq,” Applied Energy, vol. 138, pp. 775–792, 2019.

[244] L. Olatomiwa, S. Mekhilef, M. S. Ismail, and M. Moghavvemi, “Energy management strategies in hybrid renewable energy systems: A review,” Renew. Sustain. Energy Rev., vol. 62, pp. 821–835, 2016.

[245] M. Baneshi and F. Hadianfard, “Techno-economic feasibility of hybrid diesel / PV / wind / battery electricity generation systems for nonresidential large electricity consumers under southern Iran climate conditions,” Energy Convers. Manag., vol. 127, pp. 233–244, 2016.

[246] A. B. Kanase-Patil, R. P. Saini, and M. P. Sharma, “Sizing of integrated renewable energy system based on load profiles and reliability index for the state of Uttarakhand in India,” Renew. Energy, vol. 36, no. 11, pp. 2809–2821, 2011.

[247] L. O. Aghenta and M. Tariq Iqbal, “Design and dynamic modelling of a hybrid power system for a house in Nigeria,” Int. J. Photoenergy, vol. 2019, 2019. Available: 10.1155/2019/6501785.

[248] S. Biswas and M. T. Iqbal, “Dynamic Modelling of a Solar Water Pumping System with Energy Storage,” J. Sol. Energy, vol. 2018, pp. 1–12, 2018. Available: 10.1155/2018/8471715.

[249] M. Aneke and M. Wang, “Energy storage technologies and real life applications – A state of the art review,” Appl. Energy, vol. 179, pp. 350–377, 2016.

[250] A. Shahmohammadi, R. Sioshansi, A. J. Conejo, and S. Afsharnia, “The role of energy storage in mitigating ramping inefficiencies caused by variable renewable generation,” Energy Convers. Manag., vol. 162, no. February, pp. 307–320, 2018.

[251] O. Krishan and S. Suhag, “Techno-economic analysis of a hybrid renewable energy system for an energy poor rural community,” J. Energy Storage, vol. 23, no. March, pp. 305–319, 2019.

[252] M. Junaid, A. Kumar, and L. Mathew, “Techno economic feasibility analysis of different combinations of PV-Wind- Diesel-Battery hybrid system for telecommunication applications in different cities of Punjab, India,” Renew. Sustain. Energy Rev., vol. 76, no. December 2015, pp. 577–607, 2017.

[253] J. Kumar, B. V Suryakiran, A. Verma, and T. S. Bhatti, “Analysis of techno-economic viability with demand response strategy of a grid-connected microgrid model for enhanced rural electrification in Uttar Pradesh state, India,” Energy, 2019.

[254] K. Murugaperumal and P. A. D. Vimal, “Feasibility design and technoeconomic analysis of hybrid renewable energy system for rural electrification,” Sol. Energy, vol. 188, no. July, pp. 1068–1083, 2019.

[255] V. Mudgal, K. S. Reddy, and T. K. Mallick, “Techno-economic analysis of standalone solar photovoltaic-wind-biogas hybrid renewable energy system for community energy requirement,” Future Cities and Environment, vol. 5, no. 1, pp. 1-16, 2019.

[256] Y. Sawle, S. Jain, S. Babu, A. R. Nair, and B. Khan, “Prefeasibility economic and sensitivity assessment of hybrid renewable energy system,” IEEE Access, vol. 9, pp. 28260-28271, 2021.

[257] A. Chauhan and R. P. Saini, “Techno-economic optimization based approach for energy management of a stand-alone integrated renewable energy system for remote areas of India,” Energy, vol. 94, pp. 138-156, 2016. Available: https://doi.org/10.1016/J.ENERGY.2015.10.136.

[258] W. M. Amutha and V. Rajini, “Cost benefit and technical analysis of rural electrification alternatives in southern India using HOMER,” Renewable and Sustainable Energy Reviews, vol. 62, pp. 236-246, 2016. Available: https://doi.org/10.1016/J.RSER.2016.04.042.

[259] R. Sen and S. C. Bhattacharyya, “Off-grid electricity generation with renewable energy technologies in India: an application of HOMER,” Renewable Energy, vol. 62, pp. 388-398, 2014.

[260] V. K. Garg, S. Sharma, and D. Kumar, “Design and analysis of a microgrid system for reliable rural electrification,” International Transactions on Electrical Energy Systems, vol. 31, no. 2, pp. 1-20, 2021. AVAILABLE: https://doi.org/10.1002/2050-7038.12734.

[261] D. Rajavelu and B. Madasamy, “Multicriteria Decision Analysis for Renewable Energy Integration Design: For an Institutional Energy System Network,” Int. J. Photoenergy, vol. 2021, 2021. Available: 10.1155/2021/5555684.

[262] N. Jha et al., “Energy-Efficient Hybrid Power System Model Based on Solar and Wind Energy for Integrated Grids,” Math. Probl. Eng., vol. 2022, 2022. Available: 10.1155/2022/4877422.

[263] https://censusindia.gov.in/2011census/dchb/0203_PART_B_DCHB_LAHUL%20&%20SPITI.pdf. Accessed on March 28, 2022.

[264] S. Mahapatra and S. Dasappa, “Rural electrification: Optimising the choice between decentralised renewable energy sources and grid extension,” Energy Sustain. Dev., vol. 16, no. 2, pp. 146–154, 2012. Available: 10.1016/j.esd.2012.01.006.

[265] A. U. Limited 2020. Dollars to Indian Rupees. https://www.dollars2rupees.com. Accessed January 25, 2022.

[266] Global Alliance for Buildings and Construction, International Energy Agency and the United Nations Environment Programme, “2019 Global status report for buildings and construction: Towards a zero-emission, efficient and resilient buildings and construction sector,” 2019.

[267] S. Sharma, A. Verma and B. K. Panigrahi, “Robustly Coordinated Distributed Voltage Control Through Residential Demand Response Under Multiple Uncertainties,” in IEEE Transactions on Industry Applications, vol. 57, no. 4, pp. 4042-4058, July-Aug. 2021. Available: 10.1109/TIA.2021.3079135.

[268] Access to Electricity. Available at: https://ourworldindata.org/energy-access#:~:text=Citation Summary, to%20clean%20fuels%20for%20cooking. Accessed: July 2022.

[269] Energy Reports. Available at: https://mnre.gov.in/. Accessed: July 2022.

[270] UNEP, IEA. U.N. Environment and International Energy Agency: Towards a Zero-Emission, Efficient, and Resilient Buildings and Construction Sector; 2017. www.globalabc.org.

[271] Government Publications Office, International Energy Outlook 2016, with Projections To 2040. Government Printing Office, 2016.

[272] J. Kaushal and P. Basak, "A Novel Approach for Determination of Power Quality Monitoring Index of an AC Microgrid Using Fuzzy Inference System," Iranian Journal of Science and Technology, Transactions of Electrical Engineering, vol. 42, no. 4, pp. 429-450, 2018.

[273] S. Iqbal, S. Habib, M. Ali, A. Shafiq, A. ur Rehman, E. M. Ahmed, T. Khurshaid, and S. Kamel, "The Impact of V2G Charging/Discharging Strategy on the Microgrid Environment Considering Stochastic Methods," Sustainability, vol. 14, no. 20, pp. 13211, 1-22, 2022.

[274] S. Iqbal, A. Xin, M. Jan, M. A. Abdelbaky, H. Rehman, S. Salman, S. Rizvi, and M. Aurangzeb, "Aggregation of EVs for Primary Frequency Control of an Industrial Microgrid by Implementing Grid Regulation & Charger Controller," IEEE Access, vol. 8, pp. 141977-141989, 2020.

[275] Y. Ueda, K. Kurokawa, T. Tanabe, K. Kitamura, and H. Sugihara, "Analysis results of output power loss due to the grid voltage rise in grid-connected photovoltaic power generation systems," IEEE Transactions on Industrial Electronics, vol. 55, no. 7, pp. 2744-2751, 2008.

[276] S. Iqbal, A. Xin, M. U. Jan, M. A. Abdelbaky, H. U. Rehman, S. Salman, M. Aurangzeb, S. A. A. Rizvi, and N. A. Shah, "Improvement of Power Converters Performance by an Efficient Use of Dead Time Compensation Technique," Applied Sciences, vol. 10, no. 9, pp. 3121, 1-19, 2020.

[277] A. A. Alkahtani, S. T. Y. Alfalahi, A. A. Athamneh, et al., "Power Quality in Microgrids including Supraharmonics: Issues, Standards, and Mitigations," IEEE Access, vol. 8, pp. 127104-127122, 2020.

[278] M. Ahmed, L. Meegahapola, A. Vahidnia, and M. Datta, "Stability and Control Aspects of Microgrid Architectures-A Comprehensive Review," IEEE Access, vol. 8, pp. 144730-144766, 2020.

[279] S. Chandak and P. K. Rout, "The implementation framework of a microgrid: A review," International Journal of Energy Research, vol. 45, no. 3, pp. 3523-3547, 2021.

[280] T. L. Vandoorn, B. Meersman, L. Degroote, B. Renders, and L. Vandevelde, “A control strategy for islanded microgrids with DC-link voltage control,” IEEE Transactions on Power Delivery, vol. 26, no. 2, pp. 703-713, 2011.

[281] L. Wang, C. Y. Lin, and A. V. Prokhorov, “Stability analysis of a microgrid system with a hybrid offshore wind and ocean energy farm fed to a power grid through an HVDC link,” IEEE Transactions on Industry Applications, vol. 54, no. 3, pp. 2012-2022, 2018.

[282] M. Karimi, P. Wall, H. Mokhlis, and V. Terzija, “A new centralized adaptive underfrequency load shedding controller for microgrids based on a distribution state estimator,” IEEE Transactions on Power Delivery, vol. 32, pp. 370-380, 2017.

[283] R. Majumder, B. Chaudhuri, A. Ghosh, R. Majumder, G. Ledwich, and F. Zare, “Improvement of stability and load sharing in an autonomous microgrid using supplementary droop control loop,” IEEE Transactions on Power Systems, vol. 25, no. 2, pp. 796-808, 2010.

[284] E. Hossain, R. Perez, A. Nasiri, and R. Bayindir, “Stability improvement of microgrids in the presence of constant power loads,” International Journal of Electrical Power & Energy Systems, vol. 96, pp. 442-456, 2018.

[285] A. A. Nafeh, A. Heikal, R. A. El-Sehiemy, and W. A. A. Salem, “Intelligent fuzzy-based controllers for voltage stability enhancement of AC-DC micro-grid with D-STATCOM,” Alexandria Engineering Journal, vol. 61, no. 3, pp. 2260-2293, Mar. 2022. AVAILABLE: https://doi.org/10.1016/j.aej.2021.07.012.

[286] A. Abazari, M. M. Soleymani, M. Babaae, M. Ghafouri, H. Monsef, and M. Beheshti, “High penetrated renewable energy sources-based AOMPC for microgrid’s frequency regulation during weather changes, time-varying parameters and generation unit collapse,” IET Generation, Transmission & Distribution, vol. 14, no. 22, pp. 5164-5182, 2020.

[287] A. Abazari, M. Dozein, and H. Monsef, “An optimal Fuzzy-logic based frequency control strategy in a high wind penetrated power system,” Journal of the Franklin Institute, vol. 355, no. 14, pp. 6262-6285, 2018.

[288] A. Abazari, M. Dozein, H. Monsef, and B. Wu, “Wind turbine participation in micro-grid frequency control through self-tuning, adaptive fuzzy droop in de-loaded area,” IET Smart Grid, vol. 2, no. 2, pp. 301-308, 2019.

[289] Y. Song, S. Sahoo, Y. Yang, and F. Blaabjerg, “Probabilistic Risk Evaluation of Microgrids Considering Stability and Reliability,” IEEE Transactions on Power Electronics, vol. 38, no. 8, pp. 10302-10312, 2023.

[290] C. Ceballos, S. Londono, and J. Florez, “Stability analysis framework for isolated microgrids with energy resources integrated using voltage source converters,” Results in Engineering, vol. 19, pp. 1-10, 2023.

[291] K. Chen and M. Baran, “Robust Controller for Community Microgrids for Stability Improvement in Islanded Mode,” IEEE Transactions on Power Systems, vol. 38, no. 3, pp. 2472-2484, 2023.

[292] N. Diaz, F. Guinjoan, G. Quesada, A. Luna, and J. Guerrero, “Fuzzy-based cooperative interaction between stand-alone microgrids interconnected through VSC-based multiterminal converter,” International Journal of Electrical Power & Energy Systems, vol. 152, pp. 1-12, 2023.

[293] M. Leng, G. Zhou, G. Xu, S. Sahoo, X. Liu, Q. Zhou, Y. Yin, and F. Blaabjerg, “Small-Signal Stability Assessment and Interaction Analysis for Bipolar DC Microgrids,” IEEE Transactions on Power Electronics, vol. 38, no. 4, pp. 5524-5537, 2023.

[294] N. Khosravi et al., “A novel control approach to improve the stability of hybrid AC/DC microgrids,” Applied Energy, vol. 344, pp. 1-13, 2023.

[295] A. Jameel and M. Gulzar, “Load frequency regulation of interconnected multi-source multi-area power system with penetration of electric vehicles aggregator model,” Electrical Engineering, pp. 1-18, 2023.

[296] H. Abubakr et al., “Inclusion of V2G and Power System Stabilizer for Residential Microgrid Applications,” in 2023 IEEE Conference on Power Electronics and Renewable Energy (CPERE), 2023, pp. 1-6.

[297] R. Hassan, H. Wang, and R. Zane, “Continuous stability monitoring of DC microgrids using controlled injection,” in Conf. Proc. - IEEE Appl. Power Electron. Conf. Expo. - APEC, 2019, pp. 1357-1364.

[298] S. Pérez-Londoño, L. F. Rodríguez, and G. Olivar, “A simplified voltage stability index (SVSI),” International Journal of Electrical Power & Energy Systems, vol. 63, pp. 806-813, 2014. Available: 10.1016/j.ijepes.2014.06.044.

[299] S. Iqbal, A. Xin, M. U. Jan, S. Salman, A. u. M. Zaki, H. U. Rehman, M. F. Shinwari, and M. A. Abdelbaky, “V2G Strategy for Primary Frequency Control of an Industrial Microgrid Considering the Charging Station Operator,” Electronics, vol. 9, no. 4, pp. 549, 1-21, 2020.

[300] “IEEE Recommended Practice and Requirements for Harmonic Control in Electric Power Systems,” in IEEE Std 519-2014 (Revision of IEEE Std 519-1992), vol., no., pp.1-29, 11 June 2014.

[301] H. Rahman, M. Raza, P. Afsar, A. Alharbi, S. Ahmad, and H. Alyami, “Multi-Criteria Decision Making Model for Application Maintenance Offshoring Using Analytic Hierarchy Process,” Applied Sciences, vol. 11, no. 8, pp. 1-25, 2021.

[302] M. Asadabadi, E. Chang, and M. Saberi, “Are MCDM methods useful? A critical review of Analytic Hierarchy Process (AHP) and Analytic Network Process (ANP),” Cogent Engineering, vol. 6, no. 1, pp. 1-11, 2019.
[303] Y. Xi and Q. Li, “Improved AHP Model and Neural Network for Consumer Finance Credit Risk Assessment,” Advances in Multimedia, pp. 1-10, 2022.
[304] C.-L. Lin, C.-L. Fan, and B.-K. Chen, “Hybrid Analytic Hierarchy Process–Artificial Neural Network Model for Predicting the Major Risks and Quality of Taiwanese Construction Projects,” Applied Sciences, vol. 12, no. 15, pp. 7790, 1-19, 2022.
[305] İ. Kaya, M. Çolak, and F. Terzi, “Use of MCDM techniques for energy policy and decision-making problems: A review,” International Journal of Energy Research, vol. 42, pp. 2344-2372, 2018.
[306] R. Medjoudj, D. Aissani, and K. D. Haim, “Power customer satisfaction and profitability analysis using multi-criteria decision making methods,” International Journal of Electrical Power & Energy Systems, vol. 45, pp. 331-339, 2013.
[307] S. Eberlein and K. Rudion, “Small-signal stability modelling, sensitivity analysis and optimization of droop controlled inverters in LV microgrids,” International Journal of Electrical Power & Energy Systems, vol. 125, pp. 1-14, 2021.

LIST OF PUBLICATIONS FROM RESEARCH WORK

SCI-indexed journal publications

[1] Sahil Mehta & Prasenjit Basak, "A Centralized Stage-Wise Control Approach for Frequency and Voltage Regulation in PV–Wind–Storage Based Islanded Microgrid" in Electric Power Components and Systems, 2023. AVAILABLE: https://doi.org/10.1080/15325008.2023.2276829 **(IF - 1.7)**

[2] Sahil Mehta & Prasenjit Basak, "Determination of microgrid stability index based on measured electrical parameters and Mamdani fuzzy inference system", in Electrical Engineering, 2023. AVAILABLE: https://doi.org/10.1007/s00202-023-02002-2 **(IF - 1.6)**

[3] Sahil Mehta & Prasenjit Basak, "A Novel Design, Economic Assessment, and Fuzzy-Based Technical Validation of an Islanded Microgrid: A Case Study on Load Model of Kibber Village in Himachal Pradesh", in International Transactions on Electrical Energy Systems, 2022. AVAILABLE: https://doi.org/10.1155/2022/9639253 **(IF - 1.9)**

[4] Sahil Mehta & Prasenjit Basak, "A comprehensive review on control techniques for stability improvement in microgrids", in International Transactions on Electrical Energy Systems, 2022. AVAILABLE: https://doi.org/10.1002/2050-7038.12822 **(IF - 1.9)**

[5] Sahil Mehta & Prasenjit Basak, "Development of PLC-Based Hardware Test-Bench Prototype for Solar-Wind-Battery-Based Microgrid System's Control Algorithm Validation", in Electric Power Components and Systems, 2024. AVAILABLE: https://doi.org/10.1080/15325008.2024.2329326 **(IF - 1.7)**

SCOPUS-indexed journal publications

[1] Sahil Mehta & Prasenjit Basak, "Cascaded dual fuzzy logic controller for stable microgrid operation mitigating effects of natural uncertainty in solar and wind energy sources", in e-Prime - Advances in Electrical Engineering, Electronics and Energy, Volume 5, September 2023. AVAILABLE: https://doi.org/10.1016/j.prime.2023.100215

Conference publications

[1] Sahil Mehta and Prasenjit Basak, "A Case Study on PV Assisted Microgrid Using HOMER Pro for Variation of Solar Irradiance Affecting Cost of Energy," in 2020 IEEE 9th Power India International Conference (PIICON), 2020, pp. 1-6, DOI: 10.1109/PIICON49524.2020.9112894.